

REGULATION OF BLOOD PRESSURE HOMEOSTASIS

BY PANNEXIN 1 CHANNELS

Leon Joseph DeLalio

Wading River, New York

B.S. Biology, Northeastern University 2009

M.S. Biology, Northeastern University 2013

A Dissertation presented to the Graduate Faculty of the University of Virginia in
Candidacy for the Degree of Doctor of Philosophy

Department of Pharmacology

University of Virginia

October 31, 2018

ABSTRACT

The homeostatic regulation of blood pressure (BP) is multifaceted and temporally controlled by overlapping neural, vascular, and renal mechanisms. These mechanisms operate acutely in time to synchronize cardiovascular function with BP responses on a minute-to-minute basis, but also chronically over long-time scales to maintain BP within physiological limits. The integration of multivariate control mechanisms is heavily dependent on purinergic signaling, which utilizes adenosine 5'-triphosphate (ATP) as an autocrine/paracrine signal to coordinate cellular responses. The regulated release of cellular ATP and its accumulation in the extracellular space is a rate limiting step; yet the mechanisms responsible for ATP release are not well understood. Nevertheless, a primary role has been ascribed to pannexin (Panx) channels, specifically the Panx1 isoform in the vasculature. We initially focused on a role Panx1 channels in the peripheral vasculature where smooth muscle Panx1 influences acute hemodynamics involved in BP regulation. We report that phosphorylation of the intracellular loop YLK motif is directly and constitutively phosphorylated by Src kinase at tyrosine 198 (Y198). Using a Panx1-Y198 specific antibody and chemical/genetic modulators of Src kinase, we found that Src-mediated Y198 phosphorylation correlated with ATP release in vitro and ex vivo, and was necessary to support normal adrenergic vasoconstriction responses. We further demonstrated that Y198 phosphorylation was required for the presence of Panx1 at the plasma membrane, which was enriched in the smooth muscle layer of hypertensive human arteries suggestive of a contribution to hypertensive phenotypes. This discovery connects a significant purinergic vasoconstriction pathway with a previously identified, yet unexplored, tyrosine kinase-based adrenergic constriction mechanism, that causes

dysregulation of vascular hemodynamics in hypertensive disease. Delving further into a potential regulation pathway for Panx1-mediated ATP release and adrenergic vasoconstriction in smooth muscle cells, we identified a novel interaction between Panx1 and the membrane scaffold protein caveolin-1 in resistance arteries. We found that the onset of this adrenergic-stimulus dependent interaction was rapid and occurred in proximity to areas of sympathetic nerve innervation. The functional importance of this interaction was further elucidated *in vivo*, in which cell-specific caveolin-1 genetic deletion resulted in significantly blunted adrenergic-stimulated ATP release, impaired vasoconstriction, and a significant reduction in mean arterial pressure (MAP). These studies implicate plasma membrane Panx1 as a necessary component of hemodynamic control in resistance arteries. In comparison to the hemodynamic regulation of Panx1 in the peripheral vasculature, we also assessed renovascular Panx1 from renin-lineage cells, which require purinergic signaling for negative feedback control of chronic BP responses. Using a novel renin-cell Panx1 knockout model, we found that Panx1 deletion significantly alters RAAS activation and significantly increases steady-state plasma renin concentrations. In Panx1 deficient animals, high renin levels correlated with increased aldosterone levels, reduced urine volume, and a significant increase in MAP. RAAS activity and BP were only partially dependent on angiotensin type 1 receptor (AT1R) activation. Finally, we uncovered a novel Panx1-dependent function in renin-lineage cells from both renovascular and adrenocortical cell. Panx1 deficient animals exhibited impairments in adaptive cell responses that typically maintain physiological BP setpoints (renal renin recruitment and adrenal cell trans-differentiation). Thus, Panx1 channels are

novel regulators of cardiovascular feed-back mechanisms that are important in BP homeostasis.

TABLE OF CONTENTS

ABSTRACT	1
FIGURE LEGEND	6
LIST OF ABBREVIATIONS	8
DEDICATION.....	12
CHAPTER 1. GENERAL INTRODUCTION	15
1.1 ACUTE REGULATION OF BLOOD PRESSURE RESPONSES BY PURINERGIC SIGNALING: NEUROMODULATION AND HEMODYNAMIC MECHANISMS.....	16
1.2 LONG-TERM PURINERGIC CONTROL OF BLOOD PRESSURE: A ROLE FOR ATP IN RENAL FEEDBACK MECHANISMS.....	24
1.3 MECHANISMS OF ATP RELEASE	32
CHAPTER 2. MATERIALS AND METHODS	42
2.1. MATERIALS AND METHODS FOR CHAPTER 3	42
2.2. MATERIALS AND METHODS FOR CHAPTER 4	49
2.3. MATERIALS AND METHODS FOR CHAPTER 5	59
CHAPTER 3. POST-TRANSLATIONAL MODIFICATION OF PANNEXIN 1 -Y198 BY SRC KINASE	66
3.1. ABSTRACT	66
3.2. INTRODUCTION.....	68
3.3. RESULTS.....	71
3.4. DISCUSSION	100
CHAPTER 4. INTERACTION BETWEEN PANNEXIN 1 AND CAVEOLIN-1 IN SMOOTH MUSCLE CAN REGULATE BLOOD PRESSURE.....	110
4.1 ABSTRACT	110
4.2 INTRODUCTION.....	112
4.3 RESULTS.....	115
4.4 DISCUSSION	154

CHAPTER 5. PANNEXIN 1 CHANNELS REGULATE RAAS ACTIVITY, BLOOD PRESSURE, AND ADRENAL HOMEOSTASIS.....	163
5.1 ABSTRACT	163
5.2 INTRODUCTION.....	165
5.3 RESULTS.....	168
5.4 DISCUSSION	205
CHAPTER 6. GENERAL DISCUSSION AND FUTURE DIRECTIONS.....	218
CHAPTER 7. REFERENCES	233

FIGURE LEGEND

<i>Figure 1. Src family kinases regulate phenylephrine-induced Pannexin 1 channel function independent of Ca²⁺.</i>	73
<i>Figure 2. Supplement to Figure 1: Src family kinases support phenylephrine-stimulated ATP release in HEK cells.</i>	75
<i>Figure 3. Pannexin 1 tyrosine 198 is constitutively phosphorylated in vascular smooth muscle cells.</i>	79
<i>Figure 4. Supplement to Figure 3: Src kinase is sufficient to phosphorylate Pannexin 1 (Y198) in HEK cells.</i> 81	
<i>Figure 5. Src kinase activity modulates Pannexin 1 (Y198) phosphorylation.</i>	85
<i>Figure 6. Src kinase directly phosphorylates Pannexin 1 (Y198).</i>	88
<i>Figure 7. Supplement to Figure 6: Recombinant Pannexin 1 is glycosylated.</i>	90
<i>Figure 8. Pannexin1 (Y198) phosphorylation occurs at the plasma membrane in VSMCs.</i>	93
<i>Figure 9. Src-dependent Panx1-Y198 phosphorylation occurs at the plasma membrane and is detectable in hypertensive arteries.</i>	96
<i>Figure 10. Supplement to Figure 9: Total Pannexin 1 expression is increased in human hypertensive vascular biopsies.</i>	98
<i>Figure 11. Caveolae in VSMC localized adjacently to sympathetic nerves.</i>	116
<i>Figure 12. Pannexin 1 and caveolin-1 only associate after phenylephrine stimulation.</i>	120
<i>Figure 13. Z plane analysis of VSMC innervation on resistance arteries using confocal microscopy.</i>	123
<i>Figure 14. Pannexin1 and caveolin-1 localize to the plasma membrane near sympathetic nerves.</i>	126
<i>Figure 15. Supplement to Figure 14: Connexin 43 and VNUT are not found on VSMCs of resistance arteries.</i>	128
<i>Figure 16. Inducible deletion of caveolin-1 from smooth muscle cells blunts adrenergic-mediated ATP release.</i>	131
<i>Figure 17. Supplement to Figure 16: Intracellular ATP measurements in thoracodorsal arteries.</i>	133
<i>Figure 18. Effects of vascular smooth muscle cell caveolin-1 deletion on vasoconstriction and vasodilation responses in resistance arteries.</i>	136
<i>Figure 19. VSMC Caveolin-1 deletion reduces blood pressure.</i>	139
<i>Figure 20. Supplement to Figure 19: VSMC caveolin-1 deletion in SMC-Cre^{Δ/Δ} mice do not have altered renin homeostasis or blood pressure due to injection volume.</i>	141
<i>Figure 21. VSMC caveolin-1 deletion does not influence cardiac function.</i>	144
<i>Figure 22. Tamoxifen induction in Cre⁻/Cav1^{fl/fl} control mice retain normal VSMC caveolin-1 expression, phenylephrine-induced constriction, and cardiac function.</i>	148
<i>Figure 23. Caveolin-1 deletion prevents the blood pressure-lowering effects of the Panx1 inhibitory peptide (PxIL2P).</i>	152

<i>Figure 24: Generation of a renin-cell Pannexin 1 knockout model.</i>	169
<i>Figure 25. Deletion of Pannexin 1 alters baseline renin secretion, but not the distribution of JG cells in the renal cortex.</i>	173
<i>Figure 26. Supplement to Figure 25. Ren1-Panx1Δ/Δ mice have normal renal tissue morphology.</i>	175
<i>Figure 27. Renin cell Pannexin 1 is necessary for maintaining blood pressure homeostasis.</i>	180
<i>Figure 28. Supplement to Figure 27. Ren1-Panx1Δ/Δ mice have reduced urine volume.</i>	182
<i>Figure 29. Supplement to Figure 27. Effects of renovascular Panx1 deletion on vasoconstriction responses in peripheral resistance arteries.</i>	184
<i>Figure 30. Renin recruitment is impaired in Ren1-Panx1Δ/Δ mice.</i>	188
<i>Figure 31. AT1R inhibition partially mediates RAAS activity in Ren1-Panx1Δ/Δ mice.</i>	192
<i>Figure 32. Panx1 deletion from renin expressing cells causes adrenal hypertrophy and aldosterone dysregulation.</i>	196
<i>Figure 33. Supplement to Figure 32. Female Ren1-renin-cell Panx1 do not exhibit RAAS hyperactivity or adrenal gland hypertrophy.</i>	198
<i>Figure 34. Adrenocortical zonation is impaired when Panx1 is deleted from renin expressing cells.</i>	201
<i>Figure 35. Candesartan treatment normalizes adrenal hypertrophy, but not CYP11B2 dysregulation in Ren1-Panx1Δ/Δ.</i>	203
<i>Figure 36. Angiotensin II stimulated Panx1 ATP release is blunted in As4.1 cells.</i>	227
<i>Figure 37. Knockdown of Panx1 from As4.1 cells impairs cAMP-induced renin expression.</i>	229
<i>Figure 38. Panx1 deletion from renin-lineage cells results in increased adrenal cell proliferation.</i>	231

LIST OF ABBREVIATIONS

Panx1	Pannexin 1
Panx2	Pannexin 2
Panx3	Pannexin 3
α 1-AR	α 1 adrenergic receptor
SFK	Src family kinase
VSMC	Vascular smooth muscle cell
ATP	Adenosine triphosphate
NE	Norepinephrine
PE	Phenylephrine
ET1	Endothelin-1
5-HT	5-Hydroxy-tryptamine (Serotonin)
TDA	Thoracodorsal artery
hCoSMC	Human coronary smooth muscle cell
HEK	Human embryonic kidney cell

LA25	Temperature-sensitive Src normal rat kidney cells
SH2	Src homology 2 domain
SH3	Src homology 3 domain
PP2	4-Amino-5-(4-chlorophenyl)-7-(<i>t</i> -butyl)pyrazolo(3,4-d)pyrimidine
PP3	4-Amino-7-phenylpyrazol(3,4-d)pyrimidine
BAPTA-AM	Glycine, N,N'-(1,2-ethanediylbis(oxy-2,1-phenylene))bis(N-(2-((acetyloxy)methoxy)-2-oxoethyl))-, bis((acetyloxy)methyl) ester
NMDA	N-methyl-D-aspartate receptor
BP	Blood pressure
MAP	Mean Arterial Pressure
SBP	Systolic Blood Pressure
DBP	Diastolic Blood Pressure
HR	Heart rate
PxIL2P1	Pannexin 1 intracellular loop 2 mimetic peptide 1
α -AR	α -adrenergic receptor
MEJ	Myoendothelial junction

EC	Endothelial cell
SMC	Smooth muscle cell
IEL	Internal elastic lamina
RFP	Red fluorescent protein
GFP	Green fluorescent protein
VNUT	Vesicular nucleotide transporter
Cx43	Connexin43
Cav1	Caveolin-1
Acta2	Alpha 2 smooth muscle actin
CD-31	Cluster of differentiation 31
PECAM-1	Platelet endothelial cell adhesion molecule
RAAS	Renin-angiotensin-aldosterone-system
JG	Juxtaglomerular
JGA	Juxtaglomerular apparatus
GFR	Glomerular filtration rate
RBF	Renal blood flow

TGF	Tubuloglomerular feedback
P2X	Purinergic type 2 ionotropic receptor
P2Y	Purinergic type 2 metabotropic receptor
A1R	Adenosine type 1 receptor
AT1R	Angiotensin II type 1 receptor
AT2R	Angiotensin II type 2 receptor
AT3R	Angiotensin II type 3 receptor
EYFP	Enhanced yellow fluorescent protein
ZG	Zona glomerulosa
ZF	Zona fasciculata
CYP11B2	Aldosterone synthase

DEDICATION

This dissertation is dedicated to the influential and supportive people in my life: my family, my mentors, my friends and colleagues.

First and foremost, I would like to thank my family. To my mother Janice and my father Leonard, thank you for your constant love and support. No accomplishment of mine could have ever been achieved if not for the dedication and sacrifice you make for your family. You personify the values of hard work and fairness, and through that, have given me the greatest benchmark to strive for. To my sister Jessica, you are my most tenacious advocate. When times seem daunting, your youthful wisdom and loving support always guide me. To Susan, you inspire me to do great things every day. Thank you for always believing in me. I am truly thankful to have you all in my life.

I would also like to thank my mentor Brant. My time in the Isakson lab has been a transformative experience, both professionally and personally. Thank you for giving me the creative freedom to follow the science, and for always supporting me to answer the difficult questions. You have pushed me to think critically, challenged me to set high goals, and carefully guided me through the many facets of academic research. Your open candor, vigor for science, and championing of downward-held sauropod necks, is a testament to the passionate scientist and caring person I strive to emulate. I will treasure my experiences in the Isakson lab for the rest of my life. Thank you for being a great mentor and friend.

To my early mentors at Northeastern University, Dr. Rebecca Rosengaus and Dr. Wendy Smith. You welcomed me into your labs at an early age and encouraged me to

pursue a career path I would never have believed possible for myself. Thank you for nurturing my scientific curiosity and advocating for my success as both an undergraduate student and a Master's student at Northeastern. Without your early support and exemplary dedication to your students and your research I would not be where I am today. For that, I will always be grateful to you.

To my colleagues and committee members, in particular, Drs. Ariel Gomez, Thu Le, Paula Barrett, and Doug Bayliss. Thank you for your dedication, your patience, and your time in serving as my committee member. Each of you has had a profound impact on my scientific training. Thank you for welcoming me into your labs, and for teaching me the range of experimental techniques I will rely on in my future research endeavors. I am very appreciative for your sincere and informed opinions, which always pushed me to think critically. You have been supportive collaborators and true friends. Much of my success in research could not have been achieved without your guidance.

To my lab mates, thank you for fostering the caffeine-fueled, frenetic, and ambitious lab culture I love so much. To Angie, you are the most caring and considerate person I know—always willing to lend a hand. Thank you for your friendship and for listening, no matter how big a soap box I could find. To Marie, Alex, and Scott, you welcomed me to the Isakson lab when I first joined. Thank you for your friendship and for setting the high standard of achievement I will always work towards. TC Keller, “why not?” you encouraged me to tackle the challenges that seem impracticable—thank you. Alex Keller, your sharp intellect and opinionated candor were a critical part of many lab successes, thank you for your continued support and your friendship. Miranda, I am very

appreciative for your honesty and patient helpfulness. You are a trusted source of experimental expertise, and even more so, a trusted friend. Thank you for all your guidance. To Isola, Claire, Abby, and Yang, your optimism and willingness to help enriched my time in the Isakson lab, I hope it is as great an experience for you as it has been for me. Thank you all.

CHAPTER 1. GENERAL INTRODUCTION

The homeostatic regulation of blood pressure (BP) is multifaceted and temporally controlled by interacting neural, vascular, and renal mechanisms. These mechanisms operate acutely in time to synchronize BP requirements with moment-to-moment behavioral responses, and chronically to maintain BP within physiological limits. This ensures that the circulatory system can appropriately meet acute demands (e.g. support of humoral responses to insulin, epinephrine and cortisol), as well as support vital organ functions such as delivery of oxygenated blood for survival. The integration of multiple control mechanisms, and the molecular pathways that coordinate cell responses within each mechanism, establish a BP threshold necessary for homeostasis¹. Thus, these regulatory mechanisms have potent effects on shifting BP set-points, and when dysregulated result in the development, maintenance, and progression of disease phenotypes, especially hypertension². Understanding the common cellular pathways involved in setting BP thresholds is crucial for understanding how the cardiovascular system maintains homeostasis.

One common communication pathway that pervades neural, vascular, and renal regulatory systems is the use of adenosine 5'-triphosphate (ATP) as a chemical messenger, termed purinergic signaling³. The utilization of extracellular ATP as an autocrine/paracrine signal developed early in evolutionary time as a primitive cell communication system that repurposes ATP generated by oxidative phosphorylation as a diffusible messenger^{4, 5}. Autocrine/paracrine signaling mediated by ATP acts through two classes of purinergic receptors (P1 and P2), which differentially respond to ATP and its

metabolic breakdown product adenosine. The regulated release of upstream purinergic signals and the differential responses imbued by a large diversity of purinergic receptor isoforms play a fundamental role in regulating both acute and long-term cardiovascular mechanisms necessary for BP homeostasis³.

1.1 ACUTE REGULATION OF BLOOD PRESSURE RESPONSES BY PURINERGIC SIGNALING: NEUROMODULATION AND HEMODYNAMIC MECHANISMS

Acute minute-to-minute BP responses are tightly regulated at the level of the autonomic nervous system and within the peripheral vasculature. The carotid sinus and carotid body sense changes in BP directly through stretch receptors in the vascular wall or indirectly through blood metabolites^{6, 7}. However, while the carotid sinus has a cardioinhibitory effects on BP, the carotid body has cardioexcitatory effects, which relies on purinergic signaling to transduce cardiovascular information into to the central nervous system. Within the central nervous system, the nucleus tractus solitarius, which receives information from the carotid body, also utilizes purinergic signals to coordinate fast excitatory neurotransmitters and alter cardiac output and total peripheral resistance⁸. Thus, purinergic signaling facilitates rapid and acute enhancements in BP in the central nervous system. Lastly, cells of the vascular wall utilize extracellular ATP to modulate acute pressor responses and coordination of smooth muscle cell constriction that is required for altering vascular resistance. The role of extracellular nucleotides and purinergic receptors in the regulation of acute pressor responses will be reviewed.

Carotid body cells

Carotid bodies are mammalian peripheral chemoreceptors that rapidly sense alterations in arterial oxygen levels (hypoxia), carbon dioxide levels (hypercapnia), and pH necessary for maintaining cardiovascular homeostasis⁹⁻¹¹. Anatomically, carotid bodies are positioned at the internal and external carotid artery bifurcation where they transduce circulatory information directly and reflexively to autonomic respiratory and cardiovascular centers in the dorsomedial medulla oblongata^{12, 13}. When blood oxygen levels are low, or conversely, when carbon dioxide levels are elevated, carotid body cells activate afferent sensory nerve fibers, which subsequently cause increased respiration, heart rate, and blood pressure to re-establish homeostasis¹⁰. The control of this physiological reflex is maintained by heterocellular communication between glomus type I cells (chemosensory function), glomus type II cells (neuromodulatory function), and sensory afferent petrosal ganglionic neurons (transduction) which comprise the carotid body¹⁴⁻¹⁷. Due to their BP enhancing properties, dysregulation of carotid body activity has been shown to associate with several cardiovascular pathologies¹⁸⁻²⁰, especially hypertension^{21, 22}. It is well established that in hypertensive disease states, rodent model systems and humans present with enlarged carotid bodies^{23,24}. Enlargement correlated with increased mean arterial pressure and hyperventilation, indicative of enhanced carotid sinus nerve activity^{21, 25, 26}. Therapeutically, total resection of carotid bodies in rodent hypertension models (e.g. spontaneous hypertensive rats) or unilateral resection in treatment resistant hypertensive patients, prominently reduces MAP^{22,27}. Thus, signals that regulate carotid body function are intimately linked, not only with respiratory function, but also with BP regulation.

A number of neurotransmitters are involved in the activation of carotid sinus nerves by carotid bodies, which includes extracellular ATP. ATP acts as an excitatory neurotransmitter, neuromodulator, or humoral factor that is a ligand for P2 purinoceptors^{28, 29}. Early on, a role for hypoxia-induced ATP release was observed in the carotid body³⁰⁻³³. In support of this mechanism, application of extracellular ATP in vitro, induced a dose-dependent increase in chemosensory discharge in petrosal ganglionic neurons³⁴, which were mediated by P2X receptors but not P2Y receptors^{31, 35}. Similarly, in vitro whole cell patch recordings revealed a dose dependent depolarization and increase in discharge frequency of cultured petrosal ganglionic neurons³⁶. Later it was discovered that the ionotropic ATP-gated P2X2 and P2X3 receptors subtypes localize to petrosal neurons^{37, 38}, which when genetically deleted from animals, reduces chemosensory afferent responses³⁹. More recently, P2X2/P2X3 receptor antagonism has emerged as a novel therapeutic target for hypertension. P2X3 receptor mRNA was found to be upregulated in petrosal sensory neurons in spontaneously hypertensive rats and hypertensive human samples²¹. Antagonism of P2X3 receptors in this study normalized tonic drive and hyperreflexia in a hypertensive model that also correlated with reduced mean arterial pressure and reduced basal sympathetic activity in conscious rats⁴⁰. The implication of these studies highlights extracellular ATP and their cognate receptors as potent modulators of carotid body function and BP control. The mechanisms responsible for ATP release from carotid body cells are unclear, but implications for Pannexin 1 channels and connexin hemichannels, which promote cellular ATP efflux, have been purported^{41, 42}.

Nucleus tractus solitarius (NTS) communication

Within the dorsal medulla, the nucleus tractus solitarius (NTS) is a major integration site for peripheral sensory information involved in reflexive autonomic cardiovascular control⁴³⁻⁴⁵. This regulatory region receives sensory afferent information from the facial, glossopharyngeal, and vagus nerves and outputs information to multiple brain regions including presympathetic neurons of paraventricular nucleus that regulate cardiac and vasomotor activity^{43,46}. Importantly, the NTS also supports signals generated by the carotid and aortic baroreceptors, which directly sense BP in real time and generate cardiovascular depressor effects when BP becomes elevated. A large body of evidence supports the idea that purinergic signaling facilitates fast neurotransmission within the NTS and is necessary for effective reflex control⁴⁷⁻⁴⁹. In subsequent analyses, microinjection of ATP and ATP analogues (α,β -MeATP and 2-MeSATP) into the subpostremal NTS of anesthetized rats profoundly and rapidly (~1-2 min) reduced mean arterial pressure. Pre-treatment of the same region with a P2 purinoreceptor antagonist (suramin), completely blocked depressor effects of ATP and ATP analogues⁵⁰. Moreover, purinergic signaling in the NTS can also elicit differential responses depending on the site of innervation. Microinjection of ATP analogues were shown to not only reduce MAP and heart rate, but also caused a significant dose-dependent reduction in renal sympathetic nerve activity and lumbar sympathetic nerve activity⁵¹, which corresponds with dilation of renal and superior mesenteric vascular beds⁵².

In addition to ATP, adenosine also has potent neuromodulatory effects on NTS reflex control⁵³⁻⁵⁵. Ectonucleotidases are expressed within the NTS and efficiently hydrolyze ATP into adenosine^{56,57}. Adenosine receptor subtypes localize within the NTS and exhibit differential cardiovascular effects depending on the receptor isoform^{53, 58, 59}.

Early work demonstrated that microinjection of adenosine into the caudal NTS elicits a dose-dependent reduction in heart rate and MAP⁵⁴. Further studies showed cardio-depressive effects mediated by agonism of adenosine type 2 receptors (A2R), but not adenosine type 1 receptors (A1R)⁵³. Interestingly, A1R receptors have cardioexcitatory effects, which is supported by increases in MAP when animals are treated with A1R agonists⁵³. Mechanistically, A1R-dependent cardioexcitatory effects were observed to be partly mediated due to stimulated secretion of the pressor peptide vasopressin⁶⁰.

The location of adenosine receptor subtypes in the NTS also influences autonomic reflex responses. In one study activation of A2R in the caudal NTS elicited a dose-dependent cardiovascular inhibitory response that reduced MAP and induced bradycardia, and adenosine microinjection into the rostral NTS enhanced MAP and induced tachycardia, implicating signaling through A1R⁵⁵. Moreover, adenosine stimulation can elicit regional sympathetic responses in the cardiovascular system. A2R agonism in the NTS has been shown to reduce renal sympathetic nerve activity and enhance preganglionic adrenal sympathetic nerve activity⁵¹. In comparison A1R mediated pressor responses increased renal, adrenal, and lumbar sympathetic nerve activity^{58, 61}. It is evident that like ATP, adenosine also has the ability to support differential reflex control within the NTS important for modulating acute changes in BP.

Total peripheral resistance

The peripheral vasculature is another major site of purinergic control and plays a large role in modulating vascular resistance important for acute BP regulation. The controlled release of cellular ATP acts as an extracellular signaling molecule that potently

influences vascular tone. ATP is not only released from sympathetic nerve terminals, but also released from cells in the vascular wall³⁶. In resistance arteries, ATP exhibits dual activities, acting as a vasoconstrictor (smooth muscle) and a vasodilator (endothelial)³⁷. The adjustment of vessel radius by vasoconstriction and vasodilation exponentially influences vascular resistance and therefore has a profound impact on systemic BP. Although a wide array of vascular responses are influenced by purinergic signals (e.g. vascular tone, smooth muscle cell proliferation, vascular permeability, etc.), alterations in vessel radius directly and acutely influence BP⁶². In this regard, few studies have assessed purinergic-mediated vascular changes, as well as subsequent measurements of mean arterial pressure (MAP). Described here, are studies which directly highlight the acute control of vascular tone by purinergic effectors and their influence on systemic BP.

It was established early on that ATP acts as a co-transmitter with NE, which can be released from sympathetic nerves^{63, 64}. Pharmacological studies demonstrated a role for these purinergic signals in controlling arterial vasoconstriction responses and BP. In a rabbit model, pressor responses to the α -adrenergic agonist norepinephrine (NE) could be attenuated using α -adrenergic antagonist. However, pressor responses to nerve stimulation revealed an α -adrenergic independent response that was partly susceptible to purinergic desensitization by prolonged α,β -methylene ATP treatment⁶⁵. Subsequent validation experiments confirmed pressor responses in that nerve stimulation, but not NE treatment were influenced by P2 receptor antagonists⁶⁶. From the same study, reductions in pressor responses using α,β -methylene ATP coincided with reduced vas deferens contractile responses when purinergic blockade was also included with α -adrenoreceptor inhibitors. Thus, these studies established the existence of a second pressor molecule that is

independent of NE and likely co-released from sympathetic nerves to functionally regulate vascular resistance and acute BP.

In further support of purinergic vascular regulators, BP fluctuations could be induced separately by either acute injection of NE or ATP⁶⁷. These pressor molecules produced two distinct time-dependent BP frequency distributions⁶⁷. Acute administration of α,β -methylene ATP, which acts as a P2 receptor agonist, also caused a rapid rise in MAP, which was temporally distinct than prolonged pressor responses observed with NE treatment. The rapid purinergic responses were resistant to treatment with the adrenergic blocker prazosin, but were influenced by the P2 receptor blocker suramin⁶⁸. In another investigation, electrical stimulation of peripheral vascular nerves and corresponding pressor responses, could be diminished by suramin administration *in vivo*⁶⁸. These studies highlight a novel signaling axis whereby purinergic signals influence vascular responses by binding membrane associated P2 receptors. In line with this evidence, the degree of vascular responsiveness to P2 agonists differed depending on the vascular bed being assessed (pulmonary, hindquarter, and mesenteric). Moreover, pressor responses corresponded with the degree of vasoconstriction demonstrating a direct corollary between vascular resistance and BP⁶⁹. Overall, the degree of purinergic responses depends on the site receptor agonism and likely the density of receptors expressed in cells within the vascular wall.

Not only can purinergic signals invoke positive pressor responses, they can also cause rapid vasodilatory effects and negative pressor responses when intravenously administered. Injection of ATP and UTP into mice was found to rapidly reduce BP in a dose-dependent manner. Subsequently, vasodilatory responses to ATP and UTP could be

blunted by inhibiting cAMP-mediated signaling pathways in endothelial cells⁷⁰. Using a genetic deletion model, one study demonstrated that global deletion of the P2X4 isotypes suppressed flow-mediated vasodilation, which is in line with a stimulatory role for ATP in endothelial cell dependent vasodilation⁷¹. These studies also determined that P2X4 knockout altered endothelial calcium influx and nitric oxide production and caused a high BP phenotype, due to impairments in purinergic vasodilation pathways.

The transmembrane efflux of purinergic signaling molecules and the accumulation of extracellular nucleotides is a rate limiting step in initiating purinergic cascades. In the vasculature, endothelial cells and smooth muscle cells that compose the vascular wall release ATP⁷². The Pannexin 1 (Panx1) plasma membrane channel, which is highly expressed in endothelial cells and smooth muscle cells of resistance arteries has been ascribed as the predominant pathway by which ATP is released from vascular cells⁷³⁻⁷⁶. The importance of Panx1 channels was recently assessed in resistance arteries, which exhibit blunted vasoconstriction responses to P2 receptor antagonists pharmacological inhibitors of Panx1⁷⁷. Moreover, siRNA mediated knockdown of Panx1 from ex vivo arterial preparations recapitulated blunted constriction responses. A later study validated the specific effects of Panx1 function in smooth muscle cells by using an inducible cell-type specific Panx1 knockout model⁷⁸. In this study, attenuation of α -adrenergic vasoconstriction responses corresponded with reduced ATP release, and was further resistant to P2 receptor antagonists. Deletion of Panx1 from vascular smooth muscle cells also resulted in significant reductions in MAP⁷⁴. Thus, the regulation of cellular ATP release and the downstream activation of purinergic receptors plays a key role in supporting normal vascular function.

Overall, a large body of evidence demonstrates that purinergic signals are critical modulators of neural and vascular responses necessary for acutely altering systemic BP. The cellular processes regulating extracellular purine accumulation, the distribution of purinergic receptor isoforms, and the metabolism of purinergic molecules participate in fine tuning BP levels with cardiovascular demand. In the future it will be important to understand how cells intrinsically regulate cellular ATP release and assess the degree to which aberrant purinergic signaling contributes to progression of cardiovascular disease when BP set points are altered.

1.2 LONG-TERM PURINERGIC CONTROL OF BLOOD PRESSURE: A ROLE FOR ATP IN RENAL FEEDBACK MECHANISMS

BP homeostasis is strongly influenced by the relationship between renal sodium excretion and arterial pressure⁷⁹. According to the renal-volume feedback concept, acute changes in arterial pressure due to altered cardiac output or total peripheral resistance cannot be sustained unless renal sodium excretion is impaired⁸⁰. The mechanism responsible for adapting sodium excretion with BP is called pressure-natriuresis. On its own, this simple mechanism balances sodium excretion with increased pressure. Thus, acute increases in BP enhance sodium excretion, which ultimately restores BP levels through diuresis and reduced blood volume⁸¹. If sodium reabsorption is pathologically increased, the natural BP set-point becomes altered in order for pressure-natriuresis to rebalance sodium levels at the expense of increased BP.

Within the kidney, multiple autoregulatory mechanisms work in tandem to modulate (amplify or dampen) pressure-natriuresis through their combined actions on pressor hormones of the renin-angiotensin-aldosterone system (RAAS) and tubular sodium reabsorption⁸². In particular, autoregulation of afferent arterioles, tubuloglomerular feedback by macula densa cells, and tubular sodium handling in the cortical collecting duct directly participate in feedback regulation, thus ensuring pressure-natriuresis does not shift outside normal thresholds. Interestingly, all of these feedback mechanisms are strongly influenced by purinergic-mediated signaling pathways, which utilize both ATP and adenosine to coordinate sodium-responsive and pressure-dependent feedback control. Thus, purinergic signaling plays an important regulatory role in fine tuning pressure-natriuresis and merits discussion as a central regulator of long-term BP homeostasis.

Renal myogenic autoregulation

The renal afferent arteriole acts as an independent BP sensor that reflexively constricts when renal perfusion pressure is increased. This allows renal arteries to maintain a constant blood flow and glomerular filtration rate (GFR) that is independent of acute fluctuations in systemic BP⁸². This mechanism also ensures that filtration rates are optimized since secretion of the pressor hormone renin are inversely related to renal perfusion pressure. Thus, the afferent arteriole self-regulates renal blood flow and systemic BP. Mechanistically, increased renal vascular pressure has been shown to activate purinergic signaling pathways necessary for reflexive vasoconstriction. Extracellular ATP produces afferent arteriolar vasoconstriction in isolated perfused systems, as well as in cortical slices stimulated with exogenous ATP^{83,84}. The purinergic receptor responsible for

ATP-dependent responses is strongly linked to activation of P2X1 receptors, which in the rat kidney are extensively expressed along the preglomerular vasculature, but not in renal tubules, glomeruli, or efferent arterioles^{85, 86}. Moreover, pharmacological inhibition of P2X1 using suramin or a specific inhibitor (NF279) completely abolished pressure-mediated vasoconstriction when perfusion pressure was altered from 100 to 160mmHg^{87, 88}. These pharmacological effects were validated using a P2X1 genetic knockout model, which exhibited similar impairments in pressure-mediated vasoconstriction, but not other vasoconstriction pathways mediated by angiotensin II, potassium chloride, and adenosine^{88, 89}.

In addition to ATP, adenosine also influences afferent arteriolar vasoconstriction. Adenosine receptors localizes to smooth muscle cells of the afferent arteriole⁹⁰ and coordinate vasoconstriction responses in the renal microvasculature^{91, 92}. Constriction responses are more dramatic at the distal end of afferent arterioles when stimulated with adenosine and are mechanistically coupled with activation of adenosine type 1 receptors (A1R)^{93, 94}. It is interesting to note that adenosine signaling seems to be dispensable for pressure-induced responses⁸⁸, but as a diffusible messenger can still cause concentration-dependent and spatially distinct vascular responses between cortical and juxtamedullary nephrons. In the cortex, adenosine elicits dose dependent constrictions, while in juxtamedullary nephrons constriction occurs at low concentrations and dilation occurs at high concentrations^{95, 96}.

The global effect of altered renal vascular resistance directly impacts renal blood flow (RBF) and GFR, but is also connected to two regulatory mechanisms: TGF in the macula densa and the secretion of renin from JG cells. In this feedback loop, lowered GFR–

which is indicative of reduced BP— results in reduced sodium chloride delivery to the macula densa, reduced inhibitory signaling to JG cells and afferent arteriolar smooth muscle, elevation of renin secretion, and generation of angiotensin II. These responses increase BP levels to restore renal perfusion, which in turn causes activation of TGF and inhibition of renin secretion. Normally, this feedback loop acts to stabilize renal filtration and sodium excretion with BP. However, if dysregulated as in A1R knockout animals, impairment leads to enhanced renin secretion and a high blood pressure phenotype^{88,97}. Thus, purinergic signals in the afferent arteriole are critical in coupling local renal hemodynamics and RAAS hormone secretion with pressure-natriuretic feedback control.

Tubuloglomerular feedback (TGF)

TGF is a key mediator of intrarenal feedback control that links the renal tubules with the vasculature using purinergic signaling⁹⁸. Macula densa cells in thick ascending limb of Henle initiate TGF responses by sensing tubular sodium chloride concentrations and releasing nucleotides into the renal interstitium. These signals activate mesangial cells⁹⁹, cause afferent arteriolar vasoconstriction, and inhibit renin secretion by JG cells⁹⁹⁻¹⁰². The overall effect of this process is a negative feedback loop that matches the delivery of ultrafiltrate with the regulation of systemic BP.

ATP is a key mediator of TGF and was identified in early investigations to dose-dependently constrict afferent arterioles by stimulating renal P2-receptors^{87, 88}. These observations were later validated by genetic knockout of the P2X1 receptors⁹⁷. It was also demonstrated using microdialysis that increases in renal perfusion-pressure, which initiates TGF inhibitory responses, concomitantly increase in arterial pressure⁹⁵. At the time, the

release of extracellular ATP was thought to occur due to vascular shear stress^{103, 104}. However, it is now well accepted that a primary source of extracellular ATP important for TGF originates from macula densa cells and is mechanistically regulated by maxi anion channels^{100, 105}. In this study, ATP biosensors were used to demonstrate increased ATP release from the basolateral membrane of the macula densa in response to increased sodium chloride concentration. Moreover, a second study corroborated these results, this time by detecting ATP induced calcium events by mesangial cells that anatomically link the macula densa with the renal vasculature¹⁰⁶. It is interesting to note, that ATP release by maxi anion channels is probably not the only mode of ATP efflux. Other cells in the juxtaglomerular apparatus can release ATP such as mesangial cells, which use purinergic signals to support calcium wave propagation important for autoregulation, but also for controlling renin secretion by JG cells^{99, 107}. Thus, ATP mediated signaling is required for TGF-mediated inhibition. The molecular mechanisms that support channel-mediated ATP efflux from macula densa cells are currently under investigation, as these pathways have the greatest upstream influence on regulating purine release.

Adenosine was one of the first purine nucleotides suspected to control TGF through its effects on afferent arteriolar vasoconstriction, as well as observations that adenosine receptor antagonists could prevent TGF responsiveness¹⁰⁸. Later studies confirmed these effects using more specific and potent adenosine receptor antagonists^{91, 109, 110}. Subsequently, studies using genetic knockout mice that globally targeted the type 1a adenosine receptor (A1AR) definitively demonstrated the requirement for A1AR in TGF, which was completely eliminated in knockout mice, but not controls^{111, 112}. However, evidence also suggested that the transmission of purine signals within the renal interstitium

is not mediated by adenosine, but is mediated by ATP^{99, 113}. Thus, a consensus has emerged in which ATP release initiates purinergic signaling, but adenosine facilitates cell responses through A1AR activation. Furthermore, adenosine has potent inhibitory effects on renin secretion from JG cells in the afferent arteriole. A1AR knockout mice exhibit significant reductions in pressure-induced renin secretion, while direct treatment with adenosine influences calcium-mediated signaling in JG cells and has a suppressive effect on renin expression and secretion¹¹⁴⁻¹¹⁶. These inhibitory effects also enhance TGF responses on a global scale as reduced pressor hormone production results in lowered BP and reduced renal perfusion pressure.

Therefore, an inextricable linkage exists in the renal vasculature and tubules that couples the regulation of local renal dynamics with the regulation of systemic BP. During pressure-natriuresis, these regulatory mechanisms work together to ensure that renal perfusion pressure, and thus systemic BP, do not fluctuate far outside physiologic levels, thus preserving both filtration and homeostasis. The importance of purinergic signaling and its integration into many renal cell types, likely stems from the diverse number of cellular responses necessary to maintain homeostasis that can be generated from a small number of diffusible messengers

Tubular sodium/fluid reabsorption

The cortical collecting duct (CCD) plays a vital role in regulating natriuretic processes. It participates in both sodium reabsorption and fluid transport to move solutes and water from the tubular lumen back into the blood. Moreover, the CCD is highly responsive to RAAS hormones, which work in concert with renal autoregulatory feedback

loops to amplify anti-natriuresis responses. A large body of evidence supports a role for purinergic signaling in the CCD, which expresses a large number of purinergic receptors and directly influences epithelial sodium channel (ENaC) function and water reabsorption by aquaporin channels (AQP) in the nephron. Overall, data suggests that ATP promotes natriuresis in the CCD by inhibiting both sodium and water reabsorption, likely acting as a counterregulatory mechanism for RAAS stimulation.

In early water retention studies, infusion of ATP into isolated perfused rabbit CCD prevented vasopressin-induced water permeability¹¹⁷. The effect of ATP infusion could be recapitulated using an ATP analogue, but could not be inhibited using a P1-adenosine receptor antagonist suggestive of P2-purinoreceptor function. Subsequent validation studies in rats also demonstrated that ATP and UTP could reversibly inhibit vasopressin-induced water permeability and that ATP caused internalization of membrane associated AQP2 in vitro, consistent with reduced water reabsorption^{118, 119}. The P2Y2 receptor was quickly proposed as the key mediator of ATP inhibitory effects, since P2Y2 mRNA and protein localize to the apical and basolateral membrane of the CCD and could regulate calcium-mediated cell responses required for vasopressin-induced permeability^{117, 120}. In support of this function, mice genetically deleted of P2Y2 were found to have enhanced membrane associated AQP2 channels, increased fluid reabsorption, and a low renin hypertension that is associated with expanded blood volume^{121, 122}.

In the CCD, sodium transport is also required for movement of fluid from the tubules back into the circulation. ENaC channels promote sodium transport and their activity at the apical membrane of CCD cells maintains anti-natriuretic responses. Using pharmacological ENaC inhibitors, early in vitro reports using isolated CCD cells

demonstrated that ATP and UTP application inhibited sodium transport and that P2Y2 receptors likely played a role in this inhibition (197). Further support for a purinergic inhibitory mechanism was provided by localization studies that observed the presence of P2 receptors in mouse CCD cell lines including P2Y2 variant¹²³. In these cells extracellular ATP blunted sodium reabsorption and the mechanisms purported was through the regulation of serum/glucocorticoid-inducible kinase-1, which is responsible for the insertion of ENaC channels into the apical membrane¹²⁴. In isolated perfused collecting ducts observations of ATP- and UTP- inhibited sodium transport corroborated the idea that P2Y2 receptors functionally regulate sodium transport, and the promotion of anti-natriuresis could be recapitulated in P2Y2 receptor knockout mice. More recently, activation of P2Y2 receptors using a novel agonist (INS45973), dose-dependently decreased BP and promoted sodium natriuresis in wildtype mice, but not in P2Y2 knockout mice¹²⁵. This supports the idea that activation of P2Y receptors promotes natriuresis. It should be noted, that despite the large role for P2Y2 receptors in the CCD, other P2Y receptors (i.e. P2Y12) have been shown to influence sodium transport. In one study P2Y12 receptors found to immunolocalized with AQP2 CCD positive cells could be irreversibly inhibited using clopidogrel bisulfate. The effect of inhibition caused upregulated AQP2 protein abundance and reduced aquauresis responses, which is similar to responses made when P2Y2 is inhibited¹²⁶.

These evidence supports the idea that purinergic signaling, mediated by extracellular ATP and P2Y2 receptors, plays a large role in influencing sodium and water reabsorption in the CCD. These signals provide feedback inhibition of anti-natriuretic function, which potently increases systemic BP to maintain renal perfusion. In this context

purinergic signaling directly enhances pressure-natriuresis responses, and likely co-opts molecular pathways to ensure that systemic BP elevations return to normal physiological levels. However, the source of extracellular nucleotides, and the mechanisms by which extracellular ATP accumulates within the interstitium and tubules is still under investigation.

1.3 MECHANISMS OF ATP RELEASE

An accumulation of evidence supports the idea that extracellular nucleotides regulate diverse physiologic functions that are spatially mediated by the expression profile of purinergic receptors (P1 and P2) and are temporally regulated by ectonucleotidase metabolism of active signaling products¹²⁷. Although much is known about the functional aspects of purinergic signaling, less is known about the mechanisms and conditions that support cellular efflux of nucleotides, especially ATP, into the extracellular space. Many membrane-associated proteins and pathways have been implicated in the regulated release of ATP, and have been previously reviewed^{72, 128-130}. In summary, channel-mediated ATP release mechanisms have emerged as dominant pathways in which ATP is released under physiological and pathological conditions. The role of these mechanisms in neural, vascular, and renal feedback mechanisms important for BP homeostasis is less clear; yet, a case could be made for channel-mediated processes that support purinergic paracrine feedback responses. Currently, there are five proposed channel types that have supporting evidence to regulate ATP efflux from cells. These include volume-regulated anion channels (VRAC), calcium homeostasis modulator 1 channels (CALHM1), maxi-anion channels, connexin hemichannels (Cx), and pannexin 1 channels (Panx1).

Volume-Regulated Anion Channels (VRAC)

VRAC channels are ubiquitously expressed anion selective channels that cause efflux of ions and cellular metabolites due to hypotonic cell-swelling^{131, 132}. Recently, it was determined that channel oligomerization relies on heteromeric association of LRRC protein members, particularly LRRC8A, which is a critical component of VRAC activity¹³³. The ability of VRAC channels to permeate ATP was first assessed in reconstituted cell systems in which injection of *Xenopus* oocytes with LRRC8 exhibited accumulation of extracellular ATP when bathed in hypotonic solution¹³⁴. These observations coincided with increase in channel current. It should be noted that observed changes in ATP release were relatively small compared to un-injected oocytes and other ATP release channels¹³⁵. Although, the function of VRAC channels are still under investigation and the involvement of VRAC-mediated ATP release in physiological pathways remains to be observed, VRAC channels could represent a novel pathway for sensing and responding to changes in osmolality, as occurs in the cardiovascular system.

Calcium Homeostasis Modulator 1 (CALHM1)

CALHM1 channels are voltage-gated, non-selective ion channels that have a primary role in regulating cellular calcium permeability and ATP efflux¹³⁶. At resting membrane potentials CALHM1 channels remain closed, but can be activated by depolarizing stimuli and become more sensitive to opening as extracellular calcium ion concentrations are reduced¹³⁶. Structurally, the topology of CALHM1 resembles those of pannexins and connexins, which are oligomerized channels composed of tetra-spanning monomers¹³⁷. Major physiological significance has been ascribed to CALHM1 channels in

the regulation of neuronal excitability^{136, 138}, taste reception¹³⁹, and urinary bladder function^{140, 141}. Interestingly, the mechanism by which CALHM1 regulates taste reception and urinary bladder function is linked to regulated ATP release and the initiation of purinergic signaling^{139, 142}.

Evidence of CALHM1 ATP release was first described in isolated type II taste cells, in which CALHM1 expression and channel currents were observed^{139, 143}. Type II cells respond to stimuli by activating afferent sensory nerves through ATP¹⁴⁴. The strongest evidence for CALHM1-mediated ATP release stems from experiments performed in type II cell-specific CALHM1 knockout mice, which exhibit significantly reduced channel activity and ATP release as measured by the ATP biosensor technique¹⁴⁵. Knockout mice further present with an insensitivity to taste reception of sweet, salty, bitter, and umami stimuli^{139, 146}. However, a discrepancy exists in which the specific channel that causes ATP efflux is still under debate, as other proposed ATP-release channels have been localized to type II cells and partially contribute to taste sensation^{147, 148}.

In the urinary bladder ATP signaling through P2X3 receptors facilitates normal voiding responses^{140, 149}. CALHM1 expression was observed in urothelial bladder cells, which upon manipulation of hypotonicity or extracellular calcium ion concentrations evoked ATP release and CALHM1 channel activity that was sensitive to a CALHM1 blocking antibody¹⁴¹. These studies suggest a potential role for CALHM1 as a bona fide ATP release mechanism; however, the direct assessment of ATP efflux through CALHM1 channels remains to be observed. In other organ systems, such as the cardiovascular system, it is unknown if CALHM1 is expressed in, or functionally regulates, vascular cells. Moreover, the role of CALHM1 in the brain is an area of active research interest, which

has been implicated in Alzheimer diseases phenotypes¹⁵⁰. Again, the influence of CALHM1 on neural pathways that modulate homeostatic mechanism is unknown.

Maxi anion channels

Maxi anion channels are another class of membrane associated channel protein that are characteristically described by a voltage-dependence, a large conductance, and anion selectivity¹⁵¹. Under basal conditions maxi anion channels are silent, but can be activated by diverse stimuli including osmotic swelling, sodium chloride concentration, and low oxygen^{100, 152-156}. A crucial component of maxi anion channels is the SLCO2A1 protein, which constitutes the pore-forming channel subunit. Knockdown or mutation of *Slco2a1* in vitro results in reduced single channel conductance, which can be rescued by overexpression¹⁵⁷. Evidence from this report demonstrated from inside-out patch clamp recordings that maxi anion channels support cellular ATP permeation as inward currents were detected in the sole presence of an ATP containing bath solution. Functionally, these channels play a crucial role in renal TGF¹⁰⁰. Maxi anion channels localize to the basolateral side of macula densa cells and become activated by increased sodium chloride concentration¹⁰⁰. There is a linear relationship between sodium chloride concentration and ATP release from the basolateral membrane. In support of these observations it was demonstrated that macula densa cells swell and respond to changes in cell volume in vivo¹⁰⁷. It is also well established that purinergic signals mediated by macula densa cells coordinate afferent arteriolar autoregulation and JG cell renin secretion through diffusible ATP and adenosine signals in the juxtaglomerular apparatus¹⁵⁸. Thus, a direct role exists for maxi anion channels in regulating BP autoregulatory mechanisms through the sensing

of luminal sodium chloride and the release of ATP required for inhibitory purinergic signaling.

Connexin (Cx) hemichannels

The traditional view of gap junction forming proteins begins with the oligomerization of monomeric connexin proteins into hexameric connexon units. These units oligomerize and traffic to the plasma membrane where they dock with connexons of adjacent plasma membranes to support intercellular communication and electrical coupling. However, there is a non-canonical view of connexin proteins and their oligomerized connexon forms exists, in which some connexons do not enter into intercellular docked gap junctions, but rather exist as functional non-junctional channels called Cx hemichannels¹⁵⁹. These potential membrane channels have unique channel properties, which include activation at positive membrane potentials and supraphysiologic levels of extracellular calcium ion concentrations¹⁶⁰. Moreover, differential properties exist in both single channel conductance and charge selectivity, which is likely connexin-isoform specific¹⁶¹. For the most part, Cx hemichannels are basally closed under physiologic conditions, and become activated under altered physiologic conditions as occurs during pathology. There are 20 connexin isoforms, which exhibit a wide tissue distribution and complex expression profile—multiple connexins can be expressed in a single cell type^{159, 162}. Yet, the contribution of Cx hemichannels to purinergic signaling was first described in glioma cells that forcibly expressed the connexin 43 and 32 variant and subsequently released 5-15 fold greater amounts of ATP when stimulated by UTP¹⁶³. In this study, investigators assessed calcium wave propagation mediated by connexin

proteins, and observed non-junctional calcium wave propagation that was sensitive to both gap junction and P2-receptor inhibitors. The study concluded that connexin expression correlated with enhanced levels of ATP release and may support stimulated ATP efflux. A number of later studies further demonstrated a potential role for Cx hemichannels in cellular ATP efflux¹⁶⁴⁻¹⁶⁶. However, one study observed direct electrophysiological evidence that connexin 43 (Cx43) hemichannels can permeate ATP. In this study, inside-out patch recordings of C6 glioma cells expressing Cx43, detected hemichannel activity, which could be inhibited by known gap-junction blockers¹⁶⁷. Moreover, in this same configuration bioluminescence detection of ATP coincided with hemichannel activity, which were absent at negative membrane voltages when hemichannel activity is inhibited¹⁶⁷. Thus, Cx hemichannels can permeate ATP under certain conditions.

A possible physiologic role of Cx hemichannel-mediated ATP release that is in line with purinergic-feedback regulation of BP homeostasis was observed for connexin 30 (Cx30) in renal epithelial cells of the CCD. As mentioned earlier, ATP release from CCD cells cause activation of P2-receptors on the apical membrane, removal of membrane AQP2 channels, inhibition of ENaC sodium reabsorption, and increased natriuresis^{168, 169}. The source of ATP release in the CCD was unclear, but evidence suggests that Cx30 plays a role in this process. Using Cx30 global knockout mice, protein immunolocalization was observed in the distal nephron of wild type but not knockout mice. ATP release in response to changes in tubular flow or hypotonic bath solution was also found to be Cx30-dependent in microperfused CCDs¹⁷⁰. In this study ATP was detected using PC12 cell-mediated ATP biosensors. Physiologically, Cx30 knockout mice present with salt-sensitive elevations in MAP, and reductions in urinary sodium excretion¹⁷⁰ consistent with reduced natriuresis

and enhanced sodium reabsorption. In a later study, loss of Cx30-mediated ATP release due to genetic knockout caused an enhancement in ENaC channel activity on the apical side of CCD cells when sodium concentrations were increased¹⁷¹. Overall, these studies reveal a novel role of Cx30 that likely supports purinergic signaling important for natriuretic responses and BP control. It remains to be determined whether Cx30 hemichannels are the conduit by which ATP is released from cells, as has been observed for Cx43.

Pannexin 1 (Panx1) channels

The pannexin family of proteins, are channel forming glycoproteins that oligomerize into plasma membrane ion channels¹⁷². They were first identified by their homology to invertebrate innexins¹⁷³, but do form gap junctions¹⁷⁴ and do not share sequence homology with vertebrate connexin proteins despite structural similarities¹⁷⁵. Of the three pannexin isoforms, the Panx1 isoform exhibits the most diverse tissue expression profile and has been identified in a number of tissues and cell types, which importantly for this discussion includes vascular smooth muscle, endothelial cells, epithelial cells, and many others^{76, 77, 175-178}. In comparison the Panx2 and Panx3 isoforms exhibit restricted expression profiles that are limited to the central nervous system (Panx2), or the skin, skeletal muscle, and cartilage (Panx3)^{175, 176, 179, 180}.

Panx1 channels also display unique channel gating properties. The C-terminus has been shown to directly inhibit channel opening, likely by occlusion of the permeation pathway^{181, 182}. Moreover, Panx1 channels exhibits a quantized activation process, whereby individual channel subunits can be sequentially modulated to allow passage of ions and

metabolites¹⁸³. Moreover, Panx1 channels have emerged as a primary pathway by which ATP is released from various cell types to initiate purinergic signaling cascades¹⁸⁴. From initial studies, many activation mechanisms for Panx1 have been proposed, such as activation by pressure/stretch mechanosensation, elevated extracellular potassium concentrations, intracellular calcium; yet, substantive evidence in support of these mechanisms remains to be seen^{135, 185-190}. However, there are currently two purported modes of channel activation that are well supported in the literature that lead to channel opening and metabolite efflux/uptake. These mechanisms include caspase-cleavage of the C-terminus and receptor-mediated channel gating (receptor-dependent)^{77, 190-195}. An intensive research effort is underway to elucidate novel regulatory mechanisms that control the gating of Panx1 channels by these mechanisms.

Functionally, Panx1 channels have been implicated in a number of physiological and pathological conditions, which include apoptotic cell clearance, neuropathic pain induction, glucose uptake, ischemia-reperfusion injury, tumor metastasis, and blood pressure regulation^{78, 191, 196-200}. More specifically, Panx1 channels in the cardiovascular system play a key role in regulating vascular endothelial cell function and smooth muscle cell constriction. In endothelial cells, Panx1-mediated ATP release is involved in inflammatory cell recruitment and vascular permeability²⁰¹. In smooth muscle cells, Panx1 supports purinergic signaling necessary for adrenergic-mediated vasoconstriction. Early studies demonstrated that Panx1-mediated ATP release was necessary for normal adrenergic vasoconstriction responses⁷⁷. Using multiple Panx1 inhibitors (small molecule and siRNA), as well as P2-receptor antagonists, constriction response to increasing doses of α -adrenergic agonists were significantly blunted⁷⁷. In a later investigation, a genetic

approach was used to assess Panx1 function in smooth muscle cells. Using a vascular smooth muscle cell-specific tamoxifen-inducible Panx1 knockout mouse, adrenergic-stimulation ATP release and vasoconstriction were again significantly blunted⁷⁸, and in this study Panx1 knockout mice also presented with a significant reduction in MAP as measured by telemetry⁷⁸. Mechanistically, the membrane associated scaffold protein caveolin-1 was found to specifically interact with Panx1, and was required for Panx1 localization to the plasma membrane⁷³. Interestingly, deletion of caveolin-1 using the same vascular smooth muscle cell specific Cre recombinase, abrogated the interaction between Panx1 and caveolin-1, and duplicated vascular and BP phenotypes previously observed in Panx1 knockout models. In this regard, vascular Panx1 directly contributes to the regulation of systemic BP through its effects on total peripheral resistance.

Moreover, a role for Panx1-mediated ATP release has been observed in the kidney. Panx1 channels were immunolocalized to the proximal tubule, cortical collecting duct, and afferent arteriole¹⁷⁸. In the proximal tubule, Panx1-mediated ATP release is linked to immune cell infiltration and renal damage associated with acute kidney injury¹⁹⁸. Deletion of proximal tubule Panx1 prevented renal damage associated with reperfusion injury. However, in the cortical collecting ducts and afferent arterioles, the role of Panx1 is currently unknown. Given that these two sites are highly regulated by purinergic signaling and have a pronounced role on fluid/electrolyte balance and renin secretion important for long-term BP homeostasis, it is likely that Panx1 channel function may be important in initiating purinergic signaling pathways that stabilize homeostatic BP levels.

In summary, systemic BP is regulated by an integrated network of neural, vascular, and renal mechanisms, which sense and respond to changes in the cardiovascular system

by adapting the physiological BP set-point. Within these regulatory systems, purinergic signaling supports heterocellular communication important for distinct spatial and temporal regulation of cardiovascular homeostasis. A systemic dichotomy appears within the body in which purinergic signals support pressor responses in the central nervous system and vasculature, but control depressor responses in the renal vasculature and kidney. The diversity of physiological responses that are influenced by purinergic signaling suggests a fundamental role for extracellular ATP and its release by membrane-associated channels as an early and potent mechanism for coordinating homeostasis. A high translation potential therefore exists in understanding the molecular mechanisms and distinct channel properties that influence channel-mediated ATP release in the central nervous system, the peripheral vasculature, and the kidney.

CHAPTER 2. MATERIALS AND METHODS

2.1. MATERIALS AND METHODS FOR CHAPTER 3

Animals. All mice were male, 10-15 weeks of age, on a C57Bl/6 genetic background, and were cared for under the provisions of the University of Virginia Animal Care and Use Committee and followed the National Institute of Health guidelines for the care and use of laboratory animals. Wild type C57Bl/6 male mice were purchased from Taconic. All experiments were performed on a minimum of 3 mice.

Cell Culture. Primary human coronary smooth muscle cells (hCoSMCs) were purchased from Lonza (#CC-2583). All cells were maintained under standard cell culture conditions (5% CO₂ at 37°C) in smooth muscle growth media (Lonza; #CC-3181) supplemented with growth factors (Lonza; #CC-3182) and 10% fetal bovine serum (Lonza; #CC-4102D). Prior to use, primary cells were transfected with plasmids using Lipofectamine 3000 (Invitrogen; #L300015) or siRNA (RNAiMAX Invitrogen; #13778075) where noted and incubated in low serum media conditions (0.2% fetal bovine serum) for 48 hours to dedifferentiate smooth muscle cells. For siRNA-mediated knockdown of Src kinase, hCoSMCs were plated in six-well plates and grown to 70-80% confluence. Non-targeting control siRNAs or siRNAs targeting the human SRC gene (Invitrogen Silencer Select; s13414) were transfected into cells using Lipofectamine RNAiMAX reagent (Invitrogen) according to manufacturer's instructions, and knockdown efficiency was assessed via western blotting following a 48-hour incubation. Vasoconstrictive agonists and pharmacological SFK inhibitors were added after de-differentiation in low serum media.

hCoSMCs were used for experimentation up to passage 10. LA-25 cells (normal rat kidney epithelial cells containing temperature sensitive v-Src)²⁰²⁻²⁰⁴ were cultured in Dulbeccos Minimal Essential Medium (Life Technologies) supplemented with 10% fetal bovine serum and antibiotics under standard conditions and were used to specifically manipulate Src tyrosine kinase activity at the permissive (35°C) or non-permissive (40°C) temperatures. LA-25 cells were co-transfected with lab generated Panx1 (pEBB-vector) and α 1D-adrenergic receptor (OriGene; Cat# sc119760) expression plasmids, using electroporation (Lonza Nucleofector Kit T; #VCA-1002) according to manufacturer's instructions. Wild type Src kinase expression plasmids were a gift from Joan Brugge and Peter Howley (Addgene plasmid #13663). All cells were used between passages 3 and 10. Human embryonic kidney cells 293T (HEK293T) and HeLa cells were grown in DMEM supplemented with 10% FBS, 1% penicillin/streptomycin, and 1% L-glutamine. Cells were transfected using Lipofectamine 2000 (Invitrogen; Cat# L11668-019) according to the manufacturer's instructions. Cells were maintained under standard conditions and used for experimentation under passage 20. Anti GFP-antibody (abcam #13970; 1:500 dilution) was used to visualize Panx1.

Human vascular biopsies. Adipose tissue biopsy samples (approximately 1.5 g) were obtained from the gluteal region under aseptic conditions un supervision by Dr. Eugene Barrett at the University of Virginia outpatient clinic. Biopsies were obtained for research purposes from human (non-obese) adult volunteers (40 > age < 60) that were normotensive (mean arterial pressure \leq 120/80 systolic/diastolic) or hypertensive (mean arterial pressure >140/90) and not being treated with adrenergic blocking medications. Biopsies were fixed in 4% paraformaldehyde, thin sectioned (5 μ m), and immunostained as previously

described⁷³. Antibodies directed against anti-human Pannexin 1 (characterized by Penuela et al.²⁰⁵ 1:300 dilution), phospho-Panx1 (Tyr198) (Millipore; ABN1681; 1:400) (pPanx1Y198), and Acta2 (Sigma #A2547, 1:500 dilution) were used to assess tissue protein localization and to denote the vascular media. All images were acquired using an Olympus Fluoview 1000 confocal microscope.

Extracellular ATP measurements. For the measurement of extracellular ATP, intact thoracodorsal arteries (TDAs) were singly placed in a well of a 96 well plate and incubated in Krebs-HEPES physiologic solution alone or containing the SFK inhibitors PP2 (10 μ M) and dasatinib (10nM) for 1 hour or 30 min respectively. The ectonucleotidase inhibitor ARL 67156 (Tocris; Cat#1283) was added 30 minutes prior to treatment with contractile agonists as previously described²⁰⁶. The media surrounding the vessel was collected before stimulation and immediately after stimulation, placed into pre-chilled 1.5 ml Eppendorf tubes on ice, and centrifuged at 10,000g for 5 min. To chelate intracellular calcium BAPTA-AM (10 μ M) (Sigma; Cat# A1076) was added to TDA incubation media (Krebs-HEPES/2mM Ca²⁺) for 30 min prior to stimulation with vasoconstrictor compounds including: phenylephrine (PE; 20 μ M), norepinephrine (NE; 10 μ M), serotonin (100nM; 5-HT), and endothelin-1 (10nM; ET-1) (Sigma). The amount of ATP in the media was quantified using ATP bioluminescence assay kit HSII (Roche; Cat#11699709001) and a FluoStar Omega luminometer. Extracellular ATP measurements for each sample were tested in triplicate and calculated using an ATP standard curve for all experiments. Data are presented as % change of ATP from each samples baseline (pre-stimulation) level. Data are expressed as mean \pm SEM.

Pressure myography. Pressure myography was performed on thoracodorsal arteries of C57Bl/6 as previously described²⁰⁷⁻²⁰⁹. Briefly, mice were sacrificed using CO₂ asphyxia. TDAs are micro dissected, cannulated on glass pipettes in a pressure arteriography chamber, and pressurized to 80mmHg. After a 30-minute equilibration period in Krebs-HEPES with 2mM Ca²⁺, vessels were pre-incubated with SFK inhibitors as described above for ATP measurements and treated with cumulative doses of phenylephrine (PE, 10⁻¹⁰-10⁻³ M), serotonin (5-HT, 10⁻¹¹-10⁻⁵ M), and endothelin-1 (ET-1, 10⁻¹⁴-10⁻⁷ M) applied to the bath. The luminal diameter was analyzed using digital calipers using the DMT Vessel Acquisition Software (Danish MyoTechnology). Endothelial and smooth muscle cell viability was assessed using KCl or a variety of vasodilators, which included endothelial – dependent and –independent vasodilatory agents, as previously described²⁰⁷⁻²⁰⁹.

Western blot. Samples were subjected to SDS gel electrophoresis using 4-12% Bis-Tris gels (Invitrogen) and transferred to nitrocellulose membrane for immunoblotting. Membranes were blocked for 1 hour at room temperature in a solution containing 3% BSA in Tris buffered saline, then incubated overnight at 4°C with primary antibodies against Pannexin1 (Cell Signaling Technology; D9M1C mAb#91137; 1:1000), Caveolin-1 (BD Biosciences; #610059; 1:1000), Src (Cell Signaling Technology; L4A1 mAb#2110; 1:1000), phospho-Src Family (Tyr416) (Cell Signaling Technology; D49G4 mAb#6943; 1:1000), phospho-paxillin (Tyr118) (Cell Signaling Technology; #2541; 1:1000), phospho-Panx1 (Tyr198) (Millipore; ABN1681; 1:1,000), phospho-Panx1 (Tyr308) (Millipore; ABN1680; 1:1,000), β -Tubulin (Invitrogen; Cat# MA5-16308-BTIN; 1:5000), α -actin (Sigma; mAb#A2547; 1:2000) and GAPDH (Sigma; G8795; 1:10,000) or an antibody against the C-terminus of Pannexin 1²¹⁰. Membranes were washed and incubated in

LiCOR IR Dye secondary antibodies (1:15,000) for 1 hour and viewed/quantified using the LiCOR Odyssey with Image Studio software. Representative western blot images have been cropped for presentation. Data are presented as mean \pm SEM.

Co-immunoprecipitation. hCoSMCs were grown to 70-80% confluence in SMC growth media and transfected with epitope-tagged Pannexin1-pcDNA3.1-FLAG expression plasmids (wild type or mutated to Y198F) using Lipofectamine 3000 (Invitrogen Cat# L3000-015) according to the manufacturer's instructions. Plasmid mutagenesis was performed using the Q5 Site-Directed Mutagenesis Kit (New England BioLabs; E0554S) with conventional PCR and Pannexin 1 specific primers designed using NEBaseChanger analytical tools (New England BioLabs). After transfection, hCoSMCs were grown in low serum media (0.2% FBS) for 48 hours. To stimulate cells, hCoSMCs were equilibrated for 30 minutes in Krebs-HEPES supplemented with 2mM Ca^{2+} and stimulated with 20 μ M phenylephrine for 2 minutes. Cells were lysed in ice cold co-immunoprecipitation buffer 20m M Tris HCl pH 8, 120mM NaCl 1%Nonidet P-40, 2mM EDTA, 1mM sodium orthovanadate, and 20mM NaF supplemented with protease and phosphatase inhibitors (Sigma), and dounce homogenized (10 strokes) on ice. Protein extracts were incubated overnight at 4°C in 20 μ l anti-FLAG -conjugated magnetic beads (Clontech) on a tube rotator. The beads were magnetically separated and washed three times in ice cold co-immunoprecipitation buffer. Next, the beads were pulled down, eluted using a low pH elution buffer, and allowed to incubate at room temperature for 10 minutes to remove bound proteins. The eluent and beads were separated, and the eluent was incubated in Laemmli buffer for analysis by SDS gel electrophoresis. Pannexin1 was detected using

antibody against the C-terminus of Pannexin1²¹⁰ and phospho-Panx1 (Tyr198) (Millipore; ABN1681; 1:1,000).

In-vitro kinase assay. Recombinant mouse Pannexin 1 protein was purified as previously described¹⁹². To remove endogenous phosphorylation, 3.2ug of recombinant mouse Pannexin 1 protein was incubated with 2000U of recombinant lambda phosphatase (Cell Signaling Technology; P0753S) in 10X phosphatase buffer supplemented with 1mM Mn²⁺ for 16 hours at 30°C shaking at 500rpm. The enzyme mix was heat inactivated at 65°C for 1 hour and supplemented with 1mM sodium orthovanadate to inhibit phosphatase activity. To phosphorylate Pannexin 1 protein, 1.25ug of de-phosphorylated Pannexin 1 stock protein was added to a 0.6mL Eppendorph tube containing kinase assay buffer (25mM MOPS, pH 7.2, 20mM MgCl₂, 5mM EGTA, 2mM EDTA, 0.25mM DTT) diluted 1:5 with 0.05mg/ml BSA. The reaction was supplemented with 0.25mM ATP, 0.5mM MnCl₂, and 0.3ug/mL recombinant human (active) Src-GST kinase (PRECISIO© Kinase; Sigma; S1076) in a 25µl reaction volume. Samples were incubated for 1 hour at 30°C shaking 500rpm. 5X SDS buffer was added to terminate the kinase reaction. Samples were boiled for 5min at 95°C and subjected to SDS gel electrophoresis as described for western blotting. Phosphorylation was confirmed using phospho-tyrosine (P-Tyr-100) antibody (Cell Signaling Technology; mAb#9411; 1:1000), phospho-Panx1 (Tyr198) (Millipore; ABN1681; 1:1,000), phospho-Panx1 (Tyr308) (Millipore; ABN1680; 1:1,000), Pannexin1 (Cell Signaling Technology; D9M1C mAb#91137; 1:1000).

Prediction of Pannexin membrane topology and phosphorylation sites. Pannexin 1 topology map was generated using PROTTER version 1.0²¹¹. Analysis of Pannexin 1

protein linear motif sequences was performed using the Eukaryotic Linear Motif computational biology resource ²¹².

Statistics. All data were analyzed using GraphPad Prism v7.0 software. Briefly D'Agostino-Pearson tests were used to determine normality. Brown-Forsthe/Bartlett's tests were used to determine equal variance for ANOVA and F-test was used to determine equal variance for t-test. Data that passed normality tests and equal variance tests were analyzed by t-test for two groups or ANOVA for three or more groups. P value less than 0.05 was considered significant.

2.2. MATERIALS AND METHODS FOR CHAPTER 4

Animals. All animals were cared for under the provisions of the University of Virginia Animal Care and Use Committee and the National Institute of Health guidelines for the care and use of laboratory animals. Male C57BL/6 mice between 10-15 weeks of age were purchased from Taconic. Male smooth muscle myosin heavy chain-Cre recombinase modified estrogen receptor binding domain (SMMHC-CreER^{T2}) modified mice, a kind gift from S. Offermanns²¹³, were used for experimentation due to the restrictive presence of Cre recombinase on the Y chromosome. Aortae from Connexin 43 globally deficient mice (Cx43^{-/-}) were harvested at birth. Mice harboring lox-P recombination sites for caveolin-1 (Caveolin-1^{fl/fl}) were generated as previously described²¹⁴. SMMHC-CreER^{T2} mice were mated with Caveolin-1^{fl/fl} mice to specifically delete caveolin-1 from vascular smooth muscle cells. Induction of Cre-mediated deletion was performed at 6 weeks of age via ten daily intraperitoneal injections (100 µl) of tamoxifen (1 mg/kg) to generate caveolin-1 null animals (SMMHC-CreER^{T2+}/Cav1^{ΔΔ}) or ten daily 100 µl injections of peanut oil (vehicle control) to generate control animals (SMMHC-CreER^{T2+}/Cav1^{fl/fl}). All animal experiments were performed at the least 14-days from the final injection with tamoxifen and/or peanut oil since the Cre recombinase is located on the Y. Mice lacking the Cre recombinase allele were also used as tamoxifen controls. Please see the Major Resources Table in Supplemental Material for detail.

Cell Culture. Primary human vascular coronary smooth muscle cells (VSMCs) were purchased from Lonza (Cat# CC-2583). All cells were maintained under standard cell culture conditions (5% CO₂ at 37°C) in smooth muscle growth media (Lonza; Cat# CC-

3181) supplemented with smooth muscle growth factors (Lonza; Cat# CC-3182) and 10% fetal bovine serum (FBS) (Lonza; Cat# CC-4102D). Cells were used at 8 passages or fewer for in vitro experiments. For all experiments, VSMCs were serum deprived for 48hrs in 0.2% FBS to induce contractile phenotypes²¹⁵⁻²¹⁷.

Ultrastructure electron microscopy. Mouse arteries were processed for ultrastructure TEM as previously described²¹⁸. Images were obtained using a Joel 1230 transmission electron microscope at the Advanced Microscopy Core at the University of Virginia.

Proximity Ligation Assay (PLA) and Immunofluorescence. Thoracodorsal arteries (TDA) were isolated as previously described²¹⁹, incubated in Krebs-HEPES physiological saline buffer, and treated with phenylephrine (20 μ mol/L) in a single well of a 96-well dish. TDAs were then placed in a 1.5 mL Eppendorf tube, fixed in 4% paraformaldehyde, and subjected to en face proximity ligation assay using the Duolink in situ PLA detection kit (Sigma) as previously described by us²²⁰. Sympathetic nerves were labeled using anti-mouse tyrosine hydroxylase antibody (Abcam #ab112; 1:250 dilution) and visualized using an Alexa Fluor 568 secondary antibody (Life Technologies #A-21099; 1:400 dilution). Primary antibodies for PLA labeling included anti-mouse Caveolin-1 (BD Biosciences# 610406, clone 2297; 1:400 dilution) and anti-mouse Panx1 CT395 (characterized by Penuela et al,¹⁷⁶ 1:300 dilution). PLA detection was performed according to manufacturer's protocol. Immunofluorescence staining on aorta and TDAs was performed as previously described⁷⁶. Primary antibodies for immunofluorescence included anti-rabbit Cx43 antibody (Sigma #C6219; 1:300 dilution) and vesicular nucleotide transport protein (anti-mouse VNUT; a kind gift from Dr. Chen Li, 1:200 dilution). All images were acquired using an Olympus

Fluoview 1000 confocal microscope. PLA punctate spots were counted per 100 μm^2 cell area. Caveolin-1 deletion was quantified using batch-processed tissue and threshold generated images. The relative fluorescence intensity within the smooth muscle cell layer (demarcated by co-association with Acta2 staining, and between the boundary lines of the IEL and adipose tissue) was measured using ImageJ²²¹ and normalized to Acta2 positive area. Co-staining for smooth muscle cells (Acta2; Sigma #A2547, 1:500 dilution) and endothelial cells (PECAM-1; Santa Cruz #sc28188, 1:400 dilution) was performed. Data are presented as mean \pm SEM. A student's t-test was performed for statistical significance. * $p < 0.05$.

Live cell imaging. Confocal imaging was performed with a Leica TCS SP8 confocal microscope. Human VSMCs were cultured as indicated above and plated on 100 $\mu\text{g}/\text{mL}$ poly-D-lysine (PDL) on cover glass. Cells were transfected with plasmids encoding Panx1-RFP²²² and Caveolin-1-GFP using jetPRIME (Polyplus transfection/VWR) according to the manufacturer's protocol. Image acquisition and co-distribution analyses were performed double-blinded to treatment conditions with identical imaging parameters. For live imaging, baseline images were collected at 30 sec intervals for 2 min using a 20X (0.7 NA) objective. Importantly, the large cellular size (range of lengths) permitted imaging of only one cell per field of view. Treatment with phenylephrine (100 $\mu\text{mol}/\text{L}$; Sigma-Aldrich), ATP (500 $\mu\text{mol}/\text{L}$; Sigma-Aldrich) or vehicle control (water) was performed by removing half the volume of control media and replacing it with the same volume of media containing 2X agonist. Images were collected at 30 sec intervals up to 5 min. The z-section containing the largest cellular area was selected for Mander's coefficient analysis of Panx1-Cav1 co-distribution using the JACoP plugin in FIJI²²³. All post-treatment data were normalized to the average obtained at baseline. Data were collected from N=5-11 cells per

experimental condition and analyzed using a two-way ANOVA for time and treatment (Time: $F(10, 250) = 3.027$, $P = 0.0012$; Treatment: $F(2, 25) = 4.673$, $P = 0.0189$; Subjects: $F(25, 250) = 19.41$, $P < 0.0001$) with Dunnett's posthoc ($P < 0.05$ for phenylephrine at 0.5 min, for ATP) with GraphPad Prism v5.0.

Membrane fractionation and isolation of caveolin-1 enriched membrane domains.

Human VSMCs were grown to confluence and incubated in media containing 0.2% FBS for 48 hr prior to use. VSMCs were washed with PBS and re-equilibrated for 10 min in Krebs buffer (mmol/L: 118.4 NaCl, 4.7 KCl, 1.2 MgSO₄, 4 NaHCO₃, 1.2 KH₂PO₄, 10 Hepes, 6 Glucose) containing 2 mmol/L CaCl₂. VSMCs were treated with 100µmol/L phenylephrine or vehicle control, scraped with a cell scraper and lysed in ice-cold detergent-free lysis buffer (500 mmol/L Na₂CO₃, 50 mmol/L NaF, 2 mmol/L Na₃VO₄, pH 11, supplemented with 1 mg/mL of protease inhibitor cocktail (Sigma) and 1 mg/mL P2 and P3 phosphatase inhibitor cocktails (Sigma)). Lysates were homogenized using a dounce homogenizer (10 strokes) and sonication (25 pulses for 1 sec) on ice. Lysates were either fractionated using differential centrifugation (40,000 rpm; 1hr Beckman XL80 ultracentrifuge with Sw55Ti rotor) or using centrifugation across a sucrose gradient. To create a sucrose gradient, sucrose solutions were mixed in MBS-sodium carbonate buffer (25 mmol/L MES, 0.5 M NaCl, 250 mmol/L Na₂CO₃) to 85%, 30%, and 5% by mass by adding 42.5 g, 15 g, or 2.5 g of sucrose, respectively, to 50 mL of MBS. Lysates were mixed with equal volume of 85% sucrose solution to create 42.5% layer. 1.5 mL of 42.5% layer was added to the bottom of a Sw55Ti ultracentrifuge tube, after which a 5-42.5% discontinuous sucrose gradient was formed by adding, dropwise on top of previous layers, 1 mL of 30% sucrose solution followed by 1 mL of 5% sucrose solution. Gradients were

centrifuged at 42,000 rpm for 18 hr in a Beckman XL80 ultracentrifuge with Sw55Ti rotor. Ten fractions of 350 μ L each were removed starting from the top of the gradient and analyzed using western blot with antibodies for rabbit anti-human Pannexin 1 (characterized by Penuela et al. ²⁰⁵ 1:1000 dilution) and mouse anti-caveolin-1 (BD Biosciences #610406; 1:1000 dilution). Co-immunoprecipitation was performed using either Pannexin1 antibodies (1:50 dilution) in conjunction with anti-rabbit IgG Dynabeads (Invitrogen) respectively. To perform co-immunoprecipitations, caveolin-1-enriched fractions (4-5) and non-enriched fractions (7-8) were combined and total protein from each was measured by BCA assay. Equal amounts of protein from each pair of fractions was used for co-immunoprecipitation as described above. Five independent experiments were performed. The ratio of caveolin-1 signal was normalized to the amount of immunoprecipitated Pannexin 1. Data are represented as mean \pm SEM. A students t-test was performed for statistical significance, * $p < 0.05$.

Western blot. After stimulation with adrenergic agonists, human VSMCs were homogenized in ice-cold NP-40 extraction buffer (50mmol/L Tris-HCL, 150mmol/L NaCl, 5mmol/L EDTA, 1% deoxycholate, 1% NP-40 and 1% Triton-X100 in PBS and pH adjusted to 7.4) containing protease inhibitor cocktail (Sigma) and P2 / P3 phosphatase inhibitor cocktail (Sigma). Cell/tissue lysates were incubated at 4°C for 10 min to solubilize proteins, sonicated for 12 pulses for 1 sec each, and centrifuged for 10 min at 12,000 rpm to pellet cell debris. Protein concentration was determined using the BCA method (Pierce). 10-20 μ g of total protein was loaded into each sample well. Samples were subjected to SDS gel electrophoresis using 4-12% Bis-Tris gels (Invitrogen) and transferred to nitrocellulose membrane for immunoblotting. Membranes were blocked for 1 hour at room

temperature in a solution containing 3% BSA in Tris buffered saline, then incubated overnight at 4°C with primary antibodies against rabbit anti-Pannexin 1 (Cell Signaling Technology #91137 (D9M1C); 1:1000 dilution), rabbit anti-Caveolin-1 (BD Biosciences #610059; 1:1000 dilution), rabbit anti-transferrin receptor (Abcam #ab84036; 1:1000 dilution) and mouse anti-GAPDH (Sigma mAb #G8795; 1:10,000). Membranes were washed and incubated in LiCOR IR Dye secondary antibodies (1:15,000) for 1 hour and viewed/quantified using the LiCOR Odyssey with Image Studio software. Representative western blot images have been cropped for presentation.

Pressure myography. Pressure myography was performed on TDAs as previously described ²²⁴. Briefly, mice were sacrificed using CO₂ asphyxia. TDAs were microdissected, cannulated on glass pipettes in a temperature-controlled pressure arteriography chamber, and pressurized to 80mmHg. After a 30-min equilibration period in Krebs-HEPES with 2mmol/L Ca²⁺, vessels were treated with cumulative doses of phenylephrine (PE, 10⁻¹⁰-10⁻³ mol/L) applied to the bath. The luminal diameter was analyzed using digital calipers in the DMT vessel acquisition software (Danish Myo Technology). Smooth muscle cell viability was assessed using serotonin (1 μmol/L) and KCl (30 mmol/L). Endothelial-dependent vasodilation was measured using cumulative doses of acetylcholine (10⁻¹¹-10⁻² mol/L) as previously described ²²⁴. A two-way analysis of variance (ANOVA) with Bonferonni post-hoc test was performed for multiple comparisons. Concentration-effect curves were fitted to the data using four-parameter, non-linear regression curve fitting using GraphPad (version 7).

ATP measurements. For the measurement of extracellular ATP, intact TDAs of equal length were placed in individual wells of a 96-well plate in Krebs-Hepes physiologic solution for 15 min. The ectonucleotidase inhibitor ARL 67156 trisodium (Toctris; 100 μ mol/L) was added 30 min prior to treatment with contractile agonists as previously described²²⁵. Vasoconstrictor compounds were added to the incubation media for 5 min to allow ATP accumulation: Phenylephrine (PE; 20 μ mol/L), Norepinephrine (NE; 20 μ mol/L), Serotonin (5-HT; 40nmol/L), and Endothelin-1 (ET-1; 40nmol/L) (all purchased from Sigma). Following stimulation, the media surrounding the vessel was collected and immediately placed into pre-chilled 1.5 mL Eppendorf tubes on ice. All samples were centrifuged at 10,000 x g for 5 min. For intracellular ATP measurements, TDAs were micro dissected, cleaned of adventitia, and cut into equal 10.5mm vessel segments. Segments were individually lysed in ATP lysis buffer according to manufacturer's protocol, spun at 10,000 x g for 1 min, and samples collected. ATP concentration in the incubation media was quantified using the ATP bioluminescence assay kit HSII (Roche) using a FluoStar Omega plate reader luminometer. Extracellular ATP measurements for each sample were tested in triplicate and calculated using an ATP standard curve for all experiments. Intracellular ATP measurements were measured from three vessel segments (one TDA in triplicate). Data are presented as % change in ATP release from baseline (unstimulated) or as the concentration of ATP in the media compared to control samples. One-way ANOVA with Tukey's test was performed for statistical significance of extracellular ATP. A Kruskal-Wallis (one-way ANOVA on ranks) with Dunn's post-hoc test performed for intracellular ATP. Significance denoted as *p < 0.05.

Blood pressure telemetry. Blood pressure was measured using telemetry equipment as previously described ²²⁵. Briefly, telemeters (Data Sciences International; DSI) were implanted in C57BL/6 or SMMHC-CreER^{T2+}/Cav1^{fl/fl} (SMC-Cav1^{fl/fl}) mice. Under isoflurane anesthesia, the catheter of a single telemetry unit (TA11PA-C10, DSI) was implanted in the left carotid artery and the transmitter placed in a subcutaneous pouch along the right flank of the mouse. After implantation surgery, mice were allowed to recover for 7 days to re-establish normal circadian rhythms and blood pressure. For experiments using inducible Cre recombinase, mouse blood pressure baselines were continuously recorded using Dataquest A.R.T. 20 software (DSI) for 5 days after normal recovery and before starting intraperitoneal tamoxifen injections or vehicle control (peanut oil) for 10 days. Blood pressure was recorded for an additional 5 days starting 24 hr after the last tamoxifen injection. Change in MAP (Δ MAP) was calculated by subtracting the average MAP measured before tamoxifen injections to the MAP after tamoxifen injections. Diurnal (inactive period) MAP was measured during animal's light cycle: 6:00 a.m. to 5:59 p.m., and nocturnal (active period) MAP was measured during the animal's dark cycle: 6:00 p.m. to 5:59 a.m. MAPs before and after tamoxifen injections were compared with a Wilcoxon test (nonparametric paired t-test). C57BL/6 mice similarly received intraperitoneal injections of tamoxifen or vehicle control, and basal blood pressure was measured as for transgenic animals. For assessment of the blood pressure effects of the P α IL2P peptide inhibitor (formerly referred to as P α IL2P1 peptide ²²⁵), animals were intraperitoneally injected with saline vehicle control or peptide (20 mg/kg in a volume not exceeding 100 μ L). Blood pressure was recorded for 2 hr after injection, and the MAP data was averaged and compared to the basal blood pressure. Change in MAP (Δ MAP) was calculated by

subtracting the baseline MAP 30 min before injection from the MAP measured during the final 30 min of the 2 hr treatment period. Data represent mean \pm SEM. Two-way ANOVA with Tukey post-hoc test was performed for assessment of MAP before and after tamoxifen/vehicle control induction and for mice treated with scrambled peptide or PxIL2P peptide inhibitor.

Cardiac magnetic resonance imaging and histology. All MRI animal studies were performed under protocols that comply with the Guide for the Care and Use of Laboratory Animals (NIH publication no. 85-23, Revised 1996) and were approved by the Animal Care and Use Committee at our institution (ACUC, UVA). Mice were positioned supine in the scanner and body temperature was maintained at $36 \pm 0.5^\circ\text{C}$ using thermostatic circulating water. Anesthesia used was 1.25% isoflurane in O_2 inhaled through a nose cone during imaging. A 30 mm-diameter cylindrical birdcage RF coil (Bruker) with an active length of 70 mm was used, and heart rate, respiration, and temperature were monitored during imaging using a fiber optic, MR-compatible system (Small Animal Imaging Inc., Stony Brook, NY). MRI was performed on a 7 Tesla (T) Clinscan system (Bruker, Ettlingen, Germany) equipped with actively shielded gradients with a full strength of 650 mT/m and a slew rate of 6666 mT/m/ms. Baseline LV structure and function were assessed²²⁶. Six short-axis slices were acquired from base to apex, with slice thickness equal to 1mm, in-plane spatial resolution of $0.2 \times 0.2 \text{ mm}^2$, and temporal resolution of 8–12 ms. Baseline ejection fraction (EF), end-diastolic volume (EDV), end-systolic volume (ESV), myocardial mass, wall thickness, and wall thickening were measured from the cine images using the freely available software Segment version 2.0 R5292 (<http://segment.heiberg.se>).

EDV and ESV were then indexed to body mass (EDVI and ESVI, respectively). Mass to volume ratio (MVR) was calculated as the ratio of myocardial mass to EDV.

Plasma Renin ELISA. Mice were anesthetized using 2,2-Dicholor-1,1-difluoroethyl methyl ether (ThermoFisher; #76-38-0). 100-150 μ l of whole blood was collected from mouse tail veins using heparinized capillary tubes into 1.5mL Eppendorf, stored on ice, and centrifuged for 15 minutes at 1000rpm. Plasma was aliquoted, snap frozen, and stored at -80°C. Plasma renin concentration was measured using a total renin ELISA (RayBio; #ELM-Ren1) against a renin standard curve with 1:15 dilution of samples. Student's t-test (two tailed) was performed for significance.

Statistics. All data were analyzed using GraphPad Prism v5.0 for live cell image analysis or v7.0 software for all other analyses. Briefly, D'Agostino-Pearson tests were used to determine normality. Brown-Forsythe/Barlett's tests were used to determine equal variance for ANOVA and F-test was used to determine equal variance for t-test in GraphPad Prism v7.0 software. Data that passed normality tests and equal variance tests were analyzed by t-test for two groups or ANOVA for three or more groups. Data that were not normally distributed were analyzed by Kruskal-Wallis test (three or more groups). Post-hoc analysis for multiple comparisons were selected as appropriate to test for statistical significance; * $p < 0.05$, ** $p < 0.01$, *** $p < 0.001$. Results are presented as mean \pm SEM.

2.3. MATERIALS AND METHODS FOR CHAPTER 5

Animals. All animals were cared for under the provisions of the University of Virginia Animal Care and Use Committee and the National Institute of Health guidelines for the care and use of laboratory animals. Renin (Ren1^d) Cre recombinase modified mice, as previously described²²⁷, were mated with mice harboring lox-P recombination sites flanking exon 3 of Pannexin 1 ($\text{Panx1}^{fl/fl}$)²²⁸ thus producing conditional Pannexin 1 knockout mice ($\text{Ren1-Panx1}^{\Delta/\Delta}$) and control animals ($\text{Ren1-Panx1}^{wt/wt}$). Male mice ages 10-25 weeks old were used for experimentation on the basis that significant hormonal and blood pressure phenotypes were observed in male, but not female mice. To generate mice with renin cell fluorescence reporters, we mated Ren1-Cre Panx1 animals with mice containing alleles for R26R-EYFP transgene ($\text{B6.Cg-Gt(ROSA)26Sor}^{tm3(CAG-EYFP)Hze/J}$) purchase from The Jackson Laboratory (Stock No: 007903) and maintained in the University of Virginia vivarium ($\text{Ren1-Panx1}^{\Delta/\Delta (EYFP)}$ and $\text{Ren1-Panx1}^{wt/wt (EYFP)}$).

Cell Culture. As4.1 mouse kidney cells were purchased from the American Type Culture Collection (ATCC, CRL-2193). All cells were maintained under standard cell culture conditions (5% CO_2 at 37°C) and were cultured in Dulbecco's modified Eagle's medium (DMEM, Gibco; Cat# 1196b 092) supplemented with 10% fetal bovine serum (FBS) and penicillin-streptomycin (VENDOR#). For knockdown experiments, 70% confluent cells were transfected with either silencer select negative control siRNA (ThermoFisher; Cat# 4390843) or silencer select mouse Panx1 siRNA (ThermoFisher ; Cat# S79965) using Lipofectamine 3000 (ThermoFisher; Cat# L3000008) according to manufacturer's instructions in low serum (0.2%) media. Cells were analyzed for knockdown using qRT-

PCR and western blot. Experiments were performed 48hrs after knockdown. Cells were stimulated with Angiotensin II (Tocris; Cat# 1158) or 8Br-cAMP, sodium salt (Tocris; Cat# 1140).

Blood Sampling. The collection of blood samples was performed under limited-stress conditions to avoid influences of animal handling on measured metabolites. In all instances, blood sampling took place during the animal's inactive period (08:00-10:00h) and during the active period (20:00-22:00h). Mice were quickly anesthetized using 2,2-Dichloro-1,1-difluoroethyl methyl ether (ThermoFisher; #76-38-0). 100-150 μ l of whole blood was collected from mouse tail veins using Li-heparin-coated capillary tubes to allow repeated sampling no sooner than one week after initial collection. Blood was stored in 1.5mL Eppendorf on ice during the collection period. After centrifugation (1500rpm x 15min) at 4°C, the plasma was separated, flash frozen, and stored at -80°C for hormone measurements. For metabolic analyses, blood was terminally collected from mice using cardiac puncture, stored on ice in Na-EDTA or Li-Heparin blood collection tubes, and analyzed at the University of Virginia Clinical Pathology Core facilities.

Hormone Measurements. Plasma renin concentration was measured using a total renin ELISA (RayBio; #ELM-Ren1) using a 1:10 dilution of mouse plasma samples measured in duplicate according to manufacturer's instructions. Absorbance was measured at 450nm using the a FLUOstar Omega (BMG Labtech) plate reader. Plasma and urinary aldosterone concentrations were measured using solid-phase Aldosterone RIA (CT) (IBL International; MG13051). Collected plasma was diluted 1:10 fold and urine diluted 1:20 fold in supplied zero calibrator buffer and incubated for 16hrs according to manufacturer's instructions.

Radioactivity was measured at 37°C for samples, calibrators, and the standard curve using a Gamma Counter. For calculating results, the blank values were subtracted from each sample value and was multiplied by the dilution factor.

Metabolic cage experiments. Mice were kept in metabolic cages (Techniplast, Buguggiate, Italy) and 24-hour urine volume and water consumption were collected and monitored daily. Urine samples were stored at -80°C and creatinine measured by ELISA using creatinine colorimetric assay kit (Cayman; Cat #500701). Candesartan cilexetil (10 mg/kg/day) was administered via drinking water for 12 days. The dosage regimen for candesartan cilexetil was selected on preliminary telemetry recordings to be sufficient to reduce mean arterial pressure. Daily water consumption was monitored (4 days) and the appropriate amount of drug added to drinking water to achieve accurate dosages. Candesartan cilexetil (Sigma; Cat# SML0245) was dissolved in 10 times the final concentration in a vehicle of polyethylene glycol 400 (10% v/v), ethanol (5% v/v), cremophor EL (2% v/v), and tap water (83% v/v) prior to dilution to a final concentration in tap water, as previously described^{229,230}. To elicit recruitment of renin-expressing cells, mice were administered a low-sodium diet (0.05%, Envigo) and captopril (0.5g/L) (Sigma; Cat# C4042) in the drinking water.

Histological procedures. Paraffin sections (5-8 µm) of kidney and the central adrenal gland were rehydrated using 3 min incubations in each one of the following solutions: 2× xylene, 2× 100% ethanol, 2× 95% ethanol, 1× 70% ethanol, and 1× ddH₂O. Sections were stained with hematoxylin–eosin for morphological evaluation. Hematoxylin–eosin-stained adrenal sections were examined with a standard light microscope. Serial sections were made

through the entire adrenal gland and five subsequent central sections were imaged and measured for surface area of the adrenal cortex and medulla using FIJI²²¹. Hematoxylin–eosin and Masons Tri Chrome staining was performed on kidney sections at the University of Virginia Research Histology Core.

Immunofluorescence. Organs and tissues were collected from euthanized mice, cleaned of surrounding adipose tissue, and fixed in 4% PFA/PBS overnight (kidneys) or for 4 hours (adrenal glands). Tissues were subsequently dehydrated, paraffin embedded, and thinly sectioned (5-8um) to be mounted onto glass slides. After removal of paraffin and rehydration, antigen retrieval was performed using Vector Antigen Unmasking Solution Tris based (Vector Lab; Cat# H-3301) for adrenal tissue or citric acid based (Vector Lab; Cat# H-3300) for renal tissue. Slides were quenched in 3% peroxide in methanol (10 minutes) and washed 3x in TBS. Non-specific binding sites were blocked by incubating tissue sections in blocking solution containing 10% normal serum, 3% BSA, 0.5% SDS in TBS for 45min at room temperature. Samples were subsequently incubated overnight in primary antibodies diluted in a buffer contain 10% normal serum, 3% BSA, and 0.2% Tween20. Primary antibodies used included: anti-Renin mAb (abcam# ab212197; 1:500 dilution), anti- α SMActin mAb (Acta2; Sigma# A2547, 1:500 dilution), anti-GFP Rb pAb (abcam# ab6556), anti-GFP chk pAb (abcam# ab13970, 1:500 dilution), anti-tyrosine hydroxylase (abcam# Ab113, 1:800 dilution), anti-CYP11B2 (a kind gift from Dr. Celso Gomez Sanchez)²³¹. Tissue sections were washed 3x in TBS and incubated for 1 hour at room temperature with secondary antibodies: anti-rabbit Alexa Fluor 647 F(ab')₂ (Cat# A21246), anti-mouse Alexa Fluor 594 F(ab')₂ (Cat# A11020), anti-mouse Alexa Fluor 488 F(ab')₂ (Cat# A11017), anti-chicken Alexa Fluor 594 (Cat# A11042), Streptavidin Alex

Fluor conjugated 594 and 488 (Cat# S11277; Cat# S32354), and anti-sheep Alexa Fluor 488 (Cat# A11015). All secondary antibodies were used at a 1:400 dilution. For renin staining of drug treated animals, Alexa Fluor 647 Tyramide SuperBoost Kit (ThermoFisher; Cat# B40926) was used according to the manufacturer's instructions to enhance resolution and reduce autofluorescence. Slides were washed and mounted with coverslips using Ampliglod anti-fade DAPI mounting media. All images were taken on Olympus FV1000 confocal microscope and analyzed using Fluoview1000 software.

Western blot. Mouse As4.1 cells and tissues were homogenized in ice-cold RIPA extraction buffer (10mmol/L Tris-HCL pH 8.0, 150mmol/L NaCl, 1mmol/L EDTA, 0.5% SDS, 1% Triton-X100) containing protease inhibitor cocktail (Sigma; Cat# 8340) and P2 / P3 phosphatase inhibitor cocktail (Sigma; Cat# P5725 & P0044). Cell/tissue lysates were incubated at 4°C for 10 min to solubilize proteins, sonicated for 12 pulses for 1 sec each, and centrifuged for 10 min at 12,000 rpm to pellet debris. Protein concentration was determined using the BCA method (Pierce; ThermoFisher; Cat# 23225). 10-20 µg of total protein was loaded into each sample well. Samples were subjected to SDS gel electrophoresis using 4-12% Bis-Tris gels (Invitrogen) and transferred to nitrocellulose membrane for immunoblotting. Membranes were blocked for 1 hour at room temperature in a solution containing 3% BSA in Tris buffered saline, then incubated overnight at 4°C with primary antibodies: anti-Pannexin 1 (Cell Signaling Technology #91137 (D9M1C); 1:1000 dilution), mouse anti- α SMactin (ACTA2; Sigma #A2547, 1:1000 dilution). Membranes were washed and incubated in LiCOR IR Dye secondary antibodies (diluted 1:15,000) for 1 hour and viewed/quantified using the LiCOR Odyssey with Image Studio software. Representative western blot images have been cropped for presentation.

Pressure myography. Pressure myography was performed on TDAs as previously described²²⁴. Briefly, mice were sacrificed using CO₂ asphyxia. TDAs were micro dissected, cannulated on glass pipettes in a temperature-controlled pressure arteriography chamber, and pressurized to 80mmHg. After a 30-min equilibration period in Krebs-HEPES with 2mmol/L Ca²⁺, vessels were treated with cumulative doses of phenylephrine (PE, 10⁻¹⁰-10⁻³ mol/L) applied to the bath. The luminal diameter was analyzed using digital calipers in the DMT vessel acquisition software (Danish Myo Technology). Smooth muscle cell viability was assessed using KCl (30 mmol/L).

Blood pressure telemetry. Blood pressure was measured using telemetry equipment as previously described²²⁵. Briefly, telemeters (Data Sciences International; DSI) were implanted in mice under isoflurane anesthesia. The catheter of a single telemetry unit (TA11PA-C10, DSI) was implanted in the left carotid artery and the transmitter placed in a subcutaneous pouch along the right flank of the mouse. After implantation surgery, mice were allowed to recover for 7 days to re-establish normal circadian rhythms and blood pressure. Blood pressure was continuously recorded using Dataquest A.R.T. 20 software (DSI) for 5 days after normal recovery. Diurnal (inactive period) BP was measured during animal's light cycle: 6:00 a.m. to 5:59 p.m., and nocturnal (active period) BP was measured during the animal's dark cycle: 6:00 p.m. to 5:59 a.m.

qRT-PCR. Total RNA was extracted from tissue and cells using Aurum Total RNA Fatty and Fibrous Tissue extraction kit (BioRad; Cat# 732-6870) according to the manufacturer's instructions and RNA concentration measured using NanoDrop1000 spectrophotometer (ThermoFisher). For FACS sorted cells total RNA was extracted using Arcturus PicoPure

RNA Isolation Kit (ThermoFisher; Cat# 12204-01). RNA was stored at -70°C or reverse transcribed using SuperScriptIII First-Strand Synthesis System (ThermoFisher; Cat# 18080051) and random hexamer primers. qRT-PCR was performed using diluted cDNA in nuclease-free water (10ng total RNA) in triplicate using PowerUp SYBR Green Master Mix (ThermoFisher; Cat# A25742) and optimized primers for REN1: Fwd- 5'ATGCCTCTCTGGGCACTCTT; Rev- 5'GTCAAACCTTGCCAGCATGA; B2M (Sigma; ID# M_B2m_1) on a CFX Real-Time Detection System (Applied BioSystems). Pannexin expression was analyzed in triplicate PCR reactions using TaqMan Gene Expression Master Mix (2x) (ThermoFisher; Cat# 4369016) in combination with TaqMan Real-Time PCR assays for Panx1: Mm00450900_m1; Panx2: Mm01308054_m1; Panx3: Mm00552586; and B2M: Mm00437762). The threshold cycle number (CT) was used in combination with the $2^{-\Delta\Delta CT}$ method to calculate fold change from control.

Statistics. All data were analyzed using GraphPad Prism v7.0 software. A Shapiro-Wilk test was performed to determine normality. Brown-Forsythe/Barlett's tests were used to determine equal variance for ANOVA and F-test was used to determine equal variance for t-test in GraphPad Prism v7.0 software. Data that passed normality tests and equal variance tests were analyzed by t-test for two groups or ANOVA (one-way and two-way) for three or more groups. Data that were not normally distributed were analyzed by Kruskal-Wallis test (three or more groups). Post-hoc analysis for multiple comparisons were selected when appropriate to correct for multiple comparison error and test for statistical significance; * $p < 0.05$, ** $p < 0.01$, *** $p < 0.001$. Results are presented as mean \pm SEM.

CHAPTER 3. POST-TRANSLATIONAL MODIFICATION OF PANNEXIN 1 -Y198 BY SRC KINASE

3.1. ABSTRACT

In vascular smooth muscle cells of resistance arteries, Pannexin 1 (Panx1) mediated ATP release uniquely coordinates α 1-adrenergic receptor (α 1-AR) vasoconstriction, total peripheral resistance, and blood pressure homeostasis. We have recently identified amino acids 198-200 (YLK) on the Panx1 intracellular loop that are critical for phenylephrine-stimulated vasoconstriction and Panx1 channel function. We report herein that the intracellular loop YLK motif is contained within a Src homology 2 domain and is directly phosphorylated by Src kinase at Y198. We further demonstrate that Panx1-mediated ATP release occurs independently of intracellular calcium but is sensitive to Src family kinase (SFK) inhibition, suggestive of channel regulation by tyrosine phosphorylation. Using a Panx1-Y198 specific antibody, pharmacological SFK inhibitors, genetic knockdown of Src kinase, temperature sensitive on/off activation of Src kinase, and an in vitro Src kinase assay, we find that Panx1-mediated ATP release and vasoconstriction involves constitutive phosphorylation of Panx1-Y198 by Src kinase at the plasma membrane. Src-mediated Y198 phosphorylation was not induced by α 1-AR activation; however, Y198 phosphorylation was required for Panx1 presence at the plasma membrane. Lastly, we show that Panx1-Y198 immunostaining is enriched in the smooth muscle layer of hypertensive human artery biopsies, indicative of enhanced Panx1 at the plasma membrane of hypertensive humans. Our discovery that Panx1 function is supported by constitutive

Src kinase phosphorylation adds insight into the regulation of Panx1 by post-translational modifications and connects a significant purinergic vasoconstriction pathway with a previously identified, yet unexplored, tyrosine kinase-based α 1-AR constriction mechanism. This work strongly implicates a role for Src-mediated Panx1 function in normal vascular hemodynamics, as well as its involvement in hypertensive vascular pathology.

3.2. INTRODUCTION

The synchronous and coordinated constriction of vascular smooth muscle cells (VSMCs) in resistance arteries is necessary for controlling total peripheral resistance and blood pressure homeostasis²³². VSMCs on resistance arteries are innervated by sympathetic nerves²³³, which elicit local constriction events through the co-release of neuronal derived norepinephrine (NE) and presumably adenosine 5'-triphosphate (ATP)²³⁴. Following α 1-AR activation, latent VSMC-derived purinergic signals mediated by adenosine 5'-triphosphate (ATP) coordinate vasoconstriction of neighboring cells, which is likely propagated by autocrine/paracrine signaling within resistance vessels^{225, 235}. The regulated release of VSMC-derived ATP has therefore emerged as a predominant signal for controlling hemodynamics.

In the vascular wall, the location of ATP release governs its functionality— either as a vasodilator (from endothelial cells), or as a potent vasoconstrictor (from VSMCs)²³⁶. This functional dichotomy highlights a unique mechanism for the regulated release of ATP from vascular cells, which has only recently come into view²³⁷. Pannexin 1 (Panx1) channels, the prototypical member of a class of channel-forming transmembrane glycoproteins, have been established as the main conduit by which ATP is released from VSMCs²³⁸ and other cell types²³⁹ under physiological conditions. Recent work from our lab (and others) has demonstrated that Panx1-mediated ATP release uniquely couples to α 1-AR vasoconstriction in resistance arteries, where VSMC Panx1 is highly expressed^{224, 240, 241}. Moreover, we have identified an important Panx1 intracellular loop motif, residues Y198-K200 (mouse) and Y199-K201 (human), that is critical for adrenergic receptor-mediated

channel function. In *in vitro* and *in vivo* experimental models, pharmacological inhibition and genetic deletion targeting the YLK motif reduced ATP release, inhibited Panx1 current, blunted adrenergic vasoconstriction, and reduced mean arterial pressure^{225, 242}. Thus, the Panx1 YLK motif functions as an important regulatory site.

The traditional view of α 1-AR activation and subsequent VSMC constriction are mechanistically thought to couple heterotrimeric G-protein subunits to the direct generation of inositol triphosphate and increased intracellular calcium. Alternately, a number of studies have provided evidence for a secondary, and as of yet, unclear tyrosine kinase-mediated component of adrenergic constriction that might co-regulate vasoconstriction events^{206, 209, 243-245}. Recent evidence in the Pannexin literature also suggests a regulatory role for tyrosine kinases during receptor-mediated Panx1 function. Panx1 channel gating, ATP release, and neuronal cell death were dependent on Src kinase activity¹⁹⁴. Similarly, in endothelial cells of peripheral veins, receptor-mediated activation of Panx1 channels and endothelial-specific ATP release were significantly blocked using Src family kinase (SFK) inhibitors²⁴⁶. These findings suggest a common regulatory mechanism for Panx1 channel regulation that until now, has not been explored in VSMCs of resistance arteries.

Here we show that Src kinase, the archetypal SFK, is responsible for the direct phosphorylation of tyrosine 198 on the intracellular loop of Panx1 in VSMCs, and that modulation of Src activity and phospho-Y198 status is critical for supporting proper channel function. Notably, we find that phosphorylation of Y198 is constitutive in nature, and not induced upon α 1-AR stimulation. However, inhibition of SFKs, in particular Src

kinase, and the concomitant loss of tyrosine phosphorylation at Y198 is detrimental to ATP release and adrenergic vasoconstriction. Furthermore, we show that detection of Panx1-Y198 phosphorylation uniquely occurs at the plasma membrane and is present in hypertensive human vessel biopsies, which correlate with increased Panx1 protein expression in hypertensive, but not normotensive arteries. These results suggest that increased Panx1 at the plasma membrane may contribute to pathological hypertensive responses that occur in resistant hypertension.

3.3. RESULTS

Src family kinases regulate phenylephrine-induced Pannexin 1 channel function independent of Ca²⁺

We have previously shown that α 1-AR stimulated vasoconstriction uniquely couples with Panx1-mediated ATP release from VSMCs of resistance arteries and requires the Panx1 intracellular motif (YLK) ^{225, 238}. Since VSMC contraction requires increases in cytosolic calcium (Ca²⁺), we first sought to determine if adrenergic-stimulated ATP release was dependent on intracellular Ca²⁺. Isolated resistance arteries were incubated with BAPTA-AM to chelate intracellular Ca²⁺ ex vivo. Application of the α 1-AR selective agonist phenylephrine (PE; 20 μ M) caused a significant increase in extracellular ATP in the presence and the absence of BAPTA-AM (**Figure 1A**). These observations suggest a Ca²⁺-independent mechanism for regulating Panx1 channel function, at least acutely after adrenergic stimulation, and is consistent with previous observation suggesting that Ca²⁺ is not involved in Ca²⁺ mediated ATP release ²⁴⁷⁻²⁵⁰.

Next, we scanned short eukaryotic linear motif databases to analyze regions of Panx1 that might confer modifications to Panx1 independently of Ca²⁺, specifically near the intracellular loop motif (YLK). We identified a putative Src homology 2 recognition site in both mouse and human amino acid sequences, which was contained within the YLK sequence. In the mouse sequence this site localized near a Src homology 3 (proline-rich) Src-binding region indicative of regulation by SFKs (**Figure 1B**). To confirm a possible role for SFK activity in adrenergic-mediated ATP release, we measured ATP release from HEK293T cells co-expressing Panx1 and the α 1-AR in the presence of the SFK inhibitor

PP2 and the inactive analog PP3 (**Figure 2**). PE stimulated ATP release was significantly blunted by PP2 (10 μ M) treatment, but not with PP3 (10 μ M). We performed similar experiments using isolated murine resistance arteries in the presence of PP2, PP3, and the more potent tyrosine kinase inhibitor dasatinib (Figure 1C). Application of PP2 (10 μ M) significantly blunted PE and NE-induced ATP release as compared to control arteries or arteries treated with the inactive analog PP3 (10 μ M). The same inhibitory effect was observed using dasatinib (10nM). No increase in ATP release was observed when vessels were stimulated with non-adrenergic vasoconstrictors endothelin-1 (ET-1; 10nM) or serotonin (5-HT; 100nM), thus confirming the specificity of Panx1-mediated ATP release for adrenergic stimuli as previously described ²²⁵.

In addition to ATP release, we assessed vasoconstriction responses to cumulative doses of adrenergic and non-adrenergic agonists using pressure myography in isolated resistance arteries (Figure 1D-G). Pretreatment (15min) of arteries with PP2 (10 μ M) significantly blunted α 1-AR constriction as compared to control arteries or arteries treated with the inactive analog PP3 (10 μ M) (Figure 1D). Application of ET-1 or 5-HT produced strong vasoconstriction responses in the presence and absence of the PP2, highlighting again a key pathway between SFK activity and adrenergic-mediated vasoconstriction (Figure 1E-F). Similar inhibitory effects on α 1-AR vasoconstriction were observed when vessels were pretreated (15min) with dasatinib (10nM) (Figure 1G).

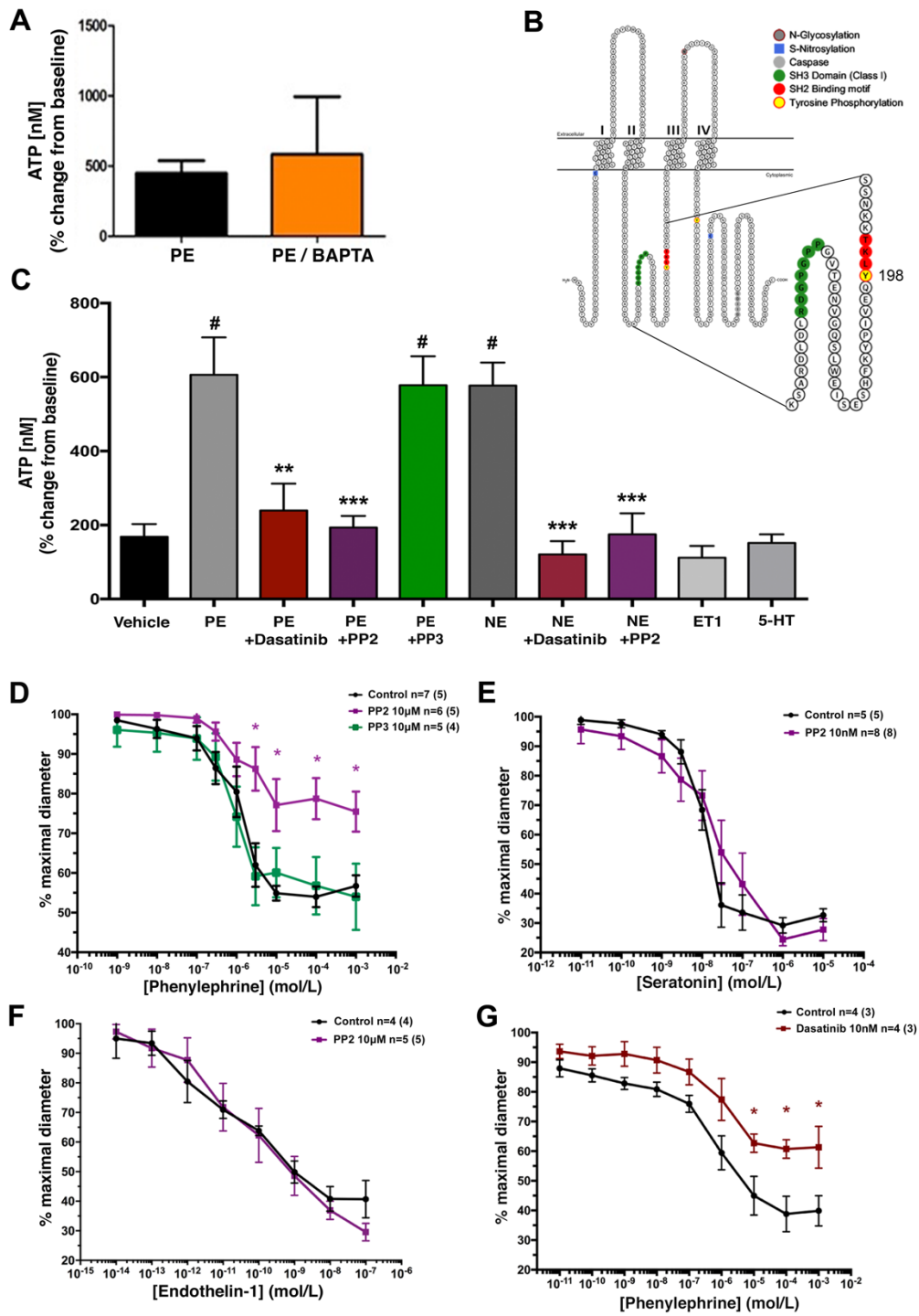


Figure 1. Src family kinases regulate phenylephrine-induced Pannexin 1 channel function independent of Ca²⁺.

Figure 1. Src family kinases regulate phenylephrine-induced Pannexin 1 channel function independent of Ca²⁺. (A) Phenylephrine (PE) stimulated ATP release from intact thoracodorsal arteries (TDAs) treated with the intracellular calcium-chelating agent BAPTA-AM. n=4 TDA (from 4 mice) Data presented as percent increase from unstimulated condition. A Students t-test was performed to test for significance. (B) Pannexin 1 membrane topology denoting Src Homology 2 linear motif (red) containing putative intracellular loop tyrosine 198 (yellow) Src phosphorylation site and the upstream proline rich Src Homology 3 binding domain (green). (C) ex vivo ATP release from TDA stimulated with PE (20μM) and norepinephrine (10μM) in the presence and absence of the SFK inhibitors PP2 (10μM), dasatinib (10nM), and negative control PP3 (10μM). The non-adrenergic vasoconstrictors serotonin (5HT; 100nM) and endothelin-1 (ET1; 10nM) were assessed. n=4 TDA (from 4 mice) per group. One-way ANOVA was performed for statistical significance. #indicates significant increase from vehicle; p<0.5. *indicates significant reduction from PE stimulated; *p< 0.05, **p<0.01, ***p<0.001. (D-G) Contractile responses to increasing concentration of adrenergic agonists (PE or norepinephrine) in the presence of SFK inhibitors PP2 (10μM; purple line), inactive control PP3 (10μM; green line), and dasatinib (10nM; red line). n=4-8 TDA (from 4-8 mice). Data presented as mean ± s.e.m. Data assessed. Using Two-way ANOVA with Bonferroni post-hoc test of multiple comparisons for significance. *p<0.05 compared to control response (black line).

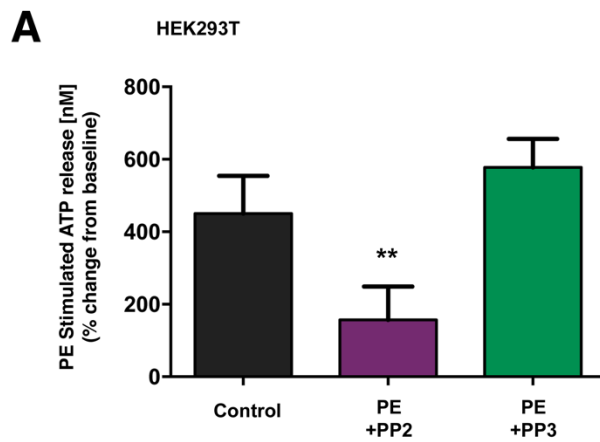


Figure 2. Supplement to Figure 1: Src family kinases support phenylephrine-stimulated ATP release in HEK cells.

Figure 2. Supplement to Figure 1: Src family kinases support phenylephrine-stimulated ATP release in HEK cells.(A) Phenylephrine-stimulated ATP release from HEK293T cells co-transfected with Pannexin 1 and α 1-adrenergic receptor expression vectors. Adrenergic-mediated ATP release blunted by incubation with SFK inhibitors PP2 (10 μ M), but not inactive analog PP3 (10 μ M). Data presented as percent change from baseline. n=4 experiments. Statistical significance tested using one-way ANOVA. **p<0.01.

Pannexin 1 tyrosine 198 is constitutively phosphorylated in smooth muscle cells

Our previously published mutagenesis experiments²²⁵ and SFK-mediated vasoconstriction impairment implicates tyrosine 198 (Y198) in the Panx1 intracellular loop motif (YLK) as a SFK phosphorylation site. To analyze the phosphorylation status of Panx1-Y198 in VSMCs after adrenergic stimulation, human coronary smooth muscle cells (hCoSMCs) were differentiated to a contractile phenotype and assessed by western blot for Panx1 expression (**Figure 3A**). Typical 48hr serum starvation upregulated smooth muscle contractile proteins, including α -smooth muscle actin and Panx1 (**Figure 3A**). We next immunoprecipitated Panx1 from hCoSMCs following PE (20 μ M) stimulation using a Panx1-specific antibody and magnetic bead separation. The status of Panx1-Y198 phosphorylation was assessed by western blot using the Y198 phospho-antibody (pPanx1Y198) (**Figure 3B; Figure 4A**). Following adrenergic stimulation, we observed similar levels of Panx1-Y198 phosphorylation both in vehicle treated and PE-stimulated samples, indicative of constitutively phosphorylation at Y198. We confirmed observations from immunoprecipitation experiments using hCoSMCs treated with pharmacological SFK inhibitors 30min prior to stimulation. As with our other assay, PE did not enhance Panx1-Y198 phosphorylation (**Figure 3C**). However, treatment with PP2 (10 μ M) and dasatinib (10nM) significantly reduced Panx1-Y198 levels. No reduction in phosphorylation was observed with the inactive control PP3 (10 μ M). These results were recapitulated in HEK293 cells expressing Panx1 (**Figure 4B**). As an additional control to confirm the detection of Y198 as a phosphorylation residue, cell lysates were treated with lambda phosphatase to completely remove phosphate groups (**Figure 3C**). A complete

reduction in pPax1Y198 levels were observed. Taken together these data suggest that SFK activity constitutively regulates Pax1-Y198 to support channel function.

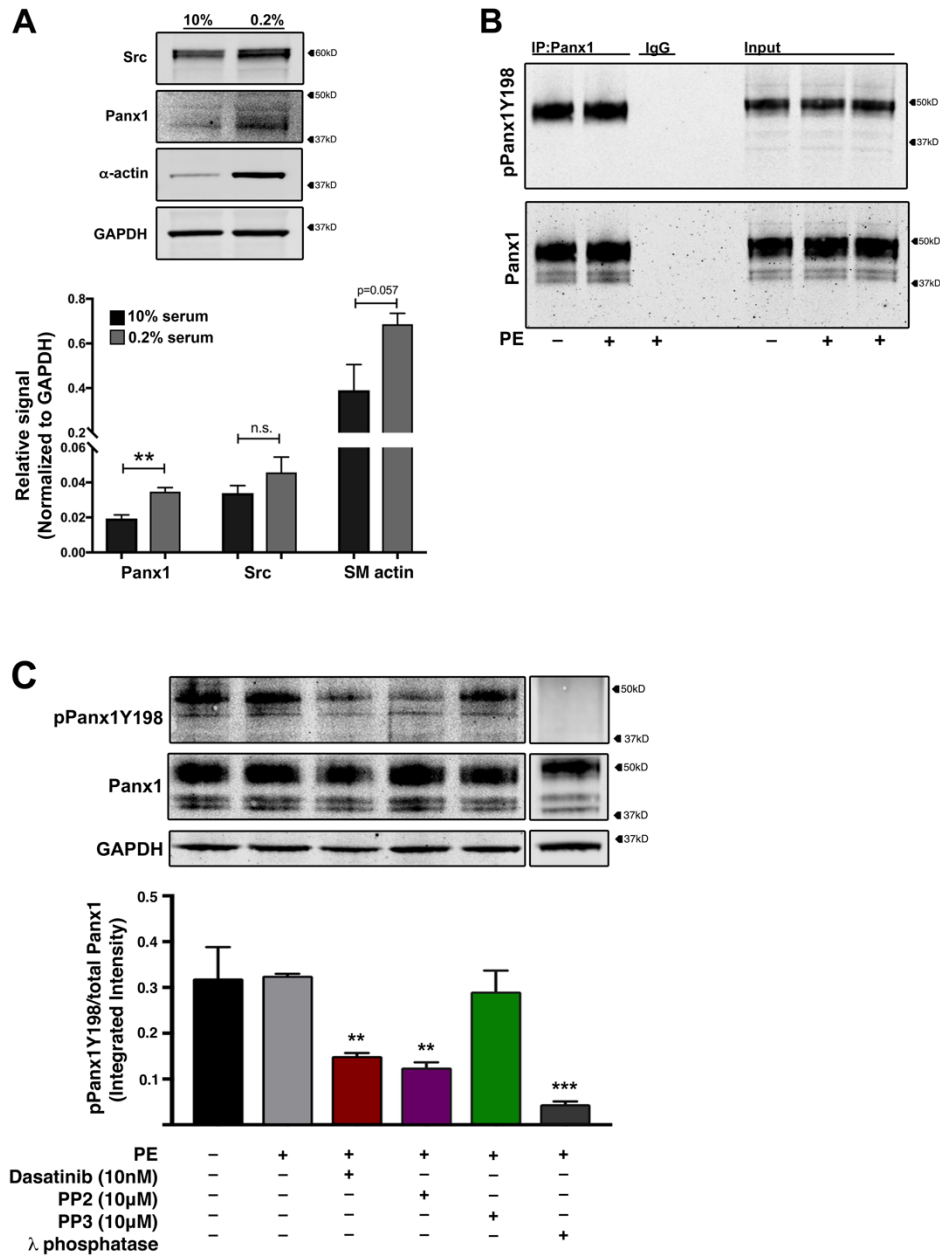


Figure 3. Pannexin 1 tyrosine 198 is constitutively phosphorylated in vascular smooth muscle cells.

Figure 3. Pannexin 1 tyrosine 198 is constitutively phosphorylated in vascular smooth muscle cells. (A) Confirmation of protein expression of Panx1 and Src kinase in smooth muscle cells following differentiation to a contractile phenotype with 48 serum starvation (0.2% FBS). Data presented as mean \pm s.e.m. n= 4 independent experiments. Student's t-test performed for statistical significance; *p< 0.05, **p<0.01 compared to high FBS level. (B) Immunoprecipitation of Panx1 from hCoSMCs stimulated with PE (20 μ M) and immunoblotted for Pannexin 1 (Y198) phosphorylation. (C) Representative western blot and quantification of phosphorylation status of Pannexin 1 Y198 in hCoSMCs treated with SFK inhibitors dasatinib (10nM; red), PP2 (10 μ M; purple), negative control PP3 (10 μ M; green). Lambda phosphatase treated lysates were used as a negative control; n=6 independent experiments. Data quantification presented as mean \pm s.e.m. **p < 0.01, ***p<0.001 compared to unstimulated control using one-way ANOVA.

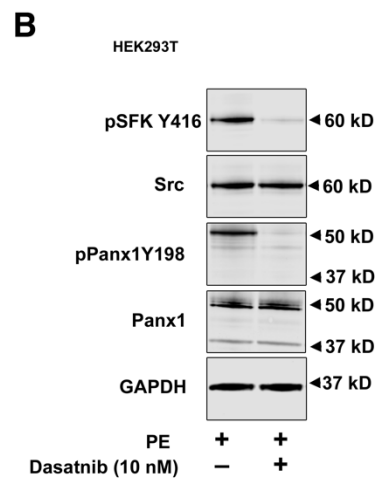
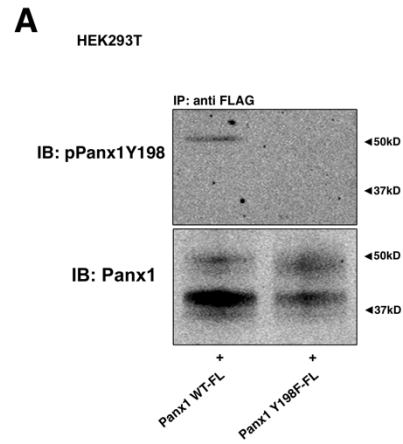


Figure 4. Supplement to Figure 3: Src kinase is sufficient to phosphorylate Pannexin 1 (Y198) in HEK cells.

Figure 4. Supplement to Figure 3: Src kinase is sufficient to phosphorylate Pannexin 1 (Y198) in HEK cells. (A) Immunoprecipitation validation of pPanx1 Y198 antibody from FLAG epitope tagged wildtype, or Y198F mutant Pannexin 1 isoforms from HEK293T cells co-expressing the α 1-adrenergic receptor. (B) Western blot analysis of Pannexin 1 (Y198) phosphorylation in HEK293T cells treated with SFK inhibitor dasatinib (10nM). SFK activity was analyzed using phospho-specific SFK antibody for activation residue (Y416) and was completely prevented with dasatinib treatment.

Src kinase modulates phosphorylation of Pannexin 1 at tyrosine 198

Due to the significant inhibitory effects of SFK-modulating agents on adrenergic-mediated vasoconstriction, ATP release, and Panx1-Y198 phosphorylation in VSMCs, we set out to specifically address if Src kinase modulates Panx1-Y198 phosphorylation—as was observed in other cell types^{194, 246}. We performed knockdown of Src kinase using Src-specific siRNA in hCoSMCs. Similar to the effects observed using SFK inhibitors, Panx1-Y198 phosphorylation was equally abundant in control and PE-stimulated conditions, yet significantly reduced after Src knockdown. No reduction in Panx1-Y198 was observed using negative control siRNA (scramble siRNA) (**Figure 5A**). To further validate the specificity of Src kinase to phosphorylate Panx1-Y198, HEK cells were transfected with expression vectors for the α 1-AR, Panx1, and mutant isoforms of Src kinase that were constitutively active (cSrc) or harbored a kinase inactivating mutation (Src-KD) (**Figure 5B**). Immunoblot detection for Src and the pSFK(Y416) auto-phosphorylation activation loop residue showed enhanced total expression of Src kinase following transfection. pSFK(Y416) was moderately increased in Src-KD, likely due to overexpression in a cell type containing native Src kinase. A greater enhancement for pSFK(Y416) was observed in conditions utilizing constitutively active cSrc. Under basal transfection conditions (only empty vector, α 1-AR, and Panx1), Panx1-Y198 phosphorylation was not different between vehicle and PE stimulation. However, transfection of the cSrc isoform generated intense hyperphosphorylation of Panx1-Y198 indicated by enhanced pPanx1Y198 signal that was absent in conditions utilizing the Src-KD isoform. Thus Panx1-Y198 phosphorylation is dependent on Src kinase activity.

Lastly, we performed a temperature-dependent Src kinase assay using LA-25 cells transfected with α 1-AR and Panx1 (**Figure 5C**). LA-25 cells harbor a temperature sensitive Src mutation²⁰⁴, which at the permissive temperature (35°C) constitutively activates Src kinase, but at the non-permissive temperature (40°C) inactivates kinase activity²⁵¹. After 30 min incubation of LA-25 cells at 35°C, Src kinase was activated as indicated by enhanced pSFK(416) autophosphorylation, as well as the phosphorylation of the Src substrate paxillin (Y118). pSFK(416) or paxillin (Y118) phosphorylation was not observed after 30min at 40°C. Analysis of Panx1 in vehicle and PE-stimulated conditions revealed constitutive phosphorylation of Panx1 (Y198) at 35°C and reduced signal at 40°C. Incubating cells with PP2 (10 μ M) at the permissive temperature was also sufficient to obstruct constitutive Src kinase activity and reduce detection of Panx1-Y198. Importantly, Panx1-Y198 signal could be rescued at the non-permissive temperature when LA-25 cells were supplemented with the constitutive cSrc isoform. These data support the notion that Src kinase activity modulates constitutive Panx1-Y198 phosphorylation.

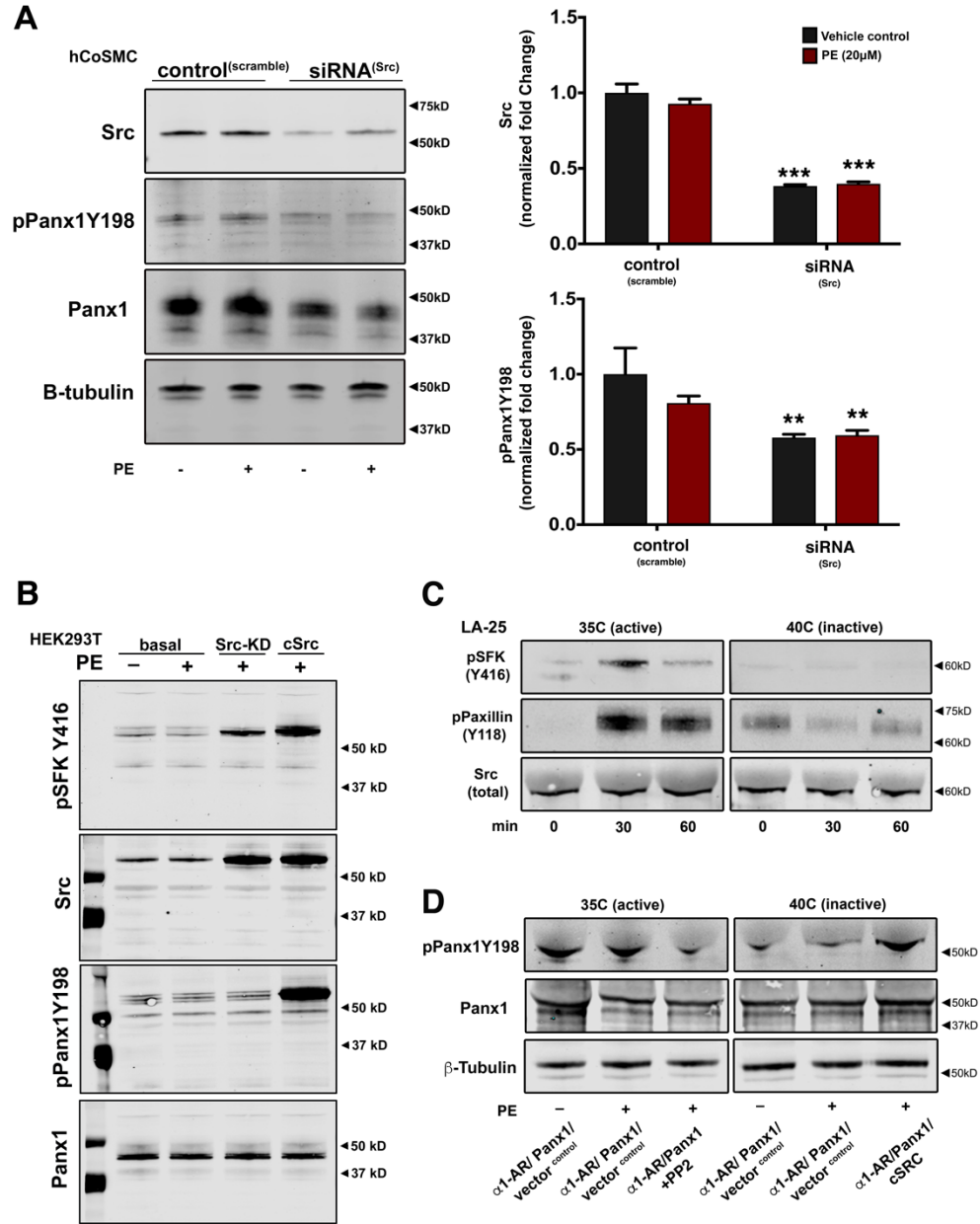


Figure 5. Src kinase activity modulates Pannexin 1 (Y198) phosphorylation.

Figure 5. Src kinase activity modulates Pannexin 1 (Y198) phosphorylation. (A) Representative western blot and quantification of Src kinase and pPanx1Y198 following siRNA-mediated knockdown of Src in hCoSMCs stimulated with PE (20 μ M). Data quantification presented as fold change \pm s.e.m. Statistical analyses performed using one-way ANOVA. * $p < 0.05$, *** $p < 0.001$. (B) *in vitro* analysis of adrenergic-stimulated Pannexin 1 (Y198) phosphorylation in HEK293T cells co-expressing the α 1-AR and Pannexin 1. Overexpression of a constitutive Src kinase isoform (cSrc) or kinase dead (Src-KD) isoform influenced pPanx1Y198 signal. (C) Time course for Src kinase activation (35 $^{\circ}$ C) and inhibition (40 $^{\circ}$ C) using mutant temperature sensitive LA-25 cells. Src activity was validated using specific antibodies for the SFK activation residue (Y416) and a Src kinase specific phosphorylation site (Y118) on the focal adhesion protein paxillin. (D) Western blot analysis of Src kinase activity on pPanx1Y198 in LA-25 cells transfected with a combination of Pannexin 1, α 1-AR, empty vector, or constitutive Src kinase (cSRC). The SFK inhibitor PP2 (10 μ M) was used to inhibit the endogenous temperature-active Src kinase. Wild type cSrc expression rescued temperature-inactive Src activity.

Src kinase directly phosphorylates Pannexin 1 (Y198)

To determine if phosphorylation of Panx1-Y198 is directly mediated by Src kinase we performed an in vitro kinase assay using recombinant Panx1 protein¹⁹² and recombinant/active Src kinase (**Figure 6A-B**). It was first necessary to dephosphorylate purified recombinant Panx1 protein using lambda phosphatase treatment. Immunoblotting with antibodies for pan-phospho-tyrosine or pPanx1Y198 antibodies revealed basally phosphorylated substrates that could be completely de-phosphorylated using lambda phosphatase (**Figure 6A**). Following dephosphorylation, Panx1 protein (Lane 4) was subsequently incubated with constitutively active Src kinase (**Figure 6B**). The addition of Src restored detection of Panx1-Y198 phosphorylation (Lane 5). As a confirmation of Src activity, the Src-dependent Panx1-Y308 phospho-site was also detectable, as supported by published literature²⁵². The presence of doublet patterns in our kinase assay was attributed to a glycosylation modification made in Sf9 cells during recombinant protein growth. To ensure doublets were due to glycosylation Panx1 was treated with N-glycosidase, which resulted in a single Panx1 species (**Figure 7**), as previously reported²⁵³. Based on these results, Src kinase directly phosphorylates Panx1 at Y198.

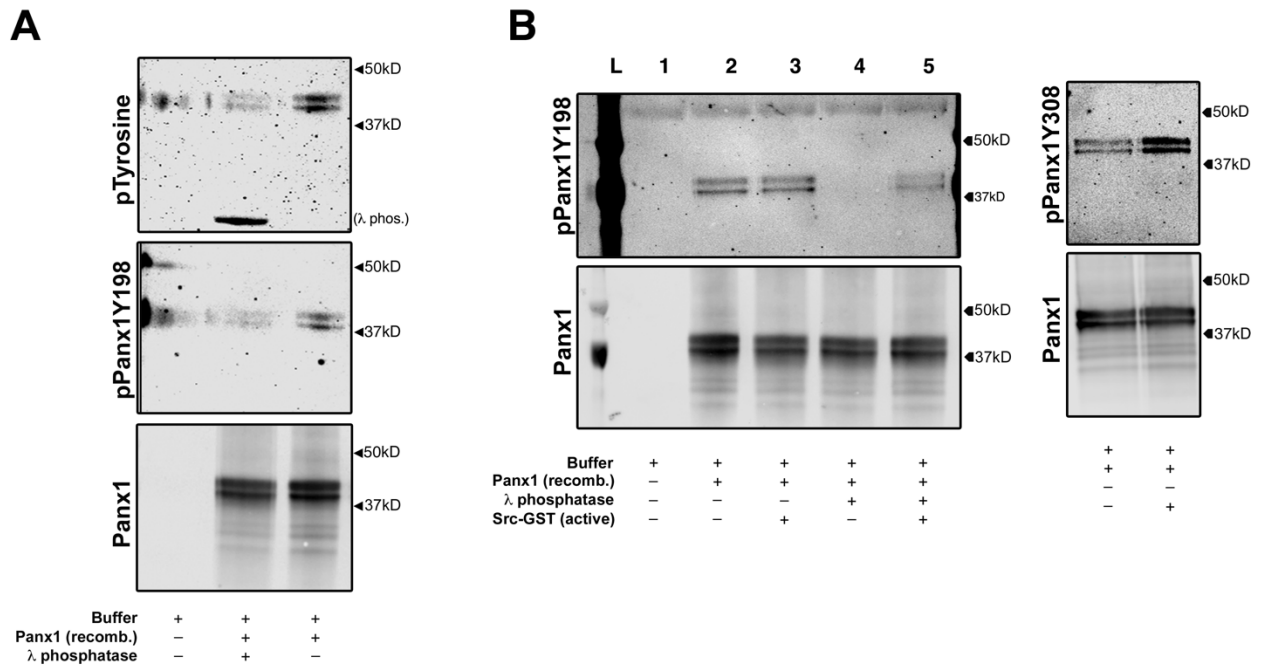


Figure 6. Src kinase directly phosphorylates Pannexin 1 (Y198).

Figure 6. Src kinase directly phosphorylates Pannexin 1 (Y198). (A) In vitro phospho-tyrosine analysis using pan-phospho-tyrosine antibody of recombinant Pannexin 1 protein treated with and without lambda phosphatase. Pannexin 1 (Y198) phosphorylation detected using pPanxY198 antibody. (B) In vitro Src kinase assay using de-phosphorylated recombinant Pannexin 1 with lambda phosphatase followed by sequential phosphorylation of Y198 residue using recombinant active Src kinase. Pannexin 1 (Y308) was assessed to validate Src activity (using pPanx1Y308 antibody).

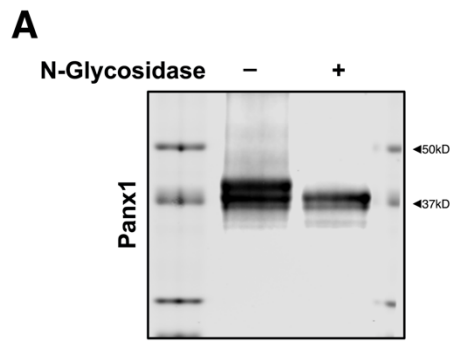


Figure 7. Supplement to Figure 6: Recombinant Pannexin 1 is glycosylated.

Figure 7. Supplement to Figure 6: Recombinant Pannexin 1 is glycosylated. (A) N-glycosidase treatment of recombinant Pannexin 1 shows double bands resultant from basal glycosylation in expression system rather than differential phosphorylation species.

Panx1-Y198 phosphorylation occurs at the plasma membrane of vascular smooth muscle cells

Functional Panx1 channels localize to the plasma membrane of VSMCs where they mediate cellular ATP release. To determine if phosphorylation of Panx1-Y198 corresponds with plasma membrane association, we performed membrane biotinylation and immunoprecipitation experiments in hCoSMCs (**Figure 8A-B**). Successful membrane biotinylation was confirmed using streptavidin conjugated antibodies after immunoprecipitation (**Figure 8A**). Panx1 protein was resolved in all VSMC fractions, with a proportion of low molecular weight Panx1 (endoplasmic reticulum-associated²⁵⁴) detected in whole cell lysates and cytoplasmic fractions, but not membrane-associated fractions. In support of Panx1-Y198 membrane-specific association, a single pPanx1Y198 band was highly enriched in immunoprecipitated fractions compared with whole cell lysates and was undetectable in cytoplasmic fractions (**Figure 8A**). When cells were stimulated with phenylephrine, there was no significant difference in Panx1-Y198 phosphorylation compared to vehicle treated controls (**Figure 8B**). Thus, constitutive phosphorylation of Panx1-Y198 likely occurs at the plasma membrane where it supports receptor-mediated channel activation.

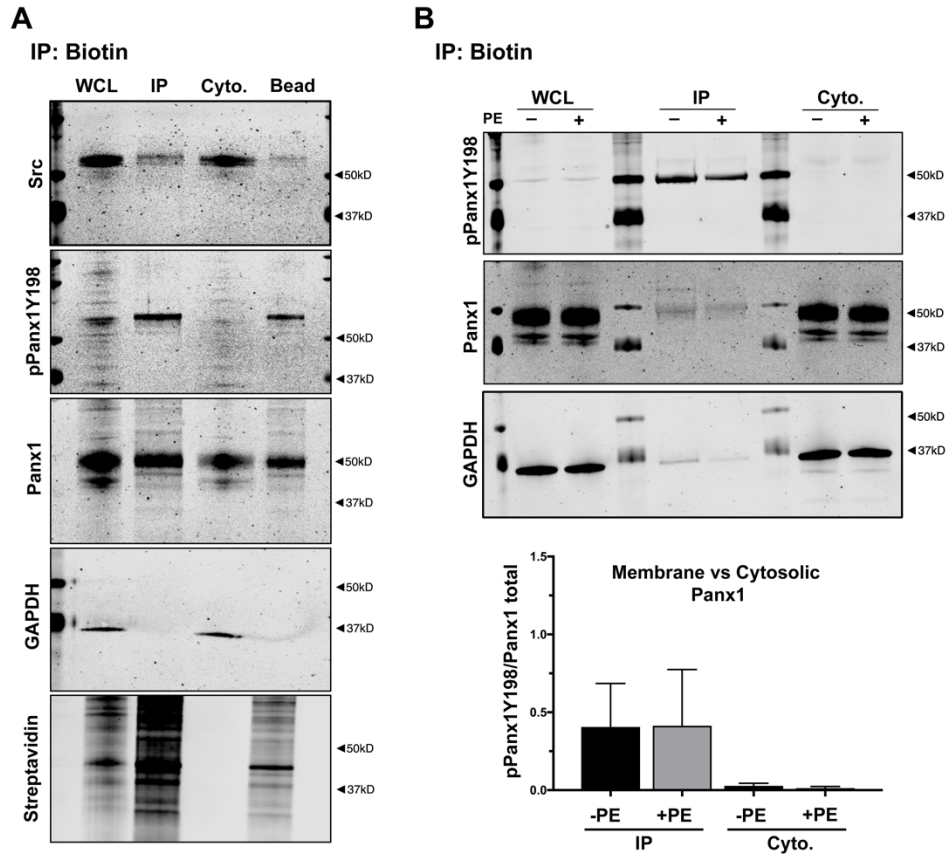


Figure 8. Pannexin1 (Y198) phosphorylation occurs at the plasma membrane in VSMCs.

Figure 8. Pannexin1 (Y198) phosphorylation occurs at the plasma membrane in VSMCs. (A) Isolation of plasma membrane proteins using membrane biotin immunoprecipitation in hCoSMCs. Phosphorylation of Pannexin 1 Y198 was assessed by western blot (pPanx1Y198) from whole cell lysate (WCL), membrane fraction (IP), cytoplasmic fraction (Cyto), or attached to isolation beads. Streptavidin conjugated antibodies were used to validate immunoprecipitation of membrane fractions. (B) Western blot analysis of membrane associated and cytoplasmic associated Pannexin 1 Y198 phosphorylation following phenylephrine stimulation (20 μ M) in hCoSMCs.

Membrane associated Panx1-Y198 is detectable in hypertensive human vessels

To further validate the finding that Src-mediated phosphorylation of Panx1-Y198 occurs at the plasma membrane, we transfected HeLa cells with a Panx1-GFP expression vector and assessed Panx1-Y198 phosphorylation at the plasma membrane. Panx1-Y198 resolved only at cell borders where it co-localized with Panx1-GFP (**Figure 9A-C**). From these findings we treated cells with PP2 to inhibit SFK activity and found a loss of pPanx1Y198 signal at the plasma membrane (**Figure 9B**). From these observations, we reasoned that the phospho-status of Panx1-Y198 was a specific marker for the pool of activatable plasma membrane-associated Panx1. Because VSMC Panx1 regulates α 1-AR-mediated vasoconstriction in resistance arteries, and since enhanced α 1-AR activation could contribute to hypertension (due to excessive sympathetic nerve activity) result in enhanced α 1-AR constriction, we tested human biopsy samples from normotensive and hypertensive (treatment-resistant) volunteers for Panx1 and phosphorylated Panx1-Y198. In hypertensive arteries, phosphorylated Panx1-Y198 was more prominently detected in the VSMC (SM α -actin positive) layer of arteries compared with normotensive arteries (**Figure 9 D-E**). No signal was detected in isotype controls. Moreover, the amount of Panx1 was found to be significantly increased in hypertensive arteries by immunolabeling (**Figure 10**). Thus, Panx1-Y198 phosphorylation is likely an important marker for the activatable pool of Panx1 channels at the plasma membrane and could be utilized to identify early vascular pathologies associated with sympathetic nerve-mediated hypertension.

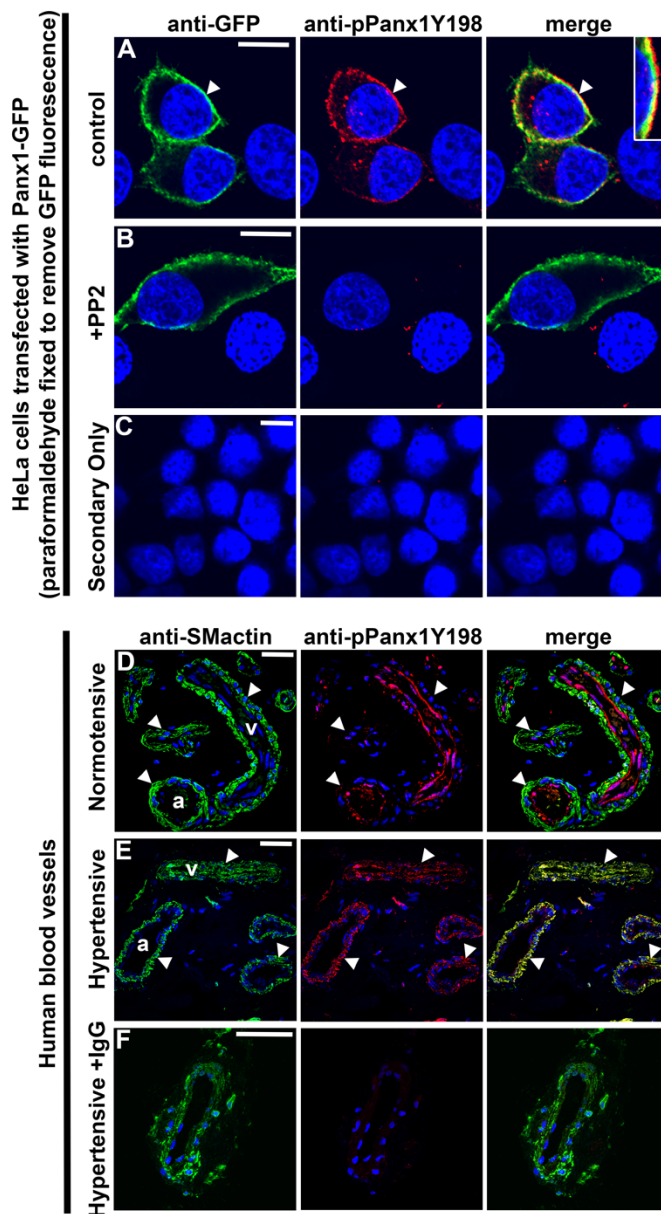


Figure 9. Src-dependent Panx1-Y198 phosphorylation occurs at the plasma membrane and is detectable in hypertensive arteries.

Figure 9. Src-dependent Panx1-Y198 phosphorylation (A) HeLa cells transfected with Panx1-GFP were treated with PP2 (10 μ M) or ATP (500 μ M) to inhibit SFK activity or internalize membrane associated Pannexin 1 respectively. Anti-GFP (green), pPanx1Y198 (red), nuclei (blue). Scale bar=10 μ m. (B) pPanx1Y198 detection in small vessels of human gluteal biopsies from normotensive or hypertensive patients. Smooth muscle α -actin positive cells (green), pPanx1Y198 (red), nuclei (blue). Asterisk denotes vessel lumen; artery (a); vein (v). Scale bar = 20 μ M

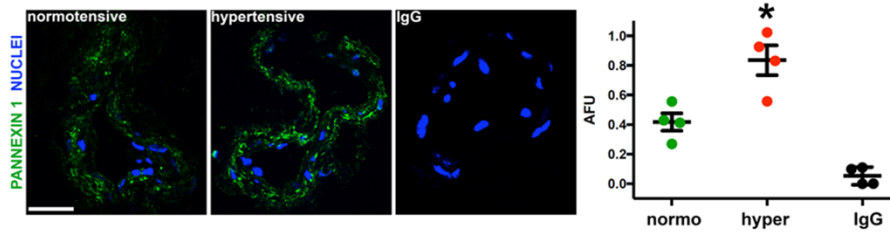


Figure 10. Supplement to Figure 9: Total Pannexin 1 expression is increased in human hypertensive vessels.

Figure 10. Supplement to Figure 9: Total Pannexin 1 expression is increased in human hypertensive vessels. Immunofluorescence analysis of total Pannexin 1 in human normotensive and hypertensive arteries isolated from gluteal biopsies. Pannexin 1 (green); nuclei (blue). Scale bar=20 μ m. Quantification of Pannexin 1 signal normalized to cell number. Data presented as mean \pm s.e.m. n=4 vessels (4 patients).

3.4. DISCUSSION

The present study demonstrates the direct phosphorylation of a critical amino acid residue (Y198) on the Panx1 intracellular loop by Src kinase in VSMCs and the sufficiency of SFK activity to modulate Panx1 channel function and adrenergic-mediated vasoconstriction. Moreover, we find that phosphorylation of the Panx1-Y198 residue by SFK activity is constitutive in nature and likely supports the initiation of purinergic signaling cascades (i.e. regulated ATP release) at the plasma membrane. We also demonstrate that enhanced VSMC Panx1 expression and Panx1-Y198 immunodetection correlates with a hypertensive vascular phenotype. Thus, our study connects two observations from the Pannexin field and the vascular biology field. The first is the modulation of Panx1 function by SFK activity in VSMCs. The second is a possible connection between Panx1-mediated ATP release and a tyrosine kinase-based α 1-AR-mediated vasoconstriction mechanism that was previously identified to influence hemodynamics in the resistance vasculature^{14-16,18,47-51}.

Currently, there are two main mechanisms ascribed to the activation of Panx1 channels following physiologic stimuli. The first mechanism is a non-reversible cleavage event of Panx1 C-terminal tails, which results in constitutive release of ATP during apoptosis^{182, 255}. The second mechanism is a reversible receptor-mediated activation of Panx1 channels by ligand gated signaling^{41, 189, 190, 238, 246, 248, 256-258}. Previous work from our lab has established a significant role for receptor-mediated Panx1 channel function in the vascular wall^{225, 238, 246}, which in VSMCs specifically couples with adrenergic stimulated events, but not with other vasoconstriction pathways²²⁵. We hypothesized that purinergic

signaling facilitates autocrine/paracrine coupling of VSMCs during tonic constriction in small resistance arteries where Panx1 is highly expressed⁷⁶.

At first, it was unclear if intracellular calcium was necessary for adrenergic-stimulated ATP release from VSMCs. Under physiologic conditions VSMCs require a rise in intracellular calcium to activate calcium-sensitive kinases and to allow contractile proteins to engage with each other, thus producing a contractile force²⁵⁹. To test the importance of calcium during adrenergic-stimulated ATP release, we measured extracellular ATP after PE stimulation from intact resistance arteries (**Figure 1A**). ATP release was unaffected by the membrane permeable calcium chelating agent BAPTA-AM indicating that VSMC Panx1 does not require intracellular calcium to function in this context and likely occurs in the early stages of adrenergic signaling events. We cannot exclude the possibility that calcium sensitive kinases, such as those involved in the canonical RhoA/ROCK sensitization pathway²⁶⁰, may further potentiate Panx1 channel opening after initial activation, although this remains to be specifically tested. In the literature, evidence of Panx1 channel gating by intracellular calcium is unclear. A handful of studies link Panx1 channel function directly to increases in intracellular calcium using ionophores¹⁸⁸, or indirectly through serotonin receptor agonism²⁶¹ or thrombin receptor activation^{189, 190}. From these studies it remains to be shown if changes in intracellular calcium directly influence Panx1 gating, or if another calcium-dependent process facilitates channel activation. In particular, calcium requirements during thrombin induced ATP release from lung epithelial cells was necessary, but not sufficient on its own to elicit a response¹⁹⁰. A similar observation was made in vein endothelial cells, in which BAPTA-AM treatment blunted thrombin induced ATP release in a similar fashion to responses from

Panx1 shRNA treated cells¹⁸⁹. Thus, a definitive calcium requirement for Panx1 channel gating has yet to be clearly delineated.

On the other hand, a number of published studies have demonstrated calcium-independent activation of Panx1 channels either by directly manipulating intracellular and extracellular calcium²⁴⁹, or through activation of P2X7 receptors^{250, 262} or NMDA receptors^{194,248}. Our observations in VSMCs and in resistance arteries support observations in these latter studies, which observed a calcium-independent function of Panx1 channels. Interestingly, the studies evidencing calcium-independent Panx1 activation have also demonstrated mechanistic regulation of Panx1 activity by tyrosine kinase activity. Thus, the necessity for increased calcium during Panx1 activation may reflect either cell-type specific or receptor-specific characteristics, that as of yet, remain to be shown.

Due to the insufficiency for intracellular calcium to influence ATP release in our *ex vivo* arterial system, we proposed that posttranslational modifications might regulate Panx1 function. A large body of evidence points to regulation of Panx1 channels by phosphorylation, predominantly tyrosine phosphorylation by Src family kinases^{194, 246, 248, 263, 264}. Moreover, in resistance arteries a tyrosine kinase-based adrenergic signaling mechanism significantly modulates tonic and phasic constriction responses to both phenylephrine and norepinephrine in different animal models^{207-209, 243-245, 265-267}. Inhibition of adrenergic constriction by tyrosine kinase inhibitors is reversible and has no direct effect on calcium-induced constriction, PKA activity, or myosin light chain kinase activity^{243, 244}. Thus, there is a strong correlation between tyrosine kinase-regulated adrenergic vasoconstriction and SFK-dependent Panx1 channel activity. In line with these studies, our

laboratory mapped and identified a regulatory region on the intracellular loop of Panx1 using mimetic peptides, VSMC-specific Panx1 knock out mice, and mutated Panx1 expression vectors²²⁵. In this current study we performed eukaryotic linear motif scanning on human (Y199-K201) and mouse (Y198-K200) Panx1 sequences²⁶⁸. We detected a putative Src homology-2 domain within the same Panx1 regulatory motif (YLK) from our previous investigation, as well as a Src homology 3 proline rich motif upstream of this regulatory motif (**Figure 1B**). SH2 and SH3 domains regulate intra- and intermolecular interactions necessary for SFK catalytic activity, localization, and recruitment of substrates²⁶⁹⁻²⁷⁵. The presence of these sequences on the Panx1 intracellular loop point to a role for SFK activity in channel function.

To test the dependence of Panx1-mediated ATP release and vasoconstriction for SFK activity, we stimulated *ex vivo* arteries with PE or NE in the presence of the SFK inhibitor PP2 and the FDA approved SRC/ABL kinase inhibitor dasatinib. Our results show that PE and NE stimulated ATP release is dependent on SFK activity in our model (**Figure 1C**), and similarly influences vasoconstriction responses in our pressure myography experiments (**Figure 1D, E, F, G**). Our findings confirm observations by Di Salvo et al. and others^{207-209, 225, 243-245, 265-267} who discovered and elaborated on a unique tyrosine kinase mediated VSMC pathway that regulates adrenergic constriction. Although our mechanistic understanding of receptor-mediated Panx1 activation remains limited, published reports evidence the potential for GPCRs to directly activate tyrosine kinases through guanine nucleotide exchange factor (GEF) interactions²⁷⁶⁻²⁷⁸. These signals could also transactivate growth/proliferation pathways through Src kinase^{245, 279}. Thus, a secondary pathway might exist in VSMCs that can regulate adrenergic-mediated responses in a non-traditional way.

Pathologically, this alternative pathway may contribute to vascular remodeling associated with human neurogenic/resistant hypertension^{7, 280}. For example, norepinephrine induced signaling has been shown to contribute to VSMC hypertrophy through trans-activation of Src kinase/ STAT3/ and MAPK pathways²⁷⁹. In line with these observations, we found a significant increase in Panx1 immunostaining in small vessels of treatment resistant hypertensive patients, as well as detection of pPanx1-Y198 phosphorylation in VSMCs (**Figure 9 & Figure 10**).

Moreover, GPCR-mediated tyrosine kinase activity may be a common mechanism for regulating cellular ATP release by Panx1. Although our VSMC models demonstrate a unique role for α -adrenergic receptors, but not serotonin or endothelin receptors in Panx1 function, we do not exclude the possibility that other cell types may couple Panx1 to these GPCRs in unique ways. Serotonin receptors, which can also activate SFKs (e.g. FYN)²⁸¹ and have been reported to activate Panx1 channels in carotid body cells²⁶¹. Evidence for angiotensin II receptor type 1 (AT1R) activation of Panx1 channels has also been implicated in carotid body cells²⁸² and in renal mesangial cells²⁸³. AT1R stimulation results in VSMC constriction, which can directly influence Src kinase activity leading to focal adhesion remodeling²⁸⁴, growth²⁸⁵, and VSMC proliferation²⁸⁶. At this time, it is unknown if AT1R activation can induce Panx1-channel activity in VSMCs, or if the AT1R and the α 1-AR share a common tyrosine kinase-mediated mechanism, but it would be interesting if $G\alpha_q$ signaling proteins were directly involved in this process.

Having established the involvement of tyrosine kinases in PE and NE-induced ATP release and vasoconstriction, we hypothesized that phosphorylation of the Panx1 tyrosine

residue (Y198), which resides in the SH2 domain, is likely mediated by SFKs. To resolve phosphorylated Panx1-Y198 we generated a phospho-antibody (pPanx1Y198), which generated a Panx1 specific band at a molecular weight corresponding to high-glycosylated (plasma membrane associated) Panx1 (**Figure 3 and Figure 4**)¹⁷². Moreover, the pPanx1Y198 signal was sensitive to phosphatase treatment and could not be detected in cells expressing the Panx1 point-mutant (Y198F) (**Figure 4A**). Using differentiated hCoSMCs, which express Panx1 and Src kinase (**Figure 3A**), we found that Panx1-Y198 was constitutively phosphorylated under basal and stimulated conditions (**Figure 3B**). Surprisingly, the addition of an adrenergic stimulus did not enhance Panx1-Y198 phosphorylation, but as hypothesized, required SFK activity (**Figure 3C and Figure 4B**). These results then suggest that while adrenergic-induced Panx1 activation requires constitutive phosphorylation at Y198, another site is likely responsible for direct channel gating. In hippocampal neurons, the Panx1-Y308 residue on the C-terminal tail was required for receptor-mediated Panx1 activation by NMDA receptor agonism, and that phosphorylation of Y308, activation of Panx1 currents, and ATP release was similarly sensitive to SFK inhibition^{194, 248}. Moreover, we cannot exclude the possibility that other non-tyrosine kinases contribute to activation state of Panx1 channels, although this was not assessed in our analysis. In the literature, c-Jun N-terminal kinase and protein kinase G have been implicated in regulating Panx1 channel activity^{287, 288}. As with the connexin family of proteins, regulation of Panx1 proteins by multi-phosphorylation could provide a central hypothesis to describe the myriad of physiological states in which Panx1 channels seem to function²⁸⁹⁻²⁹¹ and also describe the complex regulation of reversible channel gating by the C-terminal tail^{182, 183}. Phosphorylation of Panx1-Y198 could facilitate

selective binding of signaling proteins necessary for post-translational modification of C-terminal residues, which subsequently gate Panx1 channel activity, but this remains to be tested. In the literature a quantized mechanism for C-terminal channel regulation has emerged which support this concept, whereby individual regulation of C-terminal tails on oligomerized Panx1 subunits can differentially influence both receptor-independent and receptor-dependent functionality¹⁹².

Due to the constitutive nature of Panx1-Y198 phosphorylation and the necessity for tyrosine phosphorylation during adrenergic vasoconstriction, we next determined if the archetypal Src tyrosine kinase was responsible Panx1-Y198 phosphorylation. The Src family of tyrosine kinases includes nine isoforms that are expressed in mammalian cells with each kinase composed of a catalytic domain, a SH2 domain, a SH3 proline rich domain, and a unique domain for which each isoform is named ²⁹²⁻²⁹⁴. This large kinase family can be broken down into two divisions: the isoforms Src, Fyn, and Yes are ubiquitously expressed, while the isoforms Blk, Fgr, Hck, Lck, and Lyn are primarily expressed in hemopoietic cells²⁹⁴. In VSMCs Src, Fyn, and Yes activity has been directly linked to focal adhesion dynamics^{209, 295, 296} and VSMC growth/proliferation signaling^{285, 297}. We selected Src kinase because of its causal link in regulating Panx1 channel function, but also because Src activity is linked with constriction of VSMC in a number of contexts^{207-209, 243-245, 265-267}. To test the contribution of Src kinase to phosphorylate Panx1-Y198 we utilized Src kinase specific siRNA in VSMCs, catalytically dominant or kinase dead Src isoforms in HEK cells, and a temperature sensitive Src kinase cell line (LA-25) to specifically modulate kinase activity during adrenergic stimulation (**Figure 5A-C**). Consistent with experimental outcomes using pharmacological inhibitors, we show that

constitutive phosphorylation of Panx1-Y198 is directly mediated by Src activity. Moreover, we confirmed the direct phosphorylation of Panx1-Y198 by Src using recombinant Panx1 protein, constitutively-active recombinant Src kinase, and in-vitro kinase assays (**Figure 6A-B**). In this set of experiments, recombinant and glycosylated Panx1 was de-phosphorylated with lambda phosphatase and could be re-phosphorylated at the Y198 residue with the addition of active Src kinase. Our results are consistent with published findings, in which NMDA-receptor agonism leads to formation of a metabotropic signaling complex in neurons between Panx1, Src kinase, and GluN1 subunits, resulting in phosphorylation of tyrosine 308 on the Panx1 C-terminus and channel activation²⁵². Moreover, we confirmed tyrosine 308 phosphorylation in our assays, thus confirming published observations²⁵². We conclude that Panx1-Y198 is a direct post-translational modification target of Src kinase, which may facilitate multi-phosphorylation modifications, kinase binding, and channel activity—although this remains to be directly tested.

Lastly, we investigated if the Panx1-Y198 phospho-species localizes to the plasma membrane. Western blot analysis of Panx1-Y198 revealed the presence of a specific high molecular weight (~50-55kDa) Panx1 band, indicative of plasma membrane association²⁹⁸. In our membrane biotinylation experiments Panx1-Y198 was only detectable in membrane fractions and not in cytoplasmic fractions of both basally and adrenergic stimulated conditions (**Figure 8A-B**). These results were confirmed in cells expressing Panx1-GFP, in which membrane associated Panx1 co-localized with Panx1-Y198 immunostaining (**Figure 9A**). Since activation of α 1-ARs and ATP release occur at the plasma membrane, we presumed that a regulatory role for Panx1-Y198 would spatially

correlate with SFK effectors. A distinct pool of membrane-associated Src kinase also localizes to the plasma membrane by both myristoylation at the N-terminus ²⁹⁹ and molecular interactions with the caveolae scaffold protein, caveolin-1 ²⁶⁶. Recent evidence from our laboratory demonstrated an important interaction between Panx1 and caveolin-1 at the plasma membrane, which influenced channel function, adrenergic-mediated ATP release, and mean arterial pressure ²⁴². These data then suggest that interactions between Panx1 and membrane associated kinases (e.g. Src), which aggregate at unique plasma membrane domains likely supports receptor-mediated activation by placing VSMC effector molecules in close apposition with sympathetic nerves. Phosphorylation of Panx1-Y198 thus defines a distinct pool of Panx1 channels that can be activated by either Src kinase itself, or by an as of yet identified effector molecule.

Overall, our data confirm previous observations in the vasculature, in which SFKs specifically mediate adrenergic-mediated vasoconstriction and regulate extracellular ATP release by Panx1. We demonstrate that phosphorylation of the Panx1 regulatory motif at tyrosine 198 (Y198), by Src kinase, is both constitutive and required for activation by adrenergic receptors in VSMCs. The phosphorylation of Y198 likely supports activation of Panx1 channels by other kinases, which can utilize Y198 phosphorylation to localize and bind to the intracellular loop of Panx1. These data link the long-standing observation of tyrosine kinase-based adrenergic constriction with adrenergic-stimulated ATP release through the supportive activation of Panx1 channels. In the pathological context of human resistant hypertension, a Panx1-mediated constriction pathway may contribute to dysfunctional hemodynamics. The phosphorylation state of Panx1-Y198 is therefore an important marker for the distinct pool of membrane associated Panx1 that can be activated

by receptor-dependent stimuli and might be useful as a quantitative biomarker for hypertensive vascular remodeling.

CHAPTER 4. INTERACTION BETWEEN PANNEXIN 1 AND CAVEOLIN-1 IN SMOOTH MUSCLE CAN REGULATE BLOOD PRESSURE

4.1 ABSTRACT

Sympathetic nerve innervation of vascular smooth muscle cells (VSMCs) is a major regulator of arteriolar vasoconstriction, total peripheral resistance, and blood pressure (BP). Importantly, α -adrenergic receptors localize to the caveolar scaffold protein, caveolin-1, which is crucial for activation of adrenergic vasoconstriction. We have previously shown that Pannexin 1 (Panx1) channels uniquely couple with α -adrenergic receptors on VSMCs and mediate vasoconstriction through regulated ATP release. We hypothesize that localization of Panx1 to caveolin-1 promotes Panx1 channel function (stimulus-dependent ATP release and adrenergic vasoconstriction) and is important for BP homeostasis. We report that Panx1 and caveolin-1 co-localized on the VSMC plasma membrane of resistance arteries in an adrenergic stimulus-dependent manner. The onset of co-localization events was rapid (~30s) and occurs in apposition to areas of sympathetic nerve innervation following phenylephrine stimulation. To assess the functional importance of VSMC-derived caveolin-1 during adrenergic-mediated ATP release and vasoconstriction, we genetically deleted caveolin-1 using an inducible VSMC-specific mouse model. Deletion of VSMC caveolin-1 significantly blunted adrenergic-stimulated ATP release and vasoconstriction, with no direct influence on endothelium-dependent vasodilation or cardiac function. A significant reduction in mean arterial pressure (Total=

4 mmHg; Night= 7 mmHg) occurred in mice deficient for VSMC caveolin-1. These animals were resistant to further BP lowering using a Panx1 peptide inhibitor PxIL2P1, which targets an intracellular loop region necessary for channel function. We conclude that the translocation of Panx1 to caveolin-1 in VSMCs augments the release of purinergic stimuli necessary for proper adrenergic mediated vasoconstriction and BP homeostasis.

4.2 INTRODUCTION

In the peripheral circulatory system, blood pressure (BP) homeostasis is largely regulated by the contractile state of the smooth muscle cells (VSMCs) in the wall of resistance vessels. These vessels are small diameter ($\leq 200 \mu\text{m}$) arteries and arterioles that are composed of an intimal endothelial layer, a tunica media consisting of one to two VSMC layers³⁰⁰, and are functionally defined by the ability to respond to changes in intraluminal pressure to control vascular resistance and blood flow. Sympathetic nerve innervation of VSMCs is a major regulatory pathway that induces VSMC constriction, thus altering arteriolar lumen diameter and increasing the amount of vascular resistance^{301, 302}. While much is already known about the induction of rapid (purinergic) and potentiated (adrenergic) sympathetic nerve-derived stimuli on function of resistance arteries⁶², less is known about the identity of downstream VSMC signaling molecules that subsequently coordinate VSMC-derived stimuli in the arteriolar wall. Signaling through α -adrenergic receptors (α -ARs) and activation of plasma membrane-associated signaling molecules may be compartmentalized by caveolae near areas of sympathetic innervation^{301, 303-306}.

Caveolae are specialized plasma membrane domains that play an important role in intracellular signaling, cellular transport, and differentiation³⁰⁷⁻³⁰⁹. Caveolae are defined by their hallmark plasma membrane morphology, consisting of 80-100nm-wide membrane invaginations, and by their composition of oligomeric coat-forming proteins called caveolins³¹⁰. Of the three caveolin isoforms, caveolin-1 is essential for caveolae formation and function³¹¹⁻³¹³. Caveolin-1 has been shown to regulate vasoconstrictive responses in small arterioles and to influence BP homeostasis in animal models^{311, 314-316}. Importantly,

caveolin-1 is expressed in VSMCs of small arteries and acts as a membrane-scaffold protein for both α -ARs and downstream G-protein dependent vasoconstriction signaling molecules^{317, 318}, suggestive of a role in adrenergic-mediated vasoconstriction.

Recently, our group and others^{225, 238, 319, 320} have elucidated in mouse and humans an α -AR signaling axis that activates Pannexin 1 channels. Pannexins are a family of transmembrane channel-forming glycoproteins that have emerged as the physiological conduit for controlled ATP release from vascular and non-vascular cell types^{181, 197, 255}. We have previously reported that Panx1 expression is polarized within the vascular tree, with high expression levels in VSMCs of resistance arteries (e.g. mesenteric, cremasteric, thoracodorsal, and coronary), but is not present in large conduit vessels such as the femoral and carotid arteries, and the aorta⁷⁶. This expression pattern suggests a unique role for Panx1 in regulating vascular resistance. Using Panx1 pharmacological inhibitors and inducible VSMC-specific Panx1 knockout mice, we have further demonstrated that Panx1-mediated ATP release and vasoconstriction are uniquely coupled with α -adrenergic stimulation and are crucial for maintaining BP homeostasis^{225, 238}. Multiple groups have confirmed the activation of Panx1 channels by α -adrenergic stimulation^{192, 241, 321}, thus demonstrating ATP release through Panx1 as a significant physiological pathway for integrating and coordinating VSMC-derived constriction responses^{62, 72}.

In the present study, we hypothesized that caveolin-1 acts as a molecular scaffold that concentrates VSMC Panx1 to areas important for sympathetic nerve innervation, thus facilitating α -adrenergic mediated vasoconstriction and BP homeostasis. In response to the α -adrenergic agonist phenylephrine we observed a novel interaction and co-localization of

caveolin-1 and Panx1 to regions of innervation at the VSMC plasma membrane. To investigate the functional role of caveolin-1 during α -adrenergic mediated responses, we generated an inducible, VSMC-specific caveolin-1 knockout mouse model. We show that VSMC-derived caveolin-1 is required for α -adrenergic stimulated ATP release and adrenergic vasoconstriction. Deletion of VSMC caveolin-1 results in a significant reduction in mean arterial BP, particularly during the nocturnal (active) period when sympathetic drive is high. Furthermore, we suggest that caveolin-1 mediated BP effects are regulated through the Panx1 intracellular loop regulatory domain, previously identified to be indispensable for α -adrenergic vasoconstriction²²⁵.

4.3 RESULTS

Caveolae are specialized plasma membrane domains that facilitate interactions between signaling proteins (i.e. $G_{\alpha q}$, PLC, Src, etc^{266, 310, 322}) and membrane receptors (i.e. α -adrenergic receptors³²²). These structures are found in endothelium and smooth muscle; however, their signaling functions are much less studied in smooth muscle. In electron micrographs, we consistently observe caveolae contained in arteriolar smooth muscle in proximity to sympathetic nerves (**Figure 11**). For this reason, we hypothesized that the caveolin-1 protein, the main component to caveolae, may associate with Panx1, which is activated in response to adrenergic stimulation.

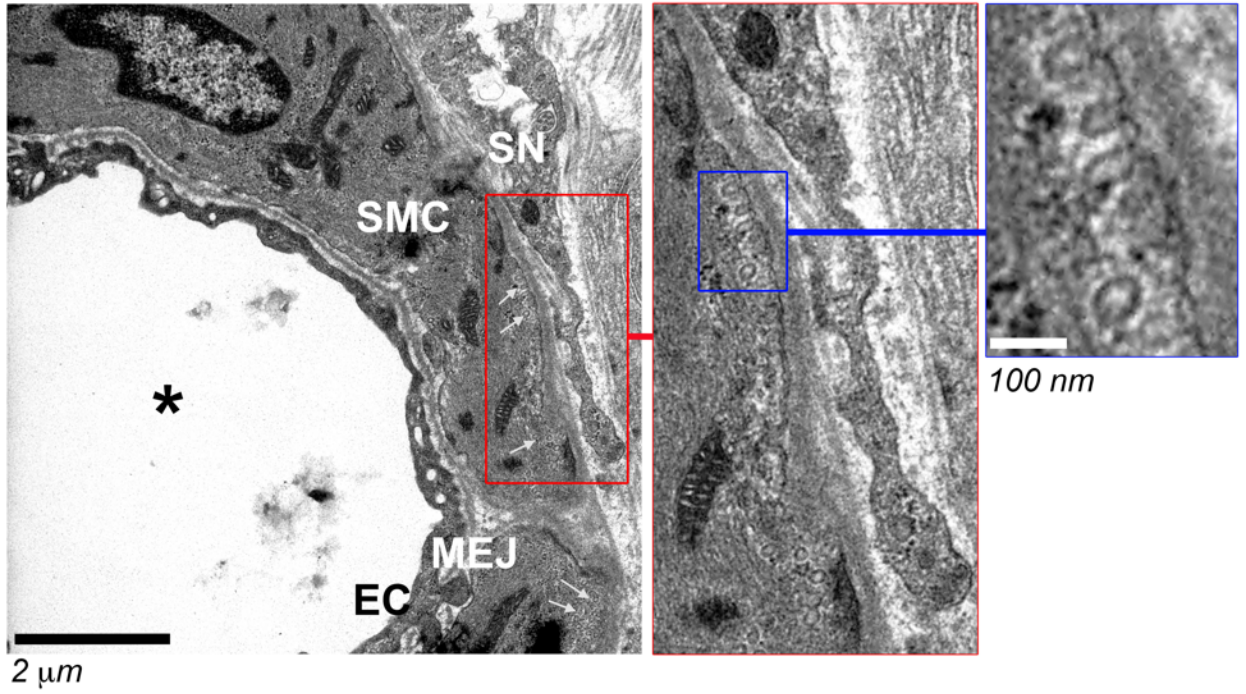


Figure 11. Caveolae in VSMC localized adjacently to sympathetic nerves.

Figure 11. Caveolae in VSMC localized adjacently to sympathetic nerves. Representative transmission electron microscopy image of terminal arteriole in mesenteric circulation. Lumen indicated by asterisk. White arrows indicate VSMC clustered membrane caveolae. Red box denotes area of VSMC-sympathetic nerve boundary containing caveolae.

In initial experiments, we performed live-cell confocal microscopy using *in vitro* human VSMC culture systems to measure the distribution and co-localization of exogenously expressed RFP-tagged Panx1 and GFP-tagged caveolin-1 following phenylephrine stimulation (**Figure 12A**). Baseline fluorescence measurements were recorded for 2 min prior to stimulation with phenylephrine (100 $\mu\text{mol/L}$), vehicle control, or high concentration ATP (500 $\mu\text{mol/L}$) to promote Panx1 internalization. A significant co-distribution was observed between caveolin-1 and Panx1 at 30 seconds of phenylephrine stimulation at the plasma membrane (**Figure 12A-B**), which persisted above control fluorescence, although not to statistically significant levels (**Figure 12B-C**). Conversely, treatment with high-concentration ATP caused a significant and continuous reduction in co-localized signal, consistent with internalization and loss of Panx1 on the cell surface^{262, 323} that is independent of caveolin-1 mediated endocytosis²²². Vehicle control-treated cells showed no changes in fluorescence co-localization from baseline.

To confirm observations from live-cell imaging experiments, we next performed *in vitro* cell fractionation and co-immunoprecipitation assays using *in vitro* VSMC culture systems to probe for endogenous interactions between Panx1 and caveolin-1 at the plasma membrane. We found that caveolin-1 and Panx1 localize to membrane-associated fractions (**Figure 12D**) and specifically overlap in caveolin-1-enriched sucrose-gradient fractions, suggesting partial localization of Panx1 to lipid microdomains containing caveolin-1 (**Figure 12E**). To determine if caveolin-1 and Panx1 interact following adrenergic stimulation, we acutely treated VSMCs with phenylephrine (20 $\mu\text{mol/L}$). Fractions enriched or deficient in caveolin-1 were isolated and Panx1 was precipitated using a protein specific antibody²⁰⁵. We found that caveolin-1 from enriched fractions significantly co-

precipitated with Panx1 after adrenergic stimulation (**Figure 12F**), suggesting that plasma membrane complexes containing caveolin-1 and Panx1 form following adrenergic stimulation and may act to facilitate channel function.

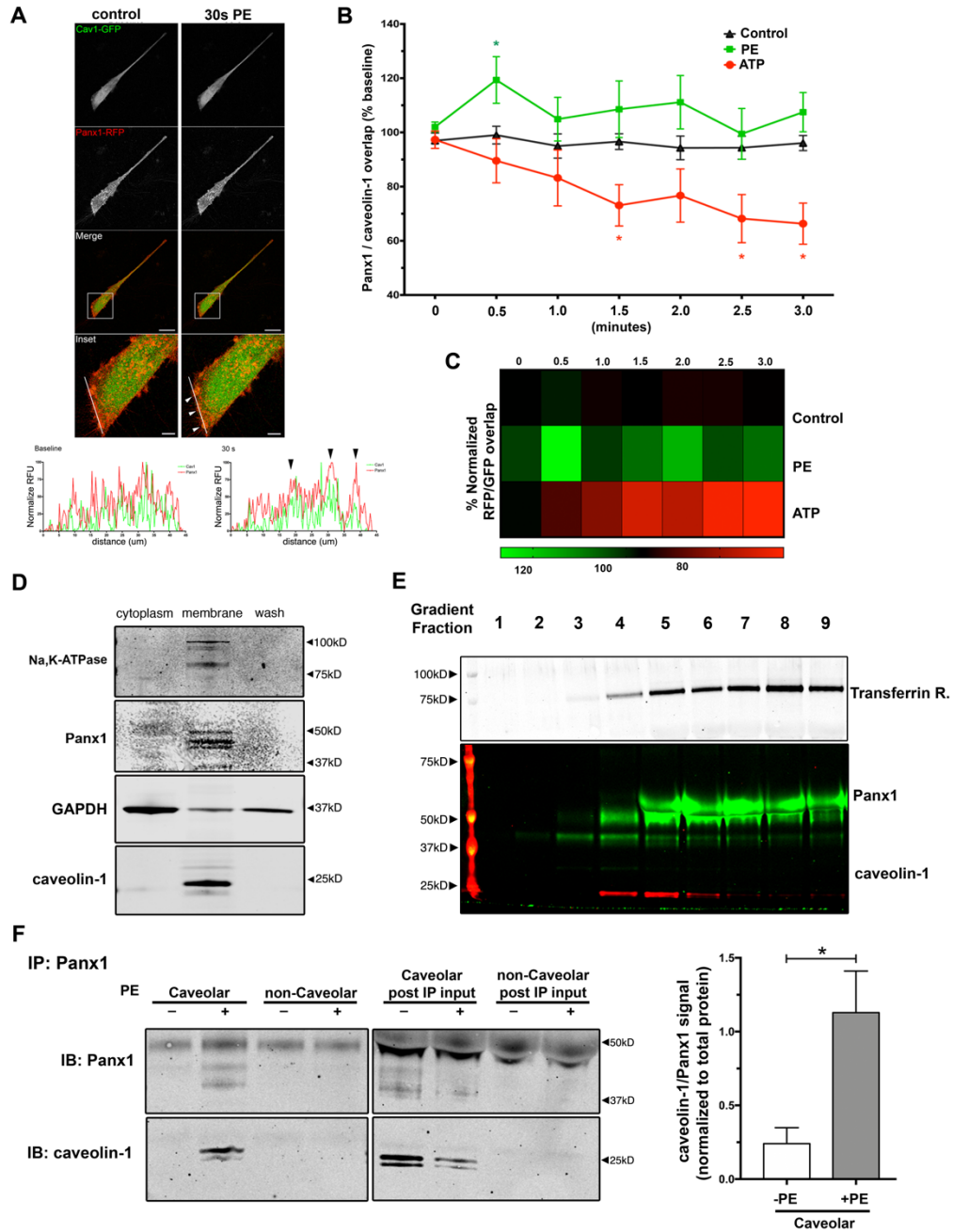


Figure 12. Pannexin 1 and caveolin-1 only associate after phenylephrine stimulation.

Figure 12. Pannexin 1 and caveolin-1 only associate after phenylephrine stimulation.

(A) Confocal images and line scan analysis of cultured human VSMCs expressing Panx1-RFP and caveolin-1 GFP following phenylephrine stimulation. Scale bar; 50 μm (low-magnification) and 10 μm (high-magnification). **(B)** Co-localization analysis of continuous time lapse confocal imaging in human VSMCs throughout acute stimulation (total time= 3 min) with vehicle control (black line; n=11), 500 $\mu\text{mol/L}$ ATP control (red line; n=5), or 100 $\mu\text{mol/L}$ phenylephrine (green line; n=10). * $p < 0.05$ compared to vehicle control using two-way ANOVA with Dunnett's posthoc. **(C)** Heat map representation of percent fluorescence co-distribution using Mander's coefficient analysis and normalized to baseline (green=positive association; red=negative association). **(D)** Membrane fractionation and western analysis of VSMCs showing endogenous distribution of Panx1 and caveolin-1 in membrane fractions. **(E)** Subcellular distribution of caveolin-1 enriched membrane domains in sodium carbonate-based detergent-free cellular fractionation using a discontinuous sucrose gradient (5%-40%), analyzed by immunoblot. Panx1 co-fractionates with caveolin-1 in lipid light rafts at the plasma membrane. **(F)** Co-immunoprecipitation and quantification of Panx1 and caveolin-1 from subcellular plasma membrane domains was measured following phenylephrine stimulation, n=5. Data analyzed by student's t-test and presented as mean \pm SEM. * $p < 0.05$.

Panx1-mediated ATP release and subsequent vasoconstriction are specifically mediated through α -AR activation^{192, 225, 238, 241, 321}. Based on our initial observations and the *in vitro* biochemical findings herein, we first tested if caveolin-1 and Panx1 similarly interact in VSMCs of *ex-vivo* isolated mouse resistance arteries. We performed proximity ligation assays (PLA) between Panx1 and caveolin-1 on TDAs having first assessed the focal plane where sympathetic nerves innervate VSMC using optical sectioning of the Z plane with a confocal microscope (**Figure 13**). Sympathetic nerves were specifically labeled with tyrosine hydroxylase. Nuclei were labeled with DAPI. On the abluminal (outer) side of the vessel wall (adventitia side) there was abundant sympathetic nerve innervation that became progressively less abundant further into the optical Z plane. Analysis was performed at the interface of sympathetic nerves and VSMCs (red box), which could be identified by their spindle shape and perpendicular arrangement to the cobble-stone shaped endothelial cells.

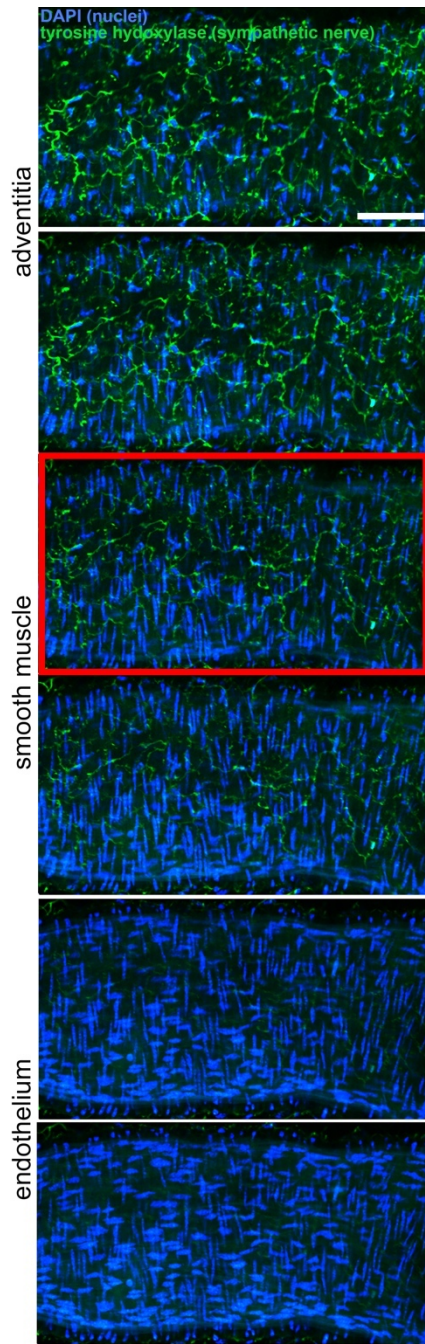


Figure 13. Z plane analysis of VSMC innervation on resistance arteries using confocal microscopy.

Figure 13. Z plane analysis of VSMC innervation on resistance arteries using confocal microscopy. Confocal optical sectioning of *en face* resistance artery used for PLA analysis. Sympathetic nerves were identified by specifically staining for tyrosine hydroxylase (green). Nuclei were stained with DAPI (blue). Optical sectioning from the outer adventitia through the vascular wall shows hallmark (circumferential) spindle shape of VSMCs, which run perpendicular to intimal endothelial cells. Red box indicates optical plane of VSMC-sympathetic nerve boundary for PLA analysis. Scale bar; 50 μ m.

In control experiments using PLA secondary antibodies alone or IgG controls, we could not detect PLA punctate signals (red puncta indicate protein associations when PLA probes <40nm in apposition) – only sympathetic nerves could be viewed (**Figure 14A-B**). Next, we performed PLA for caveolin-1 and Panx1. Here we observed relatively few positive red punctate signals under control conditions (**Figure 14C**); however, following acute (1 min) phenylephrine stimulation (20 μ mol/L), we observed an induction of PLA signal, which predominantly localized at the VSMC plasma membrane near areas of sympathetic nerve innervation (**Figure 14D-E**). As a control, TDA smooth muscle and sympathetic nerves were also analyzed for Cx43 expression, but it was not detected (**Figure 15**). The neuronal vesicular nucleotide transporter (VNUT) was also analyzed, but was only observed in sympathetic nerves, and not VSMCs as anticipated (**Figure 15**). These data demonstrate the formation of potential signaling microdomains where caveolin-1 and Panx1 are recruited together following adrenergic stimulation.

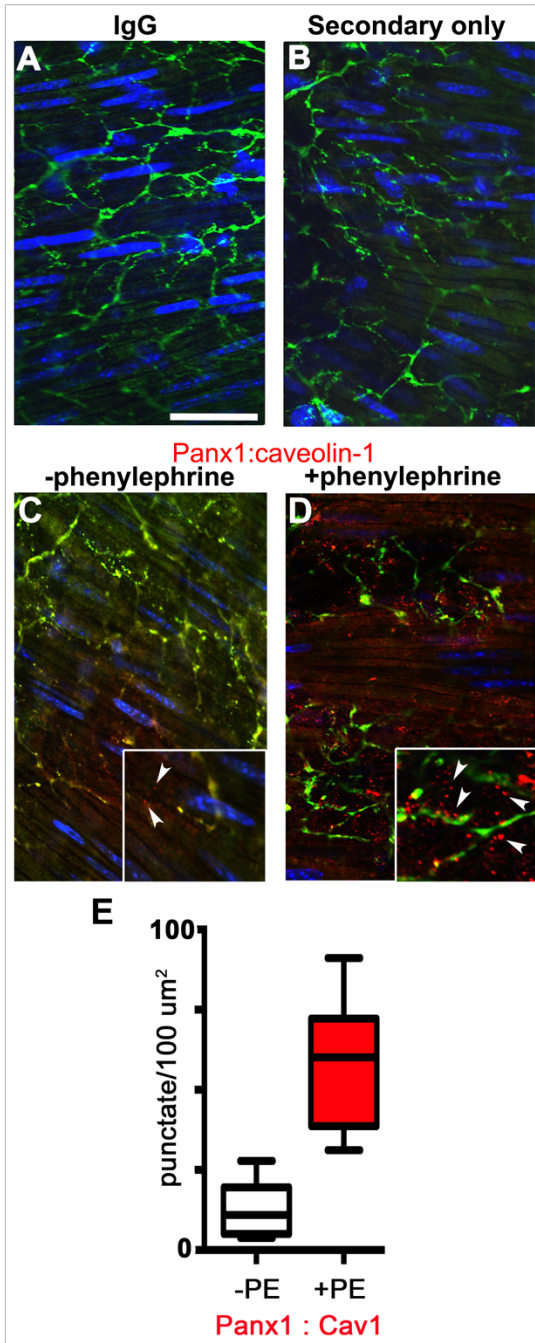


Figure 14. Pannexin1 and caveolin-1 localize to the plasma membrane near sympathetic nerves.

Figure 14. Pannexin1 and caveolin-1 localize to the plasma membrane near sympathetic nerves. *En face* immunofluorescence detection of Panx1 and caveolin-1 using proximity ligation assay (PLA) on intact TDA. Sympathetic nerves were labeled with tyrosine hydroxylase (green) and nuclei were labeled with DAPI (blue). (A) Control IgG (rabbit) staining. (B) PLA secondary probe control. (C) Lack of positive PLA between Panx1 and caveolin-1 in VSMCs at baseline conditions. (D-E) Panx1 and caveolin-1 cluster at areas of sympathetic innervation following acute (1 min) phenylephrine treatment (20 $\mu\text{mol/L}$). Positive PLA amplification is visualized as red punctate spots (white arrows). (E) Quantification of PLA signal between Panx1 and caveolin-1 before and after treatment with phenylephrine. N=3 animals per treatment group. Scale bar; 50 μm .

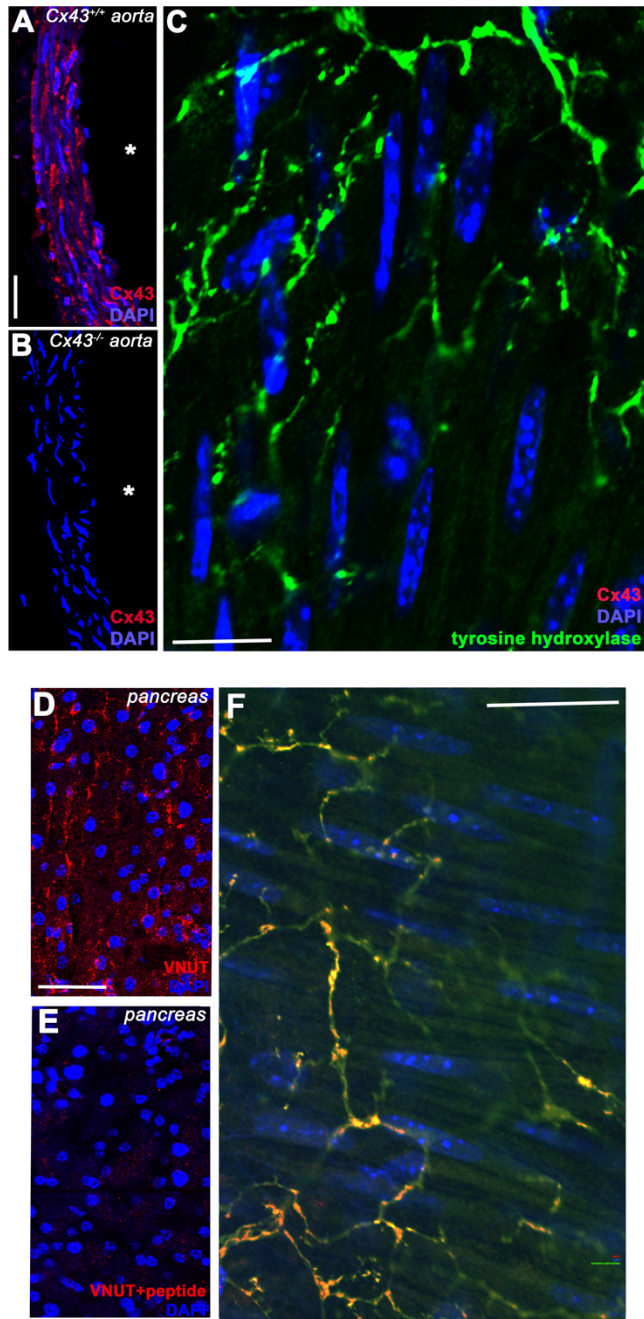


Figure 15. Supplement to Figure 14: Connexin 43 and VNUT are not found on VSMCs of resistance arteries.

Figure 15. Supplement to Figure 14: Connexin 43 and VNUT are not found on VSMCs of resistance arteries. (A) Immunofluorescence staining of transverse sections of aorta vascular wall from C57Bl/6 mouse shows expression of Connexin 43 (red) in VSMCs of large conduit artery (positive control). Nuclei stained with DAPI (blue). Scale bar; 20µm. (B) Connexin 43 immunostaining of aortic wall from global Connexin 43 (Cx43^{-/-}) knockout mouse (negative control). Nuclei stained with DAPI (blue). (C) *En face* Connexin 43 (red) immunostaining from mouse thoracodorsal artery. Tyrosine hydroxylase (green). Nuclei stained with DAPI (blue). Scale bar; Scale bar; 10µm. (D) Immunofluorescence analysis of the vesicular nucleotide transporter (VNUT) in thin sections of C57Bl/6 pancreas (positive control). Nuclei stained with DAPI (blue). Scale bar; 10µm. (E) Blocking peptide of VNUT antibody shows reduced signal in thin sections of C57Bl/6 pancreas. (F) *En face* VNUT (red) immunostaining from mouse thoracodorsal artery. No detectable signal for VNUT was found in VSMCs. Tyrosine hydroxylase (green). Nuclei stained with DAPI (blue). Scale bar; 10µm.

To investigate the functional and physiological role of VSMC caveolin-1 during α -AR vasoconstriction, we generated an inducible, VSMC-specific caveolin-1 knockout mouse model (SMC-Cav1^{fl/fl}), which upon induction of Cre recombinase deletes exon 2 of caveolin-1 (SMC-Cav1 ^{$\Delta\Delta$}) (**Figure 16A-B**). Caveolin-1 deletion was specific for VSMCs of resistance arteries, not affecting caveolin-1 expression in CD31 positive endothelial cells (**Figure 16C-D**). Due to the well-established contribution of Panx1-mediated ATP release during adrenergic stimulation^{192, 225, 238, 324}, we measured vasoconstrictor-dependent ATP release from isolated resistance arteries. Using a luminescence-based assay, we observed a caveolin-1 dependent response, whereby ATP released following adrenergic stimulation (norepinephrine 20 μ mol/L or phenylephrine 20 μ mol/L) was significantly reduced in SMC-Cav1 ^{$\Delta\Delta$} mice compared with controls (**Figure 16E**). No significant effect on ATP release was observed in any of the genotypes tested in response to agonists for other potent vasoconstriction pathways (e.g., ET-1 or 5-HT) (**Figure 16E**). Intracellular ATP concentration was also unchanged in any of the genotypes tested (**Figure 17**).

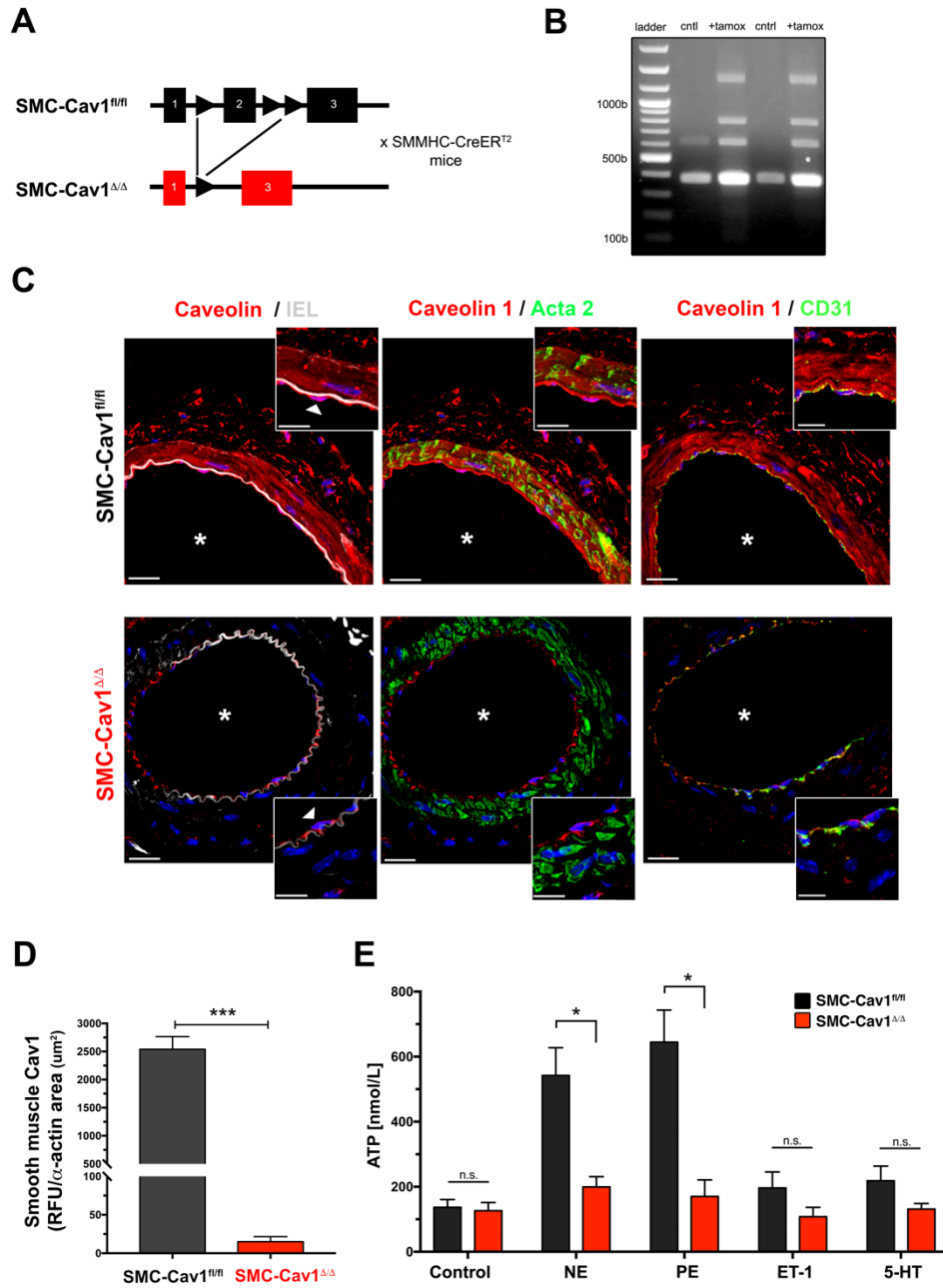


Figure 16. Inducible deletion of caveolin-1 from smooth muscle cells blunts adrenergic-mediated ATP release.

Figure 16. Inducible deletion of caveolin-1 from smooth muscle cells blunts adrenergic-mediated ATP release. (A) Inducible SMMHC-CreERT2+/Cav1fl/fl (SMC-Cav1fl/fl) mice were injected with tamoxifen (1 mg/kg) to delete caveolin-1 (SMC-Cav1Δ/Δ). (B) Agarose gel from genomic DNA showing Cre-mediated recombination at loxP site in tamoxifen treated mice. (C) Immunostaining of transverse sections of TDAs with anti-caveolin-1 (red), internal elastic lamina (gray), α-SMactin (Acta2), or CD-31 (Pecam1) (green). Nuclei are stained with DAPI (blue). *indicates vessel lumen. Scale bar; 20 μm. Arrows in high magnification indicate endothelial cells. (D) Quantification of caveolin-1 deletion from VSMCs normalized to α-SMactin positive area; n=6 mice. Students t-test was performed, significance indicated by asterisk ***p < 0.001. (E) ATP release from intact TDAs in response to adrenergic vasoconstrictors: phenylephrine (PE; 20 μmol/L) and norepinephrine (NE; 20 μmol/L), or non-adrenergic vasoconstrictors: serotonin (5-HT; 40 nmol/L) and endothelin-1 (ET-1; 40 nmol/L). N=4 mice. Data displayed as groups and represented as mean ± SEM. Two-way ANOVA and Tukey's posthoc test was performed for significance; *p < 0.05.

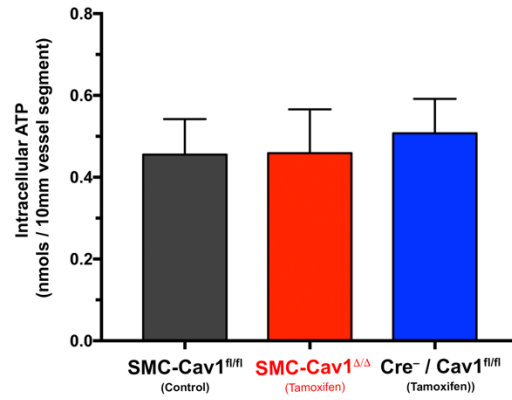
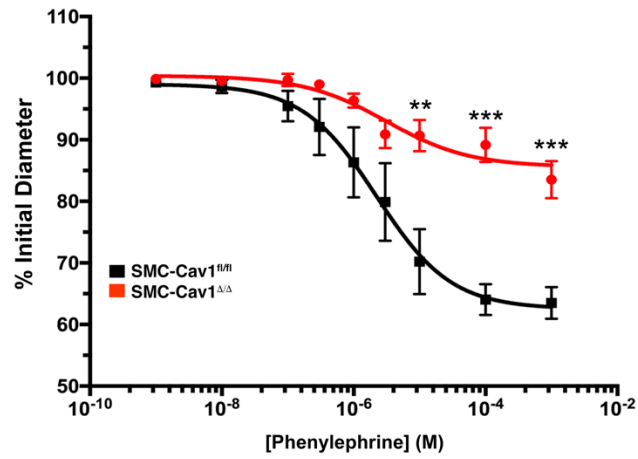


Figure 17. Supplement to Figure 16: Intracellular ATP measurements in thoracodorsal arteries.

Figure 17. Supplement to Figure 16: Intracellular ATP measurements in thoracodorsal arteries. ATP was measured from equal length segments (10mm) of isolated TDA using the ATP bioluminescence assay kit (Roche). Three segments were measured from each TDA. No significant difference was detected between any of the genotypes measured. N=3 animals (4-6) vessels per group. Data represented as mean \pm SEM and tested for significance using Kruskal-Wallis (one-way ANOVA) with Dunn's test.

In line with our ATP findings, we reasoned that blunted adrenergic-mediated ATP release in SMC-Cav1^{Δ/Δ} mice would concomitantly impair vascular responses to phenylephrine. To directly measure vasoconstriction responses in *ex vivo* resistance arteries, we assessed vascular responses to increasing concentrations of phenylephrine using pressure myography. SMC-Cav1^{Δ/Δ} mice exhibited significant reductions in phenylephrine-stimulated vasoconstriction (red line) compared with control animals (black line) (**Figure 18A**). Unlike global caveolin-1 knockout mice, which exhibit reduced expression of endothelial cell caveolin-1^{314,325}, no significant differences were observed in endothelium-dependent vasodilation (acetylcholine responses) in SMC-Cav1^{Δ/Δ} mice (**Figure 18B**). Thus, VSMC-specific deletion of caveolin-1 impairs adrenergic vasoconstriction without altering endothelial-mediated responses.

A



B

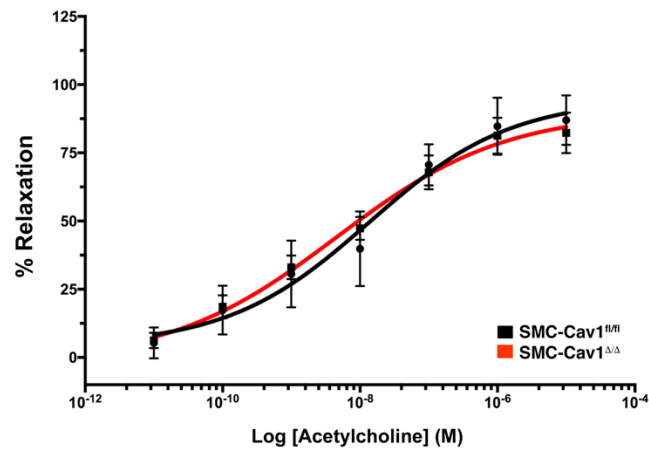


Figure 18. Effects of vascular smooth muscle cell caveolin-1 deletion on vasoconstriction and vasodilation responses in resistance arteries.

Figure 18. Effects of vascular smooth muscle cell caveolin-1 deletion on vasoconstriction and vasodilation responses in resistance arteries. (A) Contractile responses to increasing concentrations of phenylephrine in TDAs from SMC-Cav1^{fl/fl} control mice (black line; N=4 mice (7 arteries)) and SMC-Cav1^{Δ/Δ} tamoxifen-treated mice (red line; N=6 mice (8 arteries)). **(B)** Effects of VSMC caveolin-1 deletion on endothelial-dependent vasodilation to increasing concentrations of acetylcholine. Concentration-effect curves were fitted to the data using four-parameter, non-linear regression curve. Data assessed by two-way ANOVA with Bonferroni post-hoc test for multiple comparisons. **p < 0.01 ***p < 0.001.

Previously we have shown that VSMC-specific deletion of Panx1 channels results in significantly reduced BP due to blunted adrenergic-stimulated ATP release and vasoconstriction. Thus, we used telemetry to test whether SMC-Cav1^{ΔΔ} mice exhibited a similar BP phenotype. BP was assessed in individual animals before (baseline) and after induction of caveolin-1 deletion. A significant reduction in 24-hour mean arterial pressure (total MAP= -3.8 mmHg) was observed only after tamoxifen injection in SMC-Cav1^{ΔΔ} mice (**Figure 19A-B**). Moreover, a significant and greater BP reduction (Δ MAP= -6.8 mmHg) was observed during the active period, when sympathetic drive to resistance arteries is higher (**Figure 19C**) compared to the inactive period (**Figure 19D**). No significant difference in baseline MAP was observed in any other tested genotype before induction with tamoxifen, vehicle control, or saline control (**Figure 19C**; **Figure 20**). There was also no change in plasma renin concentration after caveolin-1 deletion, which was tested as a metric of altered basal renal-vasculature function (**Figure 20**).

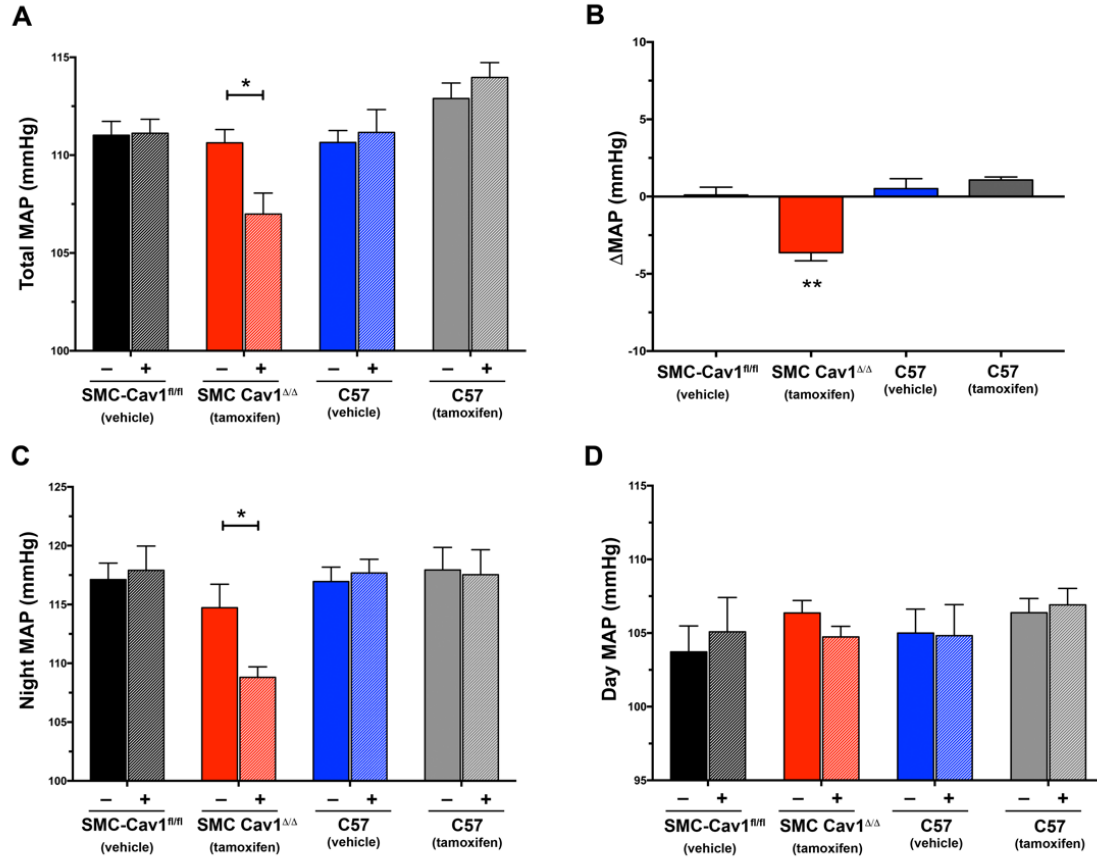


Figure 19. VSMC Caveolin-1 deletion reduces blood pressure.

Figure 19. VSMC Caveolin-1 deletion reduces blood pressure. (A) 24 hour mean arterial blood pressure (MAP) of mice across the indicated genotypes. (B) Differences in 24 hour MAP (Δ MAP) across the indicated groups of mice after treatment with tamoxifen or vehicle control. (C) MAP during the nocturnal active period (12hr dark: 6:00PM-5:59AM), and (D) MAP during the daytime inactive period (12hr light: 6:00AM-5:59PM). Baseline measurements were made for each individual animal before injections and compared to BP responses 2 weeks after tamoxifen or vehicle control injection. N=4 mice for each treatment group. * $p < 0.05$, ** $p < 0.01$, *** $p < 0.001$ compared to baseline response using one-way ANOVA (B) or two-way ANOVA (A, C, D), with Tukey's posthoc test.

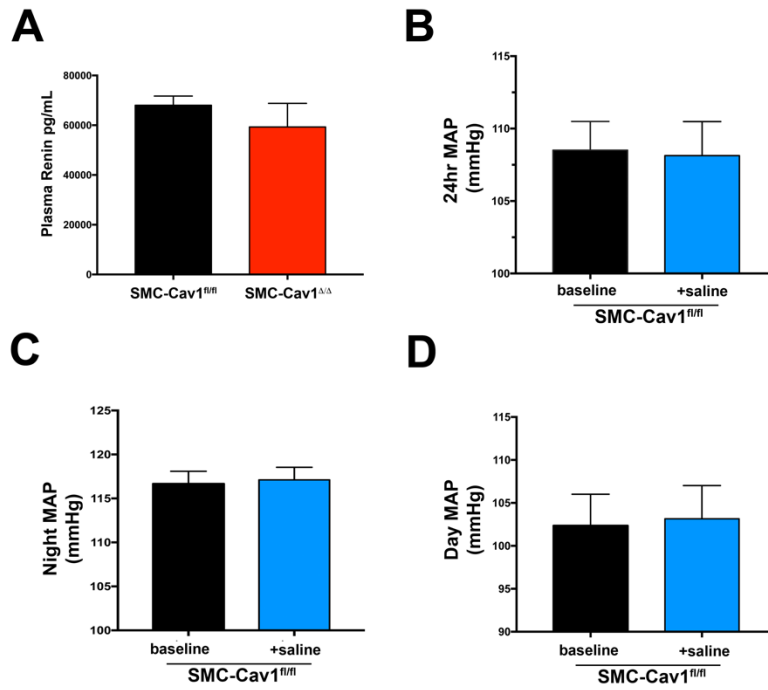


Figure 20. Supplement to Figure 19: VSMC caveolin-1 deletion in SMC-Cre^{Δ/Δ} mice do not have altered renin homeostasis or blood pressure due to injection volume.

Figure 20. Supplement to Figure 19: VSMC caveolin-1 deletion in SMC-Cre Δ/Δ mice do not have altered renin homeostasis or blood pressure due to injection volume. (A) Plasma renin measurements in SMC-Cre Δ/Δ and control mice are unaltered after induction of caveolin-1 deletion. **(B)** 24-hour mean arterial pressure (MAP). **(C)** Night (active period) MAP. **(D)** Day (inactive period) MAP. Volume controls for injections of tamoxifen or vehicle control do not alter blood pressure. N=4 mice. Data are represented as mean \pm SEM and were tested for significance using a Student's t-test.

To ensure that BP reductions in SMC-Cav1^{Δ/Δ} mice were not influenced by changes in cardiac function, we performed functional MRI analysis on SMC-Cav1^{Δ/Δ} and control animals (**Figure 21**). No significant changes in cardiac function were observed in any of the tested genotypes (**Table 1**). This includes cardiovascular changes due to heart rate, stroke volume, cardiac output, left ventricular mass, or left ventricular wall thickness—all of which can directly influence MAP. Thus, alterations in BP are modulated by deletion of caveolin-1 in smooth muscle cells and likely influence the regulation of total peripheral resistance.

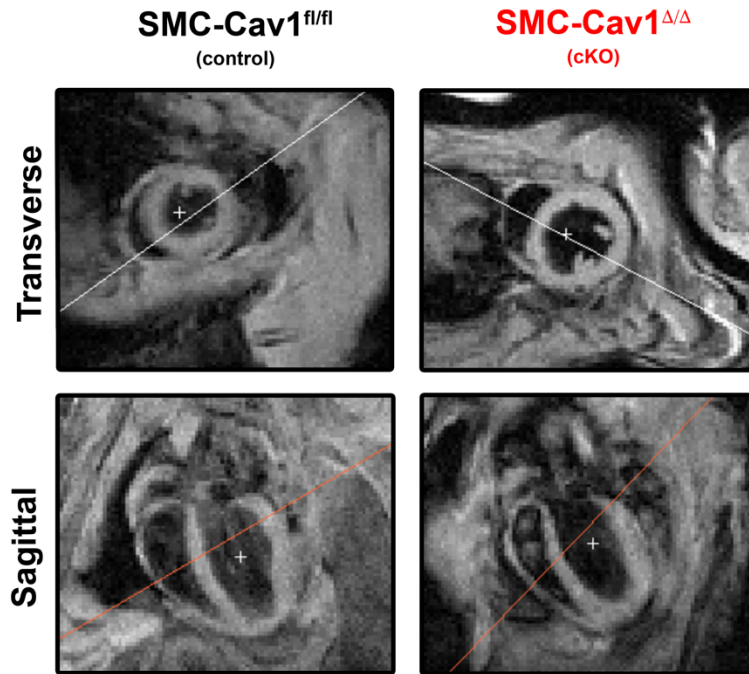


Figure 21. VSMC caveolin-1 deletion does not influence cardiac function.

Figure 21. VSMC caveolin-1 deletion does not influence cardiac function.

Representative transverse and sagittal MRI images of SMC-Cav1^{fl/fl} control and SMC-Cav1^{Δ/Δ} hearts. Six short-axis slices were acquired from base to apex, with slice thickness equal to 1mm, in-plane spatial resolution of $0.2 \times 0.2 \text{ mm}^2$, and temporal resolution of 8–12 ms. No differences in size, morphology, or function were detected as summarized in Table 1. N=4 mice.

Table 1. Cardiac function measured by MRI in SMC-Cav1^{Δ/Δ} and SMC-Cav1^{f/f} control mice. R-R wave ECG interval (R-R), Left Ventricle Mass (LVM), Cardiac output (CO), Ejection Fraction (EV), End Systolic Volume (ESV), End Diastolic Volume (EDV), Stroke Volume (SV). Data represented as mean ±SEM, n=4, 2-tail homoscedastic Student's t-test.

	SMC-Cav1 ^{f/f}		SMC-Cav1 ^{Δ/Δ}		p-value
Heart Rate (bpm)	489.35	±5.47	491.48	±19.26	0.91
R-R (ms)	122.65	±1.38	122.51	±4.89	0.98
LVM (ml)	0.099	±0.003	0.096	±0.004	0.50
LVM (g)	0.104	±0.003	0.101	±0.004	0.50
EDV (ml)	0.043	±0.003	0.040	±0.004	0.47
ESV (ml)	0.019	±0.002	0.017	±0.002	0.59
SV (ml)	0.025	±0.002	0.022	±0.004	0.59
EF (%)	57.25	±3.05	55.52	±7.29	0.81
CO (l/min)	0.012	±0.001	0.011	±0.002	0.54

Lastly, we assessed mice lacking the Cre allele, but maintaining the loxP genotype ($Cre^{-}/Cav1^{fl/fl}$) as a further control. $Cre^{-}/Cav1^{fl/fl}$ mice were analyzed for expression of caveolin-1 in resistance arteries (**Figure 22A**). Caveolin-1 immunostaining was detected in $Cre^{-}/Cav1^{fl/fl}$ VSMCs as indicated by colocalization with α SM-actin, but not in SMC- $Cav1^{\Delta/\Delta}$ knockout mice. No differences were detected in endothelial cells (CD31+) of either genotype. Consistent with these findings, $Cre^{-}/Cav1^{fl/fl}$ exhibited similar vasoconstriction responses to increasing doses of phenylephrine as did control SMC- $Cav1^{fl/fl}$ animals (**Figure 18**). SMC- $Cav1^{\Delta/\Delta}$ knockout animals still exhibited significantly blunted vascular responses to phenylephrine compared to $Cre^{-}/Cav1^{fl/fl}$ mice (**Figure 22B**), but no differences in cardiac function (**Figure 22C**; **Table 2**).

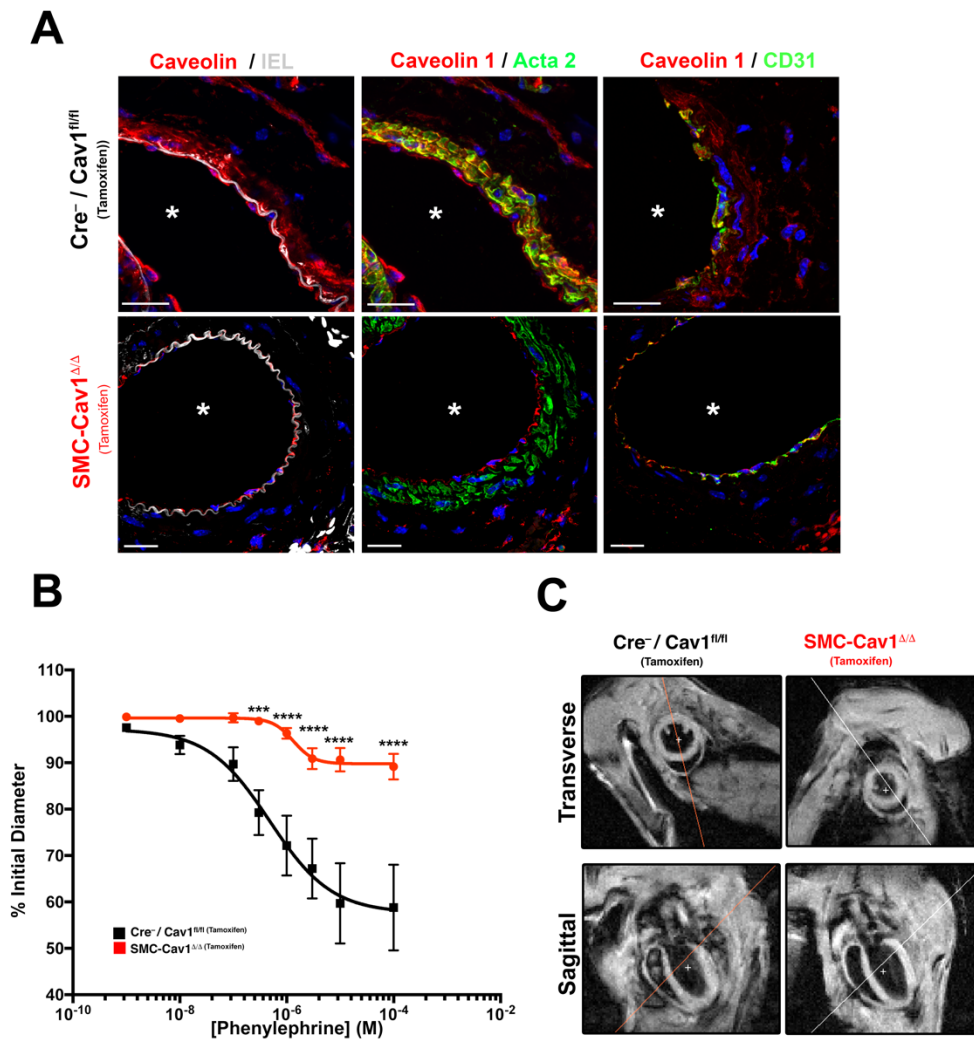


Figure 22. Tamoxifen induction in $Cre^{-}/Cav1^{fl/fl}$ control mice retain normal VSMC caveolin-1 expression, phenylephrine-induced constriction, and cardiac function.

Figure 22. Tamoxifen induction in $Cre^{-}/Cav1^{fl/fl}$ control mice retain normal VSMC caveolin-1 expression, phenylephrine-induced constriction, and cardiac function. (A) Immunostaining of transverse sections of TDAs with anti-caveolin-1 (red), internal elastic lamina (gray), α -SMactin (Acta2) or CD-31 (Pecam1) (green). Nuclei are stained with DAPI (blue). *indicates vessel lumen. Scale bar; 20um. **(B)** Effects of TDA contractile responses to increasing concentrations of phenylephrine from SMC- $Cre^{ΔΔ}$ knockout mice (red line; n=6 mice (8 arteries) or $Cre^{-}/Cav1^{fl/fl}$ control mice (black line; n=4 mice (5 arteries)). Concentration-effect curves were fitted to the data using four-parameter, non-linear regression curve. Data assessed by two-way ANOVA with Bonferroni post-hoc test for multiple comparisons. ***p < 0.001 ****p < 0.0001. **(C)** Representative transverse and sagittal MRI images of $Cre^{-}/Cav1^{fl/fl}$ control and SMC- $Cav1^{ΔΔ}$ hearts. Six short-axis slices were acquired from base to apex, with slice thickness equal to 1mm, in-plane spatial resolution of 0.2×0.2 mm², and temporal resolution of 8–12 ms. No differences in size, morphology, or function could be observed. No significant differences were found in functional analysis (Supplemental Table I). Data represented as mean \pm SEM and were tested for significance using a Student's t-test (see **Table 2**).

Table 2. Cardiac function measured by MRI in SMC-Cav1^{Δ/Δ} and Cre⁻ / Cav1^{fl/fl} tamoxifen injected control mice. R-R wave ECG interval (R-R), Left Ventricle Mass (LVM), Cardiac output (CO), Ejection Fraction (EF), End Systolic Volume (ESV), End Diastolic Volume (EDV), Stroke Volume (SV). Data represented as mean ±SEM, n=4, 2-tail homoscedastic Student's t-test.

	Cre ⁻ / Cav1 ^{fl/fl}		SMC-Cav1 ^{Δ/Δ}		p-value
Heart Rate (bpm)	466.47	±13.18	491.48	±19.26	0.26
R-R (ms)	128.85	±3.58	122.51	±4.89	0.27
LVM (ml)	0.099	±0.002	0.096	±0.004	0.56
LVM (g)	0.104	±0.002	0.101	±0.004	0.56
EDV (ml)	0.048	±0.002	0.040	±0.004	0.11
ESV (ml)	0.019	±0.001	0.017	±0.002	0.47
SV (ml)	0.030	±0.003	0.022	±0.004	0.15
EF (%)	61.27	±2.52	55.52	±7.29	0.42
CO (l/min)	0.014	±0.001	0.011	±0.002	0.17

To functionally assess whether BP reductions involving VSMC caveolin-1 are mediated through a Panx1-dependent pathway, we acutely treated animals with the Panx1 intracellular loop mimetic peptide-inhibitor PxIL2P (20 mg/kg) or scrambled control peptide (20 mg/kg). We have previously shown that PxIL2P significantly blunts phenylephrine-stimulated Panx1-channel currents, ATP release, vasoconstriction, and MAP²²⁵. Following acute injection of PxIL2P, significant BP reduction was restricted to vehicle treated SMC-Cav1^{f/f} (vehicle treated: Δ MAP= -8.83 mmHg) and C57BL/6 (vehicle treated: Δ MAP= -12.26 mmHg; tamoxifen; Δ MAP= -9.81 mmHg) control animals—both of which contain VSMC caveolin-1. Conversely, no significant changes in MAP were observed in SMC-Cav1 ^{Δ/Δ} animals, which are deficient in VSMC caveolin-1 (tamoxifen: Δ MAP= 0.73 mmHg) (**Figure 23**). Administration of a scrambled PxIL2P peptide of the same amino acid composition did not influence BP in any genotype tested. The resistance of VSMC-specific caveolin-1 deficient mice to BP lowering by PxIL2P supports the idea that VSMC caveolin-1 regulates BP homeostasis through changes in Panx1 localization and channel function.

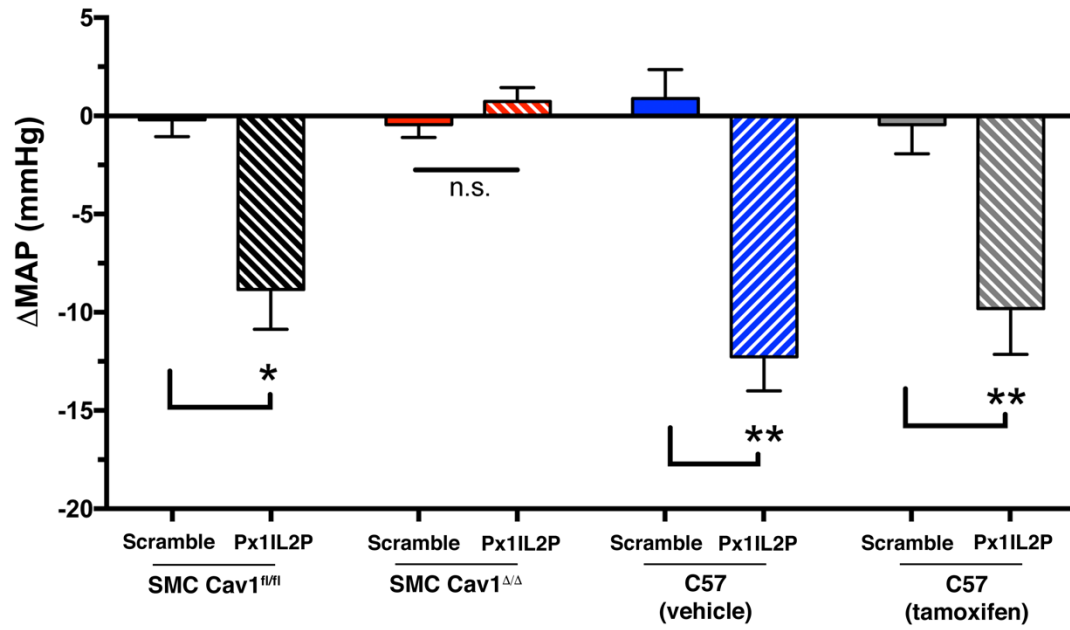


Figure 23. Caveolin-1 deletion prevents the blood pressure-lowering effects of the Panx1 inhibitory peptide (PxIL2P).

Figure 23. Caveolin-1 deletion prevents the blood pressure-lowering effects of the Panx1 inhibitory peptide (PxIL2P). Differences in MAP (Δ MAP) measured at baseline and 2 hrs after treatment with the Panx1 inhibitory peptide PxIL2P (20 mg/kg) or scramble control (20 mg/kg) in SMC-Cav1^{fl/fl}, SMC-Cav1 ^{Δ/Δ} , or C57BL/6 mice. Changes in MAP were calculated using each animal's individual baseline pretreatment. n=4 mice for each treatment group; *p< 0.05 and **p< 0.01 compared to individual baseline response using two-way ANOVA and Tukey's test.

4.4 DISCUSSION

Sympathetic-mediated vasoconstriction plays a central role in controlling BP homeostasis. This process occurs in part due to the release of norepinephrine from sympathetic nerves, subsequent activation of VSMC α -ARs, and coordinated constriction between VSMCs, thus producing a unified vasoconstriction response. Recent work from our group revealed that VSMC Panx1 channels²³⁸ are a primary regulator of α -AR mediated vasoconstriction. Using VSMC-specific Panx1 knockout mice and genetic rescue experiments we demonstrated that ATP release from these channels was necessary for proper adrenergic vasoconstriction^{78, 238}. In this regard, ATP acts as an autocrine/paracrine signaling molecule that initiates vasoconstriction responses in resistance arteries. However, less is known about the intracellular signaling molecules responsible for supporting Panx1 channel function following adrenergic stimulation. Here we have identified a novel interaction between Panx1 and the caveolae structural protein caveolin-1. Caveolin-1 and Panx1 localize to areas of the plasma membrane innervated by sympathetic nerves and associate with each other following stimulation of α -ARs with phenylephrine. Using a novel, inducible, VSMC-specific caveolin-1 knockout mouse, we also demonstrate that caveolin-1 functionally regulates adrenergic-mediated ATP release, vasoconstriction, MAP, and Panx1 dependent BP responses.

Plasma membrane caveolae influence vascular homeostasis and assist in the localization of key VSMC vasoconstriction signaling molecules such as α -AR and Gq coupled effector molecules in small arteries^{317, 322, 326}. From electron microscopy observations (**Figure 11**), we often observe caveolae localized near sympathetic nerves,

and thus predicted that this unique vascular feature may beget vascular function. Our live cell, fluorescent tracking experiments, allowed us to examine caveolin-1 and Panx1 interactions in response to stimulation with phenylephrine. Activation of α -AR resulted in a rapid co-association of the two proteins at the plasma membrane (**Figure 12A-B**). These temporal effects are consistent with previous constriction recordings following adrenergic stimulation in resistance arteries ^{234, 306}. Moreover, we treated VSMCs with a high concentration of ATP (500 μ mol/L), a manipulation that promotes active internalization of membrane associated Panx1 ³²³, to determine if caveolin-1 association correlates with Panx1 endocytosis. Here we observed a significant decrease in co-localization between Panx1 and caveolin-1 following ATP stimulation (**Figure 12A-C**), indicating that Panx1 endocytosis occurs independently of a caveolin-1 association.

Recent studies by Boyce et al. ³²³ and Gehi et al. ²²² report similar co-distributions of Panx1 with caveolin-1 in cell lines. In contrast to the phenylephrine-induced Panx1/caveolin-1 clustering observed herein, a similar decrease in overlap with caveolin-1 was observed following ATP application in N2a cells ³²³. It is important to note in this context that caveolin-1-enriched caveolae are only one specialized variety of cholesterol-enriched membrane microdomain or lipid raft ³⁰³. In fact, ATP-mediated Panx1 internalization is cholesterol-dependent ^{262, 323} but dynamin- and clathrin-independent ^{222, 323}, suggestive of a non-canonical endocytosis mechanism. Our novel results then suggest that inclusion of Panx1 in VSMC caveolae may alter channel activity (such as increased open probability ³²⁷⁻³²⁹) rather than trafficking, although this remains to be explicitly tested. In light of this work, and because of the strong association between caveolin-1 and Panx1 following adrenergic stimulation, we tested whether an endogenous interaction occurs in

VSMCs. The same culture model also showed a specific protein interaction using immunoprecipitation of membrane fractions after phenylephrine stimulation (**Figure 12D-F**), which was absent in non-caveolar Panx1-containing fractions. In these experiments, we observed multiple glycosylation species of Panx1^{172, 298} (between 37-55kDa) after immunoprecipitation, perhaps indicative of the recruitment of more Panx1 channels from intracellular stores following stimulation. Panx1 channels are oligomers of Panx1 subunits. It is unknown how many units within the channel must be glycosylated to allow for the appropriately trafficking of plasma membrane channels. It is plausible that Panx1 subunits are differentially regulated, which has been strongly suggested in other published work¹⁹². It also remains unknown whether binding of Panx1 to caveolin-1 after phenylephrine stimulation requires a direct interaction, as observed for other membrane channels³²⁷⁻³²⁹, or if other membrane associated effector molecules are required, such as Src family kinases^{273, 330}.

Panx1 plays a vital role in α -AR vasoconstriction, but not in other constriction pathways²²⁵. We reasoned that caveolae might engender the formation of α -AR membrane microdomains near the VSMC membrane innervated by sympathetic nerves. Using intact mouse resistance arteries in conjunction with PLA, we observed an adrenergic-induced interaction of caveolin-1 and Panx1 preferentially localized around sympathetic nerves (**Figure 14D-E**). These observations suggest that caveolae may support the formation of a signaling microdomain important for Panx1 activation²²⁵. Moreover, resistance arteries are characterized by multiunit neural innervation to VSMCs, whereby small patches of VSMCs are contacted by sympathetic nerves to allow for finer individual control of vasoconstriction²³³. This innervation pattern differs from the unitary innervation, which is

observed in visceral organs and large arteries, and feature a single VSMC neural input that relies on gap junction connectivity to synchronize constriction responses. In this study as in previously published findings²³⁸, we detect a scarcity of gap junction connectivity between VSMCs in our models by Cx43 immunostaining herein (**Figure 11**) or electron microscopy²³⁸. These results suggest that resistance arteries may preferentially utilize autocrine/paracrine-mediated signals to couple VSMC constriction responses and may further utilize purinergic signaling pathways mediated through Panx1 to facilitate this function.

The idea that spatially localized signals support vascular function has been extensively characterized in the endothelium, where regulation of tyrosine kinases and endothelial nitric oxide synthase is dependent on caveolin-1³⁰³; however, less is known about these processes in VSMCs, which utilize sympathetic innervation to adjust vascular resistance for proper blood pressure control³³¹. Perturbations to this adrenergic signaling axis may underlie clinical pathologies in patients suffering from treatment-resistant hypertension who present with enhanced sympathetic drive, norepinephrine spillover, and excessive vascular resistance³³²⁻³³⁴.

To explore the functional role of caveolin-1 in VSMCs we generated an inducible VSMC-specific caveolin-1 knockout mouse (**Figure 16A-B**) to selectively removed caveolin-1 from the vascular media (**Figure 16C**). Importantly, caveolin-1 expression remained present in the vascular endothelium (CD31-positive cells) between control and knockout mice. No gross alterations in the medial wall thickness or cell number were observed in TDAs (data not shown) as was described for pulmonary arteries in the

constitutive global knockout³¹¹. It is likely that the utilization of an inducible Cre-recombinase system in adult mice curtailed any negative compensatory effects seen in constitutive systems.

Using ATP bioluminescence assays, we measured phenylephrine-stimulated ATP release from *ex vivo* arteries, a process that our laboratory has shown uniquely couples with Panx1 activation²²⁵. In all cases, caveolin-1 deletion significantly reduced phenylephrine- and norepinephrine-stimulated ATP release, similar to observations in Panx1 VSMC-knockout mice²²⁵ (**Figure 16E**). From our immunofluorescence analyses, it seems likely that Panx1 is the primary conduit for ATP release from VSMCs, as VNUT and Cx43 were not detected in VSMCs of our vessels (**Figure 15**). These data suggest that caveolin-1 is involved upstream of Panx1 activation and influences the ATP release typically ascribed to Panx1 function. It remains to be demonstrated if a direct interaction between caveolin-1 is sufficient to induce Panx1 channel opening.

In the vasculature, a primary role for caveolin-1 is ascribed to negative regulation of endothelial nitric oxide synthase (eNOS) activity in the endothelium^{335, 336}. Global deletion of caveolin-1 increases eNOS activity, resulting in higher concentrations of cGMP, increased NO release, and alterations in myogenic tone and dilation responses to acetylcholine^{314, 325}. However, the role of VSMC-derived caveolin-1 has not been specifically examined in resistance arteries. Using pressure myography, we found that VSMC caveolin-1 deletion significantly blunts phenylephrine-stimulated vasoconstriction responses, but does not change vasodilation responses to acetylcholine (**Figure 18A-B**), indicating that reduced vasoconstriction is not dependent on endothelial-derived

mechanisms observed in global caveolin-1 knockout models³¹¹. ATP release from the vascular wall exhibits dual activities in resistance arteries depending on which cell type release ATP (vasoconstriction in smooth muscles and vasodilation in endothelial cells). The subtypes of purinergic receptors that are activated by ATP can also influence responses within the vascular wall with the largest contribution in smooth muscle being mediated by P2X1 ionotropic receptors²³⁵. Our laboratory has demonstrated the existence of purinergic component to adrenergic mediated vascular events whereby incubation of vessels with the ATP degrading enzyme apyrase or pharmacological blockers of purinergic receptors (P2X) prevents adrenergic vasoconstriction²³⁸. Thus, we conclude that caveolin-1 in our model functionally regulates the initial and upstream release of ATP utilized to activate downstream purinergic receptors after adrenergic stimulation.

VSMC-specific deletion of caveolin-1 results in reduced adrenergic ATP release and vasoconstriction, a similar vascular phenotypic observed when Panx1 is specifically deleted from VSMCs. We predicted that a similar dysregulation in BP would then occur after caveolin-1 deletion as observed in Panx1 knockout models: specifically, a reduction in MAP predominantly during the animal's active period (night MAP), when sympathetic drive is high. Indeed, *in vivo* BP monitoring revealed a significant reduction in 24-hour MAP (**Figure 19A-B**) with a greater reduction occurring at night (**Figure 19C**) in caveolin-1-deficient animals, but not during the day (inactive period) (**Figure 19D**). The effect size of BP lowering due to caveolin-1 deletion (~4 mmHg, 24 hour MAP; ~6 mmHg, Night MAP) was nearly identical to BP reductions in VSMC-Panx1 knockout animals⁵³. To further confirm that alterations in MAP were due to vascular changes (reduced vascular resistance), we assessed cardiac function using MRI. No measurable morphological

differences were detected in our analysis and all animals were functionally similar (e.g., heart rate, stroke volume; **Table 1**). Therefore, alterations in vascular resistance due to VSMC caveolin-1 deletion are likely responsible for observed reductions in MAP.

To determine if caveolin-1 dependent BP responses utilize in part a Panx1-dependent pathway, we acutely treated animals with PxIL2P peptide to pharmacologically lower blood pressure. PxIL2P has previously been shown to significantly reduce adrenergic stimulated Panx1 channel opening and ATP release, and also potently lowers blood pressure in mice. In the current analysis, wild-type and control mice dramatically respond to PxIL2P treatment (i.e reduced blood pressure lowering), with no effects due to scrambled control peptide ²²⁵. However, conditional deletion of VSMC caveolin-1 are completely protected to BP lowering by PxIL2P treatment. This strongly suggests that caveolin-1 is a key intermediary necessary for normal Panx1 function (**Figure 23**). These data further highlight the Panx1 intracellular loop as an important target for Panx1 activation. Previous work from our group has demonstrated that the region mapping to the PxIL2P peptide contains a regulatory motif, which upon genetic mutation negatively influences Panx1 channel function and adrenergic mediated vasoconstriction ²²⁵. Future studies are needed to determine if caveolin-1 directly influences the Panx1 intracellular loop, or if associative factors bound to caveolin-1 are required for proper channel function.

In this analysis, we explore a novel adrenergic vasoconstriction pathway that has previously been shown to coordinate constriction responses through the release of ATP by Panx1. We describe the impact of caveolin-1 deletion in the peripheral vasculature and on systemic BP regulation using a novel smooth muscle-specific mouse model. We have

limited changes due to compensatory deletion-effects by utilizing an inducible Cre-lox system in adult mice. Based on our analyses we found no additional phenotypes outside of the cardiovascular phenotypes reported in this study. Although, direct experimental evidence and future studies are required to determine if additional phenotypes exist. Here we show that the localization of Panx1 to plasma membrane caveolae and the scaffold protein caveolin-1 promotes a novel interaction important for regulating BP. It remains to be observed whether other scaffold proteins or cytoskeletal proteins contribute to the localization and formation of this unique membrane domain near sympathetic nerve terminals in VSMC. Panx1 has been shown to directly interact with the actin cytoskeleton³³⁷ and its modulator actin-related protein 3^{338, 339}, and treatment with cytochalasin B destabilized Panx1 plasma membrane distribution *in vitro*³³⁷. It is also unknown which intracellular mediators are mechanistically required for activation of Panx1 by α -AR in VSMCs, which will be especially important to determine.

Overall, our data demonstrate that Panx1 and caveolin-1 functionally couple with each other in VSMCs. Using immunofluorescence co-localization and co-immunoprecipitation, we show that caveolin-1 and Panx1 interact at distinct areas of VSMC plasma membrane innervated by sympathetic nerves, suggesting the existence of an adrenergic micro-signaling domain. This interaction was induced by α -AR stimulation and is necessary for adrenergic-mediated vasoconstriction and ATP release from resistance arteries. We found that VSMC caveolin-1 is necessary to control systemic BP responses through modulation of Panx1 function and may facilitate appropriate channel function through the Panx1 intracellular loop region.

Disclaimer

Portions of this chapter (text and figures) were written as in DeLalio L. et al. (2018). Interaction between Pannexin 1 and Caveolin-1 in Smooth Muscle can regulate blood pressure. *Arteriosclerosis, thrombosis, and vascular biology*, 2018 Jul 19 pii: ATVBAHA.118.311290. doi: 10.1161/ATVBAHA.118.311290.

CHAPTER 5. PANNEXIN 1 CHANNELS REGULATE RAAS ACTIVITY, BLOOD PRESSURE, AND ADRENAL HOMEOSTASIS

5.1 ABSTRACT

Purinergic signaling plays a key role in regulating kidney function and blood pressure (BP) homeostasis. The controlled release of cellular ATP, which is a rate limiting step in initiating autocrine/paracrine purinergic signaling cascades, strongly influence renal hemodynamics, fluid electrolyte balance, and renin secretion from juxtaglomerular (JG) cells. The coordination of renal function by purinergic signals ensures that systemic BP is maintained at an optimal physiologic set point. When BP homeostasis is threatened, a coordinated response reactivates dormant renin-lineage smooth muscle cells to augment renin expression and compensate for physiologic demand. The mechanisms controlling dynamic renin expression are unclear but purinergic signaling plays a fundamental role in their regulation. Pannexin 1 (Pax1) channels, which localize to the afferent arteriole and JG cells, are transmembrane conduits by which cellular ATP is released. We hypothesized that Pax1 channels in the renal vasculature support ATP release necessary for the control of renin secretion *in vivo*. Using a novel renin-cell Pax1 knockout model, we found that Pax1 deletion results in RAAS activation and significant increases in steady-state plasma renin concentration. Pax1 deficient animals exhibit increased plasma aldosterone levels and a concomitant increase in mean arterial pressure, which is partially dependent on angiotensin type 1 receptor (AT1R) activation. Moreover, Pax1 deficient animals have an impaired cellular response to renin recruitment mechanism, in which lineage fate switching

does not occur and JG cells hypertrophy to meet demand. These pathological features were further highlighted by adrenal gland hypertrophy and delocalization of aldosterone producing cells in the adrenal cortex, which become uncoupled from AT1R signaling and are suggestive of defective cell differentiation mechanisms. Thus, Panx1 channels in renin lineage cells directly influence renin dynamics and RAAS activity necessary for stabilizing physiologic BP levels and are novel regulators of renin cell fate and plasticity.

5.2 INTRODUCTION

Long-term blood pressure (BP) control is multifaceted and highly regulated by the renin-angiotensin-aldosterone system (RAAS). This complex system is controlled by overlapping hormonal, neural, and physical stimuli, which work at the local organ level (i.e. kidney and adrenal glands) as well as through circulating factors to maintain fluid/electrolyte balance, intravascular fluid volume, and thus BP³⁴⁰⁻³⁴³. A critical regulator of RAAS activity is the temporal control of renin secretion by juxtaglomerular (JG) cells in the afferent arteriole³⁴⁴. JG cells respond to changes in BP by synthesizing and secreting the aspartyl protease renin– the rate-limiting step in producing angiotensin-derived pressor peptides³⁴⁵. In homeostasis, JG cells localize to the preglomerular afferent arterioles and release renin from dense core granules in response to acute stimuli (β -adrenergic mediated, pressure mediated, and osmo-regulated)^{98, 346-348}. However, when BP homeostasis is threatened and there is a persistent demand to elevate BP, renin recruitment occurs in which preglomerular smooth muscle cells re-engage their fetal renin gene programs to bolster renin secretion³⁴⁹⁻³⁵¹. The mechanisms coordinating JG cell dynamics are still incompletely understood, however many of the regulatory mechanisms involved in controlling JG cell function converge on purinergic signaling pathways⁹⁰.

Initiation of purinergic signaling cascades by extracellular ATP significantly influences renovascular function⁹⁰. The renal tubules and renal vasculature express a wide array of purinergic receptors, which include the P2 family of ligand gated ionotropic (P2X) and metabotropic (P2Y) receptors, as well as the P1 family of adenosine receptors^{90, 352, 353}. Signaling mediated by these receptors directly augments renal vascular resistance^{83, 87, 354},

regulates tubuloglomerular feedback from the macula densa^{102, 105, 355}, and directly influences the secretion of renin from JG cells³⁵⁶⁻³⁶⁰. It is also well understood that the breakdown of ATP into adenosine augments renin secretion³⁶¹⁻³⁶⁴. Activation of adenosine type 1 receptors (A1R) on JG cells directly increases intracellular calcium ion concentrations resulting in reduced renin secretion³⁶⁵⁻³⁶⁷. Indirectly, A1R receptors in preglomerular smooth muscle cells are required for pressure induced renin suppression^{112, 368}. A purinergic equilibrium therefore exists between the amount of extracellular ATP and the rate of ATP degradation within the juxtaglomerular apparatus. The mechanisms underpinning how cellular ATP is released into the extracellular space are critical for the appropriate regulation of renin secretion and RAAS activation. However, these mechanisms are incompletely understood.

The novel family of Pannexin 1 (Pannx1) channels have emerged as a primary mode of regulated transmembrane ATP efflux^{72, 135, 255}. A strong physiological role for Pannx1-mediated ATP release has been established in diverse cell types and organ systems^{181, 197, 255}, and is capable of mediating physiological and pathological processes in the kidney^{178, 198, 369} and the vasculature^{76, 77, 224, 225}. Work from our laboratory and others have shown that Pannx1 is expressed within the murine kidney^{76, 205} and co-localizes with α -actin positive smooth muscle cells in the afferent arteriole¹⁷⁸. Given the cellular localization of Pannx1 and the functional role of purinergic signaling in regulating renin secretion, we hypothesized that Pannx1 channels coordinate purinergic signaling important for renin secretion, renin recruitment, and RAAS activation. To test this hypothesis, we generated a renin-cell (Ren1^{d-Cre}) Pannx1 knockout mouse model (Ren1-Pannx1 ^{Δ/Δ}) to selectively delete Pannx1 from renin lineage cells targeting the juxtaglomerular apparatus. Under steady state

conditions Panx1 deficient mice exhibit heightened, sex-dependent RAAS activation, marked by an increase in plasma renin and aldosterone concentration, as well as elevated mean arterial pressure. When challenged with chronically lowered BP, a manipulation that increases renin expression, Panx1 deficient mice present with an impaired capacity of afferent arteriolar smooth muscle cells to recruit renin. Instead, knockout mice enhanced renin secretion through an alternate mechanism that resulted in JG cell hypertrophy. Moreover, pathological elevation of plasma aldosterone and MAP were only partially mediated by AT1R activation, which corresponded with adrenocortical hyperplasia. The detection of aberrant adrenocortical zonation and ectopic expression of aldosterone synthase in the adrenal cortex revealed a secondary defect resulting in reduced urine excretion. We conclude that renin-lineage cell Panx1 controls steady-state renin secretion necessary for establishing physiological BP set points. In addition, Panx1 channels influence the ability of renal and adrenal cells to undergo cell autonomous fate-switching necessary for adrenal function and BP homeostasis indicating novel roles for Panx1 in regulating RAAS.

5.3 RESULTS

Generation of a renin-cell Pannexin 1 knockout model

To investigate the functional role of Panx1 channels in renin expressing cells of the renal vasculature, and assess the physiological influence on renin secretion, we generated a renin-cell specific Panx1 knock out mouse (Ren1-Panx1^{Δ/Δ}) using the Ren1^d-Cre mouse line³⁷⁰ (**Figure 24A**). Recombination of loxP sites flanking Panx1 was analyzed by PCR and yielded an amplicon of predictable size (371bp) for deletion of exon 3 from Panx1 (**Figure 24B**). Additionally, Ren1-Panx1^{Δ/Δ} and control animals were bred with mice harboring the stop-flox R26R EYFP allele to assess Cre-mediated labeling of renovascular cells. In Ren1-Panx1^{Δ/Δ}(EYFP) animals whole mount detection of endogenous fluorescence was detected in the juxtaglomerular apparatus, renal arterioles, and a subset of proximal tubular cells as previously described²²⁷ (**Figure 24C**). Using qRT-PCR, we next assessed Panx1 expression levels in the renal cortex from Ren1-Panx1^{Δ/Δ} and control mice. Kidneys were micro-dissected to enrich for cortical cells. Using Panx1 gene specific primers a significant reduction (~60%) of Panx1 mRNA was observed from Ren1-Panx1^{Δ/Δ}, compared to control animals (**Figure 24D**). Deletion of Panx1 did not alter the expression of other Pannexin isoforms, which were detected in very low abundance.

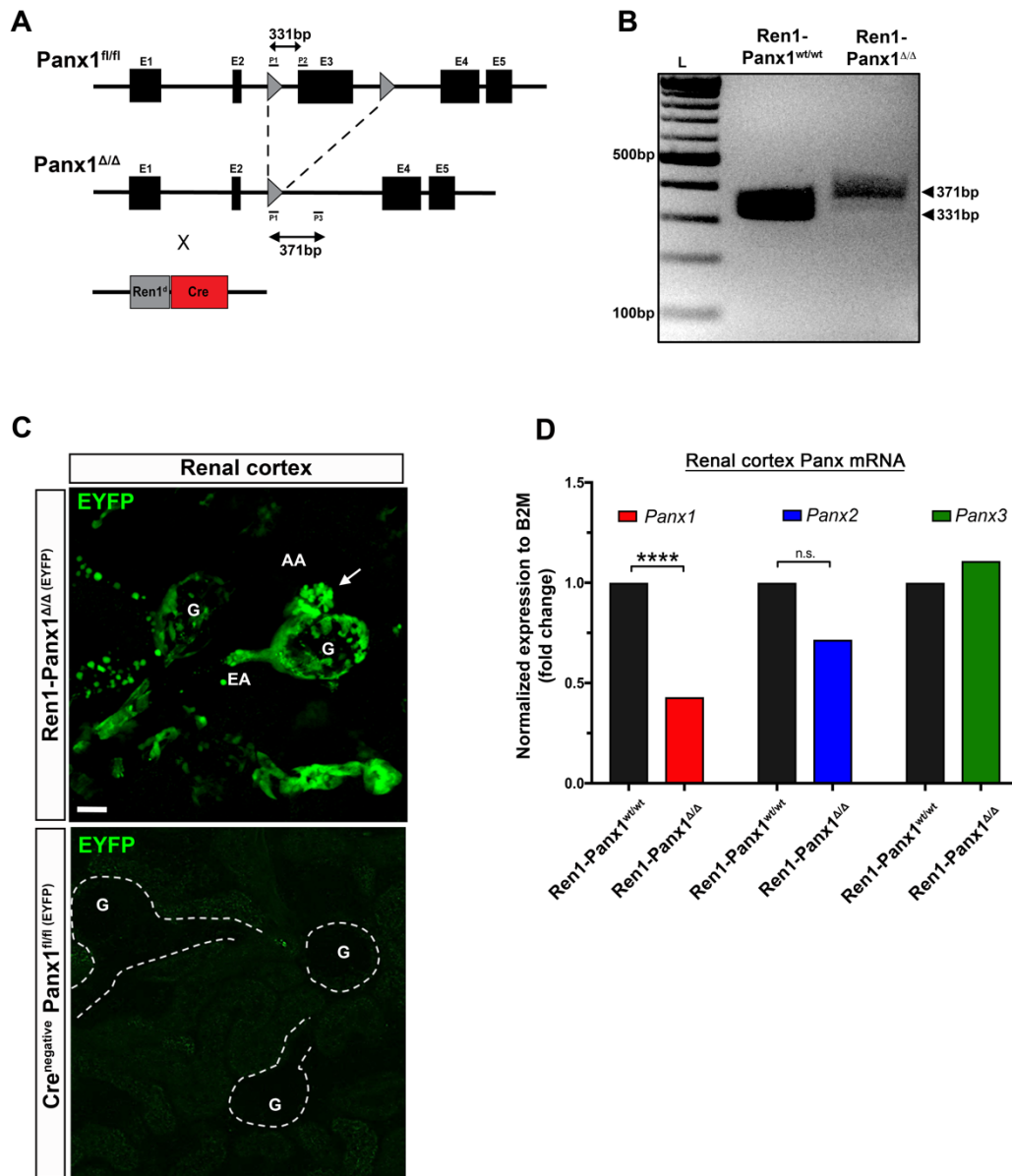


Figure 24: Generation of a renin-cell Pannexin 1 knockout model.

Figure 24: Generation of a renin-cell Pannexin 1 knockout model. (A) Gene targeting construct indicating recombination sites flanking Panx1 exon 3. Deletion of Panx1 achieved using animals harboring one allele for Cre recombinase (Ren1^d) and one wild type allele. **(B)** Validation of recombination from PCR amplification products run on agarose gel from Ren1-Panx1^{wt/wt} control (331bp) and Ren1-Panx1^{Δ/Δ} knockout mouse (371bp). **(C)** Whole mount images of genetically labeling renin lineage cells in juxtaglomerular apparatus with EYFP after breeding R26R-EYFP (Gt(ROSA)26Sor^{tm1(EYFP)Cos}) with Ren1-Panx1^{Δ/Δ} and Ren1-Panx1^{wt/wt} mice. Glomerulus (G), afferent arteriole (AA), efferent arteriole (EA) Scale bar; 20μm. Arrow indicates cluster of preglomerular renin cells. **(D)** qRT-PCR analysis of Panx1 expression from micro dissected renal cortex; N=6. Students t-test (two tailed) was performed, significance indicated by asterisk ****p<0.001.

Deletion of Pannexin 1 channels from renin expressing cells alters baseline renin secretion, but not the distribution of JG cells in the renal cortex

Next, we evaluated the effect of Panx1 deletion on systemic RAAS activity by quantifying the plasma renin concentration from Ren1-Panx1^{ΔΔ} and control mice using ELISA. Blood samples were collected during the active period (night; 20:00-22:00) and the inactive period (day; 08:00-10:00). Renin levels were enhanced in Ren1-Panx1^{ΔΔ} mice (32.20 compared to 48.48 ng/mL; 50.52% increase from control) during the inactive period and significantly increased (32.82 to 47.03 ng/mL; 43.30% from control) during the active period (**Figure 25A**). Due to the increase in plasma renin concentration we also assessed plasma aldosterone levels as a second measure of enhanced RAAS activity due to Panx1 deletion. Similarly, plasma aldosterone levels were significantly increased during both the inactive (77.7 compared to 165.5 pg/mL; 112.9% increase from control) and inactive (65.8 compared to 221.93 pg/mL; 237.6% increase from control) sampling periods (**Figure 25B**). Due to the stimulatory effect of renin observed in Ren1-Panx1^{ΔΔ} mice, we assessed the distribution of renin expressing cells in the renal cortex using immunostaining for renin and α SM-actin to demarcate renal arterioles (**Figure 25C-F**). Compared with control mice, Ren1-Panx1^{ΔΔ} mice retained a positionally normal distribution of renin positive cells, which were detected at the preglomerular afferent arteriole and co-localized with smooth muscle cells. Similarly, quantification of renin immunofluorescence showed no baseline differences in the amount of renin between Ren1-Panx1^{ΔΔ} and controls (**Figure 25G**), nor differences in the tissue expression of renin mRNA assessed by qPCR (**Figure 25H**). Moreover, renal tissue was free of glomerular or tubular pathologies as assessed by H&E and Trichrome staining (**Figure 26**) and retained normal filtration as indicated by blood

metabolic profiling (Table 3). Thus, deletion of Panx1 from renin expressing cells influences steady-state secretion of renin enzyme resulting in enhanced RAAS activity.

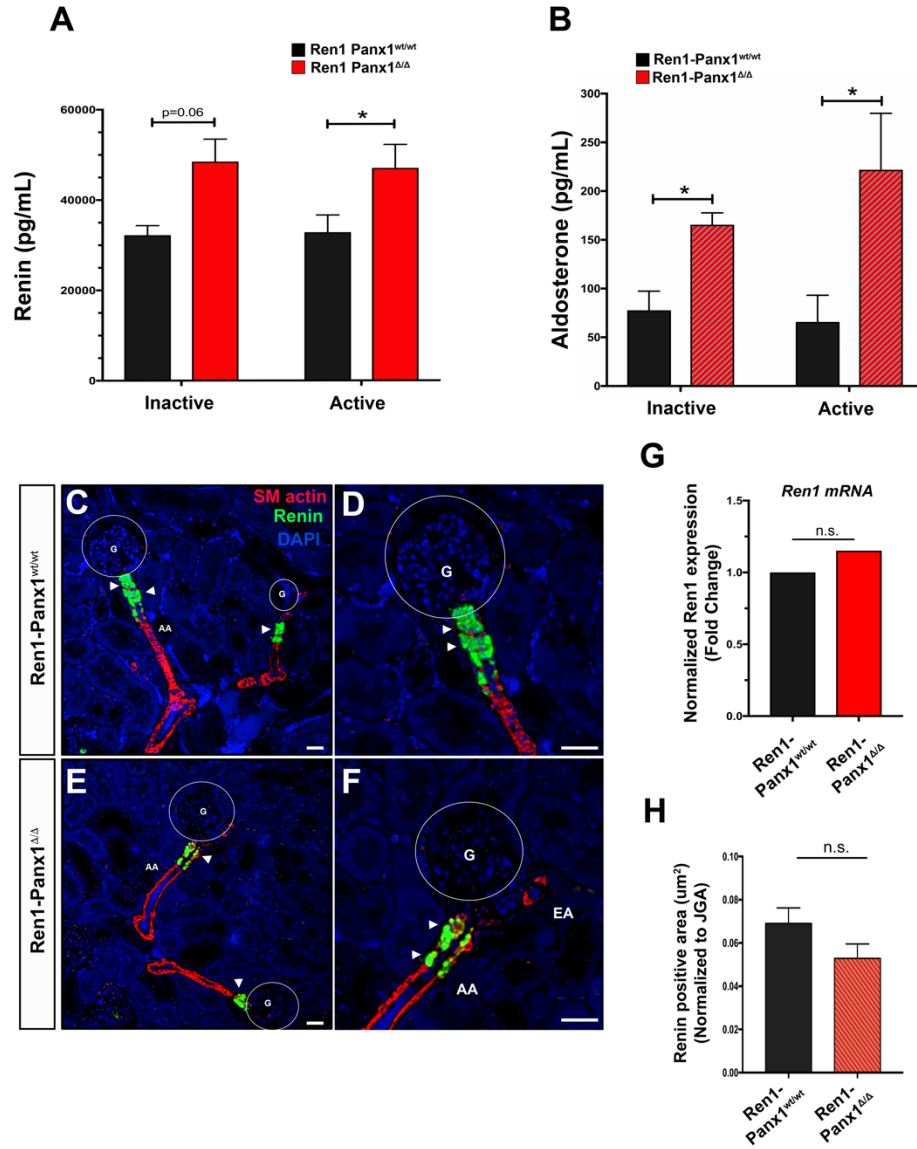


Figure 25. Deletion of Pannexin 1 alters baseline renin secretion, but not the distribution of JG cells in the renal cortex.

Figure 25. Deletion of Pannexin 1 alters baseline renin secretion, but not the distribution of JG cells in the renal cortex. (A) Plasma renin concentrations measured using Ren1-specific ELISA and collected during the inactive period (Day; 09:00-10:00) and the active period (Night; 16:00-17:00). Data displayed as mean \pm s.e.m. N=8 control; 10 knockout mice. * p <0.05 compared to baseline response using two-way ANOVA with repeated measures and Sidak correction. (B) Plasma aldosterone concentration measured using RIA from samples collected during the inactive and active period. Data displayed as mean \pm s.e.m. N=5 control; 7 knockout mice. * p <0.05 compared to control using two-way ANOVA with repeated measures and Sidak correction. (C-F) Tissue distribution of renin expression in renal cortex slices assessed by immunofluorescence. Immunostaining for renin (green), α -SMactin (red), and nuclei stained with DAPI (blue). Circles denote glomeruli (G), afferent arterioles (AA), efferent arterioles (EA), arrows indicate renin positive cells. Scale bar; 20 μ m. (D) qRT-PCR expression analysis of tissue renin levels from isolated cortical total RNA isolation and normalized to B2M expression levels using $2^{-\Delta\Delta C_t}$ method. N=4 control; 5 knockout mice. Data displayed as the average fold change. A student's t-test (two-tailed) was performed for significance. (E) Blinded renin quantification of the amount of renin positive area normalized the number of renin positive juxtaglomerular apparatus (JGA) from non-consecutive tissue sections. N=3 control; 4 knockout mice. Data represented as mean \pm s.e.m. A student's t-test (two-tailed) was performed for significance.

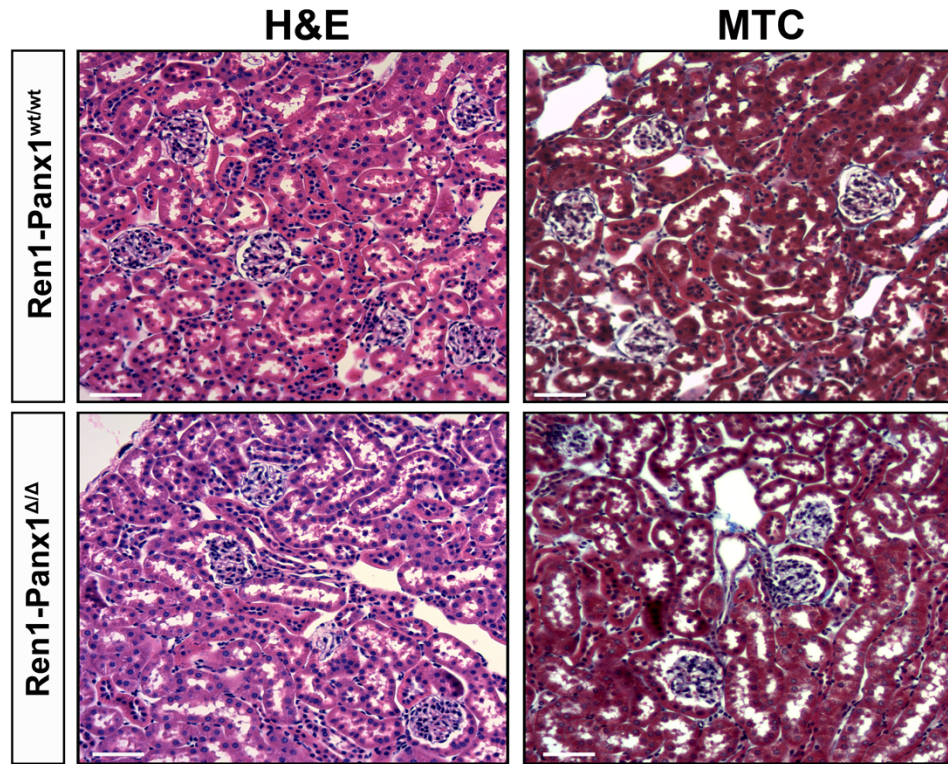


Figure 26. Supplement to Figure 25. Ren1-Panx1 Δ/Δ mice have normal renal tissue morphology.

Figure 26. Supplement to Figure 25. Ren1-Panx1 Δ/Δ mice have normal renal tissue morphology. Representative hematoxylin-eosin (H&E) and Masson's Trichrome (MTC) stain of kidney tissue. Glomerular size, distribution, and morphology are normal in Panx1 knockouts. No fibrosis or collagen deposition detected in the renal interstitium. N= 3 control; 3 knockout animals. Scale bar = 100 μ m.

Table 3. Metabolic blood data in Ren1-Panx1^{wt/wt} and Ren1-Panx1^{Δ/Δ} mice. Blood samples were collected from mice by cardiac puncture into EDTA- or Li-heparin collection tubes and stored on ice. Blood metrics were analyzed at the University of Virginia Pathology Laboratory.

	Ren1-Panx1 ^{wt/wt}		Ren1-Panx1 ^{Δ/Δ}		p-value
Na (mM)	150.6	±0.57	151.5	±1.28	0.53
K (mM)	5.6	±0.24	5.9	±0.22	0.42
Cl (mM)	115.6	±0.77	115.9	±0.77	0.83
Ca (mM)	10.0	±0.22	10.0	±0.21	0.63
BUN (mg/dL)	25.5	±1.00	24.0	±0.65	0.20
Creatinine (mM)	0.39	±0.03	0.38	±0.02	0.77
Glucose (mg/dL)	237.0	±22.0	225.8	±13.8	0.65
Results shown are mean ± SEM. Student's t-test performed for statistical significance.					

Renin cell Pannexin 1 is necessary for maintaining blood pressure homeostasis.

Increased RAAS activity directly correlates with increases BP. The BP elevating effects of pressor hormones influences vasoconstriction in the peripheral circulatory system and increased cardiac output through renal water reabsorption and blood volume expansion. Due to the significantly elevated renin and aldosterone in our animal model we tested 24-hour mean arterial pressure (MAP) in Ren1-Panx1^{Δ/Δ} and control mice using telemetry (**Figure 27A-D**). Ren1-Panx1^{Δ/Δ} exhibited an increase in MAP (104.1 mmHg) compared with Ren1-Panx1^{wt/wt} (97.2 ± mmHg), which was significantly different during the active period (104.1 compared to 97.2 mmHg). MAP elevation was significantly influenced by both increased systolic BP (120.3 mmHg compared to 113.2 mmHg) and diastolic. No differences were observed in heart rate. Due to significantly increased systolic pressure (indicative of increased cardiac output) we measured 24-hour urine excretion and water consumption in Ren1-Panx1^{Δ/Δ} mice as a proxy for a potential fluid retention phenotype. Compared with control animals, deletion of Panx1 caused a significant reduction in 24-hour urine volume (**Figure 28A**), but no difference in 24-hour water consumption (**Figure 28B**). Moreover, increased diastolic pressure, which is indicative excessive total peripheral resistance, was assessed using pressure myography. Interestingly, Ren1-Panx1^{Δ/Δ} displayed enhancements in vasoconstriction responses to increasing doses of phenylephrine (**Figure 29A**). These vascular responses co-presented with inward eutrophic vascular remodeling (increased media to lumen ratio, reduced lumen size, and no change in media area) (**Figure 29B-E**), a characteristic of high BP phenotypes. Cre recombinase activity was not detected in the medial layer of the resistance arteries (Error! Reference source not found.**F**). Thus, deletion of Panx1 in renin expressing cells

and enhanced RAAS activity result in the resetting of normal BP setpoints through a combination of vascular and renal dysfunctions.

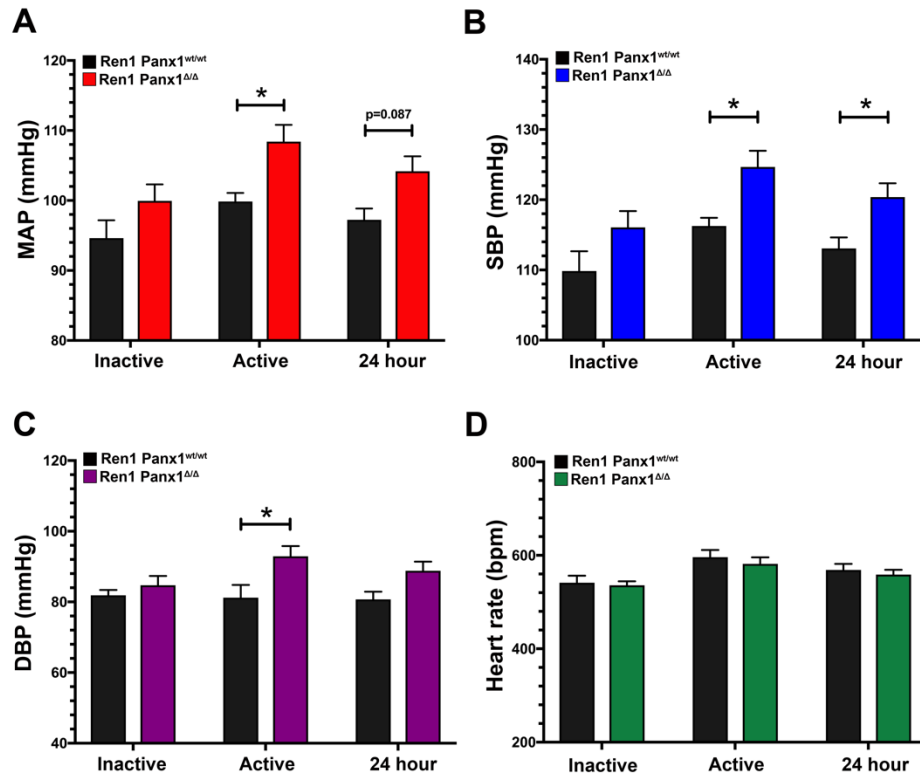


Figure 27. Renin cell Pannexin 1 is necessary for maintaining blood pressure homeostasis.

Figure 27. Renin cell Pannexin 1 is necessary for maintaining blood pressure homoeostasis. 24-hour mean arterial blood pressure (MAP) of Ren1-Panx1^{Δ/Δ} and Ren1-Panx1^{wt/wt} control mice was continuously measured using telemetry. BP was assessed during the inactive period (12hr light: 06:00-17:59) and active period (12hr dark: 18:00-05:59). **(A)** Mean arterial pressure **(B)** Systolic Pressure **(C)** Diastolic Pressure **(D)** Heart rate; N= 6 control; 7 knockout mice. Data displayed as groups and represented as mean ± s.e.m. Two-way ANOVA with repeated measures and Bonferroni posthoc test was performed for significance; *p ≤ 0.05.

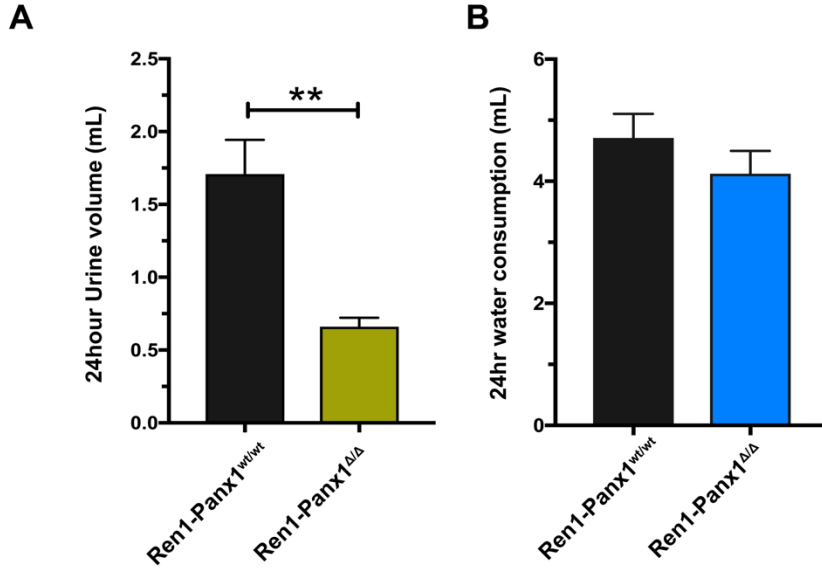


Figure 28. Supplement to Figure 27. Ren1-Panx1 Δ/Δ mice have reduced urine volume.

Figure 28. Supplement to Figure 27. Ren1-Panx1 Δ/Δ mice have reduced urine volume. Mice were individually housed in metabolic cages and 24-hour urine volume and water consumption were recorded. Mice were acclimated 3 days prior to recordings. Measurements were taken daily (18:00-19:00). **(A)** 24-hour urine volume. **(B)** 24-hour water consumption. N= 10 control; 12 knockout mice. Data are grouped and represented as the mean \pm s.e.m. 4 consecutive 24-hour recording periods were performed for each mouse. A student's t-test (two-tail) was performed for significance; **p \leq 0.01.

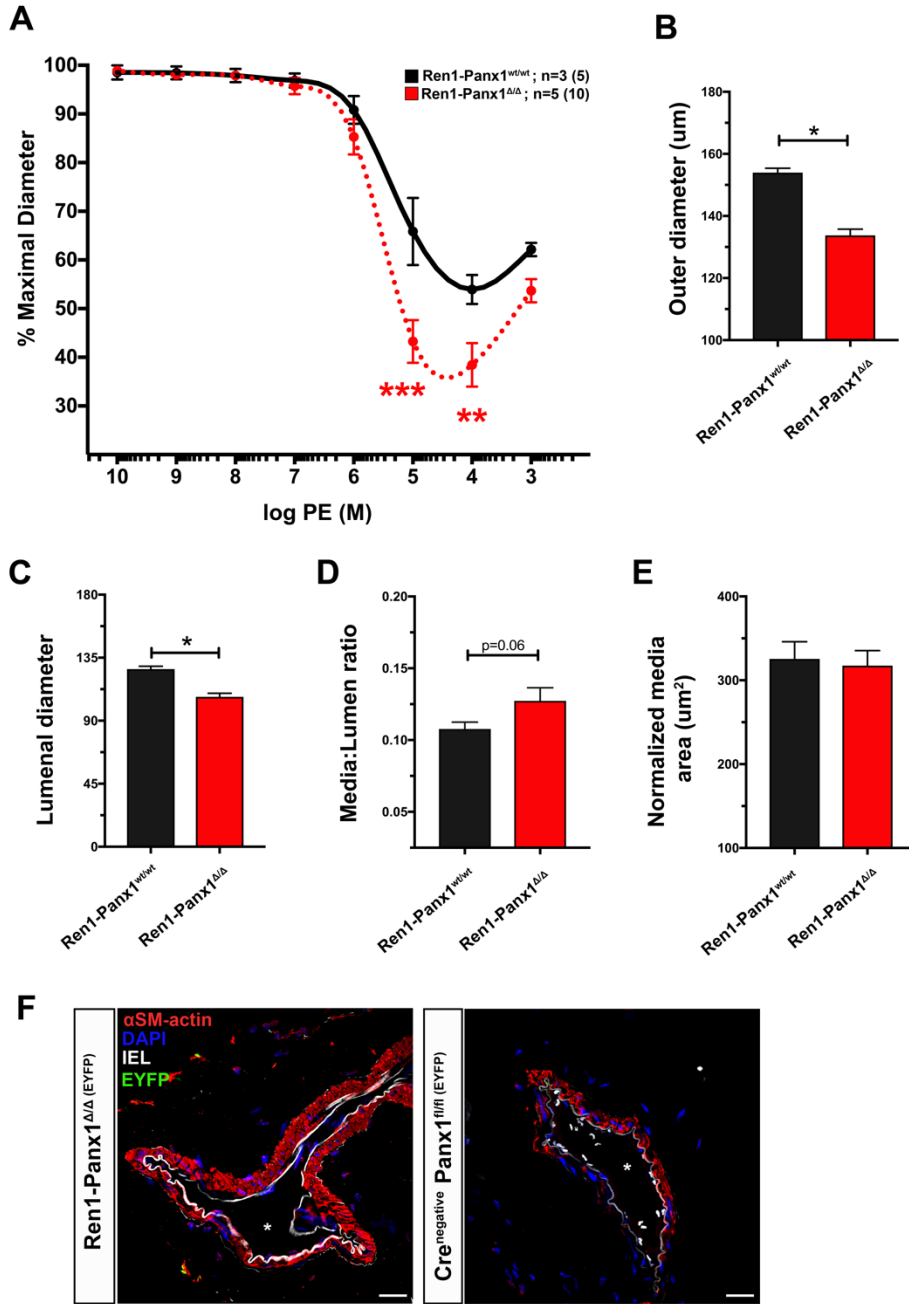


Figure 29. Supplement to Figure 27. Effects of renovascular Panx1 deletion on vasoconstriction responses in peripheral resistance arteries.

Figure 29. Supplement to Figure 27. Effects of renovascular Panx1 deletion on vasoconstriction responses in peripheral resistance arteries. (A) Contractile responses to increasing concentrations of phenylephrine in TDAs from and Ren1-Panx1^{wt/wt} control (black line; N=4 mice (7 arteries)) and Ren1-Panx1^{Δ/Δ} mice (red line; N=6 mice (8 arteries)). Concentration-effect curves were fitted to the data using four-parameter, non-linear regression curve. Data assessed by two-way ANOVA with Bonferroni post-hoc test for multiple comparisons. **p < 0.01 ***p < 0.001. **(B-E)** Vessel structural properties. **(F)** Immunostaining for EYFP expression in peripheral arteries from Ren1-Panx1^{Δ/Δ} (EYFP) reporter mice. Internal elastic lamina (white), αSM-actin (red), EYFP (green), nuclei stained with DAPI (blue); * indicates vessel lumen. Scale bar= 20μm.

Coordination of renin recruitment is impaired in mice lacking Pannexin 1

Within the afferent arteriole, vascular smooth muscle cells retain the capacity to re-activate their fetal renin gene program when BP homeostasis is challenged^{227, 371, 372}. This physiologic process is called recruitment and provides increasing renin levels when demand is needed. We predicted that Panx1 may facilitate paracrine coupling of these cell types since purinergic signals influence renin expression. To test this, we lowered BP in Ren1-Panx1^{Δ/Δ} and Ren1-Panx1^{wt/wt} mice by administering a low sodium diet (0.05%) and ACE inhibitor (captopril) in the drinking water as previously published²²⁷. The degree of renin recruitment was examined by immunofluorescence renin staining and co-localization with α -SMactin positive arterioles (**Figure 30A-D**). Following BP lowering, Ren1-Panx1^{wt/wt} control animals exhibited a typical recruitment response— α SM-actin positive cells extending distally from the entrance to the glomerulus stained positive for renin (**Figure 30A-B**). In contrast, Ren1-Panx1^{Δ/Δ} mice exhibited an abnormal recruitment response, which was marked by renin cell hypertrophy in the pre-glomerular vascular wall and a limited capacity of distal α SM-actin positive cells to re-activate renin expression (**Figure 30C-D**). Quantification of renin positive area (**Figure 30E**) and renin tissue expression levels (**Figure 30F**) similarly reflected a limited capacity to engage the renin recruitment mechanism as a significant reduction in recruitment responses were observed in Ren1-Panx1^{Δ/Δ} mice. Interestingly, Ren1-Panx1^{Δ/Δ} mice are still able to enhance plasma renin concentrations to comparable levels as control mice (**Figure 30G**), likely due to contributions from existing JG cells. Given the observed enhanced baseline plasma aldosterone levels and increased MAP in Ren1-Panx1^{Δ/Δ} mice, we predicted that Ren1-Panx1^{Δ/Δ} mice would be more sensitive to sodium depletion and captopril treatment due to

an impaired renin recruitment. However, Ren1-Panx1^{Δ/Δ} mice sufficiently maintained MAP (**Figure 32H**), as well as the plasma aldosterone concentration (**Figure 32I**) compared with Ren1-Panx1^{wt/wt} controls. These results suggest that Panx1 deletion from the renal vasculature shifts compensatory recruitment mechanisms from metaplastic differentiation to hypertrophy and increased synthesis when BP is lowered.

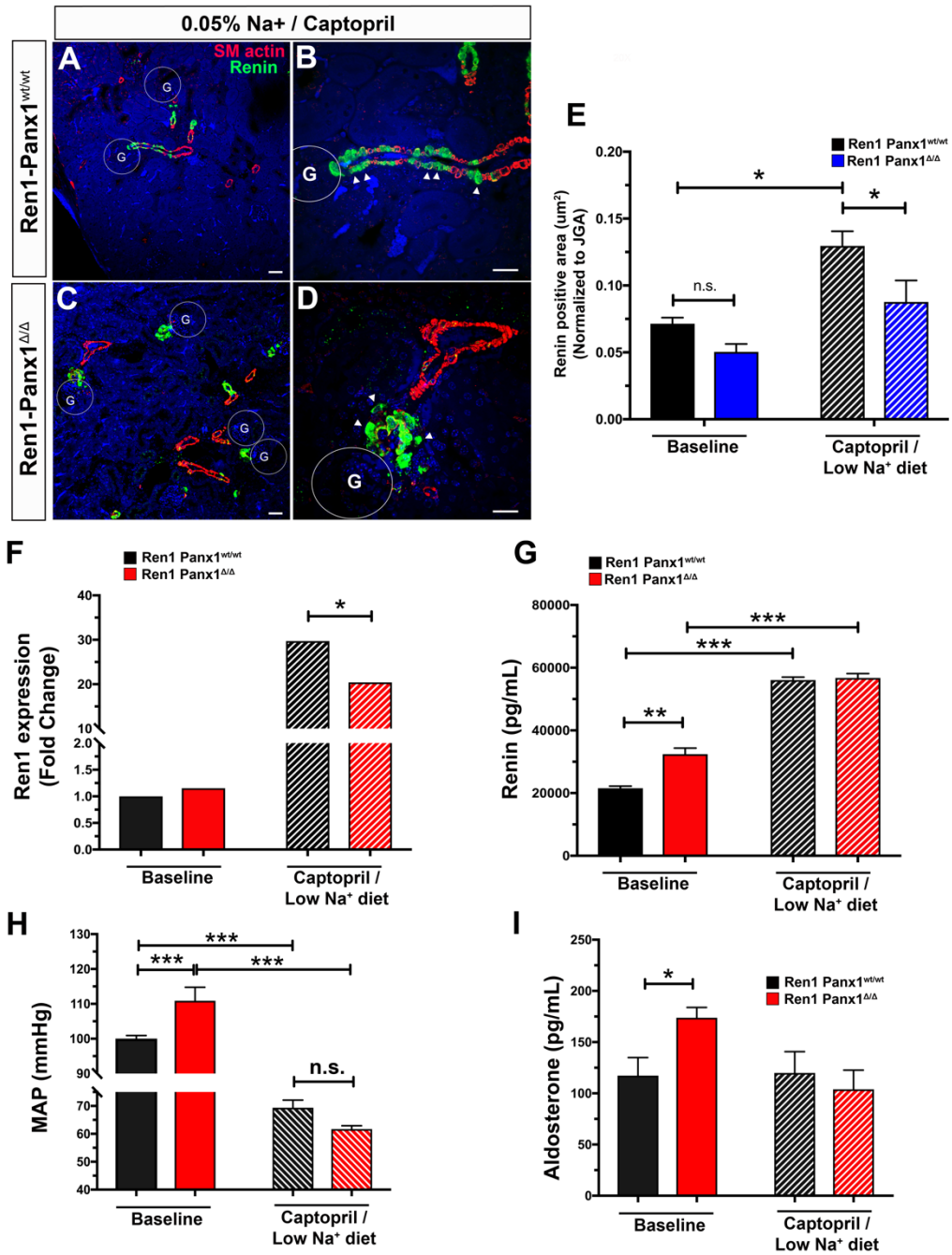


Figure 30. Renin recruitment is impaired in Ren1-Panx1^{Δ/Δ} mice.

Figure 30. Renin recruitment is impaired in Ren1-Panx1 Δ/Δ mice. (A) Immunofluorescence renin staining in kidneys of Ren1-Panx1^{wt/wt} control mice after BP lowering with low sodium (0.05%) diet and captopril (5g/L) in drinking water. Renin (green), α -SMactin (red), nuclei are stained with DAPI (blue), circles indicate glomeruli (G). Scale bar = 40 μ m. **(B)** High magnification image of (A), arrows demarcate renin cells. Scale bar = 20 μ m. **(C)** Immunofluorescence renin staining in kidneys of Ren1-Panx1 Δ/Δ mice after BP lowering. Renin (green), α -SMactin (red), nuclei are stained with DAPI (blue), circles indicate glomeruli (G). Scale bar = 40 μ m. **(D)** High magnification image of (C), arrows demarcate renin cells. Scale bar = 20 μ m. **(E)** Double blind quantification of renin positive area normalized to number of renin quantification of the amount of renin positive area normalized the number of renin positive JGA from non-consecutive tissue sections. N=4 control; 4 knockout mice. Data represented as mean \pm s.e.m. A two-way ANOVA with Sidak post-hoc test was performed for significance; *p<0.05. **(F)** qRT-PCR analysis of renin mRNA isolated from total cortex RNA at baseline and after BP lowering. Renin expression levels were normalized to B2M expression and are represented as fold change using $2^{-\Delta\Delta C_t}$ method. N= 3 control; 4 knockout mice. A two-way ANOVA with Sidak post-hoc test was performed for significance; *p<0.05. **(G)** Plasma renin concentration measured by ELISA before (N=5 control; 6 knockout) and after (N=3 control; 4 knockout) BP lowering. **(H)** 24hour mean arterial blood pressure (MAP) of Ren1-Panx1 Δ/Δ and Ren1-Panx1^{wt/wt} control mice. MAP during the inactive period (12hr light: 06:00-17:59) and active period (12hr dark: 18:00-05:59) were averaged together and represented as mean \pm s.e.m. N=3 control; 4 knockout mice. A two-way ANOVA with repeated measures and a Sidak posthoc test was performed for significance; **p < 0.01

***p < 0.001. **(I)** Plasma aldosterone levels measured by RIA before (N=4 control; 6 knockout) and after (N=3 control; 4 knockout) BP lowering. Data displayed as groups and represented as mean \pm s.e.m. A two-way ANOVA with repeated measures and a Sidak posthoc test was performed for significance; *p<0.05.

AT1R blockade is insufficient to normalize BP and aldosterone levels in Ren1-Panx1^{Δ/Δ} mice.

To determine whether elevated aldosterone and MAP in Ren1-Panx1^{Δ/Δ} mice are specifically mediated by angiotensin II type 1 receptors (AT1R), we treated Ren1-Panx1^{Δ/Δ} mice with candesartan. Mice were administered candesartan (10mg/kg/day) for 10 days in drinking water and were monitored in metabolic cages. 24-hour MAP was assessed by telemetry and aldosterone assessed by RIA. Water consumption and urine excretion volumes were also measured. At baseline Ren1-Panx1^{Δ/Δ} mice exhibited elevated MAP ($\Delta=8\text{mmHg}$) (**Figure 31A**), enhanced plasma aldosterone levels (**Figure 31B**), and significantly reduced urine volume (**Figure 31D**), which is consistent with high RAAS activity and fluid retention. In contrast, when the AT1R is inhibited, Ren1-Panx1^{Δ/Δ} and Ren1-Panx1^{wt/wt} mice exhibit a significant AT1R-dependent reduction in MAP and aldosterone with a significant MAP difference being maintained between knockout and control animals (**Figure 31A-B**). Moreover, AT1R inhibition did not influence water consumption (**Figure 31C**) or urine volume (**Figure 31D**). Thus, elevated MAP due to Panx1 deletion in renin expressing cells is partially mediated AT1R.

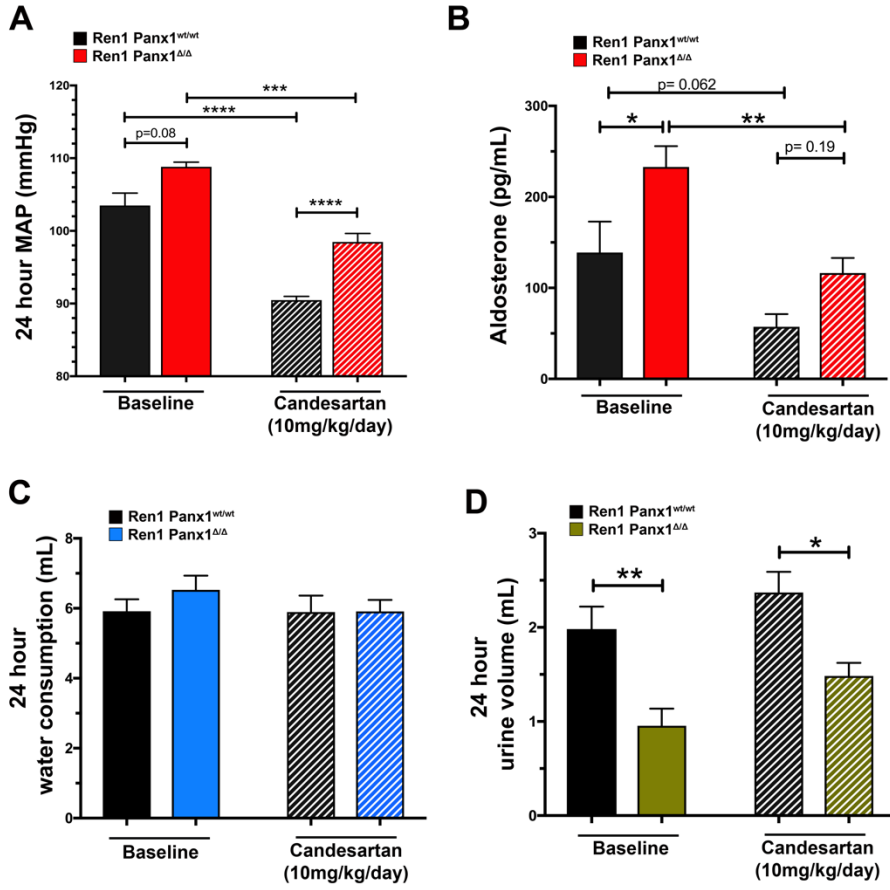


Figure 31. AT1R inhibition partially mediates RAAS activity in Ren1-Panx1^{Δ/Δ} mice.

Figure 31. AT1R inhibition partially mediates RAAS activity in Ren1-Panx1 Δ/Δ mice.

(A) 24-hour MAP measured using telemetry. N=3 control; 3 knockout mice. Data displayed as groups and represented as mean \pm s.e.m. A two-way ANOVA with repeated measured and a Sidak posthoc test was performed for significance; * $p \leq 0.05$ ** $p \leq 0.01$ *** $p \leq 0.001$ **** $p \leq 0.0001$. **(B)** Plasma aldosterone levels measured by RIA. Blood samples collected during the active period. N=3 control; 5 knockout mice. **(C)** 24-hour water consumption (4-day average) in Ren1-Panx1 Δ/Δ and Ren1-Panx1 $^{wt/wt}$ control mice treated with Candesartan (10mg/kg/day) in drinking water for 10 days. N=4 control; 7 knockout mice. **(D)** 24-hour urine volume (4-day average). N=4 control; 4 knockout mice.

Panx1 deletion from renin expressing cells causes adrenal hypertrophy and aldosterone dysregulation in male, but not female mice.

The adrenal gland and renin secreting JG cells co-modulate the maintenance of fluid and electrolyte balance critical for long-term BP regulation. Within the adrenal cortex, the outer zona glomerulosa layer acts as an extension of the RAAS and modulates aldosterone secretion through stimulation by angiotensinogen-derived peptides. Due to the incomplete normalization of MAP, plasma aldosterone, and urine volume observed in Ren1-Panx1^{ΔΔ} treated with candesartan, we examined adrenal glands from knockout and control mice for possible adrenal dysregulation. Compared with control mice, the adrenal glands of Ren1-Panx1^{ΔΔ} mice were significantly larger in overall mass (**Figure 32A**) and appeared to have a thickened cortical layer as assessed by H&E staining (**Figure 32B**). To test if Panx1 expression was altered in adrenal glands of Ren1-Panx1^{ΔΔ} mice due to the presence of a local adrenal RAAS and the expression of renin in the adrenal gland under certain circumstances³⁷³ we performed immunostaining for cre recombinase activity using our fluorescence reporting model. Adrenal glands from both Ren1-Panx1^{wt/wt} (EYFP) and Ren1-Panx1^{ΔΔ} (EYFP) had detectable levels of EYFP signal within the zona glomerulus and the zona fasciculate of the adrenal cortex (**Figure 32C**). This subset of cells spanned the length of the cortex and was not present in all adrenocortical cells or the adrenal medulla. qRT-PCR and western blot analysis furthered revealed altered Panx1 expression in our Ren1-Panx1^{ΔΔ} mice compared with controls. A significant reduction in Panx1 mRNA (**Figure 32D**), as well as protein level (**Figure 32E**) were detected. Interestingly, female Ren1-Panx1^{ΔΔ} mice did not display aberrant adrenal morphology (**Figure 33A-B**), nor did they exhibit enhancement in plasma renin concentration (**Figure 33B**) or plasma

aldosterone concentration (**Figure 33D**). Thus, Panx1 deletion from renin lineage cells of the adrenal cortex might also contribute to elevated MAP in Ren1-Panx1^{Δ/Δ} mice.

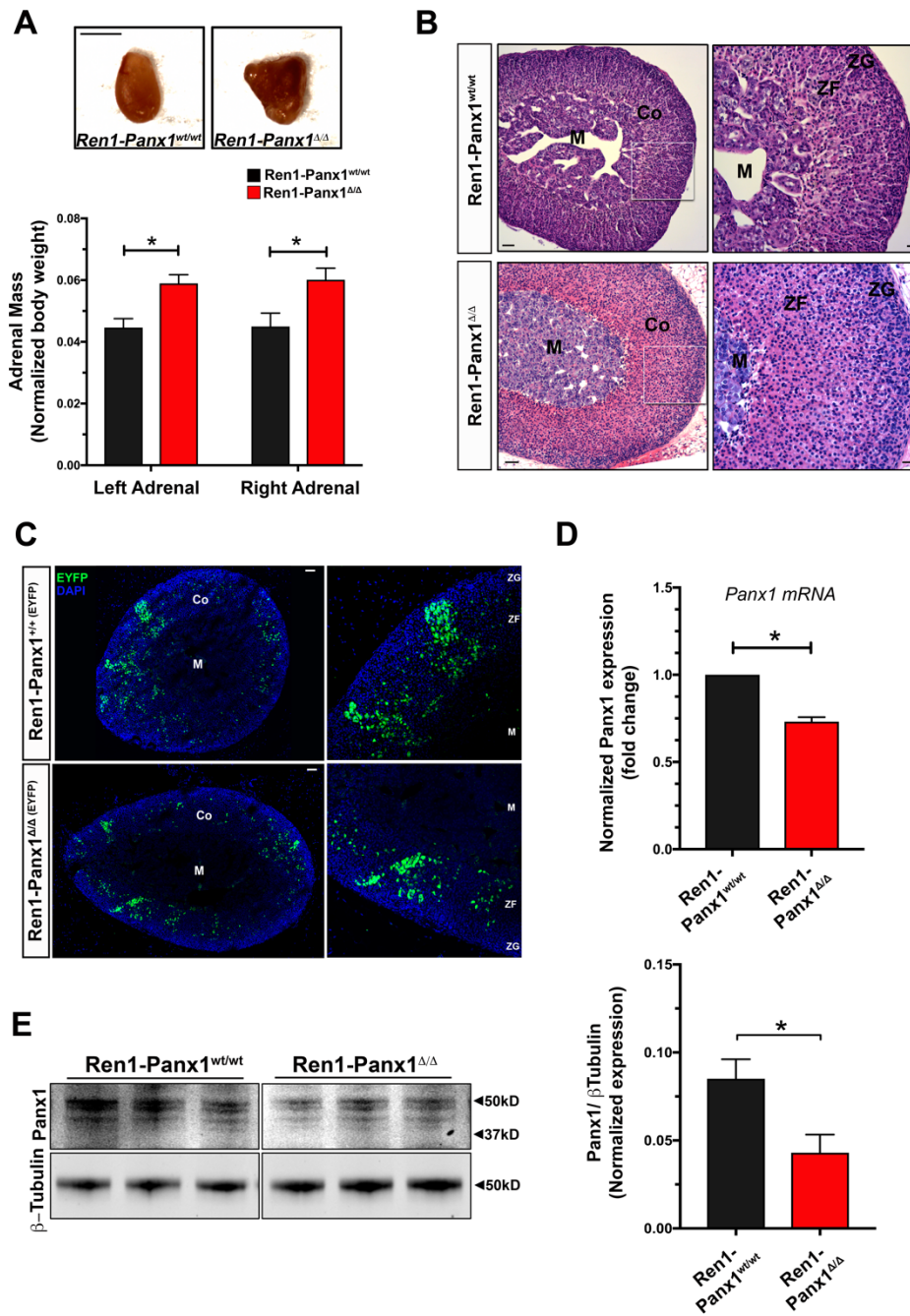


Figure 32. Panx1 deletion from renin expressing cells causes adrenal gland hypertrophy, cortical hyperplasia, and aldosterone dysregulation.

Figure 32. Panx1 deletion from renin expressing cells causes adrenal gland hypertrophy, cortical hyperplasia, and aldosterone dysregulation. (A) Representative images and normalized adrenal gland mass from Ren1-Panx1^{Δ/Δ} and Ren1-Panx1^{wt/wt} control mice. Both the right and left adrenal glands were assessed for gross morphology. Scale bar = 1mm. N= 4 control; 7 knockout mice. Data are presented as groups and represented as mean ± s.e.m. A student's t-test was performed for significance; *p<0.05. **(B)** H&E staining of adrenal gland cross-sections from Ren1-Panx1^{Δ/Δ} mice to assess adrenocortical hypertrophy. White box denotes high magnification inset (right panel), Cortex (Co), medulla (M), zona fasciculata (ZF), and zona glomerulosa (ZG). Scale bar= 50μm. **(C)** Immunofluorescence staining for Cre-dependent EYFP expression in adrenal the adrenal cortex. EYFP (green); nuclei stained with DAPI (blue). Scale bar=100μm. **(D)** qRT-PCR analysis of Panx1 from isolated total adrenal RNA. Expression levels were normalized to B2M and are represented as fold change using 2^{-ΔΔCt} method. N= 6 control; 6 knockout mice. Data presented as mean ± SEM. A student's t-test was performed for significance; *p < 0.05. **(E)** Western blot analysis of whole adrenal glands in Ren1-Panx1^{wt/wt} and Ren1-Panx1^{Δ/Δ} mice. N=3 control; 3 knockout mice. Normalized quantification represented as mean ± s.e.m. A student's t-test was performed for significance, *p < 0.05.

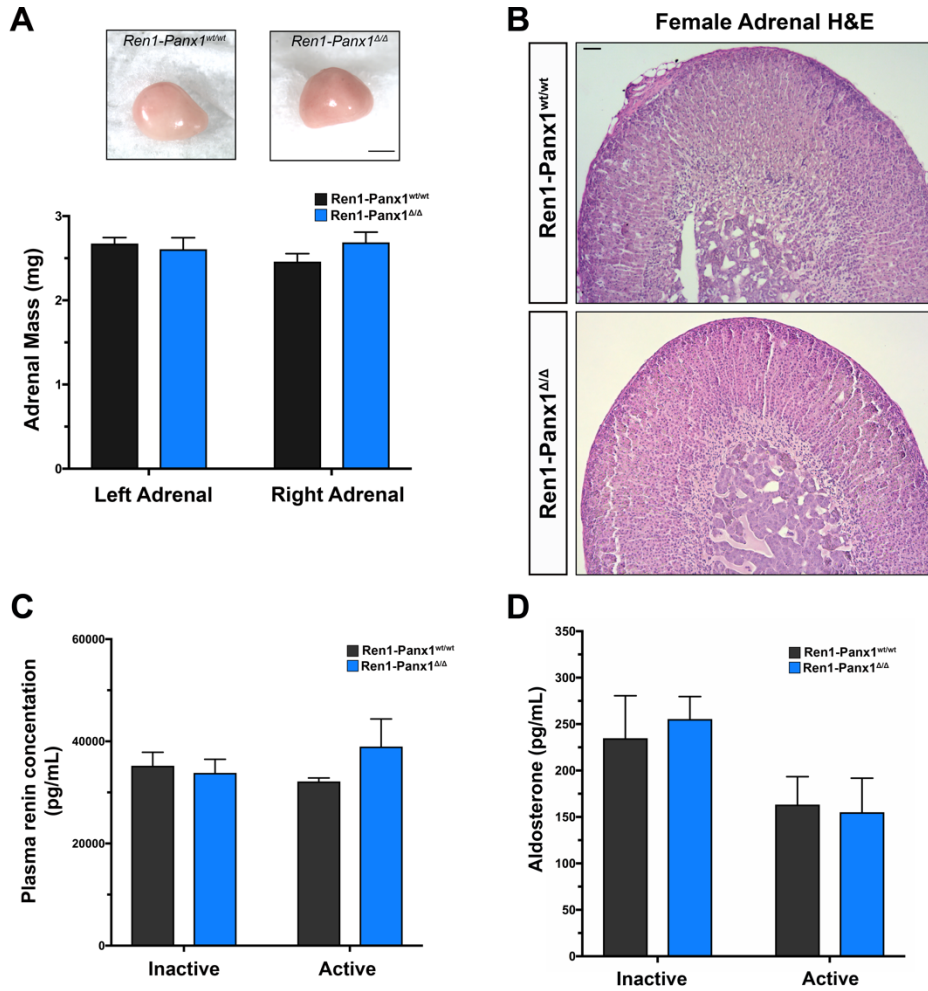


Figure 33. Supplement to Figure 32. Female *Ren1*-renin-cell *Panx1* do not exhibit RAAS hyperactivity or adrenal gland hypertrophy.

Figure 33. Supplement to Figure 32. Female Ren1-renin-cell Panx1 do not exhibit RAAS hyperactivity or adrenal gland hypertrophy. (A) Representative images of female adrenal glands and quantification of adrenal mass from Ren1-Panx1^{Δ/Δ} and Ren1-Panx1^{wt/wt} mice. Scale bar= 1mm. N=7 control; 8 knockouts. Data are presented as groups and represented as mean ± s.e.m. A students t-test was performed for significance. **(B)** Representative H&E staining of adrenal glands. Scale bar= 100μm. **(C)** Measurements of plasma renin concentration measured using ELISA during the inactive and active period. N=5 control; 5 knockout mice. **(D)** Plasma aldosterone concentration measured by RIA during the inactive and active period. N=7 control; 8 knockouts. Data are presented as groups and represented as mean ± s.e.m. A two-way ANOVA with repeated measures and a Sidak postoc test were performed for significance.

Panx1 deletion from renin-expressing cells causes dysregulation of adrenocortical zonation and ectopic CYP11B2 expression.

The steroid hydroxylase enzyme CYP11B2 (aldosterone synthase) is uniquely involved in the biosynthesis of aldosterone in the adrenal cortex. CYP11B2 expression is restricted to cells of the zona glomerulosa (ZG) which are sensitive to circulating levels of angiotensinogen-derived peptides and enhance aldosterone secretion when stimulated. Due to alterations in the adrenal cortex of Ren1-Panx1^{Δ/Δ} mice we assessed CYP11B2 expression in the adrenal cortex. Compared with Ren1-Panx1^{wt/wt} mice, which have a restricted CYP11B2 pattern in the zona glomerulosa (**Figure 34A**), Ren1-Panx1^{Δ/Δ} mice present with aberrant CYP11B2 expression (**Figure 34B**). The distribution of CYP11B2 cells were pervasive throughout the adrenal cortex and aberrantly extending into the zona fasciculata (ZF). CYP11B2 positive cells were not present in the adrenal medulla. However, due to the inability of AT1R inhibition to completely normalize BP and urine volume in Ren1-Panx1^{Δ/Δ} mice, we also assessed adrenal gland morphology following 10-day treatment with candesartan. AT1R inhibition resulted in normalization of adrenal gland mass and cortical hypertrophy (Figure 35A-C). However, AT1R inhibition was insufficient to prevent aberrant expression of CYP11B2 in the ZF of the adrenal cortex. Therefore, Panx1-dependent phenotypes impact two adrenal pathways: stimulation and hyperplasia of the adrenal cortex due to AT1R signaling, as well as an AT1R-independent mechanism regulating adrenocortical cell differentiation.

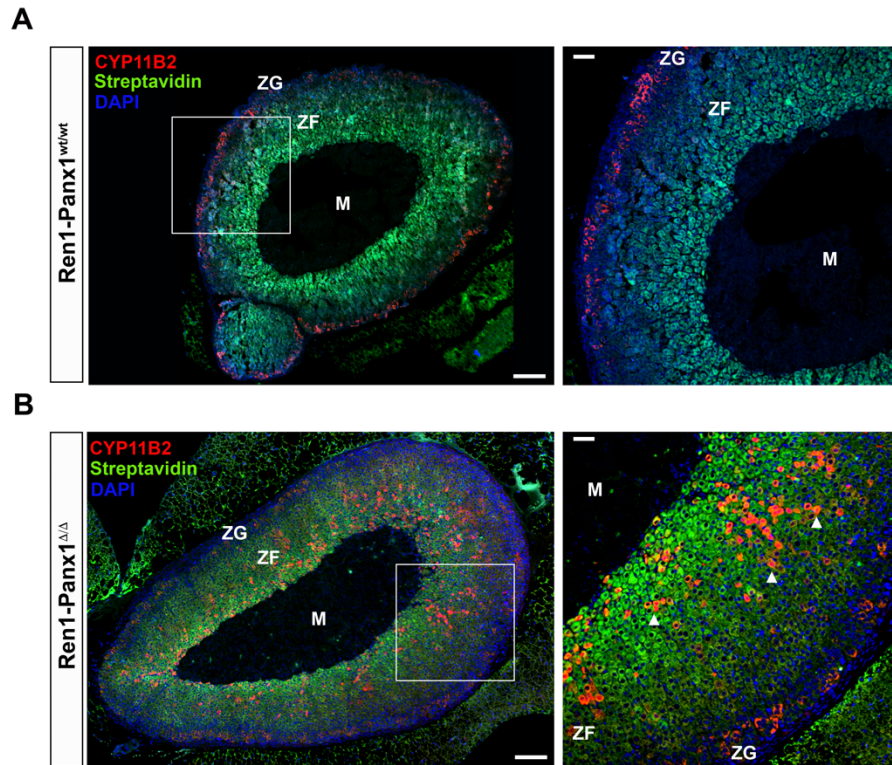


Figure 34. Adrenocortical zonation is impaired when Panx1 is deleted from renin expressing cells.

Figure 34. Adrenocortical zonation is impaired when Panx1 is deleted from renin expressing cells. Representative immunofluorescence images looking at CYP11B2 expression in Ren1-Panx1^{wt/wt} and Ren1-Panx1^{Δ/Δ} mice. **(A)** Confocal image of Ren1-Panx1^{wt/wt} adrenal gland. Scale bar =100μm. Right image is high magnification of white box. Scale bar= 20μm. **(B)** Confocal image of Ren1-Panx1^{Δ/Δ} adrenal gland. Scale bar =100μm. Right image is high magnification of white box. Scale bar= 20μm. CYP11B2 (red), streptavidin (cortex marker; green), nuclei are stained with DAPI (blue). The zona glomerulosa (ZG), zona fasciculata (ZF) and medulla (M) are labeled. White arrows indicate atypical CYP11B2 positive cells in the adrenal cortex.

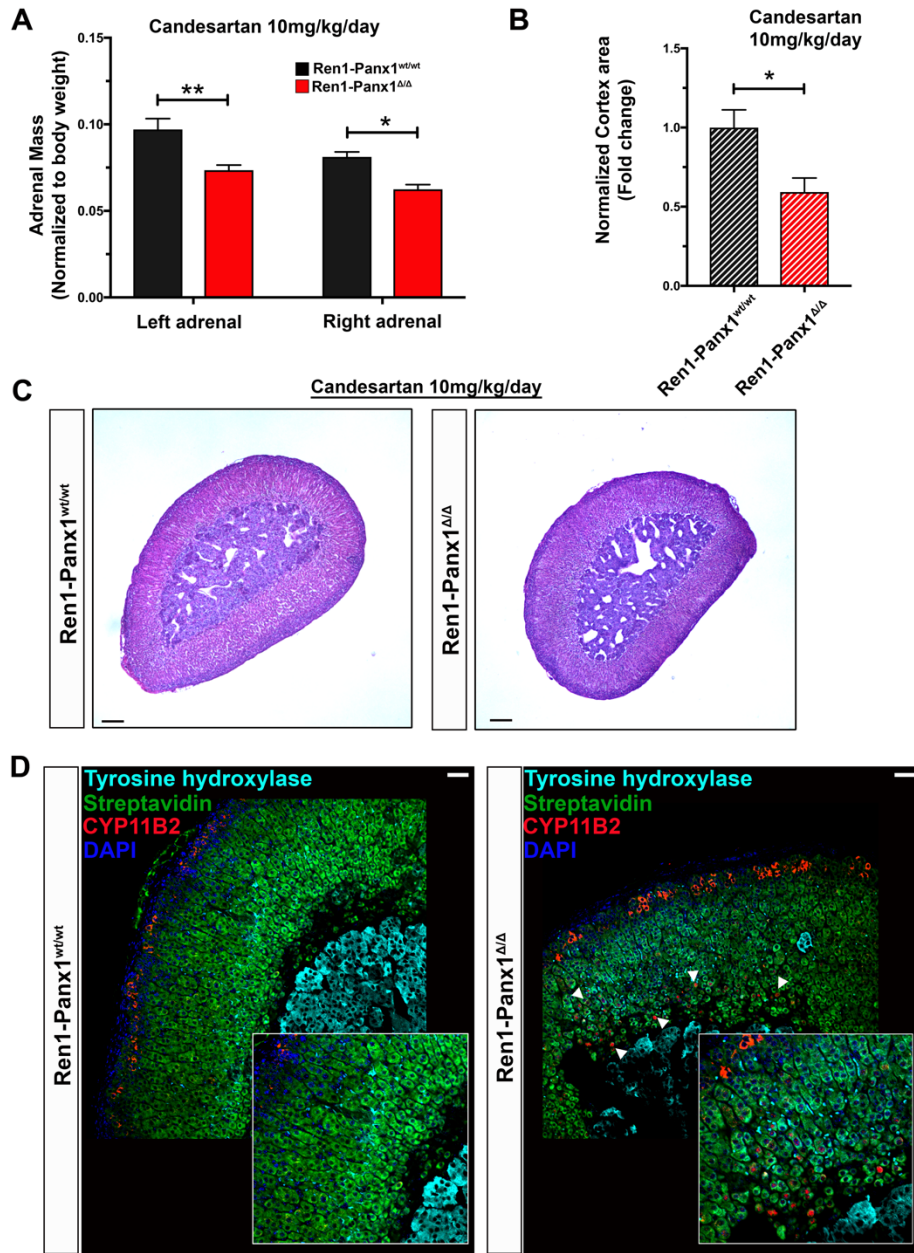


Figure 35. Candesartan treatment normalizes adrenal hypertrophy, but not CYP11B2 dysregulation in Ren1-Panx1^{Δ/Δ}.

Figure 35. Candesartan treatment normalizes adrenal hypertrophy, but not CYP11B2 dysregulation in Ren1-Panx1 Δ/Δ . (A) Normalized adrenal gland mass from Ren1-Panx1 Δ/Δ and Ren1-Panx1^{wt/wt} control mice. Both the right and left adrenal glands were assessed for gross morphology. N= 4 control; 4 knockout mice. Data are presented as groups and represented as mean \pm s.e.m. A student's t-test was performed for significance; *p<0.05, **p<0.01. (B) Quantification of adrenal cortex area from center sections of H&E staining from Ren1-Panx1 Δ/Δ mice to assess adrenocortical hypertrophy. N= 4 control; 4 knockout mice. Data are presented as groups and represented as mean \pm s.e.m. A student's t-test was performed for significance; *p<0.05. (C) Representative H&E from candesartan treated Ren1-Panx1 Δ/Δ mice and control mice. Scale bar = 1mm. (D) Confocal image of Ren1-Panx1 Δ/Δ and control adrenal glands. Right inset is high magnification adrenal cortex. Scale bar= 20 μ m. CYP11B2 (red), streptavidin (cortex marker; green), nuclei are stained with DAPI (blue), medulla stained with tyrosine hydroxylase (cyan). Scale bar =100 μ m. White arrows indicate ectopically expressed CYP11B2 positive adrenocortical cells.

5.4 DISCUSSION

The present study demonstrates a physiological role for Panx1 channels in regulating RAAS and BP homeostasis under steady-state and altered physiologic conditions. Panx1 deletion from renin lineage cells augments plasma renin and plasma aldosterone concentrations leading to a significant elevation in MAP. These pathological changes are underlined by abnormal peripheral vasoconstriction responses and fluid/electrolyte imbalances, likely due to hyperreninemia. RAAS enhancement was sex dependent in our model, with significant differences observed in male, but not female mice. The elevation in plasma aldosterone and MAP was differentially sensitive to RAAS inhibition with MAP only normalized using ACE inhibition and low salt diet. Furthermore, Panx1 deficient mice have an impaired ability of renal smooth muscle cells and adrenocortical cells to engage metaplastic differentiation and transdifferentiation mechanisms necessary for regulating renin recruitment and aldosterone production respectively. Overall, our findings suggest a suppressive role for Panx1 channels in renin-lineage cells pertaining to steady-state regulation of RAAS hormones and suppression of renal/adrenal cell differentiation important for maintaining constant BP when homeostatic set-points are altered.

Within the afferent arterioles, renal autoregulatory mechanisms temporally manage pressure changes through afferent myogenic tone and tubuloglomerular feedback (TGF)³⁷⁴. Together these two systems maintain constant renal blood flow (RBF) and glomerular filtration rates (GFR) by modulating renin secretion⁸². Any defect in the ability of these mechanisms to respond to changes in BP leads to impaired renin suppression and likely

elevated BP⁸⁰. In addition to regulation by feedback mechanisms, renin secreting JG cells in the afferent arteriole independently integrate physiologic signals to renin enhance renin secretion when BP is low. In this study, the deletion of Panx1 from renin-lineage cells resulted in a distinct high renin–high BP phenotype, which could be due to abnormal negative feedback loops, or alternatively, autonomous secretion of renin from JG cells³⁴⁵. In support of possible renal autoregulation defects in Ren1-Panx1 Δ/Δ mice, a body of evidence supports the direct influence of extracellular purines on autoregulation. ATP has been shown to directly influence the myogenic component of renal autoregulation⁸³. Direct administration of ATP to renal cortical slices or to the adventitial side of afferent arterioles produces vasoconstriction⁸⁴. The mechanism responsible for vascular responses are linked to activation of P2X1 receptors, which localize to the afferent arterioles^{85,86} and contribute to pressure-mediated vasoconstriction^{87, 97, 375}. Although pressure-mediated vasoconstriction remains to be specifically tested in our Ren1-Panx1 knockout model, reduced extracellular ATP would be consistent with reduced autoregulation and enhanced basal renin secretion. Recently, a role for Panx1 in controlling vasoconstriction from smooth muscle cells in peripheral resistance arteries has come into focus^{77, 78}. Pharmacological inhibition or genetic deletion of smooth muscle Panx1 channels resulted in reduced ATP release and vasoconstriction^{78, 376}. These studies support the notion that vascular Panx1-mediate ATP release influences the contractile state smooth muscle cells, which in Ren1-Panx1 Δ/Δ mice may impair purinergic signaling in the afferent arteriole.

In addition to ATP, adenosine also influences afferent arteriolar vasoconstriction. Adenosine type 1 receptors (A1R), localizes to smooth muscle cells of the afferent arteriole⁹⁰ and coordinates both vasoconstriction and renin suppression^{91, 92}. In A1R-

deficient animals, autoregulation mechanisms of RBF and GFR are impaired, as assessed using isolated perfused systems, which resulted in enhanced renin secretion^{88, 97}. In this context, Ren1-Panx1^{Δ/Δ} mice that contain Cre activity in afferent arterioles and have reduced renal Panx1 expression may also have reduced adenosine levels due to diminished accumulation of extracellular ATP and the subsequent lack of ATP metabolism by renovascular ectonucleotidases^{364, 377}. As previously demonstrated, reduced afferent vascular resistance highly correlates with reduced interstitial ATP concentration⁹⁵. Although the concentration of interstitial ATP and adenosine remain to be specifically measured, impairments in pressure-induced renin suppression due to impaired efflux of extracellular purine nucleotides, could contribute to dysregulation of renin and high BP levels in our model.

In concert with myogenic mechanisms, TGF also regulates the degree of autoregulation within the JGA through purinergic signaling⁹⁸. Macula densa cells in the thick ascending limb of Henle are anatomically coupled to mesangial cells and smooth muscle cells in the afferent arteriole³⁷⁸. This cellular arrangement facilitates heterocellular communication important for JG cell function⁸². When BP is elevated, and there is a corollary increase in GFR, macula densa cells convert elevated tubular sodium chloride concentration into an inhibitory ATP signal that traverses the basolateral membrane^{100, 101}, activates mesangial cells⁹⁹, and inhibits renin secretion through an adenosine-dependent process¹⁰². In our study, enhanced plasma renin concentrations in the presence of elevated BP in Ren1-Panx1^{Δ/Δ} mice might further be explained by impaired TGF due to reduced Panx1-mediated ATP release from macula densa cells, although this was not specifically tested. Currently, the mechanism thought to facilitate cellular ATP release from macula

densa relies on the ATP-permeable large-conductance (380pS) anion selective maxi anion channel¹⁰⁰. Although maxi anion channels have distinct channel properties compared with Panx1 channels, which likely exist as outwardly rectifying, non-selective small-conductance channels (15-100pS)³⁷⁹, both channels have overlapping functions and are immunolocalized to JGA^{178,380}. Thus, future investigations may be warranted to determine if Panx1 channels specifically localize to the basolateral membrane of macula densa cells, and whether deletion of Panx1 reduces renal interstitial ATP concentration upon increasing tubular sodium chloride concentrations.

Impairments in the propagation of intercellular calcium waves across the extraglomerular mesangium might also explain a high renin–high BP phenotype observed in this study. Mesangial cells express a number of purinergic receptors¹⁵³ and have been observed to utilize an ATP-dependent mechanism to propagate intercellular calcium and suppress renin secretion³⁸¹. A recent study of mesangial cell calcium wave propagation provides evidence that ATP-mediated signals partially required to propagate intracellular calcium waves through mesangial cells necessary for heterocellular communication in TGF⁹⁹. In this study, impairments in the intracellular calcium propagation occurred using pharmacological inhibitors of P2 receptors and ATP degrading enzymes⁹⁹, but not adenosine receptor inhibitors. It should be noted that adenosine in this case is disposable for calcium wave propagation, but necessary for penultimate inhibitory effects on renin secreting JG cells³⁸². Thus, the complex regulation of purinergic signaling, which relies on extracellular ATP as a key reactant, suggests a role for ATP release in regulating TGF responses. Future studies will be important to test if functional Panx1 channels exist on

mesangial cells, and if so, to test the degree in which TGF mechanisms rely on Panx1-mediated ATP release to coordinate calcium responses in the JGA.

Lastly, renin production by JG cells may be directly influenced in our model. ATP has been previously shown to enhance renin synthesis and secretion through P2Y receptor activation and cAMP-dependent mechanisms^{356, 357}. Adenosine has the opposite effect, inhibiting renin secretion through A1R activation and intracellular calcium signaling¹¹⁵. In our model, we initially predicted that deletion of Panx1 and subsequent reductions in extracellular ATP would suppress basal renin secretion. However, we observed the opposite. Plasma renin concentrations were elevated without significant changes in tissue renin expression, thus advocating for enhanced basal renin secretion rate that could be the driving factor for higher baseline BP in Ren1-Panx1^{Δ/Δ} mice. In this model, Panx1 might facilitate inhibitory signaling mediated by extracellular ATP and its breakdown into adenosine. In support of these findings, adenosine has been shown to directly inhibit renin secretion through A1R activation^{365, 366} and deletion of A1Rs in mice have enhanced and unsuppressed renin secretion¹¹⁴. Moreover, deletion of CD73 ectonucleotidases, which are responsible for the metabolism of ATP into adenosine, also have altered renin responses and vasoconstrictive feedback to changes in tubular flow³⁶⁴. The coordinated release of ATP by Panx1 might therefore be a novel regulator of JG cell function.

In comparison to Panx1-mediated purinergic signaling, Panx1 channels could also influence JG-cell membrane potential and intracellular calcium homeostasis important for coordinating renin dynamics. Renin-secreting JG cells couple membrane electrical potentials with renin secretion that allows depolarization to inhibit renin secretion and

hyperpolarization to increase renin release³⁸³. Canonically, JG cell depolarization causes L-type calcium channel activation, increased intracellular calcium concentrations, and inhibition of the calcium-sensitive adenylyl cyclase 5. This in turn inhibits calcium-sensitive adenylyl cyclase enzymes and reduces the stimulatory effects of cAMP on renin secretion. In this regard, Panx1 acting as a non-selective ion channel could influence JG cell depolarization through its permeability to cation influx. Cationic dye transfer experiments using To-Pro or Yo-Pro dye uptake in conjunction with genetic knockout/knockdown of Panx1 provide evidence for cation permeability^{191, 193, 384}. Moreover, in an early report analyzing Panx1 ion selectivity, sodium ions and positively charged N-methyl-D-glucamine molecules could permeate Panx1 channels³⁸⁵. Although this has not been specifically tested in our model, an influx of positively charged ions and molecules through Panx1 could contribute to a depolarized JG-cell membrane potential and reduced renin secretion. Removal then of Panx1 due to genetic deletion in Ren1-Panx1^{Δ/Δ} mice could potentially shift the membrane potential to favor a hyperpolarized renin secretion state.

Similarly, Panx1 channels may also permeate calcium ions which are a key negative regulator of renin secretion from JG cells. Panx1 is a non-selective ion channel that is structurally similar to the bona fide calcium channel CALHM-1¹³⁹. Moreover, a number of studies report a link between increased calcium ion concentration and Panx1^{188, 249, 386}. Evidence indicates that increased calcium ion concentration begets Panx1 channel activation; however, these studies do not rule out the alternative possibility that Panx1 channel opening may enhance calcium responses. It is interesting then to speculate in JG cells that opening of Panx1 channels might allow calcium to diffuse down its concentration

gradient and decrease basal renin secretion rates. This hypothesis could explain autonomous renin secretion and increased RAAS in Ren1-Panx1^{Δ/Δ} mice. The mechanism responsible for Panx1 channel gating in JG cells remains, but previous work has suggested that Panx1 is weakly sensitive to changes in membrane potential under certain conditions, which in turn modulates channel gating³⁸⁷⁻³⁸⁹. The mechanism by which this happens is unclear since a voltage sensing region of Panx1 proteins has not yet been identified. However, in support of voltage modulation, mouse Panx1 channels were recently found to elicit basal channel activity, which was is different than observations made for human Panx1 isoform¹⁹². This influence of membrane voltage and basal activity, could potentially allow Panx1 channels to regulate tonic inputs to JG cells and provide a conduit for positively charged ions that produce an inhibitory effect on renin secretion. Future studies are necessary to understand endogenous Panx1 channel activity in unstimulated conditions from Ren1-Panx1^{Δ/Δ} JG cells, but changes in ion conduction and membrane potential would support autonomous renin secretion caused by Panx1 deletion.

During fetal development, renin expressing cells are found throughout the renal vasculature of the developing kidney and differentiate into vascular smooth muscle cells as development continues. In adulthood, a restricted population of renin expressing JG cells remains at the entrance of the glomerulus in unstressed adult mammals^{390, 391}. However, renin-lineage cells, which previously expressed renin during development, retain the capacity to activate fetal-renin gene programs when systemic BP is severely shifted outside of physiological thresholds³⁷⁰, thus restoring homeostasis. To test the contribution of Panx1 in this physiological process, we severely lowered systemic BP by sodium depletion and treatment with the ACE inhibitor captopril. Due to published findings that ATP enhances

JG renin expression and renin promoter activity³⁵⁷, we initially predicted that coordination of renin recruitment by Panx1-mediated ATP release would be blunted in renin-lineage smooth muscle cells. In this regard, we observed a significant impairment in renin recruitment capacity within the smooth muscle cell layer of Panx1 deficient mice. In Ren1-Panx1 Δ/Δ mice pre-existing JG cells became hypertrophied most likely due to the continued presence of physiological stressors. However, knockout mice could partially compensate the amount of BP lowering as hypertrophied JG cells were able to increase renin expression and plasma renin concentration. The mechanism responsible for altered Panx1-dependent responses remains to be determined, but may involve activation of P2-receptors that couple with cAMP generating signaling pathways.

The convergence of intrarenal signaling mechanisms on cAMP-mediated pathways is crucial for initiating and maintaining the renin recruitment phenotype^{392, 393}. The lack of renin recruitment in our mouse model supports the idea that smooth muscle cell Panx1 engages purinergic signaling pathways to promote renin-lineage cell conversation during hypotension. In renal smooth muscle cells P2X receptors are expressed in the afferent arteriole⁸³ and are fast acting ionotropic channels³⁹⁴ responsible for calcium-dependent vasoconstriction³⁹⁵. In contrast, P2Y receptors, which are also found in the afferent arteriole, are metabotropic coupled receptors that have a temporally slower signaling profile⁶² than P2X receptors. P2Y receptors are involved in both cAMP-dependent renin expression³⁵⁶ and cell differentiation³⁹⁶. P2Y2 and P2Y11 receptors have been shown to couple with the G_{as} subunit of heterotrimeric G-proteins, which results in the generation of cAMP in MDCK-D1 epithelial cells and Calu6 renin secreting cells^{357, 397, 398}. Transfection of a DNA-luciferase reporter linked to the REN human promoter in Calu6-P2Y11

containing renin expressing cells exhibits reporter activity when stimulated with exogenous ATP. These effects were abolished by mutation of the -222 upstream cAMP response elements of the REN promoter³⁵⁷ connecting an ATP-mediated signaling pathway with cAMP-dependent renin expression. Thus, in our model, a continued hypotensive stimulus may cause accumulation of Panx1-dependent extracellular ATP and a shift in purinergic signaling towards a latent P2Y cAMP-mediated renin phenotype. The expression and function of P2Y receptor isotypes remains to be tested in our mouse model. It should be noted that the rodent P2Y11 homolog of human P2Y11 receptors is absent from the rats and mice³⁹⁹. In its place is a P2Y11-like receptor that may have similar functionality to human P2Y11⁴⁰⁰, but more research is needed to define this receptors mechanism of action. It will be important in the future to measure interstitial ATP concentrations in response to BP lowering, and to determine if the concentration of ATP levels or the time dependency of a purinergic stimulus is sufficient to shift intracellular signaling pathways to facilitate smooth muscle to renin-cell lineage conversion.

The adrenal cortex is the major biosynthetic source of steroid hormone production including glucocorticoids (i.e. cortisol/corticosterone) and mineralocorticoids (i.e. aldosterone). One important facet of systemic BP regulation is the appropriate regulation of aldosterone from the adrenal zona glomerulosa (ZG) in the outer zone of the adrenal cortex. Unlike other secreted hormones (i.e. renin), there is no releasable pool of aldosterone from ZG cells. Instead, biosynthesis is enhanced when there is demand, which is driven by upregulation of CYP11B2 (aldosterone synthase) expression, as well as dynamic changes in adrenal cortex size and cellular composition⁴⁰¹. In Ren1-Panx1 $\Delta\Delta$ mice, hyperreninemia corresponds with enhanced plasma aldosterone concentrations

(**Figure 25B**), high BP (**Figure 27A-D**), and an impairment in fluid retention— indicated by significantly lower urine volumes and no change in water consumption (**Figure 28**). Additionally, no alterations in kidney function or blood metabolite/ion concentrations were detected (**Table 3**). These observations suggest that heightened RAAS stimulation alters pressure natriuresis to maintain sodium balance at the expense of high BP.

Furthermore, the effects of Panx1 deletion on renal sodium handling are likely compounded by elevated circulating aldosterone levels and water retention. We observed concerted changes in MAP and plasma aldosterone reduction when animals were treated with low sodium diet/ACEi (normalizes both factors to control levels) or AT1R inhibition (both parameters are lowered, but not normalized to controls). The similarities in reducing both parameters indicate that aldosterone levels directly contribute to the high BP phenotype and is partly mediated by AT1R, a key regulator of aldosterone secretion^{363, 401}. Hyper-stimulation of AT1R receptors and adrenal hyperplasia found in Ren1-Panx1^{Δ/Δ} mice (**Figure 32A-B**) was reversed with AT1R inhibition (**Figure 35A-C**) and is consistent with other reports showing AT1R-dependent adrenal hypertrophy^{402, 403}. Differences in BP lowering and aldosterone sensitivity between low sodium diet/ACE inhibition and AT1R inhibition may be controlled by signaling through AT2R in the adrenal cortex. One report has previously shown that agonism of AT2R by angiotensin III causes aldosterone secretion from rat adrenal glomerulosa cells that is blocked by the AT2R inhibitor PD123319, but not the AT1R inhibitor candesartan⁴⁰⁴. Furthermore, evidence indicates the existence of purinergic-mediate signaling in the adrenal cortex. Although it has been shown that exogenous ATP is capable of stimulating steroidogenesis in bovine adrenocortical cells through activation of P2 receptors^{405, 406}, adenosine has been shown to have inhibitory

effects on basal and ACTH induced aldosterone production⁴⁰⁷. Notably, ectonucleotidases are present in the adrenal capsule and ZG, which further implicates the potential breakdown of ATP into adenosine as a signal contributing to phenotypes in Panx1 deficient animals⁴⁰⁸.

On the other hand, our results also suggest that Panx1 deletion influences adrenal cell plasticity and differentiation. In the adrenal gland subcapsular adrenal progenitor cells centripetally migrate through the adrenal cortex to the corticomedullary boundary⁴⁰⁹, differentiating into aldosterone producing ZG cells and subsequently into glucocorticoid producing cells⁴¹⁰. The remodeling and turnover of the adrenal cortex maintains normal hormone biosynthesis⁴⁰¹. Ren1-Panx1^{Δ/Δ} mice present with unrestricted localization of CYP11B2 positive cells outside of the ZG within the ZF. The inappropriate localization of CYP11B2 in the adrenal cortex was resistant to AT1R inhibition, despite a reversal in adrenal hypertrophy compared to controls. In the literature, a novel role for Panx1 has been established in the regulation of cell differentiation in a number of cell types and cancers⁴¹¹. Recently, Panx1 has been shown to influence the expression of β-catenin necessary for driving the differentiation state of keratinocytes and myocytes^{412,413}. The regulation of Wnt signaling pathways and the downstream regulation of β-catenin also plays a critical role in controlling differentiation state of adrenocortical cells in the ZG. β-catenin expression is restricted to the ZG⁴¹⁴ and deletion using an adrenal cortex specific Cre recombinase, results in loss of the adult adrenal cortex⁴¹⁵. Furthermore, conditional activation of beta-catenin directly influences adrenal zonation, which leads to ectopic expression of CYP11B2 in ZF cells^{416,417}. In support of a novel link between Panx1 and beta-catenin, the Panx1 intracellular region (Y198-205)⁷⁴ harbors a regulatory site for glucose synthase

kinase 3, a key regulator of β -catenin degradation. Thus, failure of CYP11B2 expressing cells to differentiate from a ZG cell phenotype may be due to the accumulation of nuclear β -catenin, whereby Panx1 deletion reduces β -catenin degradation, which has been previously found to influence CYP11B2 expression^{373, 418}. Future analyses are needed to understand the influence of purinergic signaling in adrenocortical maintenance and zonation. In conclusion, deletion of renin-cell Panx1 causes two distinct adrenal phenotypes: first, it influences steady-state suppression of aldosterone secretion due to hyperstimulation by RAAS hormones. Second, Panx1 deletion influences the differentiation state of ZG cells, which causes ectopic expression of aldosterone production indicative of impaired transdifferentiation processes.

Within the cardiovascular system the physiological and pathophysiological control of BP exhibits clear sex-differences⁴¹⁹. It is interesting to note from our study of renin-cell Panx1 function that Ren1-Panx1 Δ/Δ female mice did not exhibit RAAS hormone dysregulation, whereas male mice did. Furthermore, the adrenal glands of female mice, while more massive, were identical between Ren1-Panx1 Δ/Δ and control animals. The size of female adrenal glands are attributed to growth rate differences and larger demand for hormone biosynthesis⁴²⁰. The observed differences in circulating renin levels in our model, is also in agreement with other published studies. In comparison to males, renin levels are suppressed in female humans and rodents, and this suppression is thought to be mediated by estrogen hormone status⁴²¹⁻⁴²³. The mechanism by which sex hormones modify RAAS activation is unclear, but in our analysis, it is likely that sex-differences in renin cell function explain the observed sex-dependent phenotype in our model, rather than the

deletion of Panx1, which has not been linked to sex differences in other cell types^{196, 424,}
425.

Overall, our data demonstrate the importance of renin-cell Panx1 channels in stabilizing the BP setpoint. We found that deletion of Panx1 from a subset of renal and adrenal cells has a profound influence on RAAS hormone secretion, which become untethered from negative feedback mechanisms and lead to increased BP. The effects of enhanced RAAS hormones on MAP and fluid/electrolyte imbalance are partially mediated through AT1R-dependent pressor pathways and may indicate . Our analysis also demonstrates a role for Panx1 channels within the renal vasculature and adrenal cortex that regulates adaptive cell differentiation mechanisms to assist in renin recruitment and maintain appropriate adrenocortical zonation. Thus, Panx1 channels are a critical regulator of renin-cell function and are novel regulators of cell differentiation pathways. The appropriate control of purinergic signaling within renin cells and the coordination of RAAS dynamics by Panx1, highlights the importance of purinergic signaling in long-term BP homeostasis.

CHAPTER 6. GENERAL DISCUSSION AND FUTURE DIRECTIONS

Purinergic signaling plays a vital role in coordinating short-term and long-term BP homeostasis. In the vasculature, the regulated release of cellular ATP is a rate limiting step that initiates autocrine/paracrine purinergic signaling cascades. Importantly, the balance between extracellular ATP accumulation and metabolic breakdown into adenosine influences physiologic and pathological responses throughout the cardiovascular system that have been previously shown to regulate reactive hyperemia^{426, 427}, hypoxia-induced vasodilation^{428, 429}, adrenergic vasoconstriction⁷⁴, smooth muscle cell proliferation in atherosclerosis^{430, 431}, vagal cardiovascular reflexes⁴³², and hypertension^{115, 377, 382, 433}. Understanding how ATP is released from cells is therefore a critical first step in understanding how purinergic signaling networks influence homeostasis. Until now, many mechanisms for ATP release have been proposed (e.g. vesicular exocytosis, ABC transporters, F₁F₀-ATPase, and connexin hemi-channels)⁷². However, the family of Pannexin (Panx) proteins have emerged as the predominant mechanism by which cellular ATP is released from diverse cell types^{178, 255, 412, 413, 434-436}, especially in the vasculature^{76, 201, 225, 437}.

The Panx1 isoform is best known for its role in receptor-mediated and caspase-cleavage ATP release^{191, 291}. Panx1 proteins are oligomeric, four-transmembrane spanning glycoproteins that traffic to the plasma membrane channels^{205, 379}. Panx1 channels are governed by a unique quantized gating strategy and are thought to provide a non-selective

conduit for ions and metabolites including ATP^{379, 438}. The influence of Panx1 channels on cellular ATP release is supported by evidence utilizing a repertoire of pharmacological inhibitors^{290, 425}, global knockout mice⁴³⁹, and cell-specific Panx1 genetic models^{78, 197, 246, 440, 441}. Due to the considerable regulatory influences that purinergic pathways have on cardiovascular physiology, the release of ATP by Panx1 channels is likely a crucial signal in controlling the vascular homeostasis^{3, 442}. The work presented in this thesis centers on the functional regulation of vascular (peripheral and renovascular) Panx1 channels and their contribution in maintaining BP homeostasis.

Initially we assessed an important amino acid residue on the Panx1 intracellular loop, tyrosine 198 (Y198), which confers Panx1 channels with the ability to be reversibly activated by receptor-dependent stimuli (i.e. α 1-adrenergic receptors). Importantly, these studies showed that phosphorylation of Y198 residues are required for adrenergic-mediated vasoconstriction but were present under basal and adrenergic stimulated conditions. Using in-vitro cell culture systems, as well as ex-vivo isolated arteries the basal and stimulated release of cellular ATP corresponded with the presence or absence of Y198 phosphorylation. The presence of Panx1-Y198 phosphorylation may therefore define an activatable pool of membrane-associated Panx1. This highlights a possibility in which post-translational modification on the second intracellular loop regulate Panx1 activity. Our analysis further found that phosphorylated Y198 specifically localizes to the plasma membrane and is regulated by the prototypical Src family kinase member, Src, underscoring an alternative mechanism of adrenergic vasoconstriction that was previously unclear^{243, 244, 265} and links the potential for receptor-mediated channel activation with other Src-dependent phosphorylation sites on the Panx1 C-terminus¹⁹⁴. From a structural point

of view, it is interesting to speculate that tyrosine phosphorylation influences steric hindrance between the C-terminus and the intracellular loop in fully oligomerized Panx1 channels and allows for C-terminal displacement and channel opening¹⁸². The importance of these findings marks a key regulatory site on Panx1, which may be amenable to receptor-mediated activation in other cell systems. In the future, it will be necessary to investigate the potential for multi-site phosphorylation as other phosphorylation residues and kinases have been linked to Panx1 channel gating^{287, 288, 443}.

To further assess the plasma membrane dynamics of Panx1 in the peripheral vasculature smooth muscle cells, and its role in BP regulation, we identified an important interaction between Panx1 and the membrane scaffold protein caveolin-1²⁴². This interaction is necessary for Panx1 channel function (i.e. receptor-mediated ATP release) and supports adrenergic vasoconstriction responses in resistance arteries. Through our assessment, we determined that Panx1 and caveolin-1 interact at the plasma membrane only after adrenergic stimulation, and that this interaction was spatially restricted to membrane areas in close apposition to sympathetic nerve terminals. Finally, we assessed the physiological outcomes of genetically deleting caveolin-1 specifically in peripheral smooth muscle cells. Deletion of caveolin-1 recapitulated both the vascular and the BP phenotypes previously observed in smooth muscle specific Panx1 knockout models—namely inhibited ATP release, vasoconstriction and a significant reduction in MAP²²⁵. Thus, a functional relationship exists between Panx1 and caveolin-1 in the vasculature and suggests the possibility of signaling microdomain that supports interactions between Panx1 and kinases. While the status of phosphorylated Panx1-Y198 was not directly examined, it would be interesting if Y198 phosphorylation was required to maintain interactions with

caveolin-1. Src kinase has been shown to directly bind with caveolin-1, which targets Src kinase to the plasma membrane²⁷³. A scenario could be hypothesized in which interactions between Panx1 and caveolin-1 influence Src kinase activity at the Panx1 C-terminus— thus activating Panx1 when adrenergic stimulus is present. However, additional studies are necessary to elucidate the molecular mechanism involved in this important interaction. In conclusion, our study suggests that a novel caveolae signaling domain in the vasculature supports Panx1 channel activity that is important for regulating total peripheral resistance.

BP is maintained by two cardiovascular factors: cardiac output and total peripheral resistance. From a regulatory standpoint, alterations in systemic BP due to changes in either parameter cannot be maintained in the long-term without alterations in renal sodium and fluid balance⁸⁰. Subsequently, pressure natriuresis mechanisms will offset BP changes through countervailing increases/decreases plasma volume. One critical pressor hormone involved in stabilizing pressure natriuresis is the enzyme renin. The secretion of renin from renovascular JG cells is directly controlled by purinergic signaling⁹⁰. To assess the involvement of Panx1 in the renal vasculature, we generated a novel renin-cell Panx1 knockout mouse to target renin-lineage cells in the afferent arteriole³⁷⁰, which express Panx1¹⁷⁸. Through our functional analysis we discovered a unique a high BP–high renin phenotype in mice deficient in Panx1 due to enhanced renin secretion and plasma aldosterone concentrations. The chronic effects of circulating renin enzyme, and presumably angiotensinogen-derived peptides, contributed to a peripheral vasculature phenotype, which displayed hallmark signs of vascular remodeling and stimulus-dependent hyperreactivity; and an adrenal phenotype, which exhibited morphological hypertrophy and defects in aldosterone production. Although we found that Panx1 plays a key role in

stabilizing renin secretion and RAAS activation, it is unknown if Panx1-dependent signals are responsible for directly influencing JG cell function or impairing autoregulatory/TGF mechanisms. Future assessments are needed to directly test autoregulation mechanisms through pressure-mediated vasoconstriction, as well as testing tubuloglomerular feedback through stop-flow technique. Novel cell-specific Panx1 knockout models, preferably using inducible Cre recombinases will be important for targeting JGA cells including vascular smooth muscle cells, mesangial cells, and JG cells .

Furthermore, the effects of Panx1 deletion in renin-lineage cells has uncovered a number of distinct phenotypes driven by hyperrenemia and RAAS stimulation. It is unknown whether this high renin status is due to impaired negative feedback or autonomous JG cell renin secretion at this time. A case could be made for both scenarios and work is ongoing to test the sensitivity of RAAS to changes in sodium status, as well as the dependence of JG-cell renin secretion by secreted factors (purine efflux) or the maintenance of a depolarized membrane potential (ion influx) by Panx1. In our model RAAS inhibition results in normalization of hormone levels and a lowering in MAP, but not a normalization of MAP and fluid volume. Thus, baseline hypertensive phenotypes in Ren1-Panx1^{ΔΔ} mice are likely driven by excessive renin, while fluid balance could be altered by an alternative and as of yet identified renal Panx1 mechanism.

In support of a link between purinergic signaling and fluid/electrolyte balance, evidence supports a strong role for P2Y2 receptors in the cortical collecting duct. Activation of P2Y2 negatively influences aquaporin and sodium transporters to promote natriuresis, diuresis, and reduced MAP^{120, 444}. P2Y2 knockout mice display a high blood

pressure phenotype, excessive aquaporin 2 channel presence in the apical membrane of cortical collecting duct epithelial cells, and increased function and membrane association of the sodium transporter ENaC^{125, 169, 445}. In addition, both Panx1 and RAAS components have been found to localize to the cortical collecting duct^{178, 446, 447}. In our model, the potential removal of Panx1 from this renal site could influence fluid/electrolyte balance and blood pressure. In collecting duct cells, the mechanism of cellular ATP release is still unclear, but a case could be made that impairing purinergic signaling by Panx1 deletion results in sodium and water reabsorption that is independent of RAAS stimulation. This alteration may explain the discrepancy observed between plasma hormone levels, MAP, and urine volume in Ren1-Panx1^{ΔΔ} mice when administered an AT1R inhibitor compared with dual administration of ACE/sodium depletion. It will be interesting in the future to directly test this hypothesis using a cortical collecting duct Cre recombinase (*HOXB7*) and floxed Panx1 animals to recapitulate Ren1-Panx1^{ΔΔ} BP and fluid volume phenotypes independent of the hyperrenemia and aldosterone dysregulation observed in our analyses.

Renin secretion is also powerfully regulated by angiotensin II feedback loops in the renal vasculature. Activation of AT1R on JG cells suppresses renin secretion through calcium-dependent signaling pathways³⁸¹. It was recently shown that Panx1 channel gating is also linked to AT1R activation in carotid body cells, which was necessary for intracellular calcium mobilization⁴⁴⁸. In line with these studies, we performed initial tests from angiotensin II-stimulated ATP release from As4.1 renin-cells, which have constitutively active Panx1 channels (**Figure 36A-B**) and Panx1-dependent ATP release (**Figure 36C**). From these early studies, angiotensin II stimulation (1nM) caused a significant increase in Panx1-dependent ATP release, which was blunted by Panx1

knockdown (**Figure 36D**). From these data one could hypothesize that ATP release from Panx1 could modulate angiotensin II inhibitory signals as our Ren1-Panx1 mouse model suggests. One caveat of the As4.1 culture model is the constitutive release of both renin and prorenin, which complicates assessment of steady-state renin secretion. Other cell lines such as human Calu6 cells could potentially be used to examine renin dynamics, however analysis of isolated primary JG cells from Ren1-Panx1 mice could potentially address the sensitivity of basal renin secretion to increasing doses of angiotensin II. In the future novel in vitro renin cell models will be necessary to determine the role of Panx1 and purinergic signals involved in angiotensin II-mediated negative feedback.

Using As4.1 cells we wanted to determine if Panx1 knockdown could influence cAMP-induced renin expression, which retain proper genomic regulatory mechanisms necessary for upregulating renin⁴⁴⁹. Using 8-Br-cAMP, a membrane permeable cAMP analog, we induced renin expression in As4.1 cells (**Figure 37**). Knockdown of Panx1 significantly blunted cAMP-induced renin expression, which is in line with impaired renin recruitment responses observations in Ren1-Panx1^{Δ/Δ} mice (**Figure 30**). It is unclear if knockdown of Panx1 in As4.1 cells or genetic deletion of Panx1 in renin-lineage cells alters intracellular signaling components necessary for cAMP responses or alters autocrine/paracrine responses to acute stimuli. From these data we are interested to determine if Panx1 proteins influence cell dynamics independently of their proposed channel function, a phenomenon that has been well documented for connexins in the regulation of cell proliferation and differentiation^{450, 451}.

Lastly, our analysis revealed an important role for Panx1 and purinergic signaling in the adrenal cortex as a novel regulator of adrenocortical cell differentiation. Ren1-Panx1 knockout mice present with an AT1R-dependent adrenal hypertrophy and defective adrenocortical zonation. In support of a hyperproliferative adrenal phenotype, Ki67 staining of Ren1-Panx1^{Δ/Δ} mice was significantly enhanced compared to controls (**Figure 38A-B**). The integration of growth/proliferations pathways and adrenocortical differentiation facilitates a dual action approach to adequately matching aldosterone production with BP demand. However, enhanced proliferation does not explain unrestricted ectopic expression of CYP11B2 in the adrenal cortex of Ren1-Panx1^{Δ/Δ} mice. The transition of CYP11B2 positive cells in the adrenal ZG into other cortical cell types has been shown to require canonical Wnt signaling, activation of β-catenin, and transcription of glucocorticoid enzymes⁴⁵²⁻⁴⁵⁴. Similarly, a regulatory role for Panx1 has been shown to influence β-catenin levels and cellular differentiation responses^{73, 179, 455}. The control of this pathway by Panx1 channel function is unclear. Further research is needed to understand how Panx1 influences cell differentiation, and specific to our interests, the failure of ZG aldosterone producing cells to transdifferentiate into corticosterone producing ZF cells⁴⁵⁶. To this end, we are generating adrenocortical cell-specific Panx1 knockout models that will allow for selective targeting of adrenocortical cell types as has been described for aldosterone producing ZG cells⁴¹⁰.

It will also be important to understand how renin-lineage cells contribute to the regulation of CYP11B2 expression in the adrenal cortex. During development renin-lineage cells appear in the fetal adrenal cortex, but in adulthood repressed renin expression⁴⁴⁶. Under certain conditions though—aldosterone synthase deletion or bilateral

nephrectomy– renin production reemerges in the adrenal cortex^{373, 457}. In our mouse model, a population of renin lineage cells populate the adrenal cortex and likely influence ectopic expression of CYP11B2 when Panx1 is deleted (**Figure 32**). The fact that renin-lineage cells influence aldosterone production and can reactivate renin expression^{446, 458, 459}, indicates that a functional redundancy for RAAS hormone generation is built into the adrenocortical cells to ensure BP is maintained at all cost. In the future we hope to use single cell isolation techniques, molecular barcoding, and single cell RNA sequencing to identify differences between renin-lineage cells and other adrenocortical cell type which may provide important information in adrenocortical zonation and maintenance.

In conclusion, the Pannexin family of proteins, in particular Panx1, play a crucial role in regulating normal hemodynamic processes involved in short-term BP adaptation, as well as mechanisms involved in chronic BP homeostasis. In the peripheral vasculature Panx1 channels synchronize smooth muscle cell constriction important for total peripheral resistance, while in the renal vasculature Panx1 restrains RAAS activity necessary for BP feedback control. The controlled release of cellular ATP is a powerful homeostatic signal that coordinates cardiovascular responses and maintains a stable internal environment necessary for supporting life. Understanding the cellular characteristics and functional influences of Panx1 channels on the cardiovascular system will therefore be important should this novel channel prove therapeutically important for treating BP pathologies associated with cardiovascular disease.

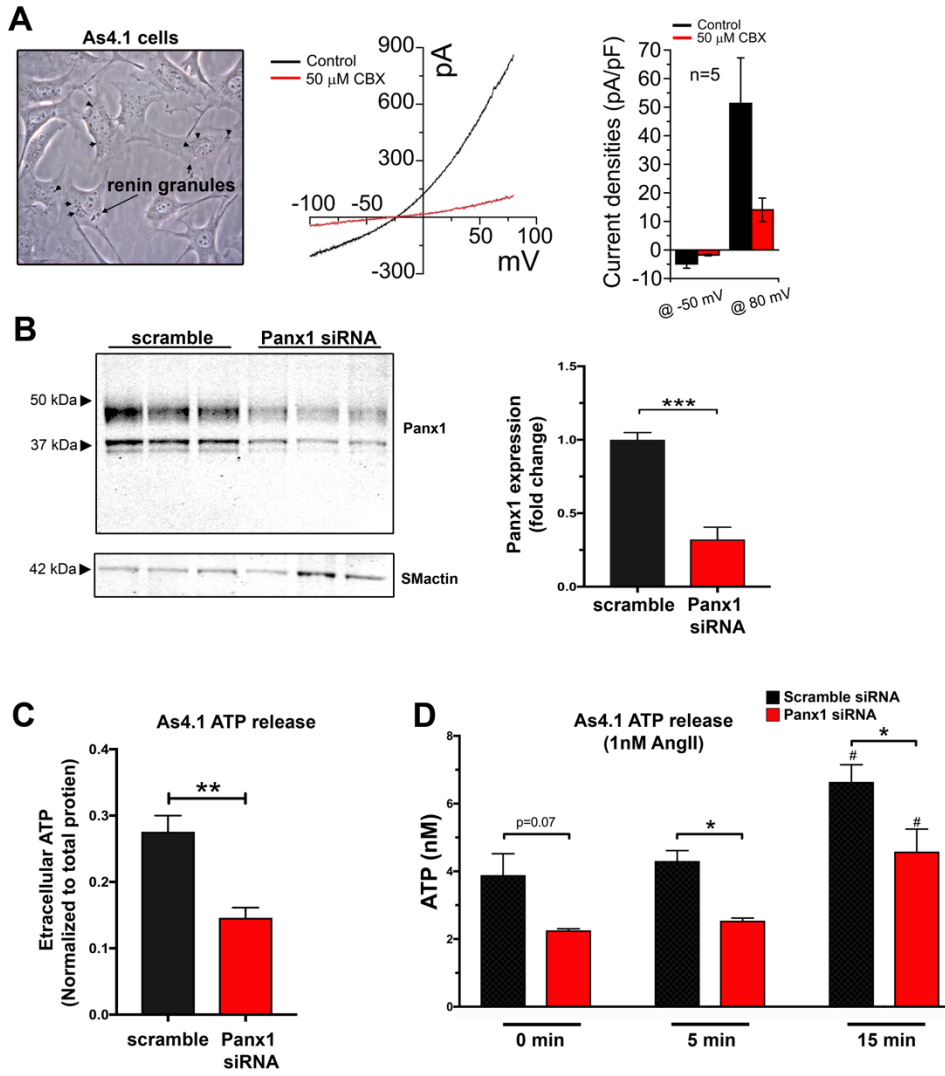


Figure 36. Angiotensin II stimulated Panx1 ATP release is blunted in As4.1 cells.

Figure 36. Angiotensin II stimulated Panx1 ATP release is blunted in As4.1 cells. (A) Representative As4.1 cell DIC image and representative current-voltage relationship from whole cell patch clamp recordings of carbenoxolone sensitive currents. Voltage ramp (100 to 80mV). Quantification of current densities at -50mV and 80mV. N=1; n=5 cells. **(B)** Representative western blot of Panx1 expression in As4.1 cells treated with control siRNA or Panx1 siRNA. N=3. Quantification of normalized Panx1 signal is presented as groups and represented as mean \pm s.e.m. A students t-test was performed for significance. **(C)** Basal ATP release from As4.1 cells after treatment with Panx1 siRNA or scramble control. N=6. Data presented as groups and represented as mean \pm s.e.m. A students t-test was performed for significance; **p<0.01. **(D)** Angiotensin II (1nM) stimulated ATP release from As4.1 cells after 15 min. N=3. Data presented as groups and represented as mean \pm s.e.m. A two-way ANOVA with Tukey post hoc test was performed for statistical significance; *p<0.05; #p<0.05 from baseline (0 min).

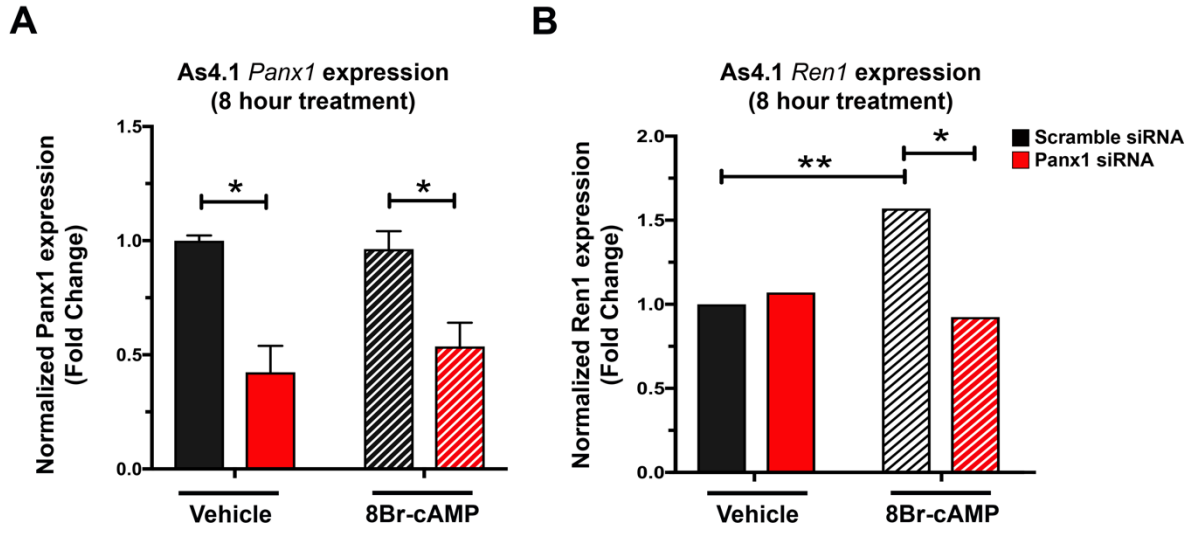


Figure 37. Knockdown of *Panx1* from As4.1 cells impairs cAMP-induced renin expression.

Figure 37. Knockdown of Panx1 from As4.1 cells impairs cAMP-induced renin expression. (A) Panx1 expression in As4.1 cells after gene specific siRNA knockdown of Panx1. N=3 experiments. Data are presented as average fold change relative to control conditions and normalized to B2M expression levels. (B) Renin expression analysis from As4.1 cells treated with 8Br-cAMP (10 μ M) for 8 hours. N=3 experiments. Data are presented as average fold change relative to control conditions and normalized to B2M expression levels. A two-way ANOVA with a Tukey post hoc test for multiple comparisons was performed for statistical significance; *p<0.05, **p<0.01.

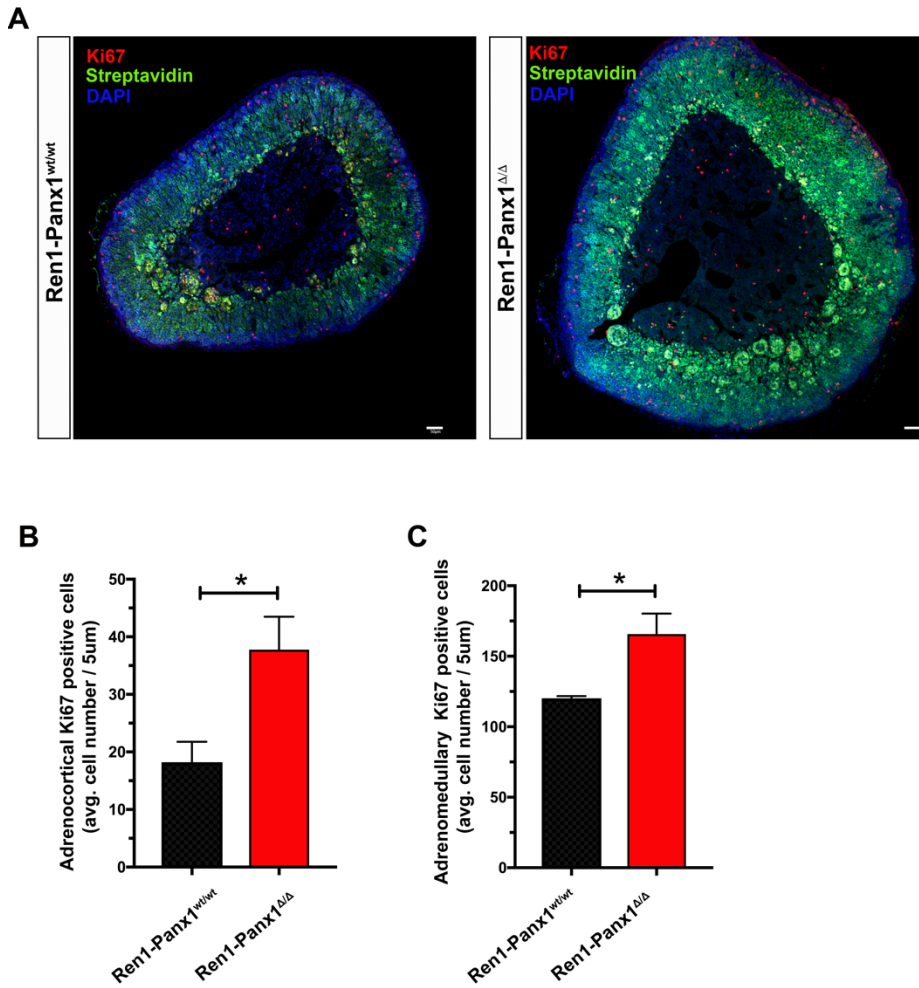


Figure 38. Panx1 deletion from renin-lineage cells results in increased adrenal cell proliferation.

Figure 38. Panx1 deletion from renin-lineage cells results in increased adrenal cell proliferation. (A) Immunohistochemical staining for proliferation marker Ki67 in adrenal glands from Ren1-Panx1^{Δ/Δ} mice and control animals. Ki67 (red), streptavidin (green), nuclei stained with DAPI (blue). Scale bar=20μm. (B) Quantification of adrenocortical Ki67 positive cell number from non-consecutive thin sections. (C) Quantification of adrenomedullary Ki67 positive cell number from non-consecutive thin sections. N=3 control; 4 knockout mice. Data are presented as groups and represented as mean ± s.e.m. A students t-test was performed for significance. *p<0.05.

CHAPTER 7. REFERENCES

1. Hall JE. Integration and regulation of cardiovascular function. *Advances in Physiology Education*. 1999;277:S174
2. Sowers JR, Epstein M, Frohlich ED. Diabetes, hypertension, and cardiovascular disease: An update. *Hypertension*. 2001;37:1053-1059
3. Burnstock G. Purinergic signaling in the cardiovascular system. *Circulation research*. 2017;120:207-228
4. Verkhatsky A, Burnstock G. Biology of purinergic signalling: Its ancient evolutionary roots, its omnipresence and its multiple functional significance. *Bioessays*. 2014;36:697-705
5. Burnstock G, Verkhatsky A. Receptors for purines and pyrimidines. *Purinergic signalling and the nervous system*. Springer; 2012:119-244.
6. Lindsey BG, Nuding SC, Segers LS, Morris KF. Carotid bodies and the integrated cardiorespiratory response to hypoxia. *Physiology*. 2018;33:281-297
7. Grassi G, Mark A, Esler M. The sympathetic nervous system alterations in human hypertension. *Circulation Research*. 2015;116:976-990
8. Joyner MJ, Charkoudian N, Wallin BG. Sympathetic nervous system and blood pressure in humans: Individualized patterns of regulation and their implications. *Hypertension*. 2010;56:10-16
9. Gonzalez C, Almaraz L, Obeso A, Rigual R. Carotid body chemoreceptors: From natural stimuli to sensory discharges. *Physiological reviews*. 1994;74:829-898
10. Marshall JM. Peripheral chemoreceptors and cardiovascular regulation. *Physiological reviews*. 1994;74:543-594
11. Nurse CA. Neurotransmission and neuromodulation in the chemosensory carotid body. *Autonomic Neuroscience*. 2005;120:1-9
12. Finley JC, Katz DM. The central organization of carotid body afferent projections to the brainstem of the rat. *Brain research*. 1992;572:108-116
13. Massari VJ, Shirahata M, Johnson TA, Gatti PJ. Carotid sinus nerve terminals which are tyrosine hydroxylase immunoreactive are found in the commissural nucleus of the tractus solitarius. *Journal of neurocytology*. 1996;25:197-208

14. Kumar P, Prabhakar NR. Peripheral chemoreceptors: Function and plasticity of the carotid body. *Comprehensive Physiology*. 2011;2:141-219
15. Lever J, Lewis P, Boyd J. Observations on the fine structure and histochemistry of the carotid body in the cat and rabbit. *Journal of anatomy*. 1959;93:478
16. Nurse CA, Leonard EM, Salman S. Role of glial-like type ii cells as paracrine modulators of carotid body chemoreception. *Physiological genomics*. 2018;50:255-262
17. Nurse CA. Synaptic and paracrine mechanisms at carotid body arterial chemoreceptors. *The Journal of Physiology*. 2014;592:n/a-n/a
18. Del Rio R, Andrade DC, Marcus NJ, Schultz HD. Selective carotid body ablation in experimental heart failure: A new therapeutic tool to improve cardiorespiratory control. *Experimental physiology*. 2015;100:136-142
19. Fletcher EC, Lesske J, Qian W, Miller 3rd C, Unger T. Repetitive, episodic hypoxia causes diurnal elevation of blood pressure in rats. *Hypertension*. 1992;19:555-561
20. Abdala AP, McBryde FD, Marina N, Hendy EB, Engelman ZJ, Fudim M, Sobotka PA, Gourine AV, Paton JF. Hypertension is critically dependent on the carotid body input in the spontaneously hypertensive rat. *The Journal of physiology*. 2012;590:4269-4277
21. Pijacka W, Moraes DJ, Ratcliffe LE, Nightingale AK, Hart EC, da Silva MP, Machado BH, McBryde FD, Abdala AP, Ford AP. Purinergic receptors in the carotid body as a new drug target for controlling hypertension. *Nature medicine*. 2016;22:1151
22. Narkiewicz K, Ratcliffe LE, Hart EC, Briant LJ, Chrostowska M, Wolf J, Szyndler A, Hering D, Abdala AP, Manghat N. Unilateral carotid body resection in resistant hypertension: A safety and feasibility trial. *JACC: Basic to Translational Science*. 2016;1:313-324
23. Heath D, Smith P, Jago R. Hyperplasia of the carotid body. *The Journal of pathology*. 1982;138:115-127
24. Smith P, Jago R, Heath D. Anatomical variation and quantitative histology of the normal and enlarged carotid body. *The Journal of pathology*. 1982;137:287-304

25. Habeck J-O. Peripheral arterial chemoreceptors and hypertension. *Journal of the autonomic nervous system*. 1991;34:1-7
26. Paton JF, Ratcliffe L, Hering D, Wolf J, Sobotka PA, Narkiewicz K. Revelations about carotid body function through its pathological role in resistant hypertension. *Current hypertension reports*. 2013;15:273-280
27. NAKAYAMA K. Surgical removal of the carotid body for bronchial asthma. *Diseases of the chest*. 1961;40:595-604
28. Burnstock G. Physiology and pathophysiology of purinergic neurotransmission. *Physiological reviews*. 2007;87:659--797
29. Burnstock G. Review lecture. Neurotransmitters and trophic factors in the autonomic nervous system. *The Journal of physiology*. 1981;313:1-35
30. Zhang M, Zhong H, Vollmer C, Nurse CA. Co-release of atp and ach mediates hypoxic signalling at rat carotid body chemoreceptors. *The Journal of Physiology*. 2000;525:143-158
31. Varas R, Alcayaga J, Iturriaga R. Ach and atp mediate excitatory transmission in cat carotid identified chemoreceptor units in vitro. *Brain research*. 2003;988:154-163
32. Icekson G, Dominguez CV, Dedios VP, Arroyo J, Alcayaga J. Petrosal ganglion responses to acetylcholine and atp are enhanced by chronic normobaric hypoxia in the rabbit. *Respiratory physiology & neurobiology*. 2013;189:624-631
33. Buttigieg J, Nurse CA. Detection of hypoxia-evoked atp release from chemoreceptor cells of the rat carotid body. *Biochemical and biophysical research communications*. 2004;322:82-87
34. McQueen D, Ribeiro J. On the specificity and type of receptor involved in carotid body chemoreceptor activation by adenosine in the cat. *British journal of pharmacology*. 1983;80:347-354
35. Alcayaga J, Cerpa V, Retamal M, Arroyo J, Iturriaga R, Zapata P. Adenosine triphosphate-induced peripheral nerve discharges generated from the cat petrosal ganglion in vitro. *Neuroscience letters*. 2000;282:185-188

36. Alcayaga C, Varas R, Valdés V, Cerpa V, Arroyo J, Iturriaga R, Alcayaga J. Atp- and ach-induced responses in isolated cat petrosal ganglion neurons. *Brain research*. 2007;1131:60-67
37. Prasad M, Fearon IM, Zhang M, Laing M, Vollmer C, Nurse CA. Expression of p2x2 and p2x3 receptor subunits in rat carotid body afferent neurones: Role in chemosensory signalling. *The Journal of Physiology*. 2001;537:667-677
38. Song X, Gao X, Guo D, Yu Q, Guo W, He C, Burnstock G, Xiang Z. Expression of p2x 2 and p2x 3 receptors in the rat carotid sinus, aortic arch, vena cava, and heart, as well as petrosal and nodose ganglia. *Purinergic signalling*. 2012;8:15-22
39. Rong W, Gourine AV, Cockayne DA, Xiang Z, Ford AP, Spyer KM, Burnstock G. Pivotal role of nucleotide p2x2 receptor subunit of the atp-gated ion channel mediating ventilatory responses to hypoxia. *Journal of Neuroscience*. 2003;23:11315-11321
40. Pijacka W, McBryde F, Ford AP, Paton JF. Ish nia os-04 p2x3 receptor activity in the carotid body (cb) of spontaneously hypertensive (sh) rats contributes to increased chemoreflex hypersensitivity and hypertension. *Journal of hypertension*. 2016;34:e42-e43
41. Zhang M, Piskuric NA, Vollmer C, Nurse CA. P2y2 receptor activation opens pannexin-1 channels in rat carotid body type ii cells: Potential role in amplifying the neurotransmitter atp. *The Journal of physiology*. 2012;590:4335-4350
42. Retamal MA, Alcayaga J, Verdugo CA, Bultynck G, Leybaert L, Sáez PJ, Fernández R, León LE, Sáez JC. Opening of pannexin-and connexin-based channels increases the excitability of nodose ganglion sensory neurons. *Frontiers in cellular neuroscience*. 2014;8:158
43. Ciriello J, Hochstenbach SL, Roder S. Central projections of baroreceptor and chemoreceptor. *Nucleus of the solitary tract*. 1993:35
44. Dampney R. Functional organization of central pathways regulating the cardiovascular system. *Physiological reviews*. 1994;74:323-364
45. Onai T, Saji M, Miura M. Functional subdivisions of the nucleus tractus solitarii of the rat as determined by circulatory and respiratory responses to electrical

- stimulation of the nucleus. *Journal of the autonomic nervous system*. 1987;21:195-202
46. Affleck V, Coote J, Pyner S. The projection and synaptic organisation of nts afferent connections with presympathetic neurons, gaba and nnos neurons in the paraventricular nucleus of the hypothalamus. *Neuroscience*. 2012;219:48-61
 47. Day TA, Sibbald JR, Khanna S. Atp mediates an excitatory noradrenergic neuron input to supraoptic vasopressin cells. *Brain research*. 1993;607:341-344
 48. Edwards FA, Gibb AJ, Colquhoun D. Atp receptor-mediated synaptic currents in the central nervous system. *Nature*. 1992;359:144
 49. Ueno S, Ishibashi H, Akaike N. Perforated-patch method reveals extracellular atp-induced k⁺ conductance in dissociated rat nucleus solitarii neurons. *Brain research*. 1992;597:176-179
 50. Ergene E, Dunbar JC, O'Leary DS, Barraco RA. Activation of p2-purinoceptors in the nucleus tractus solitarius mediate depressor responses. *Neuroscience letters*. 1994;174:188-192
 51. Scislo TJ, Augustyniak RA, Barraco RA, Woodbury DJ, O'Leary DS. Activation of p2x-purinoceptors in the nucleus tractus solitarius elicits differential inhibition of lumbar and renal sympathetic nerve activity. *Journal of the autonomic nervous system*. 1997;62:103-110
 52. Barraco RA, O'Leary DS, Ergene E, Scislo TJ. Activation of purinergic receptor subtypes in the nucleus tractus solitarius elicits specific regional vascular response patterns. *Journal of the autonomic nervous system*. 1996;59:113-124
 53. Barraco R, El-Ridi M, Ergene E, Phillis J. Adenosine receptor subtypes in the brainstem mediate distinct cardiovascular response patterns. *Brain research bulletin*. 1991;26:59-84
 54. Barraco RA, Janusz C, Polasek P, Parizon M, Roberts P. Cardiovascular effects of microinjection of adenosine into the nucleus tractus solitarius. *Brain research bulletin*. 1988;20:129-132
 55. Tao S, Abdel-Rahman AA. Neuronal and cardiovascular responses to adenosine microinjection into the nucleus tractus solitarius. *Brain research bulletin*. 1993;32:407-417

56. Zimmermann H, Zebisch M, Sträter N. Cellular function and molecular structure of ecto-nucleotidases. *Purinergic signalling*. 2012;8:437-502
57. Zimmermann H. Biochemistry, localization and functional roles of ecto-nucleotidases in the nervous system. *Progress in neurobiology*. 1996;49:589-618
58. Ichinose TK, Minic Z, Li C, O'Leary DS, Scislo TJ. Activation of nts a1 adenosine receptors inhibits regional sympathetic responses evoked by activation of cardiopulmonary chemoreflex. *American Journal of Physiology-Regulatory, Integrative and Comparative Physiology*. 2012;303:R539-R550
59. Minic Z, O'Leary DS, Scislo TJ. Nts adenosine a2a receptors inhibit the cardiopulmonary chemoreflex control of regional sympathetic outputs via a gabaergic mechanism. *American Journal of Physiology-Heart and Circulatory Physiology*. 2015;309:H185-H197
60. McClure JM, Rossi NF, Chen H, O'Leary DS, Scislo TJ. Stimulation of adenosine a1 receptors in the nucleus of the solitary tract (nts) triggers the release of vasopressin into the circulation. 2008
61. Scislo TJ, O'Leary DS. Mechanisms mediating regional sympathoactivatory responses to stimulation of nts a1 adenosine receptors. *American Journal of Physiology-Heart and Circulatory Physiology*. 2002;283:H1588-H1599
62. Burnstock G, Ralevic V. Purinergic signaling and blood vessels in health and disease. *Pharmacological Reviews*. 2013;66:102-192
63. Kasakov L, Ellis J, Kirkpatrick K, Milner P, Burnstock G. Direct evidence for concomitant release of noradrenaline, adenosine 5'-triphosphate and neuropeptide y from sympathetic nerve supplying the guinea-pig vas *Journal of the autonomic* 1988;22:75-82
64. Sneddon P, Burnstock G. Atp as a co-transmitter in rat tail artery. *European journal of pharmacology*. 1984;106:149-152
65. Grant T, Flavahan N, Greig J, McGrath J, McKean C, Reid J. Attempts to uncover subtypes of α -adrenoceptors and associated mechanisms by using sequential administration of blocking drugs. *Clinical Science*. 1985;68:25s-30s

66. Bulloch J, McGrath J. Blockade of vasopressor and vas deferens responses by α , β -methylene atp in the pithed rat. *British journal of pharmacology*. 1988;94:103-108
67. Golubinskaya VO, Tarasova OS, Borovik AS, Rodionov IM. Frequency characteristics of blood pressure oscillations evoked by sympathetic transmitters, noradrenaline and adenosine triphosphate. *Journal of the autonomic nervous system*. 1999;77:13-20
68. Schlicker E, Urbanek E, Göthert M. Atp, α , β -methylene atp and suramin as tools for characterization of vascular p2x receptors in the pithed rat. *Journal of autonomic pharmacology*. 1989;9:357-366
69. Bivalacqua TJ, Champion HC, Shah MK, De Witt BJ, Inscho EW, Kadowitz PJ. Comparative responses to α , β -methylene-atp in cat pulmonary, mesenteric, and hindquarter vascular beds. *Journal of Applied Physiology*. 2002;93:1287-1295
70. Shah MK, Kadowitz PJ. Cyclic adenosine monophosphate-dependent vascular responses to purinergic agonists adenosine triphosphate and uridine triphosphate in the anesthetized mouse. *Journal of cardiovascular pharmacology*. 2002;39:142-149
71. Yamamoto K, Sokabe T, Matsumoto T, Yoshimura K, Shibata M, Ohura N, Fukuda T, Sato T, Sekine K, Kato S. Impaired flow-dependent control of vascular tone and remodeling in p2x4-deficient mice. *Nature medicine*. 2006;12:133
72. Lohman AW, Billaud M, Isakson BE. Mechanisms of atp release and signalling in the blood vessel wall. *Cardiovascular Research*. 2012;95:269-280
73. DeLalio LJ, Keller AS, Chen J, Boyce AKJ, Artamonov M, Askew-Page HR, Keller TCS, Johnstone SR, Weaver RB, Good ME, Murphy S, Best AK, Mintz EL, Penuela S, Greenwood I, Machado RF, Somlyo AV, Swayne LA, Minshall R, Isakson BE. Interaction between pannexin 1 and caveolin-1 in smooth muscle can regulate blood pressure. *Arteriosclerosis, Thrombosis, and Vascular Biology*. 2018:ATVBAHA.118.311290
74. Billaud M, Chiu Y-H, Lohman AW, Parpaite T, Butcher JT, Mutchler SM, DeLalio LJ, Artamonov MV, Sandilos JK, Best AK, Somlyo AV, Thompson RJ, Le TH, Ravichandran KS, Bayliss DA, Isakson BE. A molecular signature in the

- pannexin1 intracellular loop confers channel activation by the α 1 adrenoreceptor in smooth muscle cells. *Science Signaling*. 2015;8:ra17-ra17
75. Lohman AW, LilaBJ, TaJS, RaSTA, AaBD, aDLJaB. Pannexin 1 channels regulate leukocyte emigration through the venous endothelium during acute inflammation. *Nature Communications*. 2015;6:1--12
 76. Lohman AW, Billaud M, Straub AC, Johnstone SR, Best AK, Lee M, Barr K, Penuela S, Laird DW, Isakson BE. Expression of pannexin isoforms in the systemic murine arterial network. *Journal of vascular research*. 2012;49:405-416
 77. Billaud M, Lohman AW, Straub AC, Looft-Wilson R, Johnstone SR, Araj CA, Best AK, Chekeni FB, Ravichandran KS, Penuela S, Laird DW, Isakson BE. Pannexin1 regulates α 1-adrenergic receptor- mediated vasoconstriction. *Circulation Research*. 2011;109:80-85
 78. Billaud M, Chiu YH, Lohman AW, Parpaite T. A molecular signature in the pannexin1 intracellular loop confers channel activation by the α 1 adrenoreceptor in smooth muscle cells. *Science*. 2015;8:ra17-ra17
 79. Guyton AC. *Arterial pressure and hypertension*. Saunders WB Co; 1980.
 80. Hall JE, Mizelle HL, Hildebrandt DA, Brands MW. Abnormal pressure natriuresis. A cause or a consequence of hypertension? *Hypertension*. 1990;15:547-559
 81. Ivy JR, Bailey MA. Pressure natriuresis and the renal control of arterial blood pressure. *The Journal of physiology*. 2014;592:3955-3967
 82. Carlström M, Wilcox CS, Arendshorst WJ. Renal autoregulation in health and disease. *Physiological reviews*. 2015;95:405-511
 83. Inscho EW, Ohishi K, Navar L. Effects of atp on pre-and postglomerular juxtamedullary microvasculature. *American Journal of Physiology-Renal Physiology*. 1992;263:F886-F893
 84. Inscho EW, Cook AK, Mui V, Miller J. Direct assessment of renal microvascular responses to p2-purinoceptor agonists. *The American journal of physiology*. 1998;274:F718-727
 85. Chan C, Unwin R, Bardini M, Oglesby I, Ford A, Townsend-Nicholson A, Burnstock G. Localization of p2x1 purinoceptors by autoradiography and

- immunohistochemistry in rat kidneys. *American Journal of Physiology-Renal Physiology*. 1998;274:F799-F804
86. Turner C, Vonend O, Chan C, Burnstock G, Unwin R. The pattern of distribution of selected atp-sensitive p2 receptor subtypes in normal rat kidney: An immunohistological study. *Cells Tissues Organs*. 2003;175:105-117
87. Inscho EW, Cook AK, Navar LG. Pressure-mediated vasoconstriction of juxtamedullary afferent arterioles involves p2-purinoceptor activation. *American Journal of Physiology-Renal Physiology*. 1996;271:F1077-F1085
88. Inscho EW, Cook AK, Imig JD, Vial C, Evans RJ. Physiological role for p2x1 receptors in renal microvascular autoregulatory behavior. *The Journal of clinical investigation*. 2003;112:1895-1905
89. Mulryan K, Gitterman D, Lewis C, Vial C, Leckie B, Cobb A, Brown J, Conley E, Buell G, Pritchard C. Reduced vas deferens contraction and male infertility in mice lacking p2x 1 receptors. *Nature*. 2000;403:86
90. Burnstock G, Evans LC, Bailey MA. Purinergic signalling in the kidney in health and disease. *Purinergic signalling*. 2014;10:71-101
91. Osswald H, Schmitz HJ, Kemper R. Renal action of adenosine: Effect on renin secretion in the rat. *Naunyn-Schmiedeberg's Archives of Pharmacology*. 1978;303:95-99
92. Tagawa H, Vander AJ. Effects of adenosine compounds on renal function and renin secretion in dogs. *Circulation Research*. 1970;26:327-338
93. Dietrich M, Endlich K, Parekh N, Steinhausen M. Interaction between adenosine and angiotensin ii in renal microcirculation. *Microvascular research*. 1991;41:275-288
94. Holz FG, Steinhausen M. Renovascular effects of adenosine receptor agonists. *Kidney and Blood Pressure Research*. 1987;10:272-282
95. Nishiyama A, Majid DS, Walker III M, Miyatake A, Navar LG. Renal interstitial atp responses to changes in arterial pressure during alterations in tubuloglomerular feedback activity. *Hypertension*. 2001;37:753-759

96. Yaoita H, Ito O, Arima S, Endo Y, Takeuchi K, Omata K, Ito S. Effect of adenosine on isolated afferent arterioles. *Nihon Jinzo Gakkai shi*. 1999;41:697-703
97. Inscho E, Cook A, Imig J, Vial C, Evans R. Renal autoregulation in p2x1 knockout mice. *Acta physiologica Scandinavica*. 2004;181:445-453
98. Peti-Peterdi J, Harris RC. Macula densa sensing and signaling mechanisms of renin release. *Journal of the American Society of Nephrology*. 2010:ASN. 2009070759
99. Peti-Peterdi J. Calcium wave of tubuloglomerular feedback. *American Journal of Physiology-Renal Physiology*. 2006;291:F473-F480
100. Bell PD, Lapointe JY, Sabirov R, Hayashi S, Peti-Peterdi J, Manabe K-I, Kovacs G, Okada Y. Macula densa cell signaling involves atp release through a maxi anion channel. *Proceedings of the National Academy of Sciences of the United States of America*. 2003;100:4322-4327
101. Peti-Peterdi J, Bebok Z, Lapointe J-Y, Bell PD. Novel regulation of cell [na⁺] in macula densa cells: Apical na⁺ recycling by hk-atpase. *American Journal of Physiology-Renal Physiology*. 2002;282:F324-F329
102. Nishiyama A, Navar LG. Atp mediates tubuloglomerular feedback. *American Journal of Physiology-Regulatory, Integrative and Comparative Physiology*. 2002;283:R273-R275
103. Bodin P, Burnstock G. Purinergic signalling: Atp release. *Neurochemical Research*. 2001;26:959-969
104. Milner P, Kirkpatrick KA, Ralevic V, Toothill V, Pearson J, Burnstock G. Endothelial cells cultured from human umbilical vein release atp, substance p and acetylcholine in response to increased flow. *Proc. R. Soc. Lond. B*. 1990;241:245-248
105. Bell PD, Komlosi P, Zhang Z-R. Atp as a mediator of macula densa cell signalling. *Purinergic signalling*. 2009;5:461-471
106. Komlosi P, Peti-Peterdi J, Fuson AL, Fintha A, Rosivall L, Bell PD. Macula densa basolateral atp release is regulated by luminal [nacl] and dietary salt intake. *American Journal of Physiology-Renal Physiology*. 2004;286:F1054-F1058

107. Peti-Peterdi J, Fintha A, Fuson AL, Tousson A, Chow RH. Real-time imaging of renin release in vitro. *American Journal of Physiology-Renal Physiology*. 2004;287:F329-F335
108. Schnermann J, Osswald H, Hermle M. Inhibitory effect of methylxanthines on feedback control of glomerular filtration rate in the rat kidney. *Pflügers Archiv*. 1977;369:39-48
109. Ren Y, Carretero OA, Garvin JL. Role of mesangial cells and gap junctions in tubuloglomerular feedback. *Kidney International*. 2002;62:525-531
110. Huang DY, Vallon V, Zimmermann H, Koszalka P, Schrader J, Osswald H. Ecto-5'-nucleotidase (cd73)-dependent and-independent generation of adenosine participates in the mediation of tubuloglomerular feedback in vivo. *American Journal of Physiology-Renal Physiology*. 2006;291:F282-F288
111. Brown R, Ollerstam A, Johansson B, Skøtt O, Gebre-Medhin S, Fredholm B, Persson AEG. Abolished tubuloglomerular feedback and increased plasma renin in adenosine a1 receptor-deficient mice. *American Journal of Physiology-Regulatory, Integrative and Comparative Physiology*. 2001;281:R1362-R1367
112. Sun D, Samuelson LC, Yang T, Huang Y, Paliege A, Saunders T, Briggs J, Schnermann J. Mediation of tubuloglomerular feedback by adenosine: Evidence from mice lacking adenosine 1 receptors. *Proceedings of the National Academy of Sciences of the United States of America*. 2001;98:9983-9988
113. Toma IaBEaMEJaKJJaVSLaP-PJ. Connexin 40 and atp-dependent intercellular calcium wave in renal glomerular endothelial cells. *American Journal of Physiology-Regulatory, Integrative and Comparative Physiology*. 2008;294:R1769--1776
114. Schweda F, Segerer F, Castrop H, Schnermann Jr, Kurtz A. Blood pressure-dependent inhibition of renin secretion requires a1 adenosine receptors. *Hypertension*. 2005;46:780-786
115. Ortiz-Capisano MC, Atchison DK, Harding P, Lasley RD, Beierwaltes WH. Adenosine inhibits renin release from juxtaglomerular cells via an a1 receptor-trpc-mediated pathway. *American journal of physiology. Renal physiology*. 2013;305:F1209-1219

116. Ortiz-Capisano MC, Ortiz PA, Harding P, Garvin JL, Beierwaltes WH. Decreased intracellular calcium stimulates renin release via calcium-inhibitable adenylyl cyclase. *Hypertension*. 2007;49:162-169
117. Rouse D, Leite M, Suki WN. Atp inhibits the hydrosmotic effect of avp in rabbit cct: Evidence for a nucleotide p2u receptor. *American Journal of Physiology-Renal Physiology*. 1994;267:F289-F295
118. Kishore BK, Chou CL, Knepper MA. Extracellular nucleotide receptor inhibits avp-stimulated water permeability in inner medullary collecting duct. *American Journal of Physiology-Renal Physiology*. 1995;269:F863-F869
119. Wildman SS, Boone M, Peppiatt-Wildman CM, Contreras-Sanz A, King BF, Shirley DG, Deen PM, Unwin RJ. Nucleotides downregulate aquaporin 2 via activation of apical p2 receptors. *Journal of the American Society of Nephrology*. 2009;20:1480-1490
120. Kishore BK, Ginns SM, Krane CM, Nielsen S, Knepper MA. Cellular localization of p2y2 purinoceptor in rat renal inner medulla and lung. *American Journal of Physiology-Renal Physiology*. 2000;278:F43-F51
121. Rieg T, Bunday RA, Chen Y, Deschenes G, Junger W, Insel PA, Vallon V. Mice lacking p2y2 receptors have salt-resistant hypertension and facilitated renal na⁺ and water reabsorption. *The FASEB Journal*. 2007;21:3717-3726
122. Vallon V. P2 receptors in the regulation of renal transport mechanisms. *AJP: Renal Physiology*. 2007;294:F10-F27
123. McCoy DE, Taylor AL, Kudlow BA, Karlson K, Slattery MJ, Schwiebert LM, Schwiebert EM, Stanton BA. Nucleotides regulate nacl transport in mimcd-k2 cells via p2x and p2y purinergic receptors. *American Journal of Physiology-Renal Physiology*. 1999;277:F552-F559
124. Li L, Wingo CS, Xia S-L. Downregulation of sgk1 by nucleotides in renal tubular epithelial cells. *American Journal of Physiology-Renal Physiology*. 2007;293:F1751-F1757
125. Rieg T, Gerasimova M, Boyer JL, Insel PA, Vallon V. P2y2 receptor activation decreases blood pressure and increases renal na⁺ excretion. *American Journal of*

Physiology-Regulatory, Integrative and Comparative Physiology.
2011;301:R510-R518

126. Zhang Y, Peti-Peterdi J, Muller CE, Carlson NG, Baqi Y, Strasburg DL, Heiney KM, Villanueva K, Kohan DE, Kishore BK. P2y12 receptor localizes in the renal collecting duct and its blockade augments arginine vasopressin action and alleviates nephrogenic diabetes insipidus. *Journal of the American Society of Nephrology.* 2015;26:2978-2987
127. Burnstock G. The past, present and future of purine nucleotides as signalling molecules. *Neuropharmacology.* 1997;36:1127-1139
128. Lohman AWAIBE. Differentiating connexin hemichannels and pannexin channels in cellular atp release. *FEBS letters.* 2014;588:1379--1388
129. Burnstock G. Historical review: Atp as a neurotransmitter. *Trends in Pharmacological Sciences.* 2006;27:166-176
130. Taruno A. Atp release channels. *International journal of molecular sciences.* 2018;19:808
131. Nilius B, Eggermont J, Voets T, Buyse G, Manolopoulos V, Droogmans G. Properties of volume-regulated anion channels in mammalian cells. *Progress in biophysics and molecular biology.* 1997;68:69-119
132. Okada Y. Volume expansion-sensing outward-rectifier cl-channel: Fresh start to the molecular identity and volume sensor. *American Journal of Physiology-Cell Physiology.* 1997;273:C755-C789
133. Voss FK, Ullrich F, Münch J, Lazarow K, Lutter D, Mah N, Andrade-Navarro MA, von Kries JP, Stauber T, Jentsch TJ. Identification of lrcc8 heteromers as an essential component of the volume-regulated anion channel vrac. *Science.* 2014;344:634-638
134. Gaitán-Peñas H, Gradogna A, Laparra-Cuervo L, Solsona C, Fernández-Dueñas V, Barrallo-Gimeno A, Ciruela F, Lakadamyali M, Pusch M, Estévez R. Investigation of lrcc8-mediated volume-regulated anion currents in xenopus oocytes. *Biophysical journal.* 2016;111:1429-1443
135. Bao L, Locovei S, Dahl G. Pannexin membrane channels are mechanosensitive conduits for atp. *FEBS letters.* 2004;572:65-68

136. Ma Z, Siebert AP, Cheung K-H, Lee RJ, Johnson B, Cohen AS, Vingtdeux V, Marambaud P, Foskett JK. Calcium homeostasis modulator 1 (calhm1) is the pore-forming subunit of an ion channel that mediates extracellular ca^{2+} regulation of neuronal excitability. *Proceedings of the National Academy of Sciences*. 2012;109:E1963-E1971
137. Siebert AP, Ma Z, Grevet JD, Demuro A, Parker I, Foskett JK. Structural and functional similarities of calcium homeostasis modulator 1 (calhm1) ion channel with connexins, pannexins, and innexins. *Journal of Biological Chemistry*. 2013;288:6140-6153
138. Dreses-Werringloer U, Lambert J-C, Vingtdeux V, Zhao H, Vais H, Siebert A, Jain A, Koppel J, Rovelet-Lecrux A, Hannequin D. A polymorphism in calhm1 influences ca^{2+} homeostasis, $a\beta$ levels, and alzheimer's disease risk. *Cell*. 2008;133:1149-1161
139. Taruno A, Vingtdeux V, Ohmoto M, Ma Z, Dvoryanchikov G, Li A, Adrien L, Zhao H, Leung S, Abernethy M. Calhm1 ion channel mediates purinergic neurotransmission of sweet, bitter and umami tastes. *Nature*. 2013;495:223
140. Vlaskovska M, Kasakov L, Rong W, Bodin P, Bardini M, Cockayne DA, Ford AP, Burnstock G. P2x3 knock-out mice reveal a major sensory role for urothelially released atp. *Journal of Neuroscience*. 2001;21:5670-5677
141. Sana-Ur-Rehman H, Markus I, Moore KH, Mansfield KJ, Liu L. Expression and localization of pannexin-1 and calhm1 in porcine bladder and their involvement in modulating atp release. *American Journal of Physiology-Regulatory, Integrative and Comparative Physiology*. 2017;312:R763-R772
142. Nakagomi H, Yoshiyama M, Mochizuki T, Miyamoto T, Komatsu R, Imura Y, Morizawa Y, Hiasa M, Miyaji T, Kira S. Urothelial atp exocytosis: Regulation of bladder compliance in the urine storage phase. *Scientific reports*. 2016;6:srep29761
143. Moyer BD, Hevezi P, Gao N, Lu M, Kalabat D, Soto H, Echeverri F, Laita B, Yeh SA, Zoller M. Expression of genes encoding multi-transmembrane proteins in specific primate taste cell populations. *PloS one*. 2009;4:e7682

144. Murata Y, Yasuo T, Yoshida R, Obata K, Yanagawa Y, Margolskee RF, Ninomiya Y. Action potential-enhanced atp release from taste cells through hemichannels. *Journal of Neurophysiology*. 2010;104:896-901
145. Romanov RA, Rogachevskaja OA, Khokhlov AA, Kolesnikov SS. Voltage dependence of atp secretion in mammalian taste cells. *The Journal of general physiology*. 2008;132:731-744
146. Tordoff MG, Ellis HT, Aleman TR, Downing A, Marambaud P, Foskett JK, Dana RM, McCaughey SA. Salty taste deficits in calhm1 knockout mice. *Chemical senses*. 2014;39:515-528
147. Huang YA, Roper SD. Intracellular ca²⁺ and trpm5-mediated membrane depolarization produce atp secretion from taste receptor cells. *The Journal of physiology*. 2010;588:2343-2350
148. Huang Y-J, Maruyama Y, Dvoryanchikov G, Pereira E, Chaudhari N, Roper SD. The role of pannexin 1 hemichannels in atp release and cell-cell communication in mouse taste buds. *Proceedings of the National Academy of Sciences of the United States of America*. 2007;104:6436-6441
149. Cockayne DA, Hamilton SG, Zhu Q-M, Dunn PM, Zhong Y, Novakovic S, Malmberg AB, Cain G, Berson A, Kassotakis L. Urinary bladder hyporeflexia and reduced pain-related behaviour in p2x 3-deficient mice. *Nature*. 2000;407:1011
150. Lambert J-C, Slegers K, González-Pérez A, Ingelsson M, Beecham GW, Hiltunen M, Combarros O, Bullido MJ, Brouwers N, Bettens K. The calhm1 p86l polymorphism is a genetic modifier of age at onset in alzheimer's disease: A meta-analysis study. *Journal of Alzheimer's disease*. 2010;22:247-255
151. Blatz AL, Magleby KL. Single voltage-dependent chloride-selective channels of large conductance in cultured rat muscle. *Biophysical journal*. 1983;43:237-241
152. Sabirov RZ, Dutta AK, Okada Y. Volume-dependent atp-conductive large-conductance anion channel as a pathway for swelling-induced atp release. *The Journal of general physiology*. 2001;118:251-266

153. Schwiebert EM. Atp release mechanisms, atp receptors and purinergic signalling along the nephron. *Clinical and experimental pharmacology & physiology*. 2001;28:340-350
154. Schwiebert E, Mills JW, Stanton B. Actin-based cytoskeleton regulates a chloride channel and cell volume in a renal cortical collecting duct cell line. *Journal of Biological Chemistry*. 1994;269:7081-7089
155. Liu H-T, Sabirov RZ, Okada Y. Oxygen-glucose deprivation induces atp release via maxi-anion channels in astrocytes. *Purinergic Signalling*. 2008;4:147-154
156. Dutta AK, Sabirov RZ, Uramoto H, Okada Y. Role of atp-conductive anion channel in atp release from neonatal rat cardiomyocytes in ischaemic or hypoxic conditions. *The Journal of physiology*. 2004;559:799-812
157. Sabirov RZ, Merzlyak PG, Okada T, Islam MR, Uramoto H, Mori T, Makino Y, Matsuura H, Xie Y, Okada Y. The organic anion transporter slco2a1 constitutes the core component of the maxi-cl channel. *The EMBO journal*. 2017;36:3309-3324
158. Castrop H. Mediators of tubuloglomerular feedback regulation of glomerular filtration: Atp and adenosine. *Acta physiologica*. 2007;189:3-14
159. Esseltine JL, Laird DW. Next-generation connexin and pannexin cell biology. *Trends in cell biology*. 2016;26:944-955
160. Lopez W, Ramachandran J, Alsamarah A, Luo Y, Harris AL, Contreras JE. Mechanism of gating by calcium in connexin hemichannels. *Proceedings of the National Academy of Sciences*. 2016;113:E7986-E7995
161. Sáez JC, Retamal MA, Basilio D, Bukauskas FF, Bennett MV. Connexin-based gap junction hemichannels: Gating mechanisms. *Biochimica et Biophysica Acta (BBA)-Biomembranes*. 2005;1711:215-224
162. Goodenough DA, Paul DL. Beyond the gap: Functions of unpaired connexon channels. *Nature reviews Molecular cell biology*. 2003;4:285
163. Cotrina ML, Lin JH-C, Alves-Rodrigues A, Liu S, Li J, Azmi-Ghadimi H, Kang J, Naus CC, Nedergaard M. Connexins regulate calcium signaling by controlling atp release. *Proceedings of the National Academy of Sciences*. 1998;95:15735-15740

164. Stout CE, Costantin JL, Naus CC, Charles AC. Intercellular calcium signaling in astrocytes via atp release through connexin hemichannels. *Journal of Biological Chemistry*. 2002;277:10482-10488
165. Pearson RA, Dale N, Llaudet E, Mobbs P. Atp released via gap junction hemichannels from the pigment epithelium regulates neural retinal progenitor proliferation. *Neuron*. 2005;46:731-744
166. Zhao H-B, Yu N, Fleming CR. Gap junctional hemichannel-mediated atp release and hearing controls in the inner ear. *Proceedings of the National Academy of Sciences*. 2005;102:18724-18729
167. Kang J, Kang N, Lovatt D, Torres A, Zhao Z, Lin J, Nedergaard M. Connexin 43 hemichannels are permeable to atp. *Journal of Neuroscience*. 2008;28:4702-4711
168. Zhang Y, Peti-Peterdi J, Müller CE, Carlson NG, Baqi Y, Strasburg DL, Heiney KM, Villanueva K, Kohan DE, Kishore BK. P2y12 receptor localizes in the renal collecting duct and its blockade augments arginine vasopressin action and alleviates nephrogenic diabetes insipidus. *Journal of the American Society of Nephrology*. 2015:ASN. 2014010118
169. Kishore BK, Nelson RD, Miller RL, Carlson NG, Kohan DE. P2y2 receptors and water transport in the kidney. *Purinergic signalling*. 2009;5:491-499
170. Sipos A, Vargas SL, Toma I, Hanner F, Willecke K, Peti-Peterdi J. Connexin 30 deficiency impairs renal tubular atp release and pressure natriuresis. *Journal of the American Society of Nephrology*. 2009;20:1724-1732
171. Mironova E, Peti-Peterdi J, Bugaj V, Stockand JD. Diminished paracrine regulation of the epithelial na⁺ channel by purinergic signaling in mice lacking connexin 30. *Journal of Biological Chemistry*. 2011;286:1054-1060
172. Penuela S, Bhalla R, Nag K, Laird DW. Glycosylation regulates pannexin intermixing and cellular localization. *Molecular biology of the cell*. 2009;20:4313-4323
173. Panchin Y, Kelmanson I, Matz M, Lukyanov K, Usman N, Lukyanov S. A ubiquitous family of putative gap junction molecules. *Current Biology*. 2000;10:R473-474

174. Sosinsky GE, Boassa D, Dermietzel R, Duffy HS, Laird DW, MacVicar B, Naus CC, Penuela S, Scemes E, Spray DC. Pannexin channels are not gap junction hemichannels. *Channels*. 2011;5:193-197
175. Baranova A, Ivanov D, Petrash N, Pestova A, Skoblov M, Kelmanson I, Shagin D, Nazarenko S, Geraymovych E, Litvin O. The mammalian pannexin family is homologous to the invertebrate innexin gap junction proteins. *Genomics*. 2004;83:706-716
176. Penuela S, Bhalla R, Gong X-Q, Cowan KN, Celetti SJ, Cowan BJ, Bai D, Shao Q, Laird DW. Pannexin 1 and pannexin 3 are glycoproteins that exhibit many distinct characteristics from the connexin family of gap junction proteins. *Journal of Cell Science*. 2007;120:3772-3783
177. Seminario-Vidal L, Okada SF, Sesma JI, Kreda SM, van Heusden CA, Zhu Y, Jones LC, O'Neal WK, Penuela S, Laird DW, Boucher RC, Lazarowski ER. Rho signaling regulates pannexin 1-mediated atp release from airway epithelia. *Journal of Biological Chemistry*. 2011;286:26277-26286
178. Hanner F, Lam L, Nguyen MTX, Yu A, Peti-Peterdi J. Intrarenal localization of the plasma membrane atp channel pannexin1. *AJP: Renal Physiology*. 2012;303:F1454-F1459
179. Celetti SJ, Cowan KN, Penuela S, Shao Q, Churko J, Laird DW. Implications of pannexin 1 and pannexin 3 for keratinocyte differentiation. *Journal of Cell Science*. 2010;123:1363-1372
180. Iwamoto T, Nakamura T, Doyle A, Ishikawa M, de Vega S, Fukumoto S, Yamada Y. Pannexin 3 regulates intracellular atp/camp levels and promotes chondrocyte differentiation. *The Journal of biological chemistry*. 2010;285:18948-18958
181. Sandilos JK, Chiu YH, Chekeni FB, Armstrong AJ, Walk SF, Ravichandran KS, Bayliss DA. Pannexin 1, an atp release channel, is activated by caspase cleavage of its pore-associated c-terminal autoinhibitory region. *J Biol Chem*. 2012;287:11303-11311
182. Sandilos JK, Chiu Y-H, Chekeni FB, Armstrong AJ, Walk SF, Ravichandran KS, Bayliss DA. How the tail of pannexin 1 inhibits the atp release channel : Pannexin 1, an atp release channel, is activated by caspase cleavage of its pore-associated c-

- terminal autoinhibitory region. *Journal of Biological Chemistry*. 2012;287:11303-11311
183. Chiu Y-H, Jin X, Medina CB, Leonhardt SA, Kiessling V, Bennett BC, Shu S, Tamm LK, Yeager M, Ravichandran KS. A quantized mechanism for activation of pannexin channels. *Nature Communications*. 2017;8
184. Lohman AW, Isakson BE. Differentiating connexin hemichannels and pannexin channels in cellular atp release. *FEBS letters*. 2014;588:1379-1388
185. Silverman WR, Vaccari JPDR, Locovei S, Qiu F, Carlsson SK, Scemes E, Keane RW, Dahl G. The pannexin 1 channel activates the inflammasome in neurons and astrocytes. *Journal of Biological Chemistry*. 2009:jbc. M109. 004804
186. Wang J, Ambrosi C, Qiu F, Jackson DG, Sosinsky G, Dahl G. The membrane protein pannexin1 forms two open-channel conformations depending on the mode of activation. *Sci. Signal*. 2014;7:ra69-ra69
187. Qiu F, Wang J, Spray DC, Scemes E, Dahl G. Two non-vesicular atp release pathways in the mouse erythrocyte membrane. *FEBS letters*. 2011;585:3430-3435
188. Locovei S, Wang J, Dahl G. Activation of pannexin 1 channels by atp through p2y receptors and by cytoplasmic calcium. *FEBS letters*. 2006;580:239-244
189. Gödecke S, Roderigo C, Rose CR, Rauch BH, Gödecke A, Schrader J. Thrombin-induced atp release from human umbilical vein endothelial cells. *American Journal of Physiology-Cell Physiology*. 2011;302:C915-C923
190. Seminario-Vidal L, Kreda S, Jones L, O'Neal W, Trejo J, Boucher RC, Lazarowski ER. Thrombin promotes release of atp from lung epithelial cells through coordinated activation of rho-and ca²⁺-dependent signaling pathways. *Journal of Biological Chemistry*. 2009:jbc. M109. 004762
191. Chekeni FB, Elliott MR, Sandilos JK, Walk SF, Kinchen JM, Lazarowski ER, Armstrong AJ, Penuela S, Laird DW, Salvesen GS, Isakson BE, Bayliss DA, Ravichandran KS. Pannexin 1 channels mediate 'find-me' signal release and membrane permeability during apoptosis. *Nature*. 2010;467:863-867
192. Chiu Y-H, Jin X, Medina CB, Leonhardt SA, Kiessling V, Bennett BC, Shu S, Tamm LK, Yeager M, Ravichandran KS, Bayliss DA. A quantized mechanism for activation of pannexin channels. *Nature Communications*. 2017;8:1-15

193. Chiu Y-H, Ravichandran KS, Bayliss DA. Intrinsic properties and regulation of pannexin 1 channel. *Channels (Austin, Tex.)*. 2014;8:103-109
194. Weilinger NL, Lohman AW, Rakai BD, Ma EMM, Bialecki J, Maslieieva V, Rilea T, Bandet MV, Ikuta NT, Scott L, Colicos MA, Teskey GC, Winship IR, Thompson RJ. Metabotropic nmda receptor signaling couples src family kinases to pannexin-1 during excitotoxicity. *Nature Neuroscience*. 2016;19:432-442
195. Pinheiro AR, Paramos-de-Carvalho D, Certal M, Costa C, Magalhães-Cardoso MT, Ferreira F, Costa MA, Correia-de-Sá P. Bradykinin-induced ca²⁺ signaling in human subcutaneous fibroblasts involves atp release via hemichannels leading to p2y₁₂ receptors activation. *Cell Communication and Signaling*. 2013;11:70
196. Weaver JL, Arandjelovic S, Brown G, Mendu SK, Schappe MS, Buckley MW, Chiu Y-H, Shu S, Kim JK, Chung J. Hematopoietic pannexin 1 function is critical for neuropathic pain. *Scientific reports*. 2017;7:42550
197. Adamson SE, Leitinger N. The role of pannexin1 in the induction and resolution of inflammation. *FEBS letters*. 2014;588:1416-1422
198. Jankowski J, Perry HM, Medina CB, Huang L, Yao J, Bajwa A, Lorenz UM, Rosin DL, Ravichandran KS, Isakson BE. Epithelial and endothelial pannexin1 channels mediate aki. *Journal of the American Society of Nephrology*. 2018:ASN. 2017121306
199. Furlow PW, Zhang S, Soong TD, Halberg N, Goodarzi H, Mangrum C, Wu YG, Elemento O, Tavazoie SF. Mechanosensitive pannexin-1 channels mediate microvascular metastatic cell survival. *Nature cell biology*. 2015;17:943
200. Weilinger NL, Tang PL, Thompson RJ. Anoxia-induced nmda receptor activation opens pannexin channels via src family kinases. *Journal of Neuroscience*. 2012;32:12579-12588
201. Lohman AW, Leskov IL, Butcher JT, Johnstone SR, Stokes TA, Begandt D, DeLalio LJ, Best AK, Penuela S, Leitinger N, Ravichandran KS, Stokes KY, Isakson BE. Pannexin 1 channels regulate leukocyte emigration through the venous endothelium during acute inflammation. *Nature Communications*. 2015;6:7965-7912

202. Di Salvo J, Gifford D, Kokkinakis A. Atp- and polyphosphate-mediated stimulation of pp60c-src kinase activity in extracts from vascular smooth muscle. *Journal of Biological Chemistry*. 1989;264:10773-10778
203. Poste G, Flood MK. Cells transformed by temperature-sensitive mutants of avian sarcoma virus cause tumors in vivo at permissive and nonpermissive temperatures. *Cell*. 1979;17:789-800
204. Solan JL, Lampe PD. Connexin 43 in la-25 cells with active v-src is phosphorylated on y247, y265, s262, s279/282, and s368 via multiple signaling pathways. *Cell Communication and Adhesion*. 2008;15:75-84
205. Penuela S, Gehi R, Laird DW. The biochemistry and function of pannexin channels. *Biochimica et biophysica acta*. 2013;1828:15-22
206. Hughes ADaWS. Role of tyrosine phosphorylation in excitation-contraction coupling in vascular smooth muscle. *Acta physiologica Scandinavica*. 1998;164:457--469
207. Abebe W, Agrawal DK. Role of tyrosine kinases in norepinephrine-induced contraction of vascular smooth muscle. *Journal of Cardiovascular Pharmacology*. 1995;26:153-159
208. Jin N, Siddiqui RA, English D, Rhoades RA. Communication between tyrosine kinase pathway and myosin light chain kinase pathway in smooth muscle. *The American journal of physiology*. 1996;271:H1348-1355
209. Min J, Reznichenko M, Poythress RH, Gallant CM, Vetterkind S, Li Y, Morgan KG. Src modulates contractile vascular smooth muscle function via regulation of focal adhesions. *Journal of Cellular Physiology*. 2012;227:3585-3592
210. Penuela S, Harland L, Simek J, Laird DW. Pannexin channels and their links to human disease. *Biochem J*. 2014;461:371-381
211. Omasits U, Ahrens CH, Müller S, Wollscheid B. Protter: Interactive protein feature visualization and integration with experimental proteomic data. *Bioinformatics (Oxford, England)*. 2014;30:884-886
212. Dinkel H, Van Roey K, Michael S, Kumar M, Uyar B, Altenberg B, Milchevskaya V, Schneider M, Kühn H, Behrendt A. Elm 2016—data update and

- new functionality of the eukaryotic linear motif resource. *Nucleic acids research*. 2015;44:D294-D300
213. Wirth A, Benyó Z, Lukasova M, Leutgeb B, Wettschureck N, Gorbey S, Örsy P, Horváth B, Maser-Gluth C, Greiner E, Lemmer B, Schütz G, Gutkind JS, Offermanns S. G12-g13-larg-mediated signaling in vascular smooth muscle is required for salt-induced hypertension. *Nature Medicine*. 2008;14:64-68
214. Cao G, Yang G, Timme TL, Saika T, Truong LD, Satoh T, Goltsov A, Park SH, Men T, Kusaka N, Tian W, Ren C, Wang H, Kadmon D, Cai WW, Chinault AC, Boone TB, Bradley A, Thompson TC. Disruption of the caveolin-1 gene impairs renal calcium reabsorption and leads to hypercalciuria and urolithiasis. *The American journal of pathology*. 2003;162:1241-1248
215. Han M, Dong L-H, Zheng B, Shi J-H, Wen J-K, Cheng Y. Smooth muscle $\alpha 22$ maintains the differentiated phenotype of vascular smooth muscle cells by inducing filamentous actin bundling. *Life sciences*. 2009;84:394-401
216. Zimmermann O, Zwaka TP, Marx N, Torzewski M, Bucher A, Guilliard P, Hannekum A, Hombach V, Torzewski J. Serum starvation and growth factor receptor expression in vascular smooth muscle cells. *Journal of vascular research*. 2006;43:157-165
217. Ma X, Wang Y, Stephens NL. Serum deprivation induces a unique hypercontractile phenotype of cultured smooth muscle cells. *American Journal of Physiology-Cell Physiology*. 1998;274:C1206-C1214
218. Straub AC, Lohman AW, Billaud M, Johnstone SR, Dwyer ST, Lee MY, Bortz PS, Best AK, Columbus L, Gaston B, Isakson BE. Endothelial cell expression of haemoglobin α regulates nitric oxide signalling. *Nature*. 2012;491:473-477
219. Billaud M, Lohman AW, Straub AC, Parpaite T, Johnstone SR, Isakson BE. Characterization of the thoracodorsal artery: Morphology and reactivity. *Microcirculation*. 2012;19:360-372
220. Straub AC, Butcher JT, Billaud M, Mutchler SM, Artamonov MV, Nguyen AT, Johnson T, Best AK, Miller MP, Palmer LA, Columbus L, Somlyo AV, Le TH, Isakson BE. Hemoglobin α /enos coupling at myoendothelial junctions is

- required for nitric oxide scavenging during vasoconstriction. *Arterioscler Thromb Vasc Biol.* 2014;34:2594-2600
221. Schindelin J, Arganda-Carreras I, Frise E, Kaynig V, Longair M, Pietzsch T, Preibisch S, Rueden C, Saalfeld S, Schmid B. Fiji: An open-source platform for biological-image analysis. *Nature methods.* 2012;9:676
222. Gehi R, Shao Q, Laird DW. Pathways regulating the trafficking and turnover of pannexin1 protein and the role of the c-terminal domain. *The Journal of biological chemistry.* 2011;286:27639-27653
223. Bolte S, Cordelieres FP. A guided tour into subcellular colocalization analysis in light microscopy. *Journal of Microscopy.* 2006;224:213-232
224. Billaud M, Lohman AW, Straub AC, Parpaite T, Johnstone SR, Isakson BE. Characterization of the thoracodorsal artery: Morphology and reactivity. *Microcirculation.* 2012;19:360-372
225. Billaud M, Chiu Y-H, Lohman AW, Parpaite T, Butcher JT, Mutchler SM, DeLalio LJ, Artamonov MV, Sandilos JK, Best AK, Somlyo AV, Thompson RJ, Le TH, Ravichandran KS, Bayliss DA, Isakson BE. A molecular signature in the pannexin 1 intracellular loop confers channel activation by the α 1-adrenergic receptor in smooth muscle cells. *Science Signaling.* 2015:1-63
226. Vandsburger MH, French BA, Helm PA, Roy RJ, Kramer CM, Young AA, Epstein FH. Multi-parameter in vivo cardiac magnetic resonance imaging demonstrates normal perfusion reserve despite severely attenuated β -adrenergic functional response in neuronal nitric oxide synthase knockout mice. *European heart journal.* 2007;28:2792-2798
227. Sequeira Lopez MLS, Pentz ES, Nomasa T, Smithies O, Gomez RA. Renin cells are precursors for multiple cell types that switch to the renin phenotype when homeostasis is threatened. *Developmental cell.* 2004;6:719-728
228. Poon IKH, Chiu Y-H, Armstrong AJ, Kinchen JM, Juncadella IJ, Bayliss DA, Ravichandran KS. Unexpected link between an antibiotic, pannexin channels and apoptosis. *Nature.* 2014;507:329-334

229. Seltzer A, Bregonzio C, Armando I, Baiardi G, Saavedra JM. Oral administration of an $\alpha 1$ receptor antagonist prevents the central effects of angiotensin ii in spontaneously hypertensive rats. *Brain research*. 2004;1028:9-18
230. Davies LA, Hu C, Guagliardo NA, Sen N, Chen X, Talley EM, Carey RM, Bayliss DA, Barrett PQ. Task channel deletion in mice causes primary hyperaldosteronism. *Proceedings of the National Academy of Sciences*. 2008;105:2203-2208
231. Wotus C, Levay-Young BK, Rogers LM, Gomez-Sanchez CE, Engeland WC. Development of adrenal zonation in fetal rats defined by expression of aldosterone synthase and 11β -hydroxylase. *Endocrinology*. 1998;139:4397-4403
232. Tanoue A, Nasa Y, Koshimizu T, Shinoura H, Oshikawa S, Kawai T, Sunada S, Takeo S, Tsujimoto G. The $\alpha 1d$ -adrenergic receptor directly regulates arterial blood pressure via vasoconstriction. *The Journal of clinical investigation*. 2002;109:765-775
233. Fisher SA. Vascular smooth muscle phenotypic diversity and function. *Physiological Genomics*. 2010;42A:169-187
234. Jackson WF, Boerman EM, Lange EJ, Lundback SS, Cohen KD. Smooth muscle $\alpha 1d$ -adrenoceptors mediate phenylephrine-induced vasoconstriction and increases in endothelial cell ca^{2+} in hamster cremaster arterioles. *British Journal of Pharmacology*. 2008;155:514-524
235. Burnstock G. Control of vascular tone by purines and pyrimidines. *British Journal of Pharmacology*. 2010;161:527--529
236. Burnstock G. Control of vascular tone by purines and pyrimidines. *British Journal of Pharmacology*. 2010;161:527-529
237. Lohman AW, Billaud M, Isakson BE. Mechanisms of atp release and signalling in the blood vessel wall. *Cardiovasc Res*. 2012;95:269-280
238. Billaud M, Lohman AW, Straub AC, Looft-Wilson R, Johnstone SR, Araj CA, Best AK, Chekeni FB, Ravichandran KS, Penuela S, Laird DW, Isakson BE. Pannexin1 regulates $\alpha 1$ -adrenergic receptor- mediated vasoconstriction. *Circulation Research*. 2011;109:80-85

239. Bond S, Naus CC. The pannexins: Past and present. *Frontiers in Physiology*. 2014;5:1-24
240. Nyberg M, Piil P, Kiehn OT, Maagaard C, Jørgensen TS, Egelund J, Isakson BE, Nielsen MS, Gliemann L, Hellsten Y. Probenecid inhibits α -adrenergic receptor-mediated vasoconstriction in the human leg vasculature. *Hypertension*. 2018;71:151-159
241. Angus JA, Wright CE. Novel α 1-adrenoceptor antagonism by the fluoroquinolone antibiotic trovafloxacin. *European journal of pharmacology*. 2016;791:179-184
242. DeLalio LJ, Keller AS, Chen J, Boyce AK, Artamonov M, Askew-Page HR, Keller IV TS, Johnstone SR, Weaver RB, Good MEJA, thrombosis, and vascular biology. Interaction between pannexin 1 and caveolin-1 in smooth muscle can regulate blood pressure. 2018:ATVBAHA. 118.311290
243. Di Salvo J, Steusloff A, Semenchuk L, Satoh S, Kolquist K, Pfitzer G. Tyrosine kinase inhibitors suppress agonist-induced contraction in smooth muscle. *Biochemical and Biophysical Research Communications*. 1993;190:968-974
244. Di Salvo J, Semenchuk LA, Lauer J. Vanadate-induced contraction of smooth muscle and enhanced protein tyrosine phosphorylation. *Archives of biochemistry and biophysics*. 1993;304:386-391
245. Ward DT, Alder AC, Ohanian J, Ohanian V. Noradrenaline-induced paxillin phosphorylation, erk activation and mek-regulated contraction in intact rat mesenteric arteries. *Journal of vascular research*. 2002;39:1-11
246. Lohman AW, Leskov IL, Butcher JT, Johnstone SR, Stokes TA, Begandt D, DeLalio LJ, Best AK, Penuela S, Leitinger N, Ravichandran KS, Stokes KY, Isakson BE. Pannexin 1 channels regulate leukocyte emigration through the venous endothelium during acute inflammation. *Nature Communications*. 2015;6:1-12
247. Thompson RJ, Zhou N, MacVicar BA. Ischemia opens neuronal gap junction hemichannels. *Science*. 2006;312:924-927
248. Weilinger NL, Tang PL, Thompson RJ. Anoxia-induced nmda receptor activation opens pannexin channels via src family kinases. *J Neurosci*. 2012;32:12579-12588

249. Ma W, Hui H, Pelegrin P, Surprenant A. Pharmacological characterization of pannexin-1 currents expressed in mammalian cells. *Journal of Pharmacology and Experimental Therapeutics*. 2009;328:409-418
250. Iglesias R, Locovei S, Roque A, Alberto AP, Dahl G, Spray DC, Scemes E. P2x7 receptor-pannexin1 complex: Pharmacology and signaling. *Am J Physiol Cell Physiol*. 2008;295:C752-760
251. Atkinson MM, Menko A, Johnson RG, Sheppard J, Sheridan JD. Rapid and reversible reduction of junctional permeability in cells infected with a temperature-sensitive mutant of avian sarcoma virus. *The Journal of Cell Biology*. 1981;91:573-578
252. Weilinger NL, Lohman AW, Rakai BD, Ma EM, Bialecki J, Maslieieva V, Rilea T, Bandet MV, Ikuta NT, Scott L, Colicos MA, Teskey GC, Winship IR, Thompson RJ. Metabotropic nmda receptor signaling couples src family kinases to pannexin-1 during excitotoxicity. *Nat Neurosci*. 2016;19:432-442
253. Bargiotas P, Krenz A, Hormuzdi SG, Ridder DA, Herb A, Barakat W, Penuela S, von Engelhardt J, Monyer H, Schwaninger M. Pannexins in ischemia-induced neurodegeneration. *Proc Natl Acad Sci U S A*. 2011;108:20772-20777
254. Penuela S, Bhalla R, Nag K, Laird DW. Glycosylation regulates pannexin intermixing and cellular localization. *Mol Biol Cell*. 2009;20:4313-4323
255. Chekeni FB, Elliott MR, Sandilos JK, Walk SF, Kinchen JM, Lazarowski ER, Armstrong AJ, Penuela S, Laird DW, Salvesen GS, Isakson BE, Bayliss DA, Ravichandran KS. Pannexin 1 channels mediate 'find-me' signal release and membrane permeability during apoptosis. *Nature*. 2010;467:863-867
256. Gulbransen BD, Bashashati M, Hirota SA, Gui X, Roberts JA, MacDonald JA, Muruve DA, McKay DM, Beck PL, Mawe GM. Activation of neuronal p2x7 receptor–pannexin-1 mediates death of enteric neurons during colitis. *Nature medicine*. 2012;18:600
257. Pinheiro AR, Paramos-de-Carvalho D, Certal M, Costa C, es-Cardoso MTM, Ferreirinha Ft, Costa MA, Correia-de-S P. Bradykinin-induced ca²⁺ signaling in human subcutaneous fibroblasts involves atp release via hemichannels leading to p2y₁₂ receptors activation. *Cell Communication and Signaling*. 2013;11:1-1

258. Pinheiro AR, Paramos-de-Carvalho D, Certal M, Costa MA, Costa C, Magalhães-Cardoso MT, Ferreirinha F, Sévigny J, Correia-de-Sá P. Histamine induces atp release from human subcutaneous fibroblasts, via pannexin-1 hemichannels, leading to ca²⁺ mobilization and cell proliferation. *The Journal of biological chemistry*. 2013;288:27571-27583
259. Somlyo AP, Somlyo AV. From pharmacomechanical coupling to g-proteins and myosin phosphatase. *Acta physiologica Scandinavica*. 1998;164:437-448
260. Somlyo AP, Somlyo AV. Ca²⁺ sensitivity of smooth muscle and nonmuscle myosin ii: Modulated by g proteins, kinases, and myosin phosphatase. *Physiological reviews*. 2003;83:1325-1358
261. Murali S, Zhang M, Nurse CA. Evidence that 5-ht stimulates intracellular ca²⁺ signalling and activates pannexin-1 currents in type ii cells of the rat carotid body. *The Journal of physiology*. 2017;595:4261-4277
262. Boyce AKJ, Swayne LA. P2x7 receptor cross-talk regulates atp-induced pannexin 1 internalization. *The Biochemical journal*. 2017;474:2133-2144
263. Riquelme MA, Cea LA, Vega JL, Boric MP, Monyer H, Bennett MV, Frank M, Willecke K, Saez JC. The atp required for potentiation of skeletal muscle contraction is released via pannexin hemichannels. *Neuropharmacology*. 2013;75:594-603
264. Poornima V, Vallabhaneni S, Mukhopadhyay M, Bera AK. Nitric oxide inhibits the pannexin 1 channel through a cgmp–pkg dependent pathway. *Nitric Oxide*. 2015;47:1-8
265. Di Salvo J, Pfitzer G, Semenchuk LA. Protein tyrosine phosphorylation, cellular ca²⁺, and ca²⁺ sensitivity for contraction of smooth muscle. *Canadian journal of physiology and pharmacology*. 1994;72:1434-1439
266. Li S, Couet J, Lisanti MP. Src tyrosine kinases, galpha subunits, and h-ras share a common membrane-anchored scaffolding protein, caveolin. Caveolin binding negatively regulates the auto-activation of src tyrosine kinases. *Journal of Biological Chemistry*. 1996;271:29182-29190

267. Hughes AD, Wijetunge S. Role of tyrosine phosphorylation in excitation-contraction coupling in vascular smooth muscle. *Acta physiologica Scandinavica*. 1998;164:457-469
268. Dinkel H, Van Roey K, Michael S, Kumar M. Elm 2016—data update and new functionality of the eukaryotic linear motif resource. *Nucleic acids ...* 2015
269. Yu H, Rosen MK, Shin TB, Seidel-Dugan C, Brugge JS, Schreiber SL. Solution structure of the sh3 domain of src and identification of its ligand-binding site. *Science*. 1992;258:1665-1668
270. Nakamoto T, Sakai R, Ozawa K, Yazaki Y, Hirai H. Direct binding of c-terminal region of p130 to sh2 and sh3 domains of src kinase. *Journal of Biological Chemistry*. 1996;271:8959-8965
271. Ren R, Mayer BJ, Cicchetti P, Baltimore D. Identification of a ten-amino acid proline-rich sh3 binding site. *Science*. 1993;259:1157-1161
272. Shvartsman DE, Donaldson JC, Diaz B, Gutman O, Martin GS, Henis YI. Src kinase activity and sh2 domain regulate the dynamics of src association with lipid and protein targets. *The Journal of Cell Biology*. 2007;178:675-686
273. Gottlieb-Abraham E, Shvartsman DE, Donaldson JC, Ehrlich M, Gutman O, Martin GS, Henis YI. Src-mediated caveolin-1 phosphorylation affects the targeting of active src to specific membrane sites. *Molecular biology of the cell*. 2013;24:3881-3895
274. Xing Z, Chen HC, Nowlen JK, Taylor SJ, Shalloway D, Guan JL. Direct interaction of v-src with the focal adhesion kinase mediated by the src sh2 domain. *Molecular biology of the cell*. 1994;5:413-421
275. Thomas SM, Brugge JS. Cellular functions regulated by src family kinases. *Annual Review of Cell and Developmental Biology*. 1997;13:513-609
276. Luttrell DK, Luttrell LM. Not so strange bedfellows: G-protein-coupled receptors and src family kinases. *Oncogene*. 2004;23:7969
277. McGarrigle D, Huang X-Y. Gpcrs signaling directly through src-family kinases. *Sci. Stke*. 2007;2007:pe35-pe35
278. Ma Y-C, Huang J, Ali S, Lowry W, Huang X-Y. Src tyrosine kinase is a novel direct effector of g proteins. *Cell*. 2000;102:635-646

279. Han C, Bowen WC, Michalopoulos GK, Wu T. Alpha-1 adrenergic receptor transactivates signal transducer and activator of transcription-3 (stat3) through activation of src and epidermal growth factor receptor (egfr) in hepatocytes. *Journal of Cellular Physiology*. 2008;216:486-497
280. Grassi G. Assessment of sympathetic cardiovascular drive in human hypertension: Achievements and perspectives. *Hypertension*. 2009;54:690-697
281. Yun H-M, Kim S, Kim H-J, Kostenis E, Kim JI, Seong JY, Baik J-H, Rhim H. The novel cellular mechanism of human 5-HT₆ receptor through an interaction with fyn. *Journal of Biological Chemistry*. 2006
282. Murali S, Zhang M, Nurse CA. Angiotensin II mobilizes intracellular calcium and activates pannexin-1 channels in rat carotid body type II cells via AT₁ receptors. *The Journal of Physiology*. 2014;592:4747-4762
283. Gómez GI, Fernández P, Velarde V, Sáez JC. Angiotensin II-induced mesangial cell damage is preceded by cell membrane permeabilization due to upregulation of non-selective channels. *International journal of molecular sciences*. 2018;19:957
284. Weng Y-I, Shukla SD. Angiotensin II activation of focal adhesion kinase and pp60c-src in relation to mitogen-activated protein kinases in hepatocytes. *Biochimica et Biophysica Acta (BBA)-Molecular Cell Research*. 2002;1589:285-297
285. Bokemeyer D, Schmitz U, Kramer HJ. Angiotensin II-induced growth of vascular smooth muscle cells requires an src-dependent activation of the epidermal growth factor receptor1. *Kidney international*. 2000;58:549-558
286. Li L, Zhou Y, Wang C, Zhao Y-L, Zhang Z-G, Fan D, Cui X-B, Wu L-L. Src tyrosine kinase regulates angiotensin II-induced protein kinase C ζ activation and proliferation in vascular smooth muscle cells. *Peptides*. 2010;31:1159-1164
287. Xiao F, Waldrop SL, Khimji A-k, Kilic G. Pannexin1 contributes to pathophysiological ATP release in lipopoptosis induced by saturated free fatty acids in liver cells. *American Journal of Physiology-Cell Physiology*. 2012;303:C1034-C1044

288. Poornima VaVSaMMaBAK. Nitric oxide inhibits the pannexin 1 channel through a cgmp \textendash pkg dependent pathway. *Nitric Oxide*. 2015;47:1--8
289. Good MEaBDaDLJaKASaBMaIBE. Emerging concepts regarding pannexin 1 in the vasculature. *Biochemical Society transactions*. 2015;43:495--501
290. Dahl G, Qiu F, Wang J. The bizarre pharmacology of the atp release channel pannexin1. *Neuropharmacology*. 2013;75:583-593
291. Isakson BE, Thompson RJ. Pannexin-1 as a potentiator of ligand-gated receptor signaling. *Channels*. 2014;8:118-123
292. Parsons SJ, Parsons JT. Src family kinases, key regulators of signal transduction. *Oncogene*. 2004;23:7906-7909
293. Roskoski Jr R. Src protein--tyrosine kinase structure and regulation. *Biochemical and Biophysical Research Communications*. 2004;324:1155-1164
294. Bolen JB, Brugge JS. Leukocyte protein tyrosine kinases: Potential targets for drug discovery. *Annual review of immunology*. 1997;15:371-404
295. Mitra SK, Schlaepfer DD. Integrin-regulated fak--src signaling in normal and cancer cells. *Current opinion in cell biology*. 2006;18:516-523
296. Bolós V, Gasent JM, López-Tarruella S, Grande E. The dual kinase complex fak-src as a promising therapeutic target in cancer. *OncoTargets and therapy*. 2010;3:83
297. Parsons JT, Parsons SJ. Src family protein tyrosine kinases: Cooperating with growth factor and adhesion signaling pathways. *Current opinion in cell biology*. 1997;9:187-192
298. Penuela S, Lohman AW, Lai W, Gyenis L, Litchfield DW, Isakson BE, Laird DW. Diverse post-translational modifications of the pannexin family of channel-forming proteins. *Channels*. 2014;8:124-130
299. Patwardhan P, Resh MD. Myristoylation and membrane binding regulate c-src stability and kinase activity. *Molecular and cellular biology*. 2010;30:4094-4107
300. Christensen KL, Mulvany MJ. Location of resistance arteries. *Journal of vascular research*. 2001;38:1-12
301. Tanoue A, Nasa Y, Koshimizu T, Shinoura H, Oshikawa S, Kawai T, Sunada S, Takeo S, Tsujimoto G. The alpha(1d)-adrenergic receptor directly regulates

- arterial blood pressure via vasoconstriction. *The Journal of clinical investigation*. 2002;109:765-775
302. Bennett MR. Autonomic neuromuscular transmission at a varicosity. *Progress in neurobiology*. 1996;50:505-532
303. Sowa G. Caveolae, caveolins, cavins, and endothelial cell function: New insights. *Frontiers in Physiology*. 2012;2
304. Rahman A, Swärd K. The role of caveolin-1 in cardiovascular regulation. *Acta physiologica (Oxford, England)*. 2009;195:231-245
305. Li X-A, Everson WV, Smart EJ. Caveolae, lipid rafts, and vascular disease. *Trends in Cardiovascular Medicine*. 2005;15:92-96
306. Martínez-Salas SG, Campos-Peralta JM, Pardo JP, Hernández-Muñoz R, Ibarra M, Tanoue A, Tsujimoto G, Villalobos-Molina R. $\alpha 1d$ -adrenoceptor regulates the vasopressor action of $\alpha 1a$ -adrenoceptor in mesenteric vascular bed of $\alpha 1d$ -adrenoceptor knockout mice. *Autonomic and Autacoid Pharmacology*. 2011;31:64-71
307. Predescu D, Vogel SM, Malik AB. Functional and morphological studies of protein transcytosis in continuous endothelia. *American Journal of Physiology-Lung Cellular and Molecular Physiology*. 2004;287:L895-901
308. Williams TM, Lisanti MP. Caveolin-1 in oncogenic transformation, cancer, and metastasis. *AJP: Cell Physiology*. 2005;288:C494-506
309. Patel HH, Murray F, Insel PA. G-protein-coupled receptor-signaling components in membrane raft and caveolae microdomains. In: Klussmann E, Scott J, eds. *Protein-protein interactions as new drug targets*. Berlin, Heidelberg: Springer Berlin Heidelberg; 2008:167-184.
310. Parton RG, del Pozo MA. Caveolae as plasma membrane sensors, protectors and organizers. *Nature Reviews Molecular Cell Biology*. 2013;14:98-112
311. Drab M, Verkade P, Elger M, Kasper M, Lohn M, Lauterbach B, Menne J, Lindschau C, Mende F, Luft FC. Loss of caveolae, vascular dysfunction, and pulmonary defects in caveolin-1 gene-disrupted mice. *Science*. 2001;293:2449-2452

312. Fra AM, Williamson E, Simons K, Parton RG. De novo formation of caveolae in lymphocytes by expression of vip21-caveolin. *Proceedings of the National Academy of Sciences of the United States of America*. 1995;92:8655-8659
313. Razani B, Combs TP, Wang XB, Frank PG, Park DS, Russell RG, Li M, Tang B, Jelicks LA, Scherer PE. Caveolin-1-deficient mice are lean, resistant to diet-induced obesity, and show hypertriglyceridemia with adipocyte abnormalities. *Journal of Biological Chemistry*. 2002;277:8635-8647
314. Razani B, Lisanti MP. Caveolin-deficient mice: Insights into caveolar function human disease. *The Journal of clinical investigation*. 2001;108:1553-1561
315. Albinsson S, Shakirova Y, Rippe A, Baumgarten M, Rosengren B-I, Rippe C, Hallmann R, Hellstrand P, Rippe B, Swärd K. Arterial remodeling and plasma volume expansion in caveolin-1-deficient mice. *American Journal of Physiology-Regulatory, Integrative and Comparative Physiology*. 2007;293:R1222-R1231
316. Bernatchez P, Sharma A, Bauer PM, Marin E, Sessa WC. A noninhibitory mutant of the caveolin-1 scaffolding domain enhances enos-derived no synthesis and vasodilation in mice. *The Journal of Clinical Investigation*. 2011;121:3747-3755
317. Morris JB, Huynh H, Vasilevski O, Woodcock EA. A1-adrenergic receptor signaling is localized to caveolae in neonatal rat cardiomyocytes. *Journal of molecular and cellular cardiology*. 2006;41:17-25
318. Hardin CD, Vallejo J. Caveolins in vascular smooth muscle: Form organizing function. *Cardiovascular research*. 2006;69:808-815
319. Baek PJ, Sung-Jin K. Anti-hypertensive effects of probenecid via inhibition of the α -adrenergic receptor. *Pharmacological Reports*. 2011;63:1145-1150
320. Nyberg M, Piil P, Kiehn OT, Maagaard C, Jørgensen TS, Egelund J, Isakson BE, Nielsen MS, Gliemann L, Hellsten Y. Probenecid inhibits α -adrenergic receptor-mediated vasoconstriction in the human leg vasculature novelty and significance. *Hypertension*. 2018;71:151-159
321. Kauffenstein G, Tamarelle S, Prunier F, Roy C, Ayer A, Toutain B, Billaud M, Isakson BE, Grimaud L, Loufrani L. Central role of p2y6 udp receptor in arteriolar myogenic tone. *Arteriosclerosis, thrombosis, and vascular biology*. 2016:ATVBAHA-116

322. Fujita T, Toya Y, Iwatsubo K, Onda T, Kimura K, Umemura S, Ishikawa Y. Accumulation of molecules involved in α 1-adrenergic signal within caveolae: Caveolin expression and the development of cardiac hypertrophy. *Cardiovascular research*. 2001;51:709-716
323. Boyce AKJ, Kim MS, Wicki-Stordeur LE, Swayne LA. Atp stimulates pannexin 1 internalization to endosomal compartments. *The Biochemical journal*. 2015;470:319-330
324. Chiu Y-H, Ravichandran KS, Bayliss DA. Intrinsic properties and regulation of pannexin 1 channel. *Channels*. 2014;8:103-109
325. Dubroca C, Loyer X, Retailleau K, Loirand G, Pacaud P, Feron O, Balligand J-L, Lévy BI, Heymes C, Henrion D. Rhoa activation and interaction with caveolin-1 are critical for pressure-induced myogenic tone in rat mesenteric resistance arteries. *Cardiovascular research*. 2007;73:190-197
326. Dreja K, Voldstedlund M, Vinten J. Cholesterol depletion disrupts caveolae and differentially impairs agonist-induced arterial contraction. *Hypertension*. 2002
327. Yeh Y-C, Parekh AB. Distinct structural domains of caveolin-1 independently regulate ca^{2+} release-activated ca^{2+} channels and ca^{2+} microdomain-dependent gene expression. *Molecular and cellular biology*. 2015;35:1341-1349
328. Kwiatek AM, Minshall RD, Cool DR, Skidgel RA, Malik AB, Tirupathi C. Caveolin-1 regulates store-operated ca^{2+} influx by binding of its scaffolding domain to *trpc1* in endothelial cells. *Molecular pharmacology*. 2006
329. Sundivakkam PC, Kwiatek AM, Sharma TT, Minshall RD, Malik AB, Tirupathi C. Caveolin-1 scaffold domain interacts with *trpc1* and *ip3r3* to regulate ca^{2+} store release-induced ca^{2+} entry in endothelial cells. *AJP: Cell Physiology*. 2008;296:C403-C413
330. Grande-García A, Echarri A, de Rooij J, Alderson NB, Waterman-Storer CM, Valdivielso JM, del Pozo MA. Caveolin-1 regulates cell polarization and directional migration through src kinase and rho gtpases. *The Journal of cell biology*. 2007;177:683-694

331. Fisher JP, Paton JFR. The sympathetic nervous system and blood pressure in humans: Implications for hypertension. *Journal of human hypertension*. 2012;26:463-475
332. Fisher JP, Young CN, Fadel PJ. Central sympathetic overactivity: Maladies and mechanisms. *Autonomic neuroscience : basic & clinical*. 2009;148:5-15
333. Pimenta E, Calhoun DA. Resistant hypertension: Incidence, prevalence, and prognosis. *Circulation*. 2012;125:1594-1596
334. Manolis AJ, Poulimenos LE, Kallistratos MS, Gavras I, Gavras H. Sympathetic overactivity in hypertension and cardiovascular disease. *Current vascular pharmacology*. 2014;12:4-15
335. Ju H, Zou R, Venema VJ, Venema RC. Direct interaction of endothelial nitric-oxide synthase and caveolin-1 inhibits synthase activity. *Journal of Biological Chemistry*. 1997;272:18522-18525
336. Feron O, Belhassen L, Kobzik L, Smith TW, Kelly RA, Michel T. Endothelial nitric oxide synthase targeting to caveolae specific interactions with caveolin isoforms in cardiac myocytes and endothelial cells. *Journal of Biological Chemistry*. 1996;271:22810-22814
337. Bhalla-Gehi R, Penuela S, Churko JM, Shao Q, Laird DW. Pannexin1 and pannexin3 delivery, cell surface dynamics, and cytoskeletal interactions. *The Journal of biological chemistry*. 2010;285:9147-9160
338. Wicki-Stordeur LE, Swayne LA. Panx1 regulates neural stem and progenitor cell behaviours associated with cytoskeletal dynamics and interacts with multiple cytoskeletal elements. *Cell communication and signaling : CCS*. 2013;11:62
339. Swayne LA. Powerful partnership: Crosstalk between pannexin 1 and the cytoskeleton. 2014:1-4
340. Carey RM, Siragy HM. Newly recognized components of the renin-angiotensin system: Potential roles in cardiovascular and renal regulation. *Endocrine reviews*. 2003;24:261-271
341. Atlas SA. The renin-angiotensin aldosterone system: Pathophysiological role and pharmacologic inhibition. *Journal of managed care pharmacy*. 2007;13:9-20

342. Carey RM. The intrarenal renin-angiotensin system in hypertension. *Advances in chronic kidney disease*. 2015;22:204-210
343. Kumar R, Singh VP, Baker KM. The intracellular renin–angiotensin system: A new paradigm. *Trends in Endocrinology & Metabolism*. 2007;18:208-214
344. Friis UG, Madsen K, Stubbe J, Hansen PBL, Svenningsen P, Bie P, Skøtt O, Jensen BL. Regulation of renin secretion by renal juxtaglomerular cells. *Pflügers Archiv - European Journal of Physiology*. 2013;465:25-37
345. Kurtz A. Renin release: Sites, mechanisms, and control. *Annual review of physiology*. 2011;73:377-399
346. Kopp U, Aurell M, Nilsson M, Åblad B. The role of beta-1-adrenoceptors in the renin release response to graded renal sympathetic nerve stimulation. *Pflügers Archiv*. 1980;387:107-113
347. Scholz H, Vogel U, Kurtz A. Interrelation between baroreceptor and macula densa mechanisms in the control of renin secretion. *The Journal of physiology*. 1993;469:511-524
348. Gomez RA, Lopez MLSS. Who and where is the renal baroreceptor?: The connexin hypothesis. *Kidney international*. 2009;75:460-462
349. Gomez RA, Lopez MLSS. Plasticity of renin cells in the kidney vasculature. *Current Hypertension Reports*. 2017;19:81-84
350. Lin EE, Sequeira-Lopez MLS, Gomez RA. Rbp-j in foxd1+ renal stromal progenitors is crucial for the proper development and assembly of the kidney vasculature and glomerular mesangial cells. *AJP: Renal Physiology*. 2014;306:F249-F258
351. Gomez RA, Belyea B, Medrano S, Pentz ES, Sequeira Lopez MLS. Fate and plasticity of renin precursors in development and disease. *Pediatric Nephrology*. 2013;29:721-726
352. Solini A, Usuelli V, Fiorina P. The dark side of extracellular atp in kidney diseases. *Journal of the American Society of Nephrology : JASN*. 2015;26:1007-1016
353. Vallon V, Stockand J, Rieg T. P2y receptors and kidney function. *Wiley Interdisciplinary Reviews: Membrane Transport and Signaling*. 2012;1:731-742

354. Guan Z, Inscho EW. Role of adenosine 5'-triphosphate in regulating renal microvascular function and in hypertension. *Hypertension*. 2011;58:333-340
355. Bell PD, Lapointe J-Y, Sabirov R, Hayashi S, Peti-Peterdi J, Manabe K-i, Kovacs G, Okada Y. Macula densa cell signaling involves atp release through a maxi anion channel. *Proceedings of the National Academy of Sciences*. 2003;100:4322-4327
356. Churchill PC, Ellis VR. Purinergic p2y receptors stimulate renin secretion by rat renal cortical slices. *Journal of Pharmacology and Experimental ...*. 1993
357. van der Weyden L, Adams DJ, Morris BJ. Capacity for purinergic control of renin promoter via p2y(11) receptor and camp pathways. *Hypertension*. 2000;36:1093-1098
358. Toering TJ, Gant CM, Visser FW, van der Graaf AM, Laverman GD, Danser AHJ, Faas MM, Navis G, Lely AT. Sex differences in renin-angiotensin-aldosterone system affect extracellular volume in healthy subjects. *American journal of physiology. Renal physiology*. 2018;314:F873-F878
359. Bührle C, Scholz H, Nobiling R, Taugner R. Junctional transmission in renin-containing and smooth muscle cells of the afferent arteriole. *Pflügers Archiv*. 1986;406:578-586
360. Yao J, Suwa M, Li B, Kawamura K, Morioka T, Oite T. Atp-dependent mechanism for coordination of intercellular ca²⁺ signaling and renin secretion in rat juxtaglomerular cells. *Circulation Research*. 2003;93:338-345
361. Franco M, Bell PD, Navar LG. Effect of adenosine a1 analogue on tubuloglomerular feedback mechanism. *American Journal of Physiology-Renal Physiology*. 1989;257:F231-F236
362. Shirley DG, Vekaria RM, Sévigny J. Ectonucleotidases in the kidney. *Purinergic Signalling*. 2009;5:501
363. Schweda F, Segerer F, Castrop H, Schnermann J, Kurtz A. Blood pressure-dependent inhibition of renin secretion requires a1 adenosine receptors. *Hypertension*. 2005;46:780-786
364. Castrop H, Huang Y, Hashimoto S, Mizel D, Hansen P, Theilig F, Bachmann S, Deng C, Briggs J, Schnermann J. Impairment of tubuloglomerular feedback

- regulation of gfr in ecto-5'-nucleotidase/cd73-deficient mice. *The Journal of clinical investigation*. 2004;114:634-642
365. Murray RD, Churchill PC. Effects of adenosine receptor agonists in the isolated, perfused rat kidney. *American Journal of Physiology-Heart and Circulatory Physiology*. 1984;247:H343-H348
366. Churchill PC, Churchill MC. A1 and a2 adenosine receptor activation inhibits and stimulates renin secretion of rat renal cortical slices. *Journal of Pharmacology and Experimental Therapeutics*. 1985;232:589-594
367. Ortiz-Capisano MC, Atchison DK, Harding P, Lasley RD, Beierwaltes WH. Adenosine inhibits renin release from juxtaglomerular cells via an a1 receptor-trpc-mediated pathway. *American Journal of Physiology-Renal Physiology*. 2013;305:F1209-F1219
368. Li L, Lai EY, Huang Y, Eisner C, Mizel D, Wilcox CS, Schnermann J. Renal afferent arteriolar and tubuloglomerular feedback reactivity in mice with conditional deletions of adenosine 1 receptors. *American Journal of Physiology-Renal Physiology*. 2012;303:F1166-F1175
369. Solini A, Usuelli V, Fiorina P. The dark side of extracellular atp in kidney diseases. *Journal of the American Society of Nephrology*. 2015;26:1007-1016
370. López MLSS, Pentz ES, Nomasa T, Smithies O, Gomez RA. Renin cells are precursors for multiple cell types that switch to the renin phenotype when homeostasis is threatened. *Developmental cell*. 2004;6:719-728
371. Gomez RA, Lopez MLSS. Plasticity of renin cells in the kidney vasculature. *Current Hypertension Reports*. 2017;19:14
372. Gomez D, Swiatlowska P, Owens GK. Epigenetic control of smooth muscle cell identity and lineage memory. *Arteriosclerosis, Thrombosis, and Vascular Biology*. 2015;35:2508-2516
373. Lee G, Makhanova N, Caron K, Lopez MLS, Gomez RA, Smithies O, Kim H-S. Homeostatic responses in the adrenal cortex to the absence of aldosterone in mice. *Endocrinology*. 2005;146:2650-2656
374. Walker III M, Harrison-Bernard LM, Cook AK, Navar LG. Dynamic interaction between myogenic and tgf mechanisms in afferent arteriolar blood flow

- autoregulation. *American Journal of Physiology-Renal Physiology*. 2000;279:F858-F865
375. Osmond DA, Inscho EW. P2x1 receptor blockade inhibits whole kidney autoregulation of renal blood flow in vivo. *American Journal of Physiology-Renal Physiology*. 2010;298:F1360-F1368
376. Billaud M, Sandilos JK, Isakson BE. Pannexin 1 in the regulation of vascular tone. *TCM*. 2012;22:68-72
377. Kauffenstein G, Drouin A, Thorin-Trescases N, Bachelard H, Robaye B, D'Orleans-Juste P, Marceau F, Thorin E, Sevigny J. Ntpdase1 (cd39) controls nucleotide-dependent vasoconstriction in mouse. *Cardiovascular Research*. 2009;85:204-213
378. Schnermann J, Briggs JP. Tubular control of renin synthesis and secretion. *Pflügers Archiv-European Journal of Physiology*. 2013;465:39-51
379. Chiu Y-H, Schappe MS, Desai BN, Bayliss DA. Revisiting multimodal activation and channel properties of pannexin 1. *The Journal of general physiology*. 2017:jgp. 201711888
380. Islam MR, Uramoto H, Okada T, Sabirov RZ, Okada Y. Maxi-anion channel and pannexin 1 hemichannel constitute separate pathways for swelling-induced atp release in murine 1929 fibrosarcoma cells. *American Journal of Physiology-Cell Physiology*. 2012;303:C924-C935
381. Kurtz A. Control of renin synthesis and secretion. *American journal of hypertension*. 2012;25:839-847
382. Brown R, Ollerstam A, Johansson B, Skøtt O, Gebre-Medhin S, Fredholm B, Persson AE. Abolished tubuloglomerular feedback and increased plasma renin in adenosine a1 receptor-deficient mice. *American Journal of Physiology-Regulatory, Integrative and Comparative Physiology*. 2001;281:R1362-1367
383. Friis UG, Madsen K, Stubbe J, Hansen PBL, Svenningsen P, Bie P, Skøtt O, Jensen BL. Regulation of renin secretion by renal juxtaglomerular cells. *Pflügers Archiv - European Journal of Physiology*. 2012;465:25-37

384. Locovei S, Bao L, Dahl G. Pannexin 1 in erythrocytes: Function without a gap. *Proceedings of the National Academy of Sciences of the United States of America*. 2006;103:7655-7659
385. Pelegrin P, Surprenant A. Pannexin-1 mediates large pore formation and interleukin-1 β release by the atp-gated p2x7 receptor. *The EMBO journal*. 2006;25:5071-5082
386. Iglesias R, Locovei S, Roque A, Alberto AP, Dahl G, Spray DC, Scemes E. P2x7 receptor-pannexin1 complex: Pharmacology and signaling. *AJP: Cell Physiology*. 2008;295:C752-C760
387. Chiu Y-H, Jin X, Medina CB, Leonhardt SA, Kiessling V, Bennett BC, Shu S, Tamm LK, Yeager M, Ravichandran KS, Bayliss DA. A quantized mechanism for activation of pannexin channels. *Nature Communications*. 2017;8:14324
388. Michalski K, Henze E, Nguyen P, Lynch P, Kawate T. The weak voltage dependence of pannexin 1 channels can be tuned by n-terminal modifications. *The Journal of general physiology*. 2018:jgp. 201711804
389. Sandilos JK, Bayliss DA. Physiological mechanisms for the modulation of pannexin 1 channel activity. *The Journal of Physiology*. 2012;590:6257-6266
390. Sequeira Lopez ML, Pentz ES, Robert B, Abrahamson DR, Gomez RA. Embryonic origin and lineage of juxtaglomerular cells. *AJP: Renal Physiology*. 2001;281:F345-356
391. Gomez RA, Lynch KR, Sturgill BC, Elwood JP, Chevalier RL, Carey RM, Peach MJ. Distribution of renin mrna and its protein in the developing kidney. *The American journal of physiology*. 1989;257:F850-858
392. Pentz ES, López M, Cordaillat M. Identity of the renin cell is mediated by camp and chromatin remodeling: An in vitro model for studying cell recruitment and plasticity. 2008
393. Pentz ES, Moyano MA, Thornhill BA, Sequeira Lopez MLS, Gomez RA. Ablation of renin-expressing juxtaglomerular cells results in a distinct kidney phenotype. *American Journal of Physiology-Regulatory, Integrative and Comparative Physiology*. 2004;286:R474-483

394. Puchałowicz K, Tarnowski M, Baranowska-Bosiacka I, Chlubek D, Dziedziejko V. P2x and p2y receptors—role in the pathophysiology of the nervous system. *International journal of molecular sciences*. 2014;15:23672-23704
395. Gitterman D, Evans R. Nerve evoked p2x receptor contractions of rat mesenteric arteries; dependence on vessel size and lack of role of l-type calcium channels and calcium induced calcium release. *British journal of pharmacology*. 2001;132:1201-1208
396. Zippel N, Limbach CA, Ratajski N, Urban C, Luparello C, Pansky A, Kassack MU, Tobiasch E. Purinergic receptors influence the differentiation of human mesenchymal stem cells. *Stem cells and development*. 2011;21:884-900
397. Post SR, Rump LC, Zambon A, Hughes RJ, Buda MD, Jacobson JP, Kao CC, Insel PA. Atp activates camp production via multiple purinergic receptors in mdck-d1 epithelial cells blockade of an autocrine/paracrine pathway to define receptor preference of an agonist. *Journal of Biological Chemistry*. 1998;273:23093-23097
398. Torres B, Zambon AC, Insel PA. P2y11 receptors activate adenylyl cyclase and contribute to nucleotide-promoted camp formation in mdck-d1 cells a mechanism for nucleotide-mediated autocrine-paracrine regulation. *Journal of Biological Chemistry*. 2002;277:7761-7765
399. Kennedy C. P2y 11 receptors: Properties, distribution and functions. *Protein reviews*. Springer; 2017:107-122.
400. Jacobson KA, Jayasekara MS, Costanzi S. Molecular structure of p2y receptors: Mutagenesis, modeling, and chemical probes. *Wiley Interdisciplinary Reviews: Membrane Transport and Signaling*. 2012;1:815-827
401. Pignatti E, Leng S, Carlone DL, Breault DT. Regulation of zonation and homeostasis in the adrenal cortex. *Molecular and cellular endocrinology*. 2017;441:146-155
402. Aguilar F, Lo M, Claustrat B, Saez JM, Sassard J, Li JY. Hypersensitivity of the adrenal cortex to trophic and secretory effects of angiotensin ii in lyon genetically-hypertensive rats. *Hypertension*. 2004;43:87-93

403. McEwan PE, Vinson GP, Kenyon CJ. Control of adrenal cell proliferation by at1 receptors in response to angiotensin ii and low-sodium diet. *American Journal of Physiology-Endocrinology And Metabolism*. 1999;276:E303-E309
404. Yatabe J, Yoneda M, Yatabe MS, Watanabe T, Felder RA, Jose PA, Sanada H. Angiotensin iii stimulates aldosterone secretion from adrenal gland partially via angiotensin ii type 2 receptor but not angiotensin ii type 1 receptor. *Endocrinology*. 2011;152:1582-1588
405. Kawamura M, Niitsu A, Nishi H, Masaki E. Extracellular atp potentiates steroidogenic effect of adrenocorticotrophic hormone in bovine adrenocortical fasciculata cells. *The Japanese Journal of Pharmacology*. 2001;85:376-381
406. Szalay KS, Orso E, Jurányi Z, Vinson GP, Vizi ES. Local non-synaptic modulation of aldosterone production by catecholamines and atp in rat: Implications for a direct neuronal fine tuning. *Hormone and Metabolic Research*. 1998;30:323-328
407. Matsuoka H, Yamada K, Atarashi K, Takagi M, Sugimoto T. Role of adenosine a1 and a2 receptors in the regulation of aldosterone production in rat adrenal glands. *Experientia*. 1990;46:726-728
408. Jurányi Z, Orso E, Janossy A, Szalay KS, Sperlagh B, Windisch K, Vinson G, Vizi E. Atp and [3h] noradrenaline release and the presence of ecto-ca²⁺-atpases in the capsule-glomerulosa fraction of the rat adrenal gland. *Journal of endocrinology*. 1997;153:105-114
409. Vidal V, Sacco S, Rocha AS, da Silva F, Panzolini C, Dumontet T, Doan TMP, Shan J, Rak-Raszewska A, Bird T, Vainio S, Martinez A, Schedl A. The adrenal capsule is a signaling center controlling cell renewal and zonation through rspos3. *Genes & Development*. 2016;30:1389-1394
410. Freedman BD, Kempna PB, Carlone DL, Shah M, Guagliardo NA, Barrett PQ, Gomez-Sanchez CE, Majzoub JA, Breault DT. Adrenocortical zonation results from lineage conversion of differentiated zona glomerulosa cells. *Developmental cell*. 2013;26:666-673
411. Jiang JX, Penuela S. Connexin and pannexin channels in cancer. *BMC cell biology*. 2016;17 Suppl 1:12

412. Penuela S, Kelly JJ, Churko JM, Barr KJ, Berger AC, Laird DW. Panx1 regulates cellular properties of keratinocytes and dermal fibroblasts in skin development and wound healing. *The Journal of investigative dermatology*. 2014;134:2026-2035
413. Langlois S, Xiang X, Young K, Cowan BJ, Penuela S, Cowan KN. Pannexin 1 and pannexin 3 channels regulate skeletal muscle myoblast proliferation and differentiation. *The Journal of biological chemistry*. 2014;289:30717-30731
414. Walczak EM, Kuick R, Finco I, Bohin N, Hrycaj SM, Wellik DM, Hammer GD. Wnt signaling inhibits adrenal steroidogenesis by cell-autonomous and non-cell-autonomous mechanisms. *Molecular Endocrinology*. 2014;28:1471-1486
415. Kim AC, Reuter AL, Zubair M, Else T, Serecky K, Bingham NC, Lavery GG, Parker KL, Hammer GD. Targeted disruption of β -catenin in sf1-expressing cells impairs development and maintenance of the adrenal cortex. *Development*. 2008;135:2593-2602
416. Berthon A, Drelon C, Ragazzon B, Boulkroun S, Tissier F, Amar L, Samson-Couterie B, Zennaro M-C, Plouin P-F, Skah S, Plateroti M, Lefèbvre H, Sahut-Barnola I, Batisse-Lignier M, Assié G, Lefrançois-Martinez A-M, Bertherat J, Martinez A, Val P. Wnt/ β -catenin signalling is activated in aldosterone-producing adenomas and controls aldosterone production. 2014;23:889-905
417. Berthon A, Sahut-Barnola I, Lambert-Langlais S, de Joussineau C, Damon-Soubeyrand C, Louiset E, Taketo MM, Tissier F, Bertherat J, Lefrançois-Martinez A-M, Martinez A, Val P. Constitutive beta-catenin activation induces adrenal hyperplasia and promotes adrenal cancer development. *Human molecular genetics*. 2010;19:1561-1576
418. Mizuno K, Hoffman LH, McKenzie JC, Inagami T. Presence of renin secretory granules in rat adrenal gland and stimulation of renin secretion by angiotensin ii but not by adrenocorticotropin. *The Journal of clinical investigation*. 1988;82:1007-1016
419. Bachmann J, Feldmer M, Ganten U, Stock G, Ganten D. Sexual dimorphism of blood pressure: Possible role of the renin-angiotensin system. *The Journal of steroid biochemistry and molecular biology*. 1991;40:511-IN512

420. Bielohuby M, Herbach N, Wanke Rd, Maser-Gluth C, Beuschlein F, Wolf E, Hoeflich A. Growth analysis of the mouse adrenal gland from weaning to adulthood: Time-and gender-dependent alterations of cell size and number in the cortical compartment. *American Journal of Physiology-Endocrinology and Metabolism*. 2007;293:E139-E146
421. Brosnihan KB, Weddle D, Anthony MS, Heise C, Li P, Ferrario CM. Effects of chronic hormone replacement on the renin–angiotensin system in cynomolgus monkeys. *Journal of hypertension*. 1997;15:719-726
422. Oelkers WK. Effects of estrogens and progestogens on the renin-aldosterone system and blood pressure. *Steroids*. 1996;61:166-171
423. Fischer M, Baessler A, Schunkert H. Renin angiotensin system and gender differences in the cardiovascular system. *Cardiovascular research*. 2002;53:672-677
424. Penuela S, Harland L, Simek J, Laird DW. Pannexin channels and their links to human disease. *The Biochemical journal*. 2014;461:371-381
425. Good ME, Chiu Y-H, Poon IK, Medina CB, Butcher JT, Mendu SK, DeLalio LJ, Lohman AW, Leitinger N, Barrett EJ. Pannexin 1 channels as an unexpected new target of the anti-hypertensive drug spironolactone. *Circulation research*. 2017:CIRCRESAHA. 117.312380
426. Berne RM. Cardiac nucleotides in hypoxia: Possible role in regulation of coronary blood flow. *American Journal of Physiology-Legacy Content*. 1963;204:317-322
427. Gerlach E, Deuticke B, Dreisbach R, Rosarius C. On the behavior of nucleotides and their dephosphorylation degradation products in the kidney in ischemia and short-term post-ischemic re-establishment of blood circulation. *Pflugers Archiv fur die gesamte Physiologie des Menschen und der Tiere*. 1963;278:296-315
428. Burnstock G. Hypoxia, endothelium, and purines. *Drug development research*. 1993;28:301-305
429. Bergfeld G, Forrester T. Release of atp from human erythrocytes in response to a brief period of hypoxia and hypercapnia. *Cardiovascular research*. 1992;26:40-47
430. Erlinge D. Extracellular atp: A growth factor for vascular smooth muscle cells. *General Pharmacology: The Vascular System*. 1998;31:1-8

431. Wang DJ, Huang NN, Heppel LA. Extracellular atp and adp stimulate proliferation of porcine aortic smooth muscle cells. *Journal of cellular physiology*. 1992;153:221-233
432. Pelleg A. Cardiac electrophysiology and pharmacology of adenosine and atp: Modulation by the autonomic nervous system. *The Journal of Clinical Pharmacology*. 1987;27:366-372
433. Visovatti SH, Hyman MC, Goonewardena SN, Anyanwu AC, Kanthi Y, Robichaud P, Wang J, Petrovic-Djergovic D, Rattan R, Burant CF. Purinergic dysregulation in pulmonary hypertension. *American Journal of Physiology-Heart and Circulatory Physiology*. 2016;311:H286-H298
434. Chen J, Zhu Y, Liang C, Chen J, Zhao H-B. Pannexin1 channels dominate atp release in the cochlea ensuring endocochlear potential and auditory receptor potential generation and hearing. *Scientific reports*. 2015;5:10762
435. Adamson SEaLN. The role of pannexin1 in the induction and resolution of inflammation. *FEBS letters*. 2014;588:1416--1422
436. Swayne LA, Boyce AK. Regulation of pannexin 1 surface expression by extracellular atp: Potential implications for nervous system function in health and disease. *Frontiers in cellular neuroscience*. 2017;11:230
437. Lohman AW, Weaver JL, Billaud M, Sandilos JK, Griffiths R, Straub AC, Penuela S, Leitinger N, Laird DW, Bayliss DA, Isakson BE. S-nitrosylation inhibits pannexin 1 channel function. *The Journal of biological chemistry*. 2012;287:39602-39612
438. Chiu Y-H, Jin X, Medina CB, Leonhardt SA, Kiessling V, Bennett BC, Shu S, Tamm LK, Yeager M, Ravichandran KS. A quantized mechanism for activation of pannexin channels. *Nature communications*. 2017;8:14324
439. Hanstein R, Negoro H, Patel NK, Charollais A, Meda P, Spray DC, Suadicani SO, Scemes E. Promises and pitfalls of a pannexin1 transgenic mouse line. *Frontiers in pharmacology*. 2013;4:61
440. Burma NE, Leduc-Pessah H, Trang T. Genetic deletion of microglial panx1 attenuates morphine withdrawal, but not analgesic tolerance or hyperalgesia in mice. *Channels*. 2017;11:487-494

441. Serman A, Hanstein R, Spray DC. The role of pannexin 1 in chemotherapy-induced peripheral neuropathy (cipn). 2015
442. Burnstock G. Historical review: Atp as a neurotransmitter. *Trends in Pharmacological Sciences*. 2006;27:166--176
443. Malhi H, Bronk SF, Werneburg NW, Gores GJ. Free fatty acids induce jnk dependent hepatocyte lipoapoptosis. *Journal of Biological Chemistry*. 2006
444. Zhang Y, Sands JM, Kohan DE, Nelson RD, Martin CF, Carlson NG, Kamerath CD, Ge Y, Klein JD, Kishore BK. Potential role of purinergic signaling in urinary concentration in inner medulla: Insights from p2y2 receptor gene knockout mice. *AJP: Renal Physiology*. 2008;295:F1715-F1724
445. Rieg T, Bunday RA, Chen Y, Deschenes G, Junger W, Insel PA, Vallon V. Mice lacking p2y2 receptors have salt-resistant hypertension and facilitated renal na⁺ and water reabsorption. *FASEB journal : official publication of the Federation of American Societies for Experimental Biology*. 2007;21:3717-3726
446. Gomez RA. Fate of renin cells during development and disease. *Hypertension*. 2017;69:387-395
447. Sequeira Lopez MLS, Nagalakshmi VK, Li M, Sigmund CD, Gomez RA. Vascular versus tubular renin: Role in kidney development. *American Journal of Physiology-Regulatory, Integrative and Comparative Physiology*. 2015;309:R650-657
448. Murali S, Zhang M, Nurse CA. Angiotensin ii mobilizes intracellular calcium and activates pannexin-1 channels in rat carotid body type ii cells via at1 receptors. *The Journal of Physiology*. 2014;592:4747-4762
449. Jones CA, Petrovic N, Novak EK, Swank RT, Sigmund CD, Gross KW. Biosynthesis of renin in mouse kidney tumor as4.1 cells. *European journal of biochemistry*. 1997;243:181-190
450. Johnstone SR. Going against the flow: The connexin connection in hypertension. *Hypertension*. 2015;65:502-504
451. Johnstone SR, Kroncke BM, Straub AC. Mapk phosphorylation of connexin 43 promotes binding of cyclin e and smooth muscle cell proliferation. *Circulation*. 2012

452. Drelon C, Berthon A, Mathieu M, Martinez A, Val P. Adrenal cortex tissue homeostasis and zonation: A wnt perspective. *Molecular and Cellular Endocrinology*. 2015;408:156-164
453. Berthon A, Drelon C, Ragazzon B, Boulkroun S, Tissier F, Amar L, Samson-Couterie B, Zennaro M-C, Plouin P-F, Skah S, Plateroti M, Lefèbvre H, Sahut-Barnola I, Batisse-Lignier M, Assié G, Lefrançois-Martinez A-M, Bertherat J, Martinez A, Val P. Wnt/ β -catenin signalling is activated in aldosterone-producing adenomas and controls aldosterone production. *Human Molecular Genetics*. 2014;23:889-905
454. Berthon A, Sahut-Barnola I, Lambert-Langlais S, de Jossineau C, Damon-Soubeyrand C, Louiset E, Taketo MM, Tissier F, Bertherat J, Lefrançois-Martinez A-M. Constitutive β -catenin activation induces adrenal hyperplasia and promotes adrenal cancer development. *Human molecular genetics*. 2010;19:1561-1576
455. Penuela S, Gyenis L, Ablack A, Churko JM, Berger AC, Litchfield DW, Lewis JD, Laird DW. Loss of pannexin 1 attenuates melanoma progression by reversion to a melanocytic phenotype. *The Journal of biological chemistry*. 2012;287:29184-29193
456. Wood MA, Hammer GD. Adrenocortical stem and progenitor cells: Unifying model of two proposed origins. *Molecular and Cellular Endocrinology*. 2011;336:206-212
457. Doi Y, Atarashi K, Franco-Saenz R, Mulrow PJ. Effect of changes in sodium or potassium balance, and nephrectomy, on adrenal renin and aldosterone concentrations. *Hypertension*. 1984;6:1124-129
458. Moreno C, Hoffman M, Stodola TJ, Didier DN, Lazar J, Geurts AM, North PE, Jacob HJ, Greene AS. Creation and characterization of a renin knockout rat. *Hypertension*. 2011;57:614-619
459. Raff H, Raff H, Gehrand A, Gehrand A, Bruder ED, Bruder ED, Hoffman MJ, Hoffman MJ, Engeland WC, Engeland WC, Moreno C, Moreno C. Renin knockout rat: Control of adrenal aldosterone and corticosterone synthesis in vitro and adrenal gene expression. *American Journal of Physiology-Regulatory, Integrative and Comparative Physiology*. 2015;308:R73-77

